ADAMANTANE COPOLYMERS

by

Liezel Coetzee

Dissertation presented for the Degree

Doctor of Philosophy (Polymer Science)

University of Stellenbosch

Promoter **Stellenbosch**

Dr. A.J van Reenen **December 2001**

DECLARATION

I, the undersigned, hereby declare that the work contained in this dissertation is my own original work and that I have not previously, in its entirety or in part, submitted it at any university for a degree.

ABSTRACT

This study concerns the incorporation of adamantane containing monomers 3-(1-adamantyl)-1-propene and 1-(1-adamantyl)-4-vinylbenzene into ethene, propene and higher α-olefins using different catalytic systems. The effect of the incorporation of the adamantane monomer on the physical and thermal properties of the polymers was investigated. A thorough study on the background of adamantane in general, as well as polymerization reactions involving the above–mentioned monomers and α-olefins was done.

3-(1-Adamantyl)-1-propene as well as 1-(1-adamantyl)-4-vinylbenzene was sucessfully synthesized. The homopolymers of each monomer were made. The above–mentioned monomers were also polymerized:

- 3-(1-adamantyl)-1-propene with ethene, propene and higher α-olefins,
- 1-(1-adamantyl)-4-vinylbenzene with ethene and styrene.

The copolymers of 3-(1-adamantyl)-propene as well as 1-(1-adamantyl)-4-vinylbenzene were characterized as far as possible to show the influence of the incorporation of the adamantane group on the physical and chemical properties of the polymers. A series of 3-phenyl-1-propene copolymers with higher α-olefins were synthesized to compare the influence of the phenyl group to the adamantyl group on the relevant properties of the polymers.

OPSOMMING

Hierdie studie behels die inkorporasie van adamantaan–bevattende monomere, 3-(1-adamantiel)-1-propeen en 1-(1-adamantiel)-4-vinielbenseen in eteen, propeen en hoër α-olefiene met behulp van verskillende katalitiese sisteme. Die effek wat die inkorporasie van die adamantaan monomeer op die fisiese en chemiese eienskappe van die polimere het, is ondersoek. 'n Deeglike studie van die agtergrond van adamantaan in die geheel, sowel as die polimerisasie reaksies van die bogenoemde monomere met α-olefiene, is gedoen.

3-(1-Adamantiel)-1-propeen sowel as 1-(1-adamantiel)-4-vinielbenseen is suksesvol berei. Die homopolimere van bogenoemde monomere is gesintetiseer. Bogenoemde monomere is gepolimeriseer:

- 3-(1-adamantiel)-1-propeen met eteen, propeen en hoër α-olefiene,
- 1-(1-adamantiel)-4-vinielbenseen met eteen en stireen.

Die kopolimere van 3-(1-adamantiel)-1-propeen en 1-(1-adamantiel)-4-vinielbenseen is sover moontlik gekarakteriseer om die invloed van die adamantaan groep op die fisiese en chemiese eienskappe van die polimeer te toon. 'n Reeks kopolimere van 3-(1-feniel)-1-propeen met hoër α-olefiene is gesintetiseer om die verwantskap tussen die invloed van die fenielgroep en die adamantielgroep op die relevante eienskappe van die polimere te toon.

ACKNOLEDGEMENTS

I wish to express my very sincere thanks to:

Dr A.J. van Reenen, my study leader, for his enthusiasm, encouragement and help throughout this study.

Dr M.W. Bredenkamp for all his advice, assistance and time so generously given to the organic side of this research project and for the many fruitful discussions held during the last three years.

Prof L.J. Mathias for his imput in this research project during the three months at the University of Southern Mississippi.

The Foundation for Research and Development for financial support for this research.

Dr M.J. Hurndall for the proof reading of this document.

Mrs E. Pentreath for all the NMR analyses done during this study.

Johan Eygelaar for the infrared spectroscopy analyses done during this study.

André van Zyl for all the GPC analyses done during this study.

Charl Morkel for all the DMA work done during this study.

A special word of thanks to all my friends who always supported and encouraged me.

Bernard, for always believing in me.

Special thanks for the love and support of my family.

To my husband Bernard, for always believing in me.

LIST OF CONTENTS

LIST OF FIGURES

CHAPTER 1

CHAPTER 3

CHAPTER 4

CHAPTER 5

CHAPTER 6

LIST OF TABLES

CHAPTER 3

CHAPTER 4

CHAPTER 5

CHAPTER 6

LIST OF SCHEMES

CHAPTER 1

INTRODUCTION AND OBJECTIVES

1.1 INTRODUCTION

Adamantane is the smallest repeating unit of the diamond lattice[1]. Adamantane has long been considered a strain-free molecule because its structural features are thought to be 'ideal'.

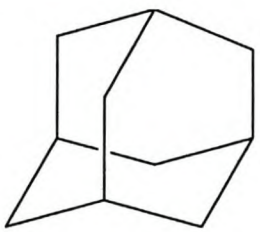

Figure 1-1: Structural Representantion of the Adamantane Molecule

Adamantane is a rigid ring system composed of three fused chair cyclohexane rings. All tertiary positions are identical and all secondary positions are equal. Carbocations can quite easily form at adamantane bridgehead positions, while the secondary positions are much less reactive[1]. Its high degree of symmetry inherently makes functionalization easier. Although substitution of the tertiary positions in adamantane generally requires more vigorous conditions than are used with nonbridgehead substrates, reactions often proceed in significantly better yields because of the lack of side reactions. Most importantly, no elimination can take place; the introduction of a double bond into the adamantane skeleton would be a violation of Bredt's rules, since a double bond would be placed at a bridgehead[2].

Much research has been devoted to the formation of all–hydrocarbon materials. They offer advantages over heteroatom-containing materials in terms of long term thermal and environmental stability, in having a low dielectric constant, and low water absorption. Strong carbon–carbon bonds also lead to improved moduli, strength and toughness. Adamantane is an ideal choice for use in such materials as it is all-hydrocarbon and its tetrahedral geometry allows for growth of hydrocarbon arms in three dimensions.

Adamantyl groups have been incorporated in polymers as part of the main chain[3-5] and as side groups[6-11]. This results in property modifications, including decreased crystallinity, increased solubility and enhanced T_g, without sacrificing thermal stability. The bulkiness of adamantane tends to inhibit packing of chains, which ultimately decreases crystallinity and increases solubility. Adamantane-containing polymers show enhanced properties such as hydrolytic and thermooxidative stability. The syntheses of adamantyl monomers are, however, expensive and cumbersome.

The use of α-olefins having adamantyl or methyladamantyl substituents have received little or no attention. In 1969 Capaldi and Borchert reported the synthesis of 3-(1-adamantyl)-1-propene and the polymerization thereof to low yield, using Ziegler–Natta catalysts[12].

Ziegler-Natta catalysts are a term that describes a large variety of transition metal-based catalysts capable of polymerizing and copolymerizing α-olefins and dienes[13-15]. The products of these reactions poly(α-olefins), polydienes and α-olefin copolymers are commercially produced in very large volumes and have numerous applications as general–purpose enginering plastics. Ziegler–Natta catalysts have different active sites and there is poor control of comonomer incorporation, which results in the production of heterogeneous polymers. The products obtained with heterogeneous Ziegler–Natta catalysts are mixtures

containing polymer molecules of different stereoregularity. In the copolymers made with Ziegler–Natta catalysts, the amount of comonomer incorporated and the regular insertion of the comonomer along the polymer chain cannot be controlled. The comonomer can act as a chain transfer agent and could cause a broad molecular mass distribution.

Metallocene–based catalysts, including the so–called 'single–site' catalysts, are bicomponents consisting of group four transition metal compounds and cocatalysts[16-18]. They generate only one kind of active center and are therefore the only catalysts that can be used to control both the molecular mass and the microstructure (tacticity, regioregularity and comonomer distribution) of polyolefins. Their use leads to homogeneous copolymers of narrow molecular mass distributions[19, 20].

1.2 OBJECTIVES

The main purpose of this work was to synthesize and characterize adamantane-containing monomers, copolymerize them with ethene, propene and higher α-olefins, and investigate the effect of the adamantane on the thermal and physical properties of the polymers.

Specific objectives were:

1.2.1 A Study of the Incorporation of Adamantane-Containing Monomers into Polymers of Ethene, Propene and Higher α-Olefins

This objective involved the following tasks:

- The synthesis of 3-(1-adamantyl)-1-propene using three different synthetic approaches.
- Homopolymerization of 3-(1-adamantyl)-1-propene.
- Copolymerization of 3-(1-adamantyl)-1-propene with ethene, propene and higher α-olefins, with different metallocene catalyst systems.

- Homopolymerization of 3-phenyl-1-propene.
- Copolymerization of 3-phenyl-1-propene with higher α-olefins, using a metallocene catalyst system.
- Synthesis of 1-(1-adamantyl)-4-vinylbenzene, using three different synthetic approaches.
- Hompolymerization of 1-vinyl(4-adamantyl)-benzene.
- Copolymerization of 1-(1-adamantyl)-4-vinylbenzene with α-olefins and styrene, using different catalytic systems.

1.2.2 Characterization of the Homo- and Copolymers

The homo-and copolymers mentioned in Section 1.2.1 were to be characterized for:

- Glass Transition and Melting Point Determination
- Composition Analyses
- Molecular Weight Determination

1.2.3 Consideration of the Relationship between the Composition and Physical Properties of the Homo-and Copolymers

The relationship between the composition and physical properties of the homo- and copolymers mentioned in Section 1.2.1 was investigated.

1.3 STRUCTURE OF MANUSCRIPT

Chapter two gives an historical overview of adamantane, its structure, formation and properties, as well as adamantane–containing polymers and their industrial applications.

Chapter three describes the different approaches used (and related difficulties) in the synthesis of 3-(1-adamantyl)-1-propene. Gas Chromatography (GC) was used to follow the progress of the monomer synthesis as well as to determine the purity of the monomer.
Characterization of 3-(1-adamantyl)-1-propene, which included determinations of the melting point by DSC, and microstructure by NMR and IR spectroscopy is also described.

Chapter four describes the homopolymerization reaction of 3-(adamantyl)-1-propene as well as the copolymerization reactions with ethene, propene and higher α-olefins. Three different metallocene catalyst systems were used, namely the C_2 symmetric ansa metallocene *rac*-[(ethylenebis(indenyl)]zirconium dichloride, the C_{2v} symmetric catalyst, bis(indenyl)zirconium dichloride, Ind_2ZrCl_2, and a half-sandwich catalyst, dimethylsilyl(t-butylamido)(tetramethylcyclopentadienyl)titaniumdimethyl. In all three systems, methylaluminoxane(MAO) was used as cocatalyst. An historical and theoretical background on metallocene catalyzed polymerization reactions with ethene, propene and higher α-olefins are discussed in this Chapter.

Chapter four also includes a discussion on an analogous series of copolymers which were made by copolymerizing 3-phenyl-1-propene with the higher α-olefins, in order to compare the relative effect of the adamantyl group and a phenyl group. This series of polymerizations was carried out using the C_2 symmetric *ansa* metallocene *rac*-[(ethylenebis(indenyl)]zirconium dichloride with MAO as cocatalyst. The properties of the 3-phenyl-1-propene polymers and copolymers were compared to those of the 3-(1-adamantyl)-1-propene polymers and the influence of the phenyl and the adamantyl groups on the properties were compared. Characterization of the 3-(1-adamantyl)-1-propene polymers and the 3-phenyl-1-propene polymers included determinations of the melting points by DSC and DMA, microstructures by NMR and IR spectroscopy.

In Chapter five, the different methods used for the preparation of 1-(1-adamantyl)-4-vinylbenzene are discussed. The effect of the incorporation of the adamantane-substituted monomer on the physical and thermal properties of the polymers was investigated.

Characterization of 1-(1-adamantyl)-4-vinylbenzene included determinations of the melting point by DSC and microstructure by NMR and IR spectroscopy. Gas chromatography was used to follow the progress of the monomer synthesis as well as to determine the purity of the monomer.

In Chapter six, the homopolymerization reaction of 1-(1-adamantyl)-4-vinylbenzene as well as the polymerization reactions with ethene, styrene and higher α-olefins are discussed. Two different metallocene catalyst systems were used, namely a half-sandwich catalyst pentamethylcyclopentadienyl zirconium trichloride, and a bridged catalyst, iso-propylindene(cyclopentadienyl)(9-fluorenyl) zirconium dichloride. Stannic chloride ($SnCl_4$) was used to catalyse cationic homopolymerizations as well as copolymerization reactions with the 1-(1-adamantyl)-4-vinylbenzene and styrene monomers. In both the metallocene catalyst systems used in the polymerization reactions, methylaluminoxane(MAO) was used as cocatalyst. Also included in this Chapter is a brief background on mainly the metallocene-catalyzed styrene polymerizations.

In Chapter seven conclusions are drawn to the objectives, as stated in Chapter one. 3-(1-Adamantyl)-1-propene and 1-(1-adamantyl)-4-vinylbenzene were successfully synthesized and subsequent polymerization reactions involving these two monomers carried out.

1.4 REFERENCES

1. Fort R.C., Jr., *Adamantane: The Chemistry of Diamond Molecules*, Grassman P.G., Ed., Studies in Organic Chemistry, Vol. 5, Marcel Dekker: New York, 1976.
2. Reichert V.R., PhD Dissertation, University of Southern Mississippi, 1994.
3. Chern Y.T., Wang J.J., *Macromolecules*, 1995, **28**, 5 554.
4. Chern Y.T., Chung W.H., *J. Polym. Sci.: Part A: Polym. Chem.*, 1996, **34**, 117.
5. Pixton M.R., Paul D.R., *Polymer*, 1995, **36**, 3 165.
6. Wang J.J., Chern Y.T., Chung M.A., *J. Polym. Sci., Polym. Chem. Ed.*, 1996, **34**, 3 345.
7. Chern Y.T., *Polym. Bull.*, 1996, **36**, 59.
8. Mathias L.J., Reichert V.R., Muir A.V.G.,*Chem. Mat.*, 1993, **5**, 4.
9. Matsumoto A., Tanaka S., Otso T., *Macromolecules*, 1991, **24**, 4 017.
10. Avici D., Kusefoglu S.H., Thompson R.D., Mathias L.J., *Macromolecules*, 1994, **27**, 2 937.
11. Tsuda T., Mathias L.J., *Macromolecules*, 1993, **26**, 4 743.
12. Capaldi E., Borchert A.E., *US Patent*, 1969, **3,457**, 318.
13. Breslow D.S., Newburg N.R., *J. Am. Chem. Soc.*, 1957, **79**, 5 072.
14. Natta G., Pino P., Mazzanti G., Giannini U., *J. Am. Chem. Soc.*, 1957, **79**,2 957.
15. Geldenhuys M., M.Sc thesis, University of Stellenbosch, 1999.
16. Sinn H., Kaminsky W., *Adv. Organomet. Chem.*, 1980, **18**, 99.
17. Kaminsky W., Kulper K., Brintzinger H.H., Wald F.R., *Angew. Chem. Int. Ed. Engl.*, 1985, **24**, 507.
18. Kaminsky W. in *History of Polyolefins*. Seymour R.B., Cheng T., Eds. Plenum Press, New York, 1987, 361.
19. Suhm J., Schneider M.J., Mülhaupt R., *J. Molecular Catalysis A: Chem.*, 1998, **128**, 215.
20. Heiland K., Kaminsky W., *Makromol. Chem.*, 1992, **193**, 601.

CHAPTER 2

HISTORICAL AND OVERVIEW OF ADAMANTANE

2.1 INTRODUCTION

This Chapter is an overview and historical in general of adamantane, its structure, formation and properties, as well as adamantane–containing polymers. This Chapter focuses on introducing the reader to adamantane, its properties, incorporation in polymers and the applications of adamantane-containing polymers in industry. A discussion in general about the effects on polymer properties, especially T_g, of different pendant groups will introduce the reader to the huge effect of incorporating adamantane as pendant group or part of the main chain in polymers.

2.2 GLASS TRANSITION TEMPERATURE (T_g) OF POLYMERS

An amorphous polymer is easy to imagine[1]. A bowl of spaghetti is a fair analogy. A bucket of worms is even better, because polymer molecules are constantly in motion. To be analogous to some common polymers, the worms would have to be 10^3 to 10^4 times longer than they are thick. Obviously, the constant motion one notes in the bucket is not of whole worms at once, but of individual segments. The analogous segmental Brownian motion in polymers is very important in explaining flow and deformation. The intensity of the motion increases with temperature. Below a certain temperature (T_g) the polymer segments do not have sufficient energy to move past one another. If the material is stressed, the only reversible response can be for bond angles and distances to be strained, since no gross movements of segments can take place. Such a material is a glass. Only if the temperature is above T_g can the segments rearrange to relieve an externally applied stress. The glass transition temperature (T_g) is called a second–order transition, since the change in volume is not discontinuous. The abruptness of the transition can be rationalized by the

concept of free volume. The segmental energy has to exceed a certain barrier value before a 'hole' of segmental dimensions can be created for diffusion.

Whether or not T_g is a thermodynamic parameter is the subject of some controversy. A statistical model put forward by Gibbs and DiMarzio predicts the existence and some of the characteristics of the glass transition[2-4]. However, attempts to verify the thermodynamic interrelation among changes in heat capacity, expansion coefficient, and compressibility at T_g have met with only occasional success. Experimentally, it is found that T_g itself depends on the time scale of the experiment in which it is measured[1].

If energy is stored in an amorphous polymer by stressing it and an attempt is made to recover the energy that was put in, there is always a certain amount of of hysteresis or mechanism loss. This loss may be small above or below T_g, but it is always a maximum at T_g. This often is a more sensitive measurement than volume change on heating. The rationalization is not difficult. In the glass, the stress is stored by bond distortions which are easily recovered. Above T_g, polymer chains can be uncoiled from their random conformation by rotations readily about successive single bonds. Only at T_g is the uncoiling hindered by intermolecular forces.

2.2.1 Effect of Chemical Structure and Pendant Groups on T_g of Polymers

Segmental mobility is highly dependant on chain stiffness and somewhat dependant on intermolecular forces[1]. It is expected that polymers with high polarity or high cohesive energy density should have higher transition temperatures than nonpolar materials. On the other hand, regularity, which is so important to crystallizability, counts for little in the amorphous transition. Since the segmental motion implies the concerted movement of many chain atoms (ten to fifty atoms), bulky side groups which hinder rotation about single bonds should raise T_g also. An interesting series in this respect is afforded by the vinyl ether polymers. As the polar ether linkage is diluted by longer alkyl side groups from

methyl to butyl, T_g decreases. However, when the alkyl group is bunched up next to the chain, as with *tert*-butyl ether, rotation about the single bonds in the chain is made difficult and T_g is raised dramatically. Chain stiffness and, consequently, T_g, increases if single bonds in the polymer chain are replaced by multiple bonds about which there can be no rotation. Ring structures in the main chain contribute inflexibility as in poly(ethylene terephthalate) or cellulose derivatives.

Since crystallinity depends strongly on regularity, but T_g does not, it is conceivable that some copolymers might form glasses before they can crystallize. This is the case for ethylene–propylene copolymers of roughly equimolar proportions. When polymerized by a catalyst which gives highly crystalline, linear polyethylene or highly crystalline, isotactic polypropylene, a mixture of the monomers gives an amorphous, rubbery material which does not crystallize but only forms a glass on cooling to about –60 °C. Another example is that by adding 20 % of phenylmethylsilanol, the crystallinity of polydimethylsilanol is destroyed without substantially raising the T_g.

2.2.2 Why did we choose Adamantane?

Adamantane was chosen because of its exceptional qualities. Adamantane is a rigid ring system composed of three fused chair cyclohexane rings[5]. Its high symmetry inherently makes functionalization easier. All tertiary positions are identical and all secondary positions are equal[6]. Carbocations can quite easily form at adamantane bridgehead positions, while the secondary positions are much less reactive. Although substitution of the tertiary positions in adamantane generally requires more vigorous conditions than are used with nonbridgehead substrates, they often proceed in significantly better yields because of the lack of side reactions. Most importantly, no elimination can take place; the introduction of a double bond into the adamantane skeleton would be a violation of Bredt's rules, since a double bond would be placed at a bridgehead[5]. There has been a lot of research devoted to the formation of all–hydrocarbon materials[7]. They

offer advantages over heteroatom containing materials in long term thermal and environmental stability, in prossessing low dielectric constant, and having low water absorption. Also, strong carbon–carbon bonds lead to improved moduli, strength, and toughness. Adamantane is an ideal choice for use in such materials in that it is all hydrocarbon and its tetrahedral geometry allows for growth of hydrocarbon arms in three dimensions.

Adamantane has also been incorporated into the backbone of many polymers including polysulfones, polyimides, and polyesters[8]. The polymers show enhanced properties such as hydrolytic and thermooxidative stability, although the syntheses of the adamantyl monomers are expensive and cumbersome.

When adamantane is incorporated as a pendant group[8] on the polymer backbone, the result is property modifications, including decreased crystallinity, increased solubility and enhanced T_g and thermal stability[8]. For example, pendant adamantane groups cause dramatic increases in T_g's and solubility without sacrificing thermal stability. The bulkiness of adamantane tends to inhibit packing of chains which ultimately decreases crystallinity and increases solubility[8].

2.3 STRUCTURE AND PROPERTIES OF ADAMANTANE

2.3.1 Structure and Properties of Adamantane

Adamantane is the smallest repeating unit of the diamond lattice[5]. Several representations of this molecule and the numbering scheme are shown as structures **[2-1]** to **[2-3]**.

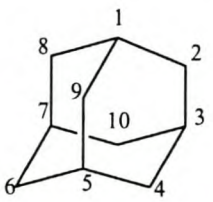

[2 - 1]

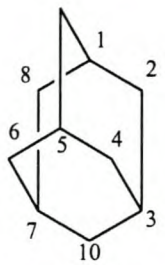

[2 - 2]

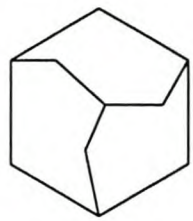

[2 - 3]

X-ray and electron diffraction studies[9–15] confirm the structure and essential normality of all C-C and C-H bond lengths. Within the limits of these studies, all C-C-C angles are tetrahedral. Adjacent carbon atoms are held in the staggered, torsionally most favorable conformation. The next higher adamantologs, diamantane **[2-4]**[16] and triamantane **[2-5]**[17], have the same sorts of structural features (nomenclature for these systems follows the suggestions of Vogl and co-workers[18]).

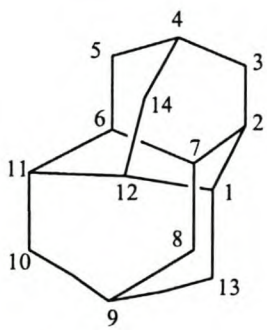

[2 - 4]

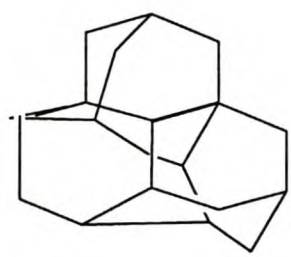

[2 - 5]

2.3.2 Strain within the Adamantane Structure

Adamantane has long been considered a strain-free molecule[19] because its structural features are thought to be 'ideal'. However, it has been proposed that, in fact, adamantane should have a nonzero strain energy[20]. Tetrahedral bond angles can only be expected for a given carbon atom when all four substituents are identical[21]. Widening of the C-C-C angles is observed in propane (112.4°)[22] and other straight chain hydrocarbons[23,24]; isobutene, has a value of 111.3°[25]. Cyclohexane also has somewhat spread angles (111.5°)[26]. From these

observations it is suggested that adamantane must have some strain, because the cage structure prevents the attainment of these preferred wider angles. Molecular mechanics calculations indicate that adamantane has a strain energy of 6-7 kcal/mol[26]. The source of strain has been assigned to C-C non-bonding interactions magnified by the rigidity of the adamantane skeleton (such are present in all cyclohexane rings)[5]. There appear to be no special effects associated with the cage structure.

Substituents may add to the strain energy of adamantane and diamantane. In adamantane, a substituent at the 2-position is axial to one of the cyclohexane rings, whereas at the 1-position, it is equatorial. Equilibration of 1- and 2-methyladamantane produces an equilibrium mixture [Eq. (2-1)].

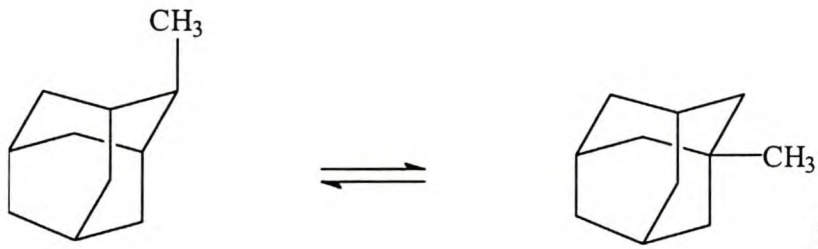

Eq. 2-1

$\Delta G° = -2.4$ kcal/mole

The enthalpy difference of 2.5 kcal/mole is somewhat larger than is typical for methyl on a cyclohexane ring, and it has been suggested that this reflects the inflexibility of the adamantane molecule. In diadamantane, the difference is between the 1-bridgehead, where a group is axial, and the 4-bridgehead, where it is equatorial [Eq. (2-2)].

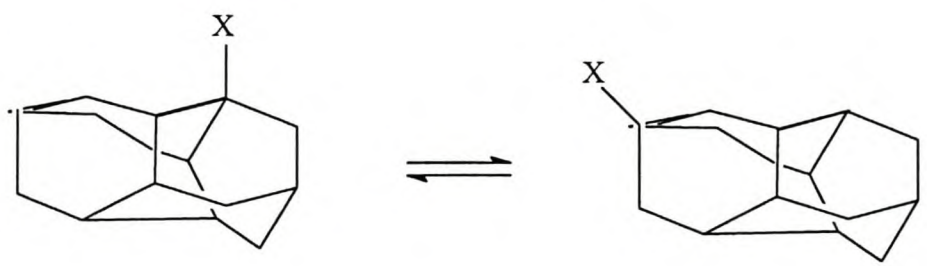

Eq. 2-2

Several equilibrations have been performed. For X = Cl, OH, and CH_3, the enthalpy term favors the equatorial 1-isomer by 0.68, 1.1, and 2.14 kcal/mole, respectively[27, 28]. These values are very similar to those obtained in cyclohexanes, which perhaps negates the 'rigidity' explanation for adamantanes.

2.3.3 Spectral Properties of Adamantane

The high symmetry of adamantane (point group T_d) has significant effects on the spectral characteristics of the hydrocarbon and its simple derivatives. The infrared spectrum of adamantane consists of 32 absorptions, only nine or ten of which are strong[29]. Those infrared spectra of 1-substituted adamantanes that have been reported have the same basic simplicity[30]. Each of the strong bands present in the spectrum of adamantane itself appears in the spectra of the substituted compounds. In addition, a number of the derivatives have an absorption in the region 1 017-1 038 cm^{-1}. The suitability of using this band as a diagnostic test for the presence of an adamantane skeleton is excluded by its occasional extremely low intensity.

Spectra of 2-substituted compounds, which are of lower symmetry (C_s) than their 1-substituted counterparts (C_{3v}), are more complex, as are spectra of 1,3-disubstituted adamantanes (C_{2v} if the substitiuents are the same, C_s if not)[31].

Nuclear magnetic resonance spectra of adamantanes are of considerably greater value than IR spectra for structure determination. They have quite characteristic features for a given substitution pattern[32] and structures are readily assigned from the chemical shifts and integrated intensities. Generally, analysis is facilitated by the absence of strong coupling.

The 60 mHz proton magnetic resonance (pmr) spectrum of adamantane consists of a sharp doublet, spacing 1.7 Hz, at 1.78 ppm and a barely discernible shoulder on the low field side of the peak. At 220 mHz, this shoulder is cleanly separated and the bridgehead protons may be identified as its source by relative

intensities[33]. The correct chemical shifts are then seen to be: CH, 1.87 ppm; CH_2, 1.74 ppm.

Examination of the resonances resulting from ^1H coupling with ^{13}C in natural abundance allows an estimate of J_{vic}, the vicinal coupling constant between the bridgehead and methylene protons. The ^{13}C satellites from the CH_2 groups are broad singlets w_h = 5.3 Hz, J_{CH} = 120 ± 1 Hz.

A unique J_{vic} cannot be obtained, but clearly it must be less than, or equal to, 5.3/2 = 2.65 Hz. This value is in good agreement with that obtained for substituted adamantanes, 2.6 ± 0.2 Hz[32], and is somewhat larger than the 1.8 Hz predicted by the Karplus relationship for a dihedral angle of 60° [34].

It is of interest to determine why so little splitting is observed in simple adamantane derivatives. One would expect, from a first-order analysis, that the β-hydrogens in a bridgehead substituted adamantane would appear as a clean doublet with a J value of about 1-3 Hz. The δ-hydrogens, which are non-equivalent, should give an AB quartet with further splitting by the two adjacent bridgehead protons. A bridgehead (γ) hydrogen resonance should be split at least seven times by three neighboring methylene groups. In fact, the β- and δ protons rarely show any splitting, and the bridgeheads always give a broad, unresolved hump. An explanation for this is that, at 60 mHz, at which most reported adamantane spectra have been recorded[32], chemical shifts are simply not large enough to allow distinction between the two types of δ hydrogens. In addition, the separations between β, γ, and δ protons are often so small that the condition for first-order interpretation (that $\delta >> J$) is not met.

Long-range couplings may also be operative in adamantanes. An examination of a model shows that both the protons of the methylene groups and those at the bridgeheads lie in the "W" arrangement that has been implicated in most four-bond couplings in saturated systems[35, 36]. There is the further possibility of a bridgehead-methylene five-bond coupling[5]. Although these interactions could

contribute significantly to line broadening, and thus to the washing out of normal coupling, their presence has not been established.

The effect of aromatic solvents upon the pmr spectra of adamantanes has received much attention[32, 37, 38]. The specific shifts, usually of only those protons furthest from the substituent, are often of substantial value in structure determination[32]. A simple example of this is the benzene solvent effect upon the spectrum of 1-chloroadamantane. In carbon tetrachloride, the β- and γ absorptions overlap, but all three of the expected resonances become visible in a benzene solution.

2.4 STEREOCHEMISTRY AND OPTICAL PROPERTIES

When one or more secondary substituents are present on the adamantane ring the stereochemical possibilities become many; some are shown as structures **[2-6]** to **[2-12]**. The various ketones, which are in fact rigid cyclohexanones, have been examined for Cotton effects. Djerassi and co-workers[39] prepared and resolved compound **[2-6]** (X = COOH) in which the substituents lie in nodal planes. As predicted by the octant rules[39], extremely low molecular amplitudes are observed for the Cotton effects; molar ellipticities from circular dichorism are also small.

Snatzke *et al*[40] have prepared compounds **[2-7]** and **[2-8]** (X = CH_3, F, Cl, Br, I, OH, OAc, ONO_2, SCN, N_3) which have the substituent axial and equatorial, respectively. All of the equatorial substituents follow the octant rules, while axial substituents either make virtually no contribution (e.g. CH_3) or show antioctant behavior. Similar results are obtained with compound **[2-9]** (X = Br, OH, OAc, OMe, COOH, etc.) and, likewise, with compounds of the types **[2-10]** or **[2-11]**. Compounds of type **[2-12]** have allene dissymmetry. One such compound 2,6-dichloro-1,3,5,7-tetracarboxyadamantane, has been resolved, and the specific rotation is found to be small.

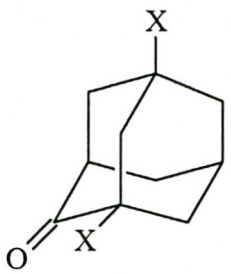

[2 - 6]

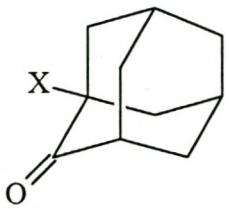

[2 - 7]

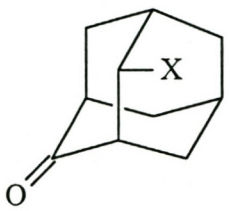

[2 - 8]

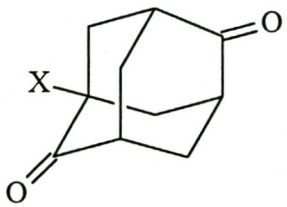

[2 - 9]

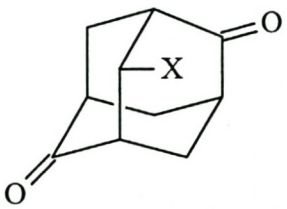

[2 - 10]

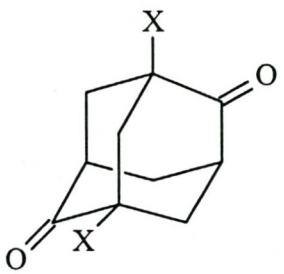

[2 - 11]

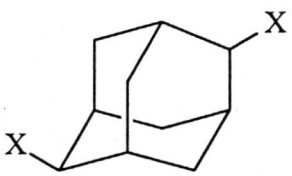

[2 - 12]

2.5 THE SOLID STATE OF ADAMANTANE

The unusual structure of adamantane has significant effects upon its crystal structure and solid-state properties[5]. Adamantane is one of the highest melting hydrocarbons known, m.p. (269 °C), and sublimes readily at atmospheric pressure and room temperature. It crystallizes in a face-centered cubic lattice. Solid adamantane is a plastic crystal, as are the solid forms of many other globular molecules. The plastic crystalline state is characterized by[41]:

1. An entropy of fusion of less than 5 cal/mole/deg, compensated by one or more transitions in the crystal.
2. High triple point pressure and temperature.
3. High symmetry, usually cubic or hexagonal.
4. Transparency, tackiness, and easy deformability.

Measurements of the heat capacity of adamantane[42, 43] reveal a pronounced lambda-type transition at 208.62 °K. This transition has also been detected by infrared spectroscopy[44], X-ray diffraction[45-47] and proton magnetic resonance. Molecules in the high-temperature state are able to rotate more freely than those in the low-temperature state.

The high triple point parameters expected for a plastic crystal are observed for adamantane. The triple point tetragonal/face-centered cubic/ liquid is found[48, 49] near 27 kbar at 460 °C. Graphitization occurs above 480 °C.

All workers in the area of adamantane chemistry are familiar with the tackiness of adamantane. The very slow sublimation of adamantane, for example, yields large transparent crystals with the consistency of paraffin wax[5].

Diamantane and some of its derivatives also show plastic crystalline behavior. The parent hydrocarbon and the 1- and 3-alcohols have two transitions below

the melting point, the other derivatives only one. It is believed that the two transitions correspond to rotational changes and a change in lattice structure[50].

Adamantane appears to form solid solutions with a number of small organic molecules. Advantage has been taken of this property to observe free radicals derived from the small molecules[51-55]. For example, γ- or X-irradiation of simple amines trapped in an adamantane crystal produces radicals by abstraction of an α-hydrogen from the amine. These radicals are stable for up to ten hours at room temperature, and have sufficient freedom of motion that high resolution electron spin resonance spectra can be obtained. This results in symmetrical line broadening, and the spectra remain interpretable.

2.6 DIPOLE MOMENTS

Extensive measurements have been made of the dipole moments of adamantane derivatives[56]. Adamantanes generally have higher moments than the corresponding *t*-butyl derivatives.

2.7 REARRANGEMENTS LEADING TO THE FORMATION OF ADAMANTANES

It has been observed that nearly all $C_{10}H_{15}$ tricyclic compounds rearrange to give adamantane at high temperatures or in the presence of catalysts[6]. This is attributed to the low strain energy of adamantane. Higher tricyclic analogues (C_{11} and above), rearrange to give bridgehead alkyl substituted adamantane derivatives. Rearrangements of tricyclic compounds provide a pathway to some tetra-substituted derivatives that otherwise require long and tedious syntheses.

2.7.1 Rearrangement Catalysts

The chemistry of diamondoid hydrocarbons is replete with examples of molecular rearrangement, the archetype of which is undoubtedly the aluminium chloride-catalyzed transformation of *endo*-tetrahydrodicyclopentadiene **[2-13]** into adamantane **[2-1]** (Eq.2-3)[57].

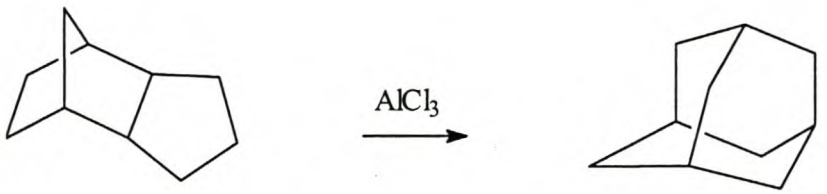

[2 - 13] [2 - 1] Eq. 2-3

An intriguing aspect of this reaction is the possibility that there may be literally hundreds of pathways, all accessible under strong Lewis acid catalysis, between precursor and product. A practical difficulty is that, because adamantane is so much more thermodynamically stable than all other isomeric tricyclic hydrocarbons, the detection and isolation of intermediates, in what is essentially an equilibrium-controlled process, is very difficult by ordinary analytical techniques. Scheme 2-1 shows several examples of Lewis acid catalyzed rearrangements[6].

The difficulties with conventional aluminium chloride catalysis are catalyst deactivation and the formation of numerous by-products which complicate the isolation of pure adamantane.

An extremely important route to alkyl adamantanes has been devised by Schneider and co-workers[58, 59]. Polycyclic aromatics are hydrogenated and contacted with an aluminum bromide sludge catalyst (*vide infra*). Perhydroacenaphtalene (mixture of isomers) gives an almost quantitative yield of 1,3-dimethyladamantane, via the first formed 1-ethyladamantane[59, 60]. The sludge is a rather viscous orange liquid, obtained by treating a cyclohexane solution of an alkyl bromide with excess aluminum bromide; the catalyst appears as a denser phase. The most commonly employed halides are *sec*-butyl and *tert*-butyl halides.

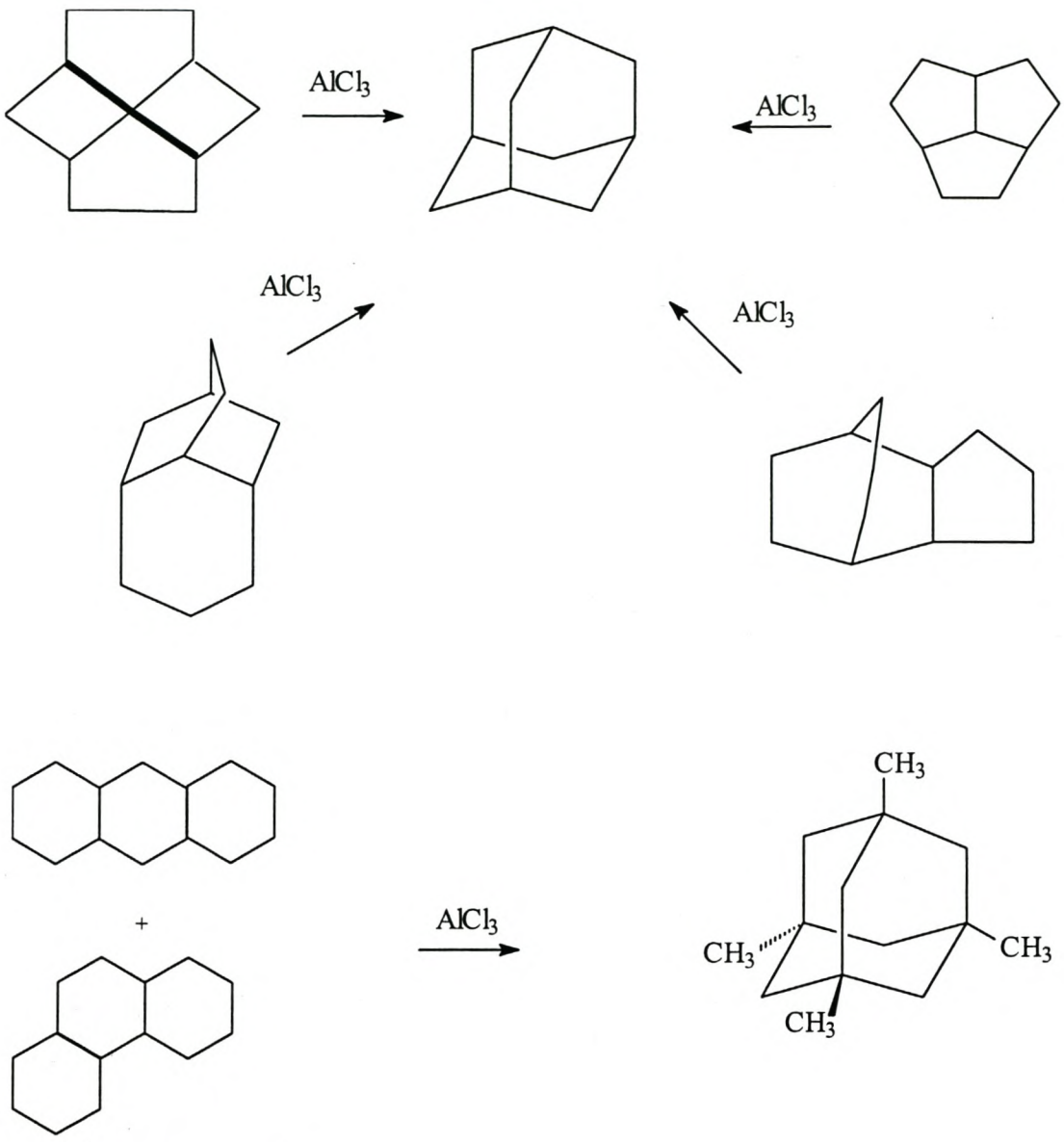

Scheme 2-1: Lewis Acid–Catalyzed Rearrangements Leading to the Formation of Adamantane

2.8 ADAMANTANE-CONTAINING POLYMERS

Incorporation of the rigid, symmetrical, low strain adamantane structure into a polymer has long attracted chemists from the standpoint of obtaining polymers with increased stiffness, thermal and oxidative stability, and solvent resistance[61].

Intuitively, the attachment of a large group, pendant from the polymer, should reduce chain mobility and raise the glass transition temperature (T_g). However, what is surprising with the adamantyl moiety is the magnitude of its effect[7]. Adamantane also maintains thermo oxidative stability because, unlike a typical linkage to a tertiary carbon (for example a *t*-butyl ester), elimination cannot easily occur at the bridgehead position which is the point of attachment.

2.8.1 Carbochain Polymers of Adamantane

Polyadamantane was first obtained from 3,3'-dibromo-1,1'-biadamantane by the Wurtz reaction[61]:

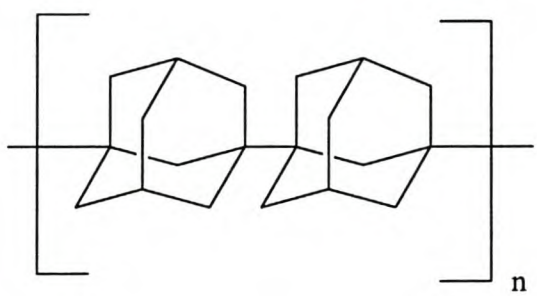

[2–14]

The polymer (melting point above 420 °C) was a white powder, insoluble in the usual organic solvents and resistant to concentrated hydrochloric acid and 5 *N* alkali. According to X-ray diffraction data[61], the polyadamantane had a degree of crystallinity in excess of 80 %.

Dehydroadamantanes may serve as another precursor of polyadamantane, 1,3-dehydroadamantane is an extremely reactive compound; on heating to 130-160 °C, it is converted into a solid polymer without fusion.

Polyadamantane is also formed by polymerization of 2,4-dehydroadamantane under the influence of aluminium chloride[62]. Interesting results have been obtained for the polycondensation of polybromoadamantanes under the influence of sodium metal[62]. The product is a three-dimensional carbon polymer

consisting of the carbon nuclei of adamantane. Oligomers consisting of two or three adamantane nuclei and short methylene chains between them have been obtained by the polycondensation of adamantane and its homologues with alkyl halides in the presence of $AlCl_3$ or $AlBr_3$[62]. The number of nuclei in the chain can be increased by using a large excess of the initial adamantane homologue.

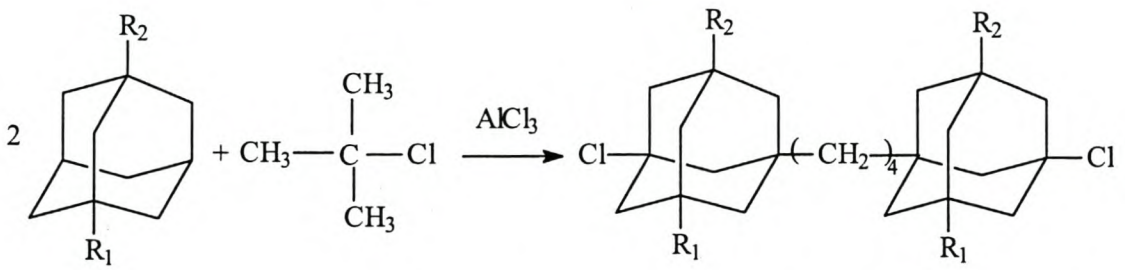

R_1 and R_2 = CH_3 or C_2H_5 Eq. 2-4

Copolymers of adamantane and benzene[62] serve as another example of mixed polyadamantanes.

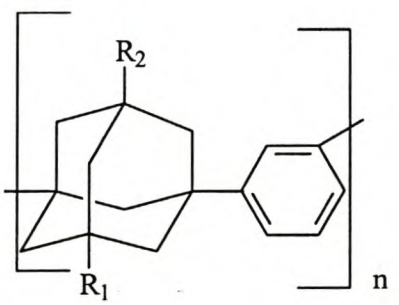

Where R_1 and R_2 = alkyl and n = 9–10.

[2–15]

Certain polymers of vinyl derivatives of adamantane are known[63]. Under the influence of $AlCl_3$ or $AlBr_3$ in methylene chloride, vinyladamantane gives rise to a solid product which is insoluble in organic solvents. On the basis of the results of elemental analysis, a formula has been proposed for the oligomer.

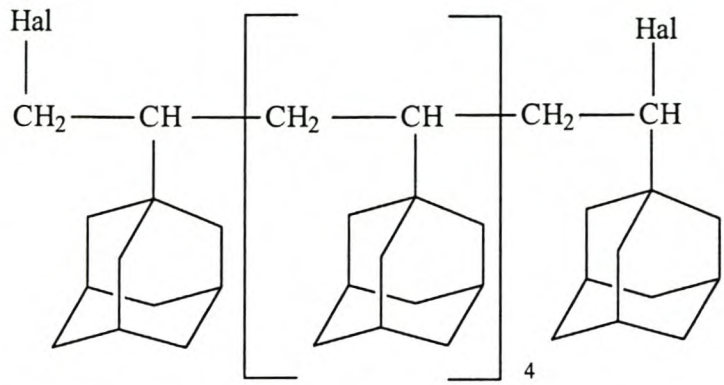

[2–16]

Adamantyl acrylates and methacrylates polymerize under the influence of free-radical and anionic catalysts and also under ultraviolet irradiation[64–66]. A study of the kinetics of the radical polymerization showed that both the methacrylates and the vinyl esters of adamantane derivatives are highly reactive, i.e. the adamantyl group does not inhibit polymerization. The principal distinctive properties of such polymers are T_g's, considerable surface hardness, brittleness and low mechanical strength, and insignificant contraction on polymerization. These properties are due to the presence of the bulky adamantyl group in the macromolecules, which increases the rigidity of the polymer chains.

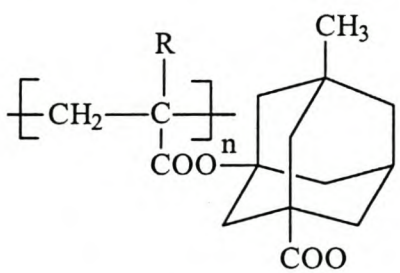

R = H or CH_3

[2–17]

Solutions of poly(adamantyl acrylates) are very viscous, which led to their use as thickening agents for lubricating oils. For example, a 1 % solution of poly (dimethyladamantyl acrylate) with a molecular weight of 80 000 has the same

viscosity as a 2 % solution of poly(methyl methacrylate) with a molecular weight of 117 000 $g.mol^{-1}$. Copolymerization with adamantyl acrylates leads to an increase in glass transition temperatures and the hardness of the copolymers.

As the size of the pendant group increases from methyl (acetate), to *t*-butyl, to phenyl (benzoate), and finally adamantane, the T_g values increase to values of 49, 100, 130, and 214 °C, respectively.

The influence of bulky substituents on the stereoregularity of the polymers of vinyl ethers and esters showed that the adamantyl group promotes a high syndiotacticity in poly(vinyl carboxylate) and isotacticity in vinyl ether[61]. The orienting effect of the adamantyl group is similar to that of the *t*-butyl group, which can be regarded as the open-chain analogue of the adamantyl group.

Like adamantyl methacrylates, poly(adamantyl vinyl ethers) have high glass transition temperatures (210–225 °C). In the homo- and copolymerization of the heterocyclic derivative 5-(1'-adamantyloxy)-2H, 2-pyrrolone with various vinyl monomers was studied. Spectroscopic investigations have shown that the polymerization takes place as a result of the partial dissociation of the C=C bond in the heterocycle.

The presence of the pyrrolone heterocycle in the polymer chain led to an investigation of the photochemical properties of the polymer films. Upon ultraviolet irradiation, photochemical transformations, accompanied by the formation of cyclopropyl isocyanate groups, take place in the polymer. The homo- and co-polymers of 5-(1'-adamantyl-oxy)-2*H*, 2-pyrrolone have high T_g's(220 – 245 °C).

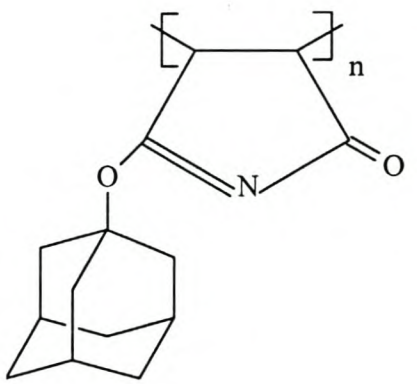

[2–18]

2.8.2 Polyethers, Polyesters and Polycarbonates of Adamantane

A polyether may have been the first polymeric heterochain derivative of adamantane obtained[61]. In their study of the possibility of synthesizing the adamantane nucleus from bicyclic systems, Stetter *et al* [67] observed that when 3-methylenebicyclo[3.3.1]-7-nonanone is heated in an inert solvent in the presence of toluene-*p*-sulphonic acid, a polyether derived from adamantane is formed in quantitative yield.

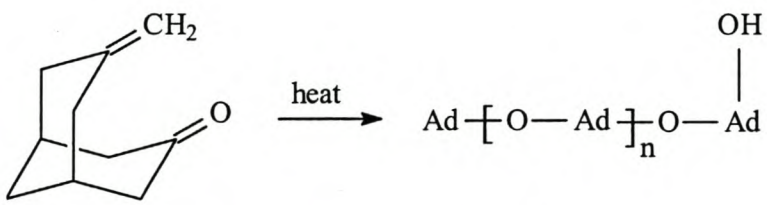

Ad = adamantane Eq. 2–5

The majority of adamantane-containing polyesters have low molecular weights, owing to the steric influence of the adamantane nucleus, for example, in the esterification of adamantane-1,3-diols by tetracarboxylic acid dianhydrides[61]. If the reaction is carried out in dimethylformamide (DMF) at a low temperature (60 °C) and in the presence of toluene-*p*-sulphonic acid, a linear non-cross-linked polyester with free carboxy-groups is obtained.

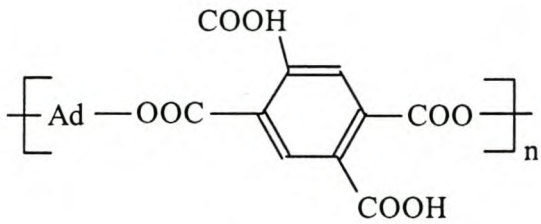

Ad = adamantane

[2–19]

Adamantane-containing polyesters have fairly high T_g's and softening temperatures. They are also highly resistant to thermal and oxidative degradation and exhibit an effective hydrolytic stability.

Both linear and cross-linked polyesters are highly resistant to the action of ultraviolet light and sunlight. These properties make adamatane-containing polyesters useful as protective coatings and packing materials.

Bisphenols derived from adamantane have been used in the synthesis of polycarbonates and copolycarbonates. Bisphenols containing the adamantane nucleus in the form of a cardo-group have also been proposed for the synthesis of polycarbonates. Depending on the method of preparation (low temperature or interfacial polycondensation), these polycarbonates have crystalline or amorphous structures.

2.8.3 Adamantane-Containing Polyamides

Polyamides are some of the first polymers for which the effectiveness of the introduction of adamantane nuclei into polymer chains was demonstrated[68]. Adamantane-containing polyamides, obtained in the melt (like nylon-6,6) from a salt of 1,3-diaminoadamantane and sebacic acid or a salt of adamantanedicarboxylic acid and 1,4-bis(aminomethyl)-cyclohexane, have low molecular weights. High-molecular-weight polyamides have the following general formula:

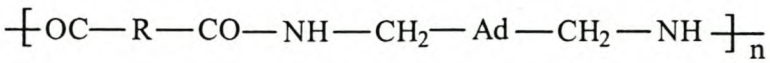

Ad = adamantane

[2–20]

Among adamantane-containing polyamides, poly(*m*-phenyleneadamantylene-1,3-dicarboxamide) - the product of the condensation of *m*-phenylenediamine with the chloride of adamantane-1,3-dicarboxylic acid – is of great interest[61].

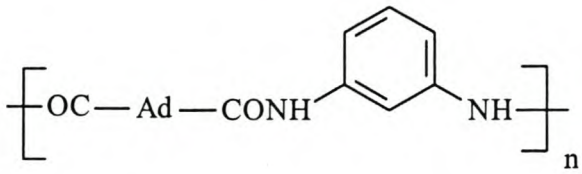

Ad = adamantane

[2–21]

A fibre can be obtained from a solution of this polyamide in DMF by the wet moulding method. An interesting feature of poly(*m*-phenyleneadamantylene-1,3-dicarboxamide) is that both the polyamide itself and the fibre obtained from it are amorphous and, in contrast to many polymers, the fibre does not crystallize when kept at temperatures in the range between the T_g and yield points. The polyamide softens at 294 °C and loses not more than 0.86 % of its weight when kept in air for two hours at 325 °C.

2.8.4 Adamantane-Containing Polyurethanes

Adamantane-containing polyurethanes can be obtained by the reaction of 1,3-adamantylene di-isocyanate or 1,3-di-isocyanato-5,7-dimethyladamantane with polyols. Polyols are usually polyalkylene or polyoxyalkelene glycols, polyester glycols, castor oil, and sorbitol polyesters[69]. The replacement of 1,3-adamantylene di-isocyanate by 1,3-bis(isocyanatomethyl)adamantane

makes it possible to obtain light-resistant polyurethanes with a higher elasticity. An increase in light resistance is also observed for cross-linked polyurethanes.

Another advantage of adamantane-containing polyurethanes is their increased hydrolytic stability[61]. This effect is particularly notable when the adamantylene group is attached to an ester group, i.e. for polyurethanes obtained from adamantane-containing oligoester-glycols. The films obtained from such a polyurethane do not change much over a period of three months in 5 % H_2SO_4 and NaOH solutions. They only swell by 3 %, while similar polyurethanes derived from aliphatic oligoester-glycols decompose after 20–25 days.

2.8.5 Epoxy Resins based on Adamantane Derivatives

Adamantane-containing epoxides have been obtained by the oxidation of the corresponding alkenyladamantanes[70, 71].

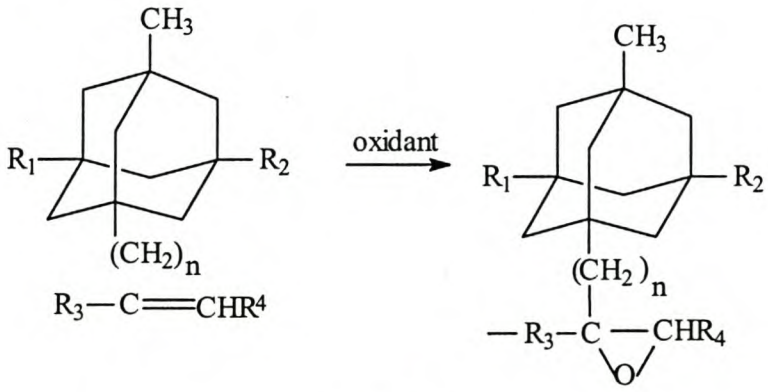

Eq 2-6

The oxidants are organic and inorganic peroxides, hydroperoxides, and hydrogen peroxide.

The hardened epoxy-resins (based on the bisphenols derived from adamantane, 1,1'-biadamantane, and isopropylidene) are superior to the polyepoxide with the isopropylidene groups as regards heat resistance and thermal stability. The softening temperatures of these resins are 250 °C and 220 °C compared with 180 °C for the polyepoxide based on isopropylidenebisphenol, while the

temperature of the onset of weight loss is 390 °C against 340 °C. In addition, they decompose at 400 °C, leaving a larger amount of carbon residue than the corresponding polyepoxides without adamantane rings.

2.8.6 Cyclochain Polymers of Adamantane

Among the cyclochain polymers with adamantane fragments in the main chain, polyimides have been most thoroughly investigated[61]. A distinctive feature of adamantane-containing polyimides is their high resistance to hydrolysis and the action of organic solvents and certain chemicals. A film made of the polyimide based on 1,3-bis(3',4'-dicarboxyphenyl)adamantane and di(4-aminophenyl)ether loses not more than 14 % of its initial strength after a five day exposure to a 10 % solution of NaOH and does not dissolve in concentrated H_2SO_4. On the other hand, the polyimide film based on pyromellitic dianhydride decomposed under analogous conditions.

A polybenzimidazole was synthesized from the diphenyl ester of adamantanedicarboxylic acid and 3,3'-diaminobenzimidine.

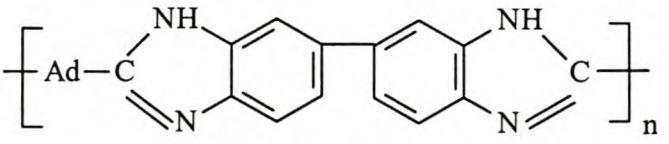

Ad = adamantane

[2–22]

The polymer has a low molecular weight and is soluble in DMF and dimethyl sulphoxide (DMSO), but its thermal stability is lower that that of aromatic polybenzimidazoles; it begins to decompose in nitrogen at 540 °C.

2.8.7 Biologically Active Adamantane-Containing Polymers

Progress in the chemistry of adamantane is to a large extent associated with the biological activity of some of its functional derivatives[72]. However, only a few studies have been made on the polymeric adamantane derivatives used in medicine. The copolymers of *N*-vinylpyrrolidinone and *N*-allylaminodamantane as well as the reduced products of the interaction of 1-aminoadamantane and the copolymer of *N*-vinylpyrrolidinone and crotonaldehyde, have been proposed as potential antiviral agents.

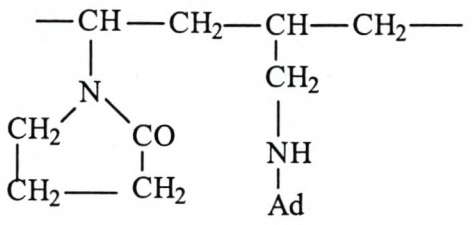

[2–23]

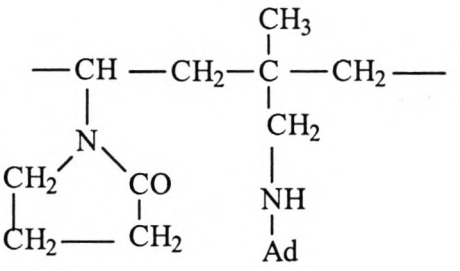

[2–24]

2.8.8 Star Polymers

Aramids are high performance, rigid rod materials, such as Kevlar and Nomex[7]. Benzoxazoles are even more rigid materials and are noted for their excellent thermooxidative stability and chemical resistance[73]. Both types of polymers are processed from lyotropic solutions into fibres or films which exhibit high moduli and tensile strengths due to the high degrees of chain orientation. The use of adamantane as a rigid core enforces a tetrahedral arrangement of the aramid and benzoxazole arms. These star polymers exhibit comparable thermal stability to and decreased viscosity compared to the linear polymer. The aramids are interesting in that they do not behave as rigid rods in solution and are more soluble than linear aramids of comparable molecular weight[74].

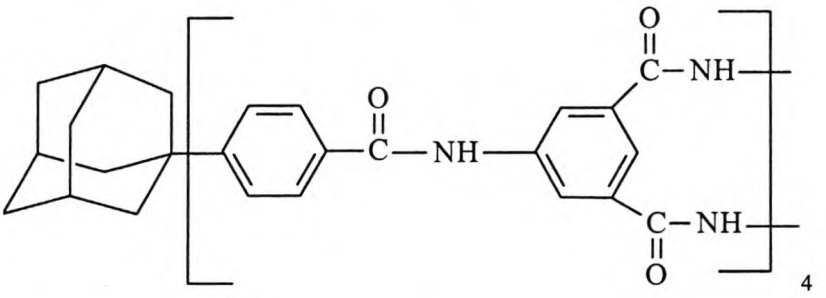

Hyperbranched aramid (adamantane core)

[2–25]

The hyperbranched aramid was partially soluble in DMSO and amide solvents such as DMF[7]. Solution and solid-state NMR spectroscopy were used to confirm the product structure. Residual solvent peaks were observed in the solid-state NMR spectra, even after extensive extraction and vacuum drying. It appears that hyperbranched structures and adamantane incorporation disrupts crystalline packing and leads to a more open and molecularly-porous branched structure that is capable of taking up and holding solvent. Thermal analysis by DSC showed no transitions below 500 °C, although gradual changes in the base line occurred above 310 and 340 °C, corresponding to the onset of weight loss as

seen in the TGA scans. Thermal decomposition began ca 80 °C lower and was more rapid above 350 °C than for linear and star-branched polymers.

It appears that the adamantane core may enhance solubility which promotes the formation of high molecular weight polymers without sacrificing thermal stability. However, in the case of highly branched aramids, the presence of adamantane units as defects to prevent close packing did not maintain solubility (probably due to crosslinking) and actually resulted in a decrease in the thermal stability of the polymer obtained.

2.8.9 Three Dimensional Hydrocarbon Networks

Much research has been carried out on the formation of all–hydrocarbon materials[7]. The latter have the following advantages over hetroatom-containing materials: long-term thermal and environmental stability, low dielectric constants, and low water absorption. Furthermore, the strong carbon-carbon bonds should lead to improved moduli, strength and toughness. Adamantane is an ideal choice for use in such materials in that it is all hydrocarbon and its tetrahedral geometry allows for the growth of hydrocarbon moieties in three dimensions.

Adamantane has been functionalized with terminal acetylene to form [2-26], phenylacetylene and diphenylacetylene groups.

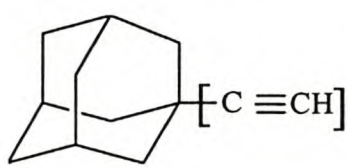

[2–26]

[2 – 26] is an example of adamantane with acetylene groups directly attached[75]. Complete cure was accomplished by heating to above 320 °C. The onset of decomposition for the cured material was 475 °C in helium. Thermal polymerization gave a complex mixture of oligomers with number-average

molecular weights ranging from 184 to 10 000 g.mol^{-1}, as measured by reverse phase HPLC. ^{13}C NMR spectra revealed the formation of a linear polyene structure containing adamantane with terminal acetylene groups.

2.8.10 Polymers with Adamantyl Pendant Groups

The bulky rigid structure of adamantane greatly increases T_g's of adamantane-containing polymers when incorporated as a pendant group into polymer backbones[7]. Generally, the attachment of a large group pendant from a polymer should reduce chain mobility and raise T_g. In the case of adamantane-containing polymers, it was found that the adamantyl moiety had a much larger effect than expected. Adamantane also maintains thermooxidative stability because, unlike a typical linkage to a tertiary carbon (for example a *t*-butyl ester), elimination cannot easily occur at the bridgehead position which is the point of attachment. A series of chain-growth polymers based on ester derivatives of ethyl α-hydroxymethylacrylate were synthesized to illustrate the adamantyl effect.

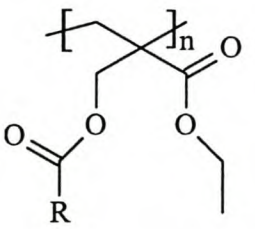

R = H, CH_3, C_6H_5, *t*-butyl, adamantyl

[2–27]

Several new monomers with pendant adamantyl groups were used in step-growth polymerizations. The monomers were synthesized by alkylating phenolics and halobenzenes with 1-bromoadamantane. 4-(1-adamantyl)phenol was obtained by simply heating 1-bromoadamantane in phenol[8]. The monomer, together with formaldehyde and acid catalyst, were used in the step-growth polymerization of monomers with adamantyl pendant groups to novolacs.

Novolacs are thermoplastic resins with molecular weights of up to 2 000 and T_g's of 45–70 °C[7]. These polymers had number-average molecular weights of ca 3 000. The T_g's observed by DSC ranged from 175–230 °C, compared to 45-70 °C for the unsubstituted analogs. The polymers exhibited a 10 % weight loss at 400 °C in nitrogen, as measured by TGA.

Another pendant adamantyl, step-growth polymer which had a significantly increased T_g was synthesized from adamantyl-substituted resorcinol and 4,4'-difluorobenzophenone to form a poly(ether ether ketone) (PEEK). The polymer had a T_g of 235 °C, 115 °C higher than that of the unsubstituted analog. The polymer was readily soluble in common organic solvents and exhibited a 5 % weight loss at > 490 °C. Films cast from 100 % adamantyl-substituted resorcinol were transparent and strong, but brittle. Films melt-pressed with copolymers containing 50 % adamantyl-substituted resorcinol were transparent, tough and flexible. A polyphenylene was formed by the step-growth polymerization of aryl halides and a $NiCl_2$/Zn/triphenylphosphine system. The polymer was soluble in chloroform and THF and had a number-average molecular weight of only 2 000. No thermal transitions were observed before the onset of decompositions at 350 °C.

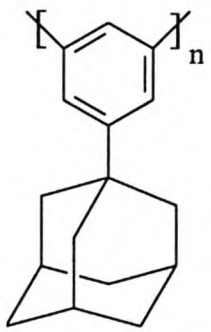

Adamantyl-substituted poly(phenylene)

[2–28]

2.9 *THERMALLY STABLE HYDROCARBON POLYMERS CONTAINING ADAMANTANE GROUPS*[76]

Only a few examples of wholly hydrocarbon polymers based on adamantane are known. Polymerization of 1–vinyladamantane with Friedel–Crafts catalysts or the reaction of adamantane with benzene yielded only low molecular weight oligomers, whereas, Wurtz–type coupling of dibromoadamantane derivatives gave crystalline polymer (polyadamantane that melted above 420 °C)[77, 78]. The metathesis reaction of 1-ethynyladamantane with molybdenum or tungsten salts yielded amorphous, insoluble powders, which decomposed at 200 °C in air and 240 °C in nitrogen[79]. In the absence of catalyst, 1-ethynyladamantane does not polymerize[80]. The polymerization of 1-ethynyladamantane and 1,3-diethynyladamantane is discussed a little more completely in the next two Sections.

2.9.1 Polymerization Reactions with 1-Ethynyladamantane [2-29] [79]

Polymerization of **[2-29]** by $MoCl_5$ and WCl_6 in toluene provided polymers in 100 % yields[79]. The $Mo(CO)_6^-$ and $W(CO)_6^-$ based catalysts also effected the polymerization. Ziegler catalysts were incapable of polymerizing this monomer. The polymerization of **[2-29]** by $MoCl_5$ and WCl_6 proceeded in high yields in hydrocarbons and halogenated hydrocarbon solvents. Polymers formed were completely insoluble. Polymers obtained at high temperature or at low monomer concentration were also insoluble.

[2-29] remained unchanged after it was heated to 250 °C for 24 hours and it partially decomposed after several days of heating above 300 °C[76]. Although **[2-29]** did not form a homopolymer, it copolymerized with 1,3-diethynyladamantane **[2-30]**, *tert*-butylacetylene and 1-decyne[76, 78].

Copolymers containing 10–47 % by weight of **[2-29]** were prepared by step-curing mixtures of **[2-30]** and **[2-29]** to 320 °C[76]. Complete incorporation of **[2-29]** into the polymer matrix was used. However, at concentrations exceeding

50 % by weight of **[2-29]**, incorporation of **[2-29]** into the polymer matrix was not observed and unreacted monomer **[2-29]** was recovered. Cooligomers were prepared by heating **[2-29]** and **[2-30]** at 210 °C for 24 hours. The rate of cooligomerization was slower than that observed for the homooligomerization of **[2-30]**, but the incorporation of the monoacetylene into the oligomer corresponded to the starting monomer ratio.

2.9.2 Polymerization Reactions with 1,3-Diethynyladamantane [2-30] [76]

In contrast to adamantane and most disubstituted adamantane derivatives, 1,3-diethynyladamantane **[2-30]** is a relatively low melting solid (mp. 46 °C)[76]. When heated to temperatures above 200 °C, **[2-30]** became a clear, brown, void-free polymeric resin and at 210 °C gelation occurred in 24–50 hours. Freshly gelled samples containing 40-45 % unreacted monomer, were step-cured by incremental temperature increases to 320 °C. Samples heated at 250 °C for several days were incompletely cured, as indicated by DSC exotherms above 300 °C. When samples that were heated above 320 °C were cooled and rescanned, no DSC transitions were observed. The fully cured sample exhibited an onset of major degradation (TGA) at 476 °C in air and 475 °C in helium. Isothermal ageing studies were conducted on 10–15 mg samples of the polymer in air. At 315 °C, the adamantane–containing polymer lost 8 % of its weight after 100 hours and was more stable than the polymer prepared from the aromatic diethynyl 4,4'-bis(3-ethynylphenoxy)diphenyl sulfone, which lost 12 % of its weight after a similar period[81]. Weight losses of 5 % and 20 % were observed for the adamantane polymer at 301 and 325 °C after 100 hours in air[76]. Although no thermal transitions were observed in the DSC between 25 and 450 °C, poly(1,3-diethynyladamantane) exhibited a glass transition temperature near 260 °C. The density of the polymer was 1.08g/cm^3, similar to that of the parent hydrocarbon, adamantane (1.09g/cm^3). The relatively high density of the polymer, as compared to conventional aliphatic hydrocarbon polymers (d < 1.0g/cm^3), suggests that the adamantane ring

remained intact during polymerization. The polymer showed no measurable weight gain in water or 10 % aqueous HCl at room temperature over several weeks. The equilibrium weight gain in water at 71 °C after 30 days was 0.7 %. The polymer was insoluble in organic solvents such as hexane and ethanol, but was swelled slightly by ethyl acetate and showed an equilibrium weight gain of 1.4 % in DMF and 0.5 % in DMSO at 20 °C.

The temperature required to initiate polymerization of **[2-30]** was reduced to below 200 °C by the use of certain catalysts. Azobis(isobutyronitrile) (AIBN) and benzoyl peroxide (BPO) lowered the onset temperature of polymerization to 185 °C.

2.10 REFERENCES

1. Rodriques F., *Principles of Polymer Systems*, McGraw-Hill, Inc., 1970, 38.

2. Gibbs J.H., *J. Chem. Phys.*, 1956, **25**, 185.

3. Gibbs J.H., DiMarzio E.A., *J. Chem. Phys.*, 1958, **28**, 373.

4. DiMarzio E.A., Gibbs J.H., *J. Chem. Phys.*, 1958, **28**, 807.

5. Fort R.C., Jr., *Adamantane: The Chemistry of Diamond Molecules*, Grassman P.G., Ed., Studies in Organic Chemistry, Vol. 5, Marcel Dekker: New York, 1976.

6. Reichert V.R., PhD Dissertation, University of Southern Mississippi, 1994.

7. Mathias L.J., Jensen J.J., Reichert V.R., Lewis C.M., Tullos G.L., *Step-Growth Polymers for High Performance Materials*, Chapter 11, 1996.

8. Mathias L.J., Jensen J.J., Grimsley M., *J. of Polym. Sci.: Part A: Polym. Chem.*, 1996, **34**, 397.

9. Nowacki W., *Helv. Chim. Acta*, 1945, **28**, 1 233.

10. Nowacki W., Hedberg K.W., *J. Am. Chem. Soc.*, 1948, **70**, 1 497.

11. Alden R.A., Kraut J., Taylor T.G., *J. Phys. Chem.*, 1967, **71**, 2 379.

12. Alden R.A., Kraut J., Taylor T.G., *J. Am. Chem. Soc.*, 1968, **90**, 74.

13. Chadwick D., Legon A.C., Millen D.J., *J. Chem. Soc. A*, 1968, 1 116.

14. Lee C.M., Dlardy J.C., *Chem. Comm.*, 1970, 716.

15. Hargittai I., Hedberg K.W., *Chem. Comm.*, 1971, 1 499.

16. Karle I.L., Karle J., *J. Am. Chem. Soc.*, 1965, **87**, 919.

17. Carrel H.L., Donohue J., *Tetrahedron Lett.*, 1969, 3 503.

18. Vogl, O., Anderson B.C., Simons D.M., *Tetrahedron Lett.*, 1966, 415.

19. Fort R.C., Jr., Scheleyer P. Von R., *Chem. Rev.*, 1964, **64**, 277.

20. Schleyer P. Von R., Williams J.E., Blanchard K.R., *J. Am. Chem. Soc.*, 1970, **92**, 2 377.

21. Mislow K., *Introduction to Stereochemistry*, Benjamin, Inc., New York, 1965, 10–13.

22. Lide D.R., Jr., *J. Chem. Phys.*, 1960, **33**, 1 514.

23. Bonham R.A., Bartell L.S., *J. Am. Chem. Soc.*, 1959, **81**, 3 491.

24. Ukaji T., Bonham R.A., *J. Am. Chem. Soc.*, 1962, **84**, 3 627.

25. Lide D.R., Jr., *J. Chem. Phys.*, 1960, **33**, 1 519.

26. Atkinson V.A., *Acta Chem. Scand.*, 1961, **15**, 559.

27. Johnston D.E., McKervey M.A., Rooney J.J., *Chem. Comm.*, 1972, 29.

28. McKervey M.A., Johnston D.E., Rooney J.J., *Tetrahedron Lett.*, 1972, 1 547.

29. Mair B.J., Shamaiengar M., Krouskop N.C., Rossini F.D., *Anal. Chem.*, 1959, **31**, 2 082.

30. Sohar P., Zubovics Z., Varsanyi G., *Chem. Abstr.*, 1970, **72**, 16 944h.

31. Warren R.W., Scheneider A., Jankowski E.J., *Appl. Spect.*, 1968, **22**, 115.

32. Fort R.C., Jr., Schleyer P. von R., *J. Org. Chem.*, 1965, **30**, 789.

33. Liggero S.H., Schleyer P. von R., Ramey K.C., *Spectros. Lett.*, 1969, **2**, 197.

34. Karplus M., *J. Chem. Phys.*, 1959, **30**, 11.

35. Sternhell S., *Rev. Pure Appl. Chem.*, 1964, **14**, 15.

36. Garbisch E., *J. Am. Chem. Soc.*, 1964, **84**, 5 561.

37. Fort R.C., Jr., Lindstrom T.R., *Tetrahedron*, 1967, **23**, 3 227.

38. Greidanus J.W., *Can. J. Chem.*, 1970, **48**, 3 530.

39. Briggs W.S., Suchy M., Djerassi C., *Tetrahedron Lett.*, 1968, 1 097.

40. Snatzke G., Ehrig B., Klein H., *Tetrahedron*, 1969, **25**, 5 601.

41. Westrum E.F., Jr., *J. Chem. Ed.*, 1962, **39**, 443.

42. Chang S.–S., Westrum E.F., Jr., *J. Phys. Chem.*, 1960, **64**, 1 547.

43. Westrum E.F., Jr., *Phys. Chem. Solids*, 1961, **18**, 83.

44. Wu P.– J., Hsu L., Dows D.A., *J. Chem. Phys.*, 1971, **54**, 2 714.

45. Nordman C.E., Schmitkons D.L., *Acta Cryst.*, 1965, **18**, 764.

46. Ito T., *Acta Cryst.*, 1973, **B29**, 364.

47. Mirskaya K.V., *Chem. Abstr.*, 1963, **59**, 1 157h.

48. Pistorius C.W.F.T., Snyman H.C., *Z. Physik Chem.*, 1964, **43**, 278.

49. Pistorius C.W.F.T., Resing H.A., *Mol. Cryst. Liq. Cryst.*, 1969, **5**, 353.

50. Clark T., Johnston D.E., Mackle H., McKervey M.A., Rooney J.J., *Chem. Comm.*, 1972, 1 042.

51. Wood D.E., Lloyd R.V., *J. Chem. Phys.*, 1970, **52**, 3 840.

52. Wood D.E., Lloyd R.V., *J. Chem. Phys.*, 1970, **53**, 3 932.

53. McIntosh A.R., Gee D.R., Wan J.K.S., *Spectros. Lett.*, 1971, **4**, 217.

54. Wolodaarsky W.H., Wan J.K.S., *Can. J. Chem.*, 1972, **50**, 1 096.

55. Lloyd R.V., Rogers M.T., *J. Am. Chem. Soc.*, 1973, **95**, 2 459.

56. Mazheika I.B., Yankovskaya I.S., Polis Ya. Yu., *J. Gen. Chem.*, 1970, **41**, 1 640.

57. McKervey M.A., *Chem. Soc. Rev.*, 1974, **3**, 479.

58. Schneider A., Warren R.W., Janaski E.J., *J. Am. Chem. Soc.*, 1964, **86**, 5365.

59. Schneider A., Warren R.W., Janaski E.J., *J. Org. Chem.*, 1966, **31**, 1 617.

60. Landa S., Podurouzkova B., Vanek J., *Chem. Abstr.*, 1972, **76**, 140 029k.

61. Khaardin A.P., Radchenko S.S., *Russ. Chem. Rev.*, 1982, **51**, 272.

62. Storesund H.I., *Tetrahedron Lett.*, 1972, 3 911.

63. Zosim L.A., Dovgan N.A., Yurchenko A.G., *USSR Patent*, 1976, 521 951.

64. Duling I.N., Schneider A., Moore R.E., *Chem. Abstr.*, 1969, **71**, 125 245.

65. Duling I.N., Schneider A., Moore R.E., *US Patent*, 1972, 3 639 362.

66. Duling I.N., *US Patent*, 1970, 3 533 947.

67. Stetter H., Gartnet J., Tacke P., *Angew. Chem.*, 1965, B77 171.

68. Elmore L.M., *US Patent*, 1965, 3 301 827.

69. Moore R.E., *US Patent*, 1972, 3 646 095.

70. Borchert A.E., Capaldi E.C., *US Patent*, 1970, 3 536 732.

71. Borchert A.E., Capaldi E.C., *US Patent*, 1972, 3 676 375.

72. Daves W.I., Grunert R.R., Hoff R.E., McGahen I.W., Neumeyer E.M., Paulshock M., Watts J.C., Wood T.R., Hermann E.C., Hoffman C.E., *Science*, 1964, **144**, 862.

73. Dotrong M., Dotrong M.H., Moore G.J., Evers R.C., *Polym. Prepr. (Am. Chem. Soc. Div. Polym. Sci.)*, 1994, **35(2)**, 673.

74. Mathias L.J., Reichert V.R., *Macromolecules*, 1994, **27**, 703.

75. Archibald T.G., Malik A.A., Baum K., *Macromolecules*, 1991, **24**, 5 261.

76. Archibald T.G., Malik A.A., Baum K., *Macromolecules*, 1991, **24**, 5 261.

77. Reinhardt H.F., *J. Polym. Sci., Polym. Lett. Ed*, 1964, **2**, 567.

78. Storesund H.J., *Tetrahedron Lett.*, 1971, 3 911.

79. Okano Y., Masuda T., Higashimura T., *J. Polym. Sci., Polym. Chem. Ed.*, 1985, 23, 2 527.

80. Brown R.F.C., Eastwood F.W., Jackman G.P., *Aust. J. Chem.*, 1977, **30**, 1 757.

81. Loughran G.A., Arnold F.E., *Polym. Prepr. (Am. Chem. Soc. Div. Polym. Chem.)*, 1980, **21** (1), 199.

CHAPTER 3

THE SYNTHESIS OF 3-(1-ADAMANTYL)-1-PROPENE

In this Chapter, the different approaches as well as the difficulties involved in the synthesis of 3-(1-adamantyl)-1-propene are discussed. 3-(1-Adamantyl)-1-propene was used as monomer in a series of polymerizations with α-olefins using different metallocene catalyst systems (discussed in Chapter four). The effect of the incorporation of the adamantane monomer on the physical and thermal properties of the polymers was also investigated (discussed in Chapter four).

3.1 INTRODUCTION

The preparation of 3-(1-adamantyl)-1-propene or allyl adamantane comprises, in effect, the allylation of adamantane. Radical allylations are of the mildest, most general methods used to introduce allyl groups into functionalized molecules. A schematic representation of radical allylation is given in Scheme 3-1. Early reagents used for the allylations of halides and phenyl selenides were based on the chemistry of the trialkyltin radical (allyl stannanes, allyl phenyl sulfides/Bu_3SnBu_3), and they transferred allyl groups or 2–carbon substituted allyl groups[1]. 2–Heteroatom substituted (Cl, Si, NO_2, SO_2) radical allylating reagents were often introduced to control the oxidation level at C_2. 2–Heteroatom substituted allylating reagents should be especially useful because the residual heteroatoms could later be used to promote ionic or radical carbon–carbon bond formation.

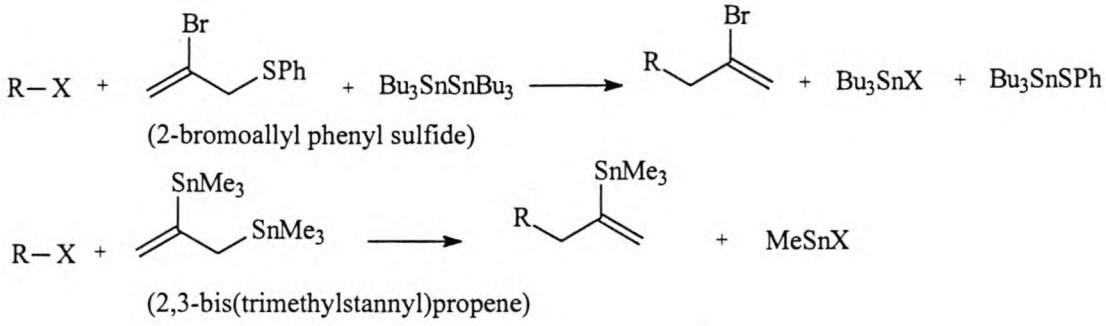

Scheme 3–1: Radical Allylations Based on the Chemistry of the Trialkyltin Radical

3.2 THE PREPARATION OF 3-(1-ADAMANTYL)-1-PROPENE

3.2.1 The Preparation of 3-(1-Adamantyl)-1-Propene by the Method of Capaldi and Borchert[2]

The process involves contacting an adamantyl halide in the presence of a Friedel-Crafts type catalyst with substituted allylhalides and olefins, producing materials consisting of adamantyl dihaloalkanes and adamantyl haloalkanes, respectively. Thereafter, the adamantyl dihaloalkane is subjected to dehalogenation and the adamantyl haloalkane to dehydrohalogenation, and the corresponding alkenyladamantanes are formed (see Scheme 3-2). The alkenyl substituted compounds are useful in the preparation of polymers with high thermal stability.

In essence, one of the more successful methods described in this patent is, as a first step, the reaction of 1-adamantyl bromide (X = Br in Scheme 3-2) with allyl bromide in the presence of $AlCl_3$ using CS_2 as solvent. This reaction is typically carried out at low temperatures (-70°C to –35°C) and gives the intermediate 1,2 dibromo-3-adamantyl propane in good yield. In the second step, this intermediate is then dehalogenated by refluxing with zinc dust in ethanol.

The first step can be carried out with a variety of Friedel-Crafts-type catalysts as well as boron trifluoride catalysts of the Friedel-Crafts type. Aside from $AlCl_3$, the patent illustrates the use of, inter alia, $FeCl_3$ and $SbCl_4$ as catalysts.

Other than CS_2, hydrocarbons like hexane and pentane were also found to be suitable solvents for this step.

In the second step, the dehalogenation reaction can be catalyzed by bivalent metals other than zinc, for example magnesium.

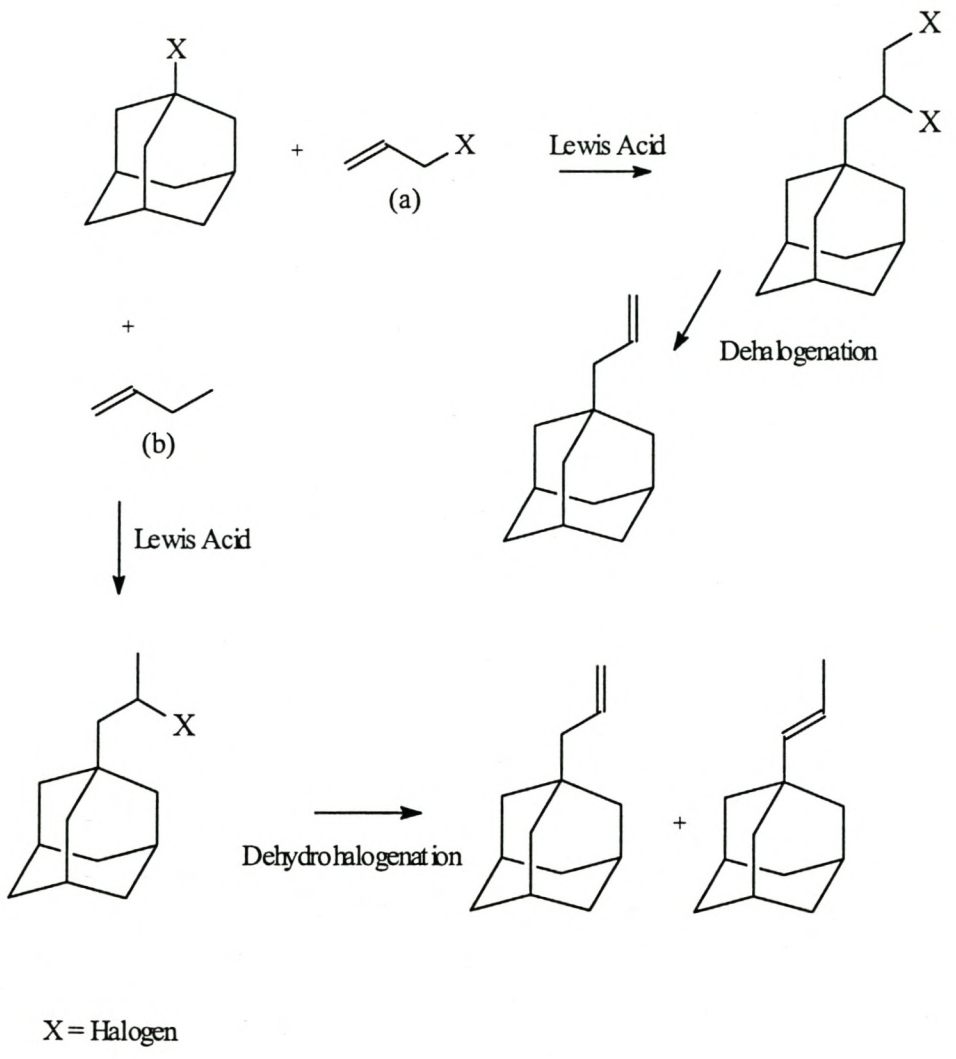

X = Halogen

Scheme 3–2: Reaction of a Haloadamantane with (a) an Allyl Halide and (b) an Olefin

3.2.2 The Substitution Reaction of 1-Adamantyl Chloride with Trimethylsilylated Unsaturated Compounds

The method for the preparation of 3-(1-adamantyl)-1-propene described by Sasaki *et al* [3] involves the reaction of chloroadamantane with allyltrimethylsilane in CH_2Cl_2 using $TiCl_4$ as catalyst. For the mode of reaction, there are three possibilities, depending on the attack site of the adamantyl group in the first step.

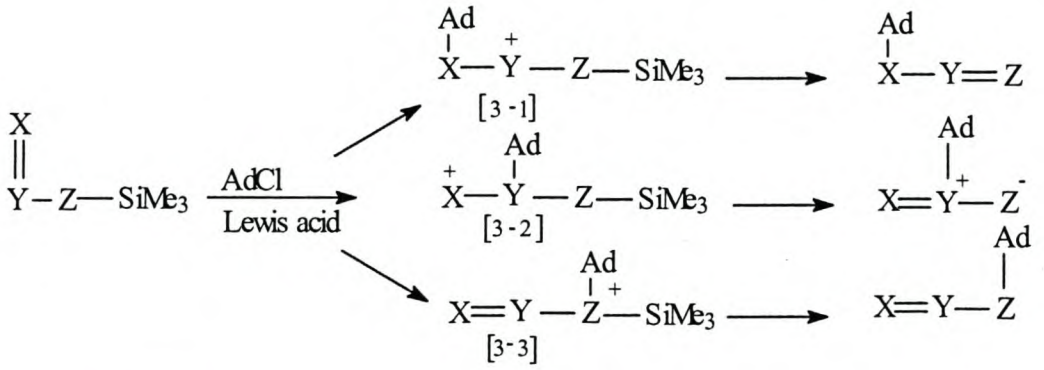

Ad = adamantane

Scheme 3–3: Three Possibilities for the Attack of the Adamantyl Group

The intermediate **[3-1]** is stabilized by σ-π conjugation between the Si–C bond and the vacant π orbital. In the second step, desilylation gives rise to adamantane–substituted products (Scheme 3-3).

A typical example of such a substitution reaction is the case where the X, Y and Z atoms are all carbon; 1-adamantyl chloride is reported to react smoothly with allyltrimethylsilane **[3–4]** at room temperature in the presence of titanium tetrachloride to give 3-(1-adamantyl)-1-propene in 85 % yield. This reactivity implies that the adamantyl cation, accordingly a tertiary cation, is also a reactive species with **[3-4]** in addition to known electrophiles like acyl, sulfenyl, alkoxycarbonium, and bromonium cations.

3.2.3 Atom–Transfer Reactions of Alkyl–Substituted Radicals

In the method described by Thoma *et al* [4], 3-(1-adamantyl)-1-propene was prepared by treating a refluxing solution of 1-adamantyl bromide and allyltributyl tin in benzene with a solution of azobis(isobutyronitrile) (AIBN) in benzene (Scheme 3-4). After work-up the method was reported to give 3-(1adamantyl)-1-propene in a 57% yield.

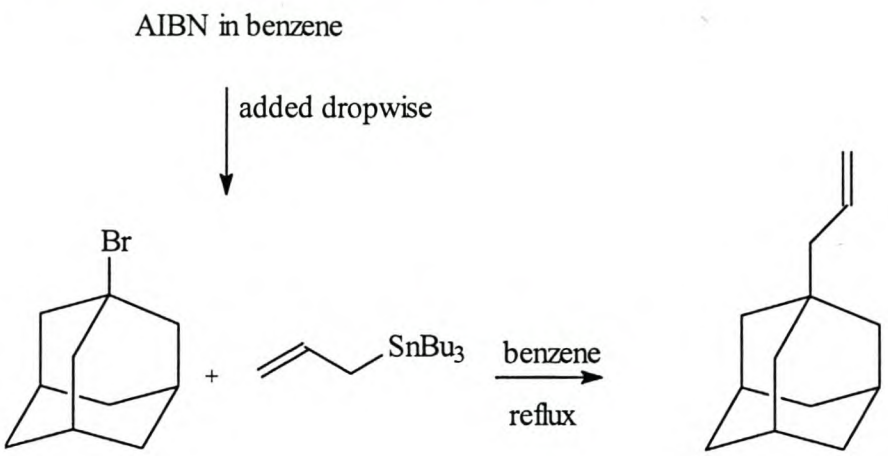

Scheme 3–4: Preparation of 3-(1-Adamantyl)-1-Propene Using the Method Described by Thoma *et al*

3.2.4 Preparation of Bridgehead Alkyl Derivatives by Grignard Coupling

The approach of using standard methods for preparing bridgehead allyl derivatives by Grignard coupling seemed a useful way to tackle the synthesis of 3-(1-adamantyl)-1propene (Scheme3-5).

Osawa *et al* [5] reported on a simple, high yield method by which to convert adamantane–type bridgehead bromides to the corresponding alkyl derivatives. In particular, treatment of 1-bromoadamantane with an excess of CH_3MgBr in ether yielded 1-methyladamantane in 83 % yield. Furthermore, it was reported that stirring a two-phase mixture of 1–bromoadamantane and magnesium actually decreased the yield of Grignard reagent required, as opposed to allowing the two–phase mixture to stand without stirring[6]. This is another example where the chemistry at the bridgehead polycyclic bridged ring systems is much 'cleaner', due to the inhibition of competing reactions.

Ordinary *tert*–halides give elimination by-products with Grignard reagents; elimination is not possible with adamantane and the other bridged ring systems studied; and yields of coupling products were enhanced as the result.

However, when alkyl groups rather than methyl were introduced, yields were reported to be less than for methyl, and adamantane is formed, in considerable amounts, as a byproduct.

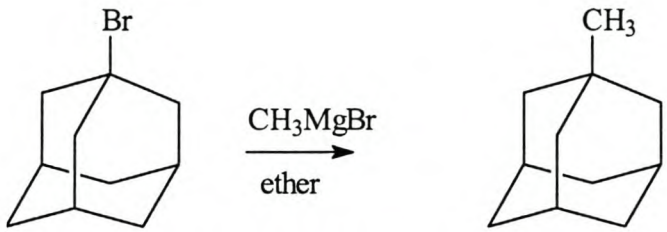

Scheme 3–5: Preparation of 1-Methyl-Adamantane by Grignard Coupling

3.3 EXPERIMENTAL APPROACHES FOR THE SYNTHESIS AND CHARACTERIZATION OF 3-(1-ADAMANTYL)-1-PROPENE

In this Section, the different methods as well as the difficulties involved in the preparation of 3-(1-adamantyl)-1-propene are discussed. The analyses of the monomer is discussed in detail in this Section. Scheme 3–6 is a summary of the three approaches which were followed to synthesize 3-(1-adamantyl)-1-propene.

Based on the available literature, the methods of Capaldi and Borchert[2], Sasaki *et al* [3] and a modified approach of Osawa *et al* [5] were evaluated. The method of Thoma *et al* [4] (90 %) was abandoned after very low yields were initially obtained.

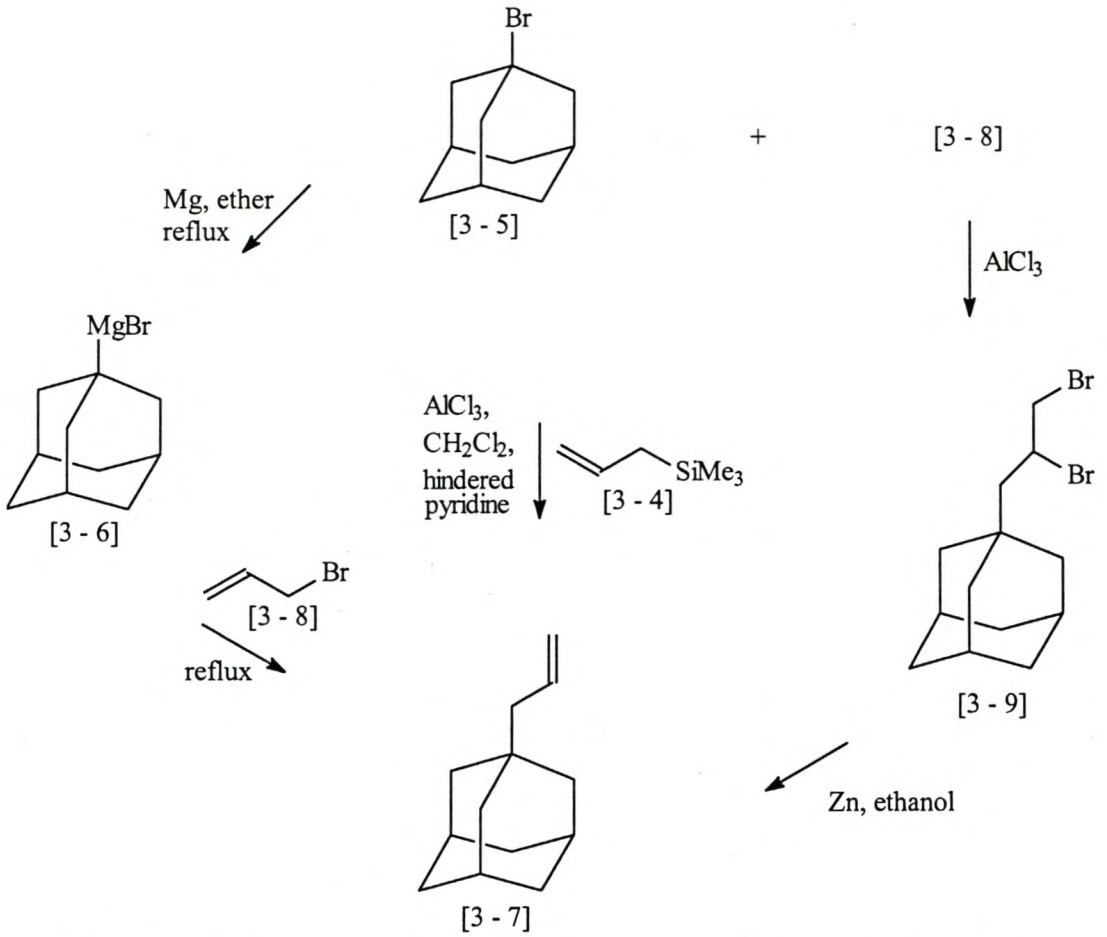

Scheme 3–6: Summary of the Three Approaches Followed to Synthesize 3-(1-Adamantyl)-1-Propene

3.4 EXPERIMENTAL

3.4.1 Materials and Methods

All experiments involving air- and moisture sensitive compounds were conducted in a nitrogen atmosphere, either by using standard Schlenk techniques or working in a Plas Labs dry box. Glassware was dried overnight at 120 °C before use, assembled hot and cooled in a nitrogen atmosphere.

3.4.1.1 Reagents

All the chemicals used were obtained from Aldrich except for the magnesium turnings, dichloromethane, carbon disulphide, ethanol, zinc powder and diethyl ether which were obtained from Saarchem.

Solvents were thoroughly dried under nitrogen before use, except for ethanol which was used as received.

Carbon Disulphide

Carbon disulphide (500 mL) was placed under a nitrogen atmosphere and purged with nitrogen before use.

Diethyl Ether

Because of the moisture sensitivity of the magnesium turnings used in the Grignard reactions, the ether had to be carefully dried. Diethyl ether (500 mL) was boiled under reflux[7] over 0.5 g of lithium aluminium hydride ($LiAlH_4$) for 30 minutes and then distilled onto 4 Å molecular sieve.

Dichloromethane

Because of the moisture sensitivity of the trimethylsilylated compound and the hindered pyridine, dichloromethane had to be carefully dried. Dichloromethane (500 mL) was dried overnight on P_2O_5 and then distilled onto 4 Å molecular sieve.

3.4.2 Equipment

Apparatus for the preparation of **adamantyl magnesium bromide [3–6]** comprised a 50 mL round bottom flask and a condenser.

Apparatus for the preparation of **3-(1-adamantyl)-1-propene [3–7]** comprised a 50 mL two-neck round bottom flask, condenser, dropping funnel, glass wool, disposable syringe, rubber septum, nitrogen inlet and a separating funnel.

Apparatus for the preparation of **1,2-dibromo-3-adamantyl propane [3–9]** comprised a 50 mL two-neck round bottom flask, condenser, dropping funnel and a separating funnel.

3.4.3 Laboratory Safety

The standard safety procedures for the preparation of a Grignard reagent were taken into account during the synthesis of **[3–6]**. High reactivity of the

magnesium with water could easily cause an explosion. Care had to be taken to exclude all moisture when drying the diethyl ether.

3.4.4 Analytical Methods and Instrumentation

3.4.4.1 Differential Scanning Calorimetry (DSC) and Thermogravimetric Analysis (TGA)

TGA analyses were performed using a SDT simultaneous DTA-TGA (TA Instruments) at a heating rate of 20 °C/min. Glass transition and melting temperatures were obtained using a DSC 2 920 Differential Scanning Calorimeter (TA Instruments) at a heating rate of 10 °C/min. Samples of the polymers (8-10 mg) were heated in aluminium pans under a nitrogen atmosphere at a rate of 20 °C/min from ambient temperature to 300 °C during the TGA experiments.

3.4.4.2 Infrared Spectroscopy (IR)

The IR spectra of the homo- and copolymers were recorded on a Perkin Elmer 1 600 Infrared Fourier Transform spectrometer (FTIR). The IR spectra of the polymers were recorded by means of a photo-acoustic detector system or by using the transmission scan method where the liquid polymers were placed on a NaCl disk and scanned. This method obviated any sample preparation.

3.4.4.3 Nuclear Magnetic Resonance Spectroscopy (NMR)

^{1}H and ^{13}C NMR spectra were recorded on a Varian VXR 300 Spectrometer at ambient temperature (20 °C) using 7 mm rotors and spinning rates of about 5 500 Hz. $CDCl_3$ was used as sample solvent throughout.

3.4.4.4 Gas Chromatography (GC)

A Hewlett Packard 5 890 Series 2 gas chromatograph was used to follow the progress of the monomer synthesis as well as to determine the purity of the monomer.

3.5 FIRST APPROACH: GRIGNARD TYPE REACTION

Grignard reagents are known to react with *tert*–halides, but low yields of alkanes are expected. With the experimental background of Osawa *et al* [5], we decided to use standard Grignard chemistry to prepare 3-(1-adamantyl)-1-propene[8]. Scheme 3–7 shows schematically the Grignard type of procedure that was followed to prepare 3-(1-adamantyl)-1-propene.

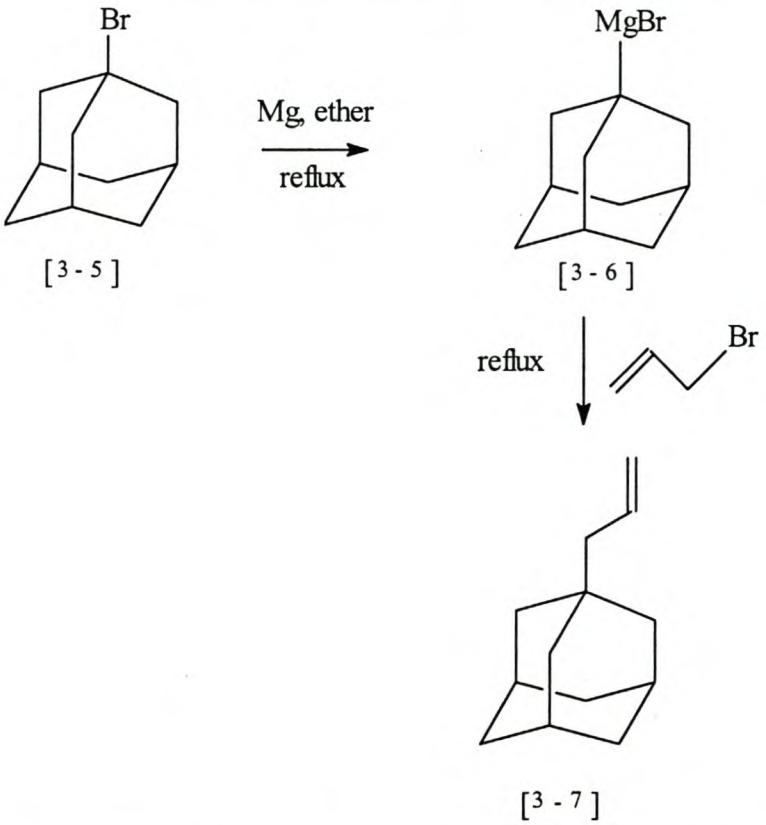

Scheme 3-7: Synthesis of [3–7] by Using a Grignard Type Reaction

3.5.1 Preparation of Adamantyl Magnesium Bromide

A solution of adamantyl magnesium bromide **[3–6]** (Grignard reagent) was prepared from magnesium turnings (1.22 g; 2 x 10^{-2} mole) and adamantyl bromide (**[3–5]**) (4.3 g; 2 x 10^{-2} mole in 10 mL of anhydrous ether) in 30 mL of anhydrous ether. The magnesium turnings were weighed out into the round bottom flask, together with 30 mL of anhydrous ether and boiled under reflux. **[3-5]** was then added dropwise, over a period of 30 minutes. After all of the **[3–5]** had been added, the mixture was refluxed for 30 minutes. The

Grignard reagent was then filtered through glass wool to get rid of the excess magnesium turnings.

3.5.2 Addition of 3-Bromo-1-Propene to Adamantyl Magnesium Bromide [3–6]

3-Bromo-1-propene (1.67 mL; 2 x 10^{-2} mole) was added dropwise to the Grignard reagent at 50 °C over a period of 30 minutes. The reaction mixture was refluxed for a further hour. The reaction mixture was then cooled and poured onto an excess of crushed ice in a large beaker to break the solid magnesium complexes. The magnesium salts were removed by adding 5 mL of diluted sulphuric acid. The ether layer was separated, washed three times with ammoniacal ammonium sulphate solution (10 mL) to remove any dissolved magnesium salts and then once with water (10 mL) to remove any excess ammonium sulphate solution. The ether layer was dried over magnesium sulphate ($MgSO_4$). After one hour, the mixture was again filtered, and the solvent removed under reduced pressure on a rotory evaporator to yield a colourless oil, 3-(1-adamantyl)-1-propene (**[3–7]**), 1.7 g, 49 %.

3.5.3 Results and Discussion

NMR analysis of **[3–7]** revealed a range of reaction products. **[3–7]** was purified by high vacuum distillation (0.05 mm Hg), but NMR analysis still showed a mixture of products. Two more attempts to purify **[3–7]**, flash chromatography and high vacuum sublimation, failed. From the NMR analysis, it was clear that both attempts to purify **[3–7]** were not successful, because there were still some byproducts present. The byproducts could be biadamantane or unreacted **[3-5]**. Because of the low yield of the Grignard reaction and the side reactions leading to the impurities present in the required product, **[3–7]**, the Corey–House reaction was considered a possible one–pot synthesis for **[3–7]**[8]. However, an extensive literature research showed that the Corey–House reaction was not suitable for the substitution of bridgehead bromine atoms by alkyl groups and that Grignard reagents were preferred over organocuprates[9-12]. It was decided that the approach of using

Grignard coupling to prepare **[3-7]** was not effective enough to give the target monomer in good yields.

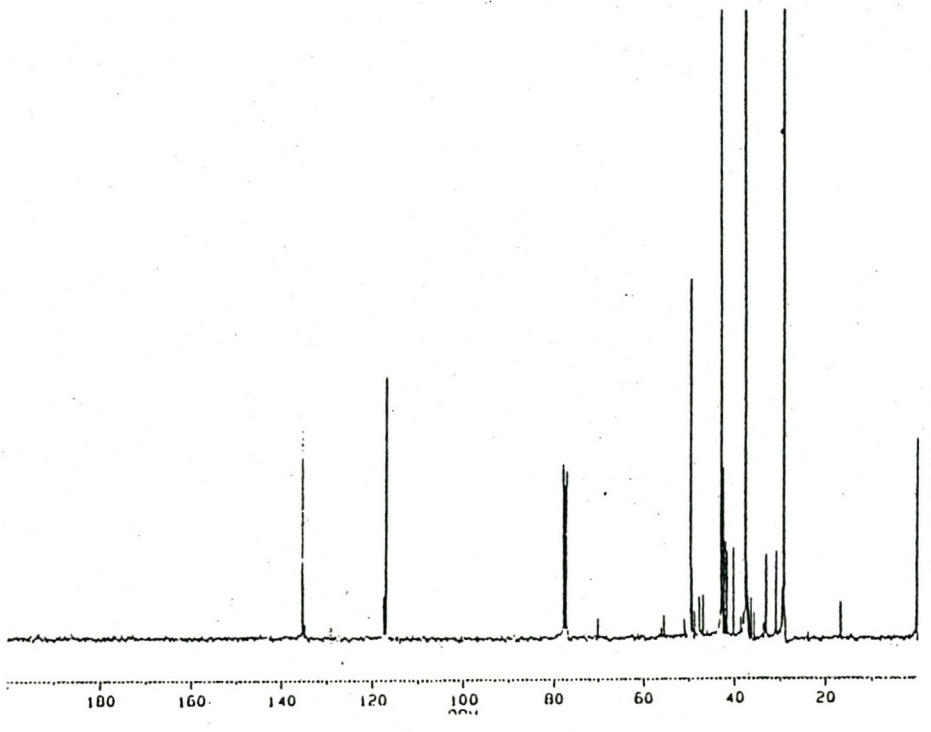

Figure 3–1: ^{13}C NMR Spectrum of [3-7] in $CDCl_3$ prepared by the Grignard Route

3.6 SECOND APPROACH: SYNTHESIS OF 3-(1-ADAMANTYL)-1-PROPENE BY USING TRIMETHYLSILYLATED UNSATURATED COMPOUNDS

In our hands, the method of Sasaki *et al* [3] yielded none of the expected product. Instead, a large amount of insoluble precipitate formed during the reaction. This precipitate appeared to be polymeric in nature, and lead to the speculation that HBr formed during the reaction by abstraction of a proton from one of the other bridgehead positions caused a number of undesirable side-reactions, not least the isomerization and cationic polymerization of the formed product. It was therefore decided to use a proton sponge during the reaction. The material of choice was a hindered pyridine.

The addition of a few drops of the pyridine prevents the formation of any hydrogen bromide which could lead to the creation of an acidic reaction medium, conducive to the occurrence of side reactions. The hindered pyridine acted thus as a proton sponge. Other proton sponges used in this reaction were 1,8-bisdimethylamino naphthalene and 4 Å molecular sieve. We found that the hindered pyridine gave the best results.

In Scheme 3–8 the preparation of **[3–7]** by using trimethylsilylated unsaturated compounds is shown schematically.

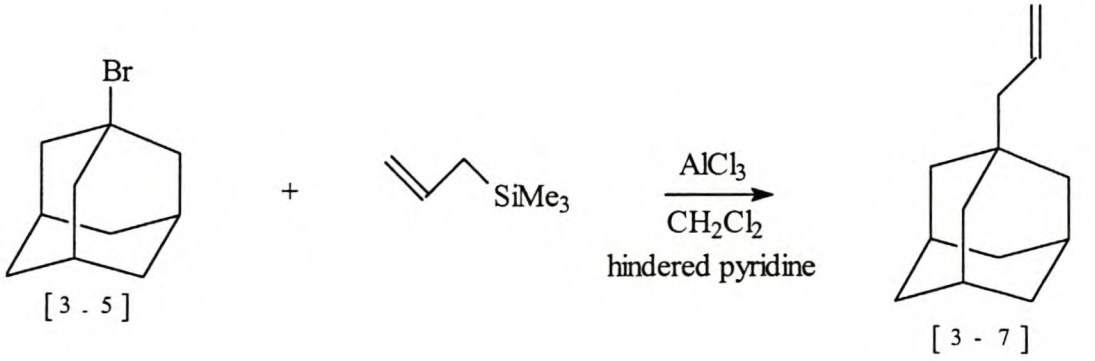

Scheme 3-8: Preparation of [3–7] Using Trimethylsilylated Unsaturated Compounds

3.6.1 Preparation of 3-(1-Adamantyl)-1-Propene [3-7]

In order to prevent any moisture in the reaction medium which could affect the experiment, the two–neck round bottom flask was sealed off with two rubber septums after **[3–5]** was weighed out. The whole experiment was conducted under nitrogen.

To a solution of **[3–5]**(2 g; 9 x 10^{-3} mole) in dichloromethane, (20 mL) under nitrogen, allyltrimethylsilane (1.05 g; 9 x 10^{-3} mole) and a few drops of 2,6-di-tert-butyl pyridine were added at –70 °C (dry ice/acetone). The reaction mixture became pale yellow-pink. After one hour the reaction mixture became, and then remained, dark yellow-pink. After 12 hours, the reaction mixture was clear and pale pink and was poured into an ice-water bath. A small quantity of methylene dichloride was added and the organic layer was extracted with water, four times. The organic layer was dried over $MgSO_4$ and after removal of the solvent under reduced pressure, an oily product was obtained. The crude product was purified by means of high vacuum sublimation at 60 °C to yield a colourless oil, **[3–7]**, 0.95 g, 60 %.

3.6.2 Results and Discussion

The ^{13}C NMR spectrum of 3-(1-adamantyl)-1-propene is shown in Figure 3–2 and the chemical shift values are given in Table 3.1.

Table 3.1: ^{13}C NMR Chemical Shifts (δ) of [3–7] in $CDCl_3$

Carbon	Chemical shift (ppm)
a	28.57
b	37.39
c	42.64
d	32.10
e	49.29
f	135.16
g	116.68

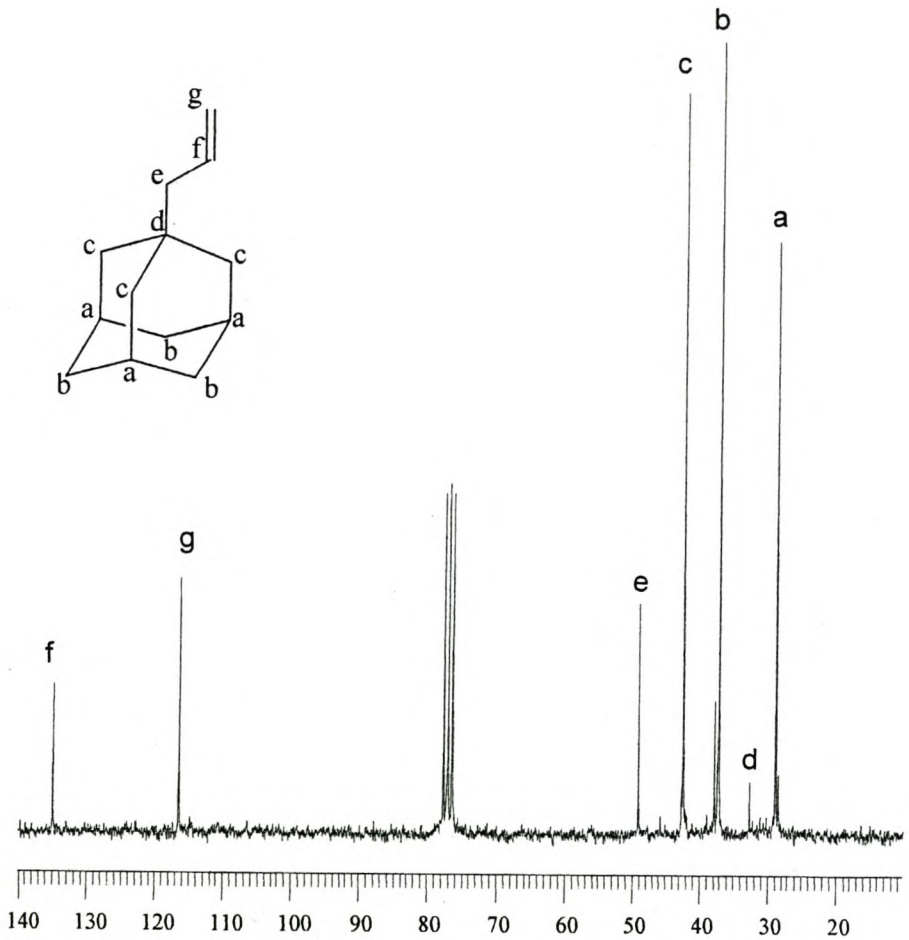

Figure 3-2: ^{13}C NMR Spectrum of [3–7] in $CDCl_3$

The ^{13}C NMR spectrum of **[3–7]** showed seven signals as expected. NMR analysis of **[3–7]** revealed that this method, where 2,6-di-tert-butyl pyridine is employed as a proton sponge to prevent the creation of an acidic medium conducive to the occurrence of side reactions, proved to be succesful for the synthesis of 3-(1-adamantyl)-1-propene of high purity. From the NMR analysis it was also evident that high vacuum sublimation was an excellent method to purify **[3-7]** (>96 % as determined by GC). High vacuum distillation (0.05 mm Hg) was also tried as a method of purification, but NMR analysis still showed a mixture of products.

A new method for the preparation of 3-(1-adamantyl)-1-propene, using the relevant literature published by Sasaki *et al* [3] and adding a proton sponge, was thus developed. The hindered pyridine, 2,6-di-tert-butyl pyridine, employed to act as a proton sponge, proved to be very efficient in preventing the creation of an acidic reaction medium conducive to the occurrence of side reactions.

The only disadvantage of this method, was that the hindered pyridine is very expensive which makes it quite expensive to produce large quantities of **[3-7]**, and it was therefore decided to attempt a less expensive method to synthesize a substantial amount of **[3–7]**.

3.7 THIRD APPROACH: PREPARATION OF 3-(1-ADAMANTYL)-1-PROPENE BY USING A FRIEDEL-CRAFTS TYPE REACTION

In this approach, the method of Capaldi *et al* [2] was followed. The outline of the reaction is shown in Scheme 3-9.

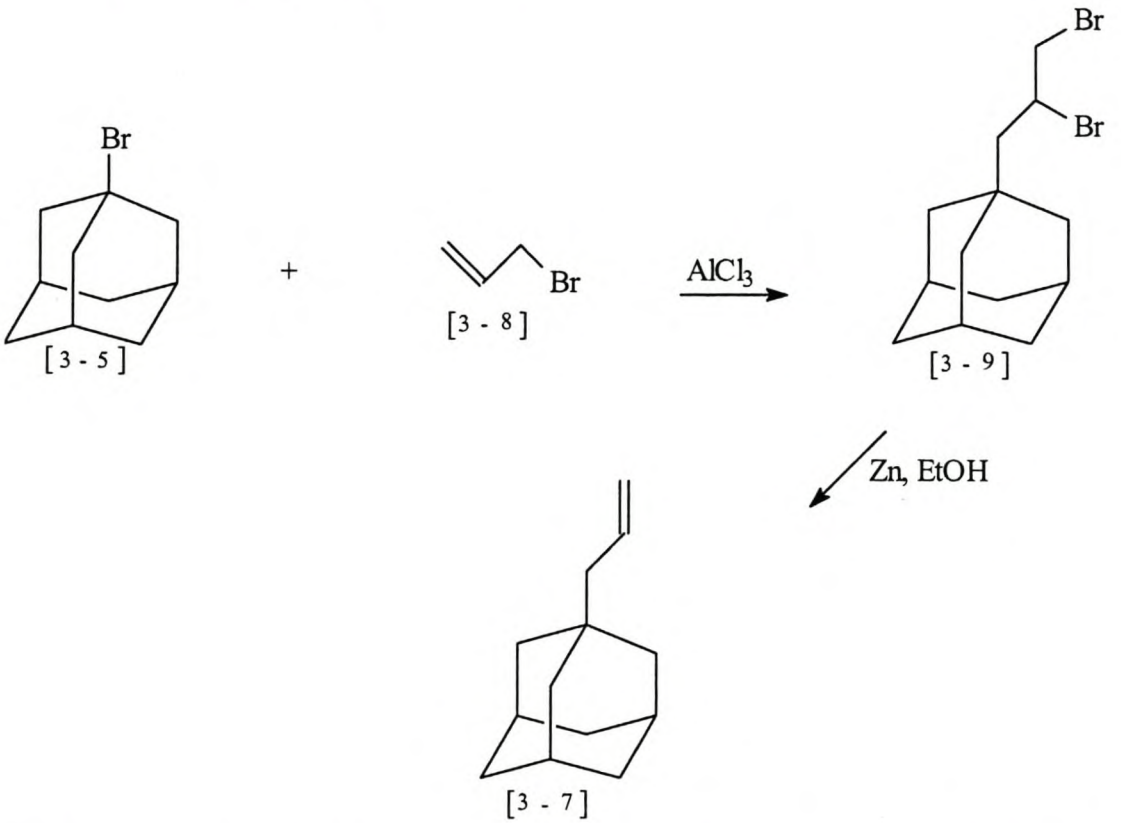

Scheme 3–9: Preparation of [3–7] by Using a Friedel–Crafts Type Reaction

3.7.1 Preparation of 1,2-Dibromo-3-Adamantyl Propane [3–9]

[3–5] (10.8 g; 5 x 10^{-2} mole) and 3-bromo-1-propene (6.05 g; 5 x 10^{-2} mole) were dissolved in 40 mL of carbon disulfide. The solution was cooled, with stirring, to below –70 °C (dry ice/acetone) and then $AlCl_3$ (0.5 g; 3.8 x10^{3} mole) added in small portions over a period of 20 minutes. The temperature was then allowed to rise slowly to between –35 °C and –30 °C and held there for a further hour.

The reaction mixture was then poured into an ice/water mixture and the organic layer extracted with a large excess of diethyl ether. The organic extract was washed with water, dried over $MgSO_4$ and the solvent removed under reduced pressure. The product was then redissolved in hexane and repeatedly extracted with water to remove the residual carbon disulfide. After further drying over $MgSO_4$ and removal of the solvent, 13.7 g (82 %) of **[3–9]** was isolated. This product was used without any further purification. Some of the product was purified for spectral analysis by sublimation under reduced pressure.

3.7.2 Preparation of 3-(1-Adamantyl)-1-Propene [3-7]

Zinc dust (3 g; 4.6 x 10^{-2} mole) was added to 20 mL of ethanol, and the mixture heated to reflux. To this was added, dropwise, over a period of 30 minutes **[3-9]** (13.7 g; 4.1 x 10^{-2} mole). When addition was complete, the resulting mixture was refluxed for a further three hours, washed with water, then dried over $MgSO_4$ and the solvent removed under reduced pressure to yield **[3–7]**. The product was purified by high vacuum sublimation (95 % purity as determined by GC) to yield a yellowish oil, 3-(1-adamantyl)-1-propene, 5.5 g, 75 %.

3.7.3 Results and Discussion

The ^{13}C NMR spectrum of **[3–9]** is shown in Figure 3–3 and the chemical shift values are given in Table 3.3.

Table 3.2: ^{1}H NMR Chemical Shifts (δ) of [3–9] in $CDCl_3$

Proton	Chemical shift (ppm)
a, d	3.6 (t)
b	2.1 (s)
c	1.7 (s)
e	1.6 (s)
f	4.2 (m)
g	3.8 (d)

Table 3.3: ^{13}C NMR Chemical Shifts (δ) of [3–9] in $CDCl_3$

Carbon	Chemical shift (ppm)
a	28.50
b	36.90
c	42.40
d	32.40
e	50.80
f	38.40
g	46.30

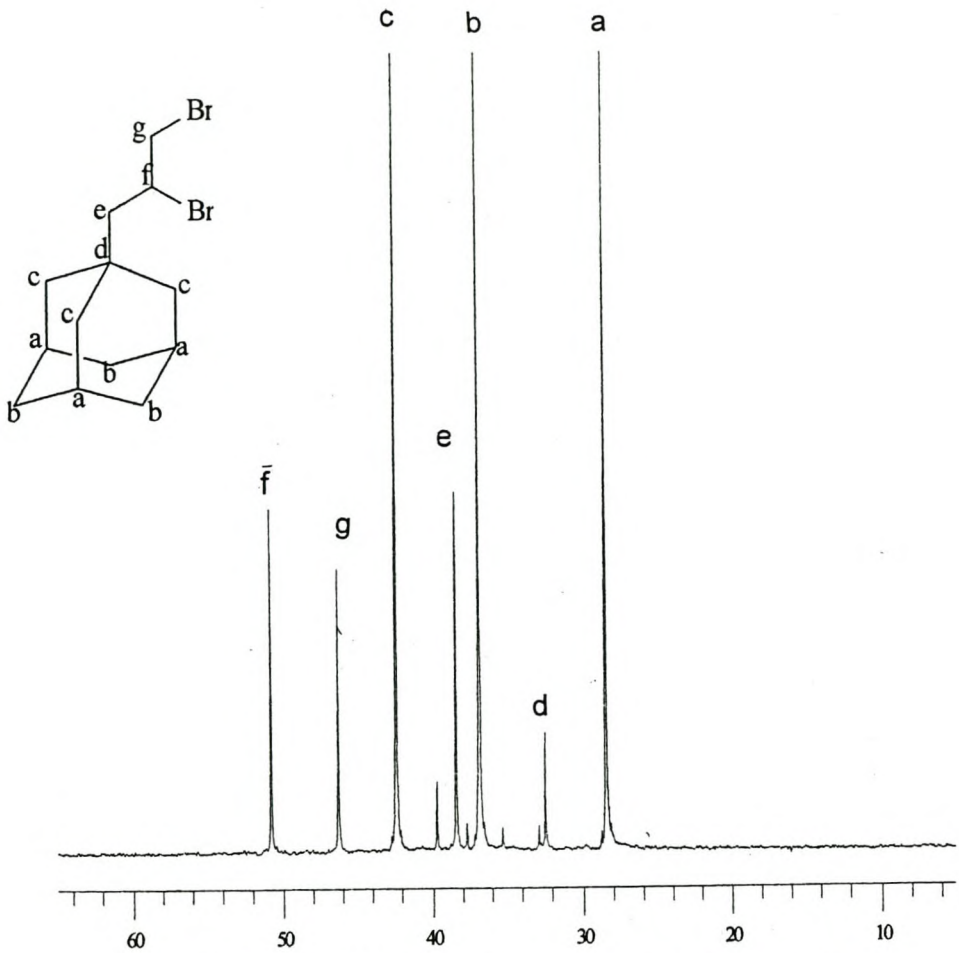

Figure 3-3: ^{13}C NMR Spectrum of [3–9] in $CDCl_3$

The ^{13}C NMR spectrum of **[3–9]** showed seven signals as expected. The spectrum is consistent with the structure shown above.

The ^{13}C NMR spectrum of **[3–7]** is shown in Figure 3–4 and the chemical shift values are given in Table 3.5.

Table 3.4: ^{1}H NMR Chemical Shifts (δ) of [3–7] in $CDCl_3$

Proton	Chemical shift (ppm)
a, d	3.6 (t)
b	2.1 (s)
c	1.7 (s)
e	1.9 (s)
f	5.7 (s)
g	5.0 (s)

Table 3.5: ^{13}C NMR Chemical Shifts (δ) of [3–7] in $CDCl_3$

Carbon	Chemical shift (ppm)
a	28.99
b	37.38
c	42.64
d	33.10
e	49.29
f	135.15
g	116.67

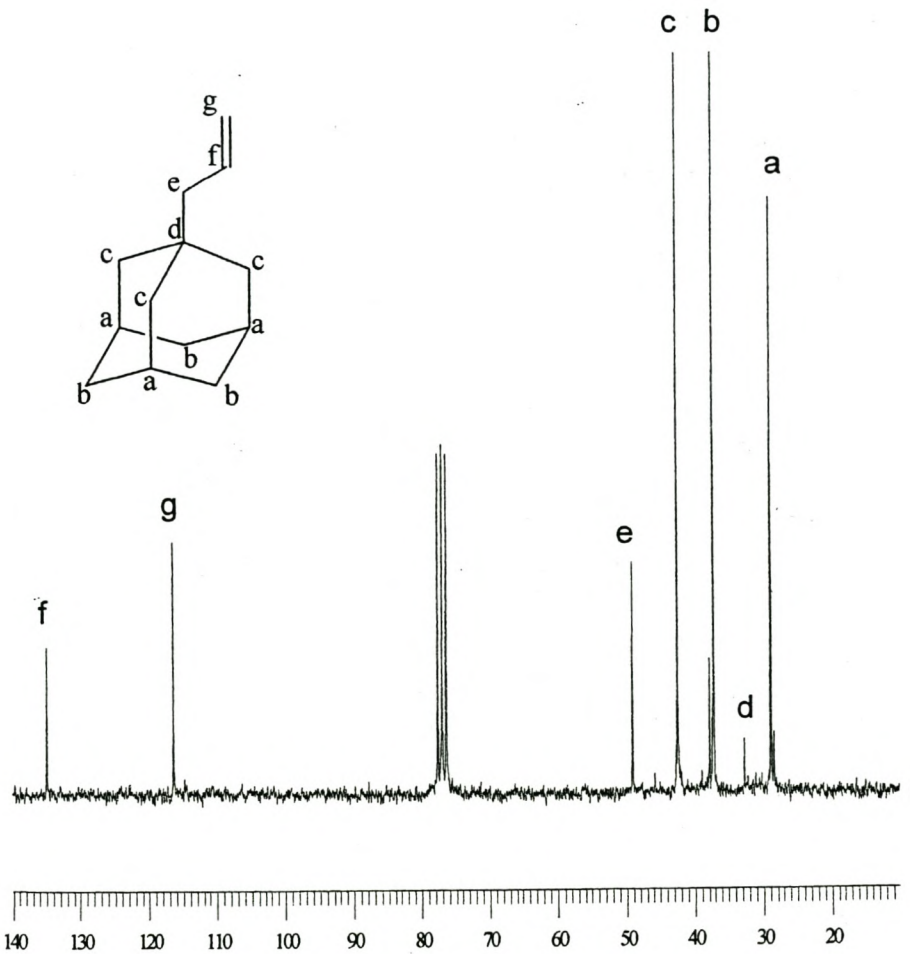

Figure 3-4: ^{13}C NMR Spectrum of [3–7] in $CDCl_3$

The ^{13}C NMR spectrum of **[3–7]** showed seven signals as expected. Analysis by FTIR spectroscopy was done to confirm the proposed structure of **[3–7]**. A Perkin Elmer FTIR instrument in conjunction with a photo–acoustic detector system was used. This method obviates sample preparation and gives spectra that compare well with those from other IR techniques.

The spectral characteristics expected for **[3–7]** can be predicted.

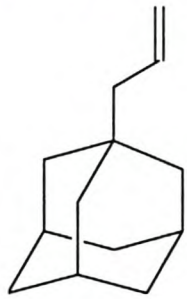

For the CH_2 – and CH - groups in the allyl group the following are expected:

- C–H stretch vibrations, both symmetrical at 2 897 cm^{-1} and asymmetrical at 2 846 cm^{-1}
- Non–conjugated C=C stretch vibrations at 1 639 cm^{-1}
- -CH_2 scissor vibrations at 1 450 cm^{-1}
- -CH_2-CH_2 skeletal vibrations at 665 cm^{-1}

For the adamantyl group:

- C-H assymetrical stretch vibrations at 2 846 cm^{-1}
- -CH_2 wag vibrations, assymetrical at 1 346 cm^{-1} due to HCC angle bending
- C-H vibrations at 1 097 cm^{-1} due to deformation
- -C-C-C angle bending vibrations at 997 cm^{-1}
- -CH_2 rock vibrations at 910 cm^{-1}

The FTIR analysis of **[3–7]** shown in Figure 3-5 confirmed the expected structure.

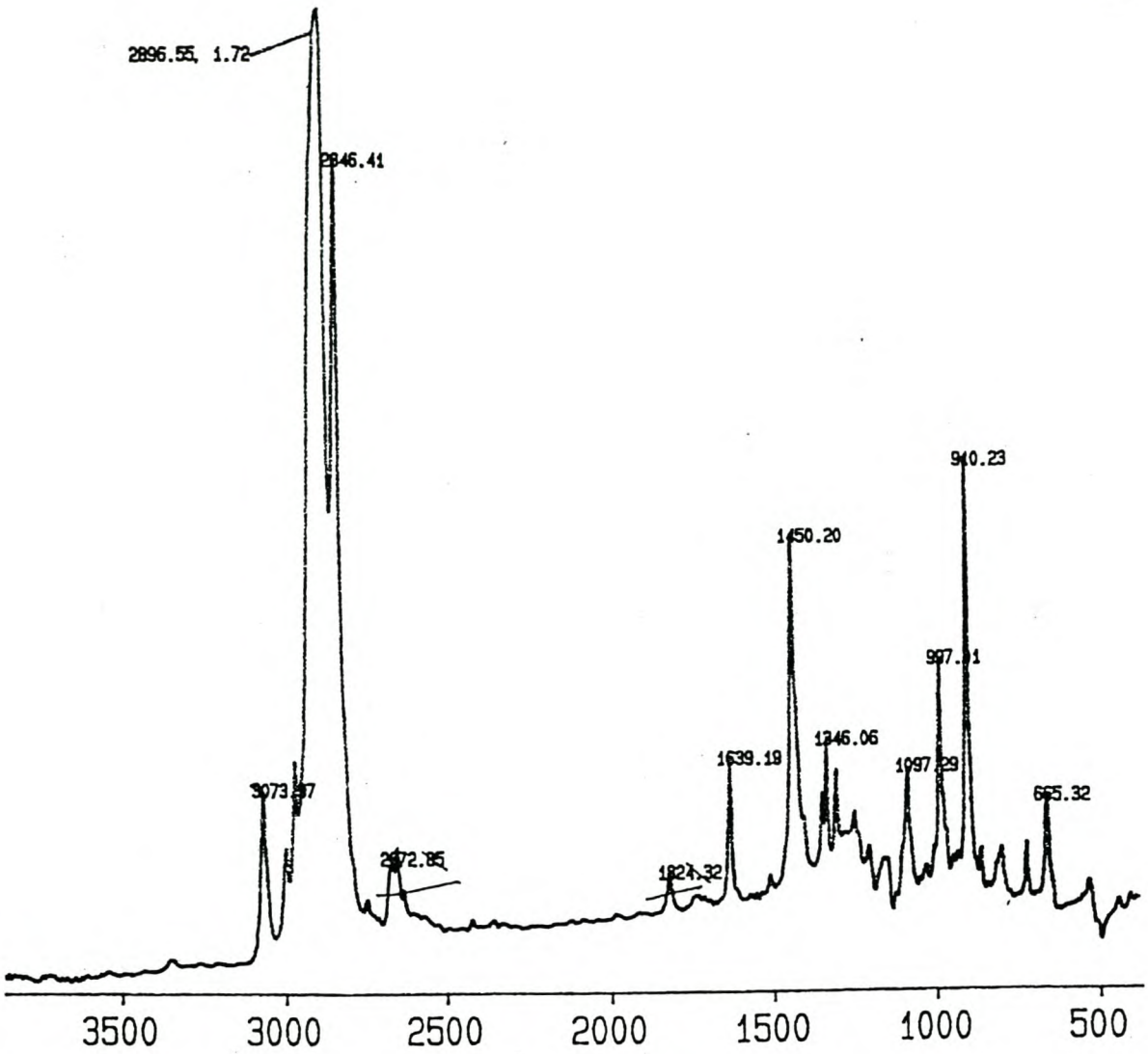

Figure 3-5: IR Spectrum of [3–7]

NMR analysis and the IR spectrum of **[3–7]** revealed that this Friedel–Crafts type method proved to be successful for the synthesis of high purity **[3–7]** which can be used as monomer in polymerization reactions. This method proved to be just as good and effective as the method used in the second approach using trimethylsilylated unsaturated compounds to synthesize **[3-7]**, although it is not that expensive.

From the NMR analysis it was clear that high vacuum sublimation was an excellent method to purify **[3–7]** (>96 % purity as determined by GC).

[3–7] synthesized by this Friedel–Crafts type reaction, was pure enough (>95 % purity determined by GC) to be polymerized or incorporated into polymers.

3.8 CONCLUSIONS

In conclusion, three different approaches were applied to synthesize **[3–7]** that was pure enough to be polymerized or incorporaterd into polymers. The first approach by which **[3-7]** was synthesized, a Grignard type reaction proved to be unsuccessful. Using this approach, only a mixture of products was obtained. Attempts to purify **[3–7]** using flash chromatography as well as high vacuum sublimation, failed. The second approach, by which **[3-7]** was synthesized using trimethylsilylated unsaturated compounds, proved to be reasonably successful, when a new method was applied, using a proton sponge in conjunction with the method of Sasaki *et al* [3]. The only disadvantage of this method is that the hindered pyridine is very expensive which makes it quite expensive to produce large quantities **[3-7]**. The third approach, by which **[3–7]** was synthesized using a Friedel–Crafts type reaction, proved to be very efficient. The use of high vacuum sublimation proved to be an excellent method to purify **[3-7]**. By this method, the purity of **[3-7]** is better than 96 % determined by GC.

3.9 REFERENCES

1. Curran D.P., Woo B., *Tetrahedron Lett.*, 1992, **33**(48), 6 931.
2. Capaldi E., Borchert A.E., *US Patent*, 1969, **3 457**, 318.
3. Sasaki T., Usuki A., Ohno T., *J. Org. Chem.*, 1980, **45**, 3 559.
4. Thoma G., Curran D.P., Geib S.V., Giese B., Damm W., Wetterich F., *J. Am. Chem. Soc.*, 1993, **115**, 8 585.
5. Osawa E., Marjerski Z., Schleyer P. von R., *J. Org. Chem.*, 1971, **36(1)**, 205.
6. Kraus T.M., Siclovan T.M., *J. Org. Chem.*, 1994, **59**, 922.
7. Grant M., M.Sc Thesis, University of Stellenbosch, 1993.
8. Furniss B.S., Hannaford A.J., Smith P.W.G., Tatchell A.R., Textbook of Practical Organic Chemistry, Fith Ed., 340.
9. Corey E.J., Postner G.H., *J. Am. Chem. Soc.*, 1967, **89**, 3 911.

10. Corey E.J., Postner G.H., *J. Am. Chem. Soc.*, 1968, **90**, 5 615.

11. Whitesides G.M., Fischer W.F., San Filippo J., Bashe R.W., House H.O., *J. Am. Chem. Soc.*, 1969, **91**, 4 871.

12. Bergbreiter D.E., Whitesides R.M., *J. Org. Chem.*, 1975, **40**, 779.

CHAPTER 4

POLYMERIZATION REACTIONS OF 3-(1-ADAMANTYL)-1-PROPENE

4.1 INTRODUCTION

In this Chapter, the homopolymerization reaction of 3-(adamantyl)-1-propene as well as the polymerization reactions with ethene, propene and higher α-olefins are discussed. Three different metallocene catalyst systems were used, namely the C_2 symmetric *ansa* metallocene *rac*-[(ethylene *bis*(1-indenyl)]zirconium dichloride (*rac*-Et(Ind)$ZrCl_2$), the C_{2v} symmetric catalyst, bis(indenyl)zirconium dichloride (Ind_2ZrCl_2), and a half-sandwich catalyst, dimethylsilyl-(t-butylamido)-(tetramethylcyclpentadienyl) titaniumdimethyl. In all three systems, methylaluminoxane (MAO) was used as cocatalyst. A historical and theoretical background on metallocene catalyzed polymerization reactions with ethene, propene and higher α-olefins are discussed in this Chapter.

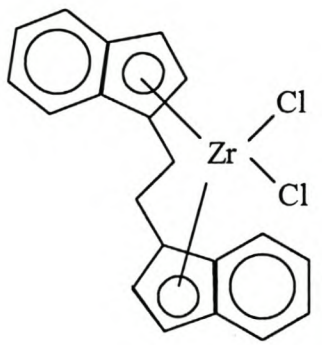

Figure 4–1: *rac*-[Ethylene *bis*-(1-Indenyl)]Zirconium Dichloride

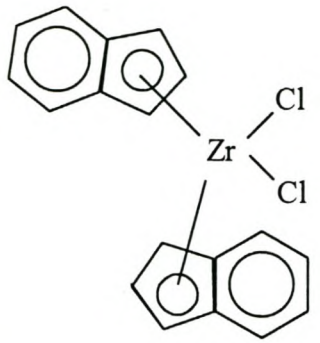

Figure 4–2: *bis*-(1-Indenyl)Zirconium Dichloride

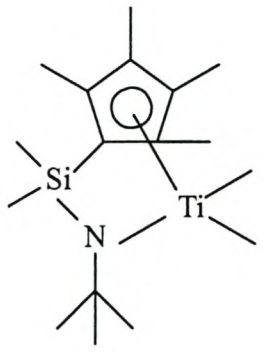

Figure 4–3: Dimethylsilyl(*t*-butylamido) (tetramethylcyclopentadienyl)titaniumdimethyl

In order to compare the relative effect of the adamantyl group and a phenyl group, an analogous series of copolymers were made by copolymerizing 3-phenyl-1-propene with the higher α-olefins using the C_2 symmetric *ansa* metallocene *rac*-[(ethylene *bis*(1-indenyl)]zirconium dichloride with MAO used as cocatalyst. The properties of the 3-phenyl-1-propene polymers and copolymers were compared to those of 3-(1-adamantyl)-1-propene polymers and copolymers and the influence of the phenyl and the adamantyl groups on the properties were compared.

4.2 *METALLOCENE CATALYZED POLYMERIZATION REACTIONS WITH ETHENE, PROPENE AND HIGHER α-OLEFINS*

4.2.1 Introduction

Metallocene catalysts for olefin polymerization were discovered by Breslow and Natta soon after the original discovery of Ziegler-Natta catalysts[1-3]. Metallocene catalysts are bicomponents consisting of group four transition metal compounds and cocatalysts. Titanocenes were the first metallocene catalysts that afforded the synthesis of ethylene copolymers with 1-butene[4] and propene[5], with a high degree of compositional uniformity. Unfortunately, these catalyst systems are only moderately active, and the molecular masses of the copolymers they produced rapidly decreased with an increase in the α-olefin content[4, 5]. In 1976 Kaminsky and Sinn developed a new class of metallocene catalysts that exhibit extremely high activity[6-8]. These catalysts and their subsequent modifications presently compete with Ziegler-Natta catalysts for many commercial applications. The evolution of metallocene catalyst structures for olefin polymerization until 1984 is tabulated in Table 4.1[9]. Since 1984, a rapid, worldwide industrial and academic development began in the field of metallocene catalysts, which continues today.

In the early 1980's Brintzinger and coworkers synthesized racemic ethylene-bridged *bis*(1-indenyl) zirconium dichloride, $Et(Ind)_2ZrCl_2$, and racemic ethylene–bridged *bis*(4,5,6,7-tetrahydro-indenyl) zirconium dichloride, $Et(H_4Ind)_2ZrCl_2$[10], as well as their titanium analogues, $Et(Ind)_2TiCl_2$ and $Et(H_4Ind)_2ZrCl_2$[11], which have both meso and racemic configurations. The sterically rigid chiral $Et(Ind)_2ZrCl_2$ and $Et(H_4Ind)_2ZrCl_2$ catalysts activated with methylalumoxane (or methylaluminoxane, MAO) catalyzed the stereoselective polymerization of propene with very high activities. This was the first time that isotactic polyolefins were obtained from homogeneous Ziegler–Natta polymerizations. This demonstrated stereochemical control by the chiral *ansa*-indenyl ligands on the transition metal ion in the selection of one of the two enantiotropic faces (re or si) of a prochiral vinyl monomer in migratory insertion. In 1988 Ewen *et al* synthesized a C_s–symmetric zirconocene $(Me_2C(Flu)(Cp)]ZrCl_2)$ which produces syndiotactic polypropene in high

quantities[12]. Table 4.1 is a summary of the historical developments in the field of metallocene research.

TABLE 4.1: Historical Developments in the Field of Metallocene Research

1952	Development of the structure of metallocenes (ferrocene) by Fischer and Wilkinson	Ref. 13
1955	Metallocene as component of Ziegler-Natta catalysts, low activity with common aluminium alkyls	Ref. 1
1973	Addition of small amount of water to increase the activity (Al:H_2O = 1:0.05 up to 1:0.3) (Reichert, Meyer and Breslow)	Ref. 14, Ref. 15
1975	Unusual increase in activity by adding water at the ratio Al:H_2O = 1:2 (Kaminsky, Sinn and Motweiler)	Ref. 16
1977	Using separately prepared methylalumoxane (MAO) as cocatalyst for olefin polymerization (Kaminsky and Sinn)	Ref. 6
1982	Synthesis of *ansa* metallocenes with C_2 symmetry (Brintzinger)	Ref. 4
1984	Polymerization of propene using a *rac/meso* mixture of *ansa* titanocenes lead to partially isotactic polypropene (Ewen)	Ref. 12
1984	Chiral *ansa* zirconocenes produce highly isotactic polypropene (Kaminsky and Brintzinger)	Ref. 7

In the field of the copolymerization of linear α-olefins, new possibilities for controlling the properties of copolymers have emerged through the development of homogeneous, chiral metallocene catalysts. Results of early studies revealed that these catalysts polymerize propene and higher α-olefins at a moderately lower rate than ethene[17-20]. Accordingly, copolymers obtained with these catalysts contain larger fractions of higher olefins than those obtained with heterogeneous catalysts, under comparable conditions[21-28]. Results of later studies, particular by the groups of Zambelli[29-32], Chien[33-38], Soga[39] and Kashiwa[40, 41] showed that copolymers produced by metallocene-based catalysts consist of uniform chains with narrow molecular mass distributions typical of single–site catalysts (see Figure 4-4).

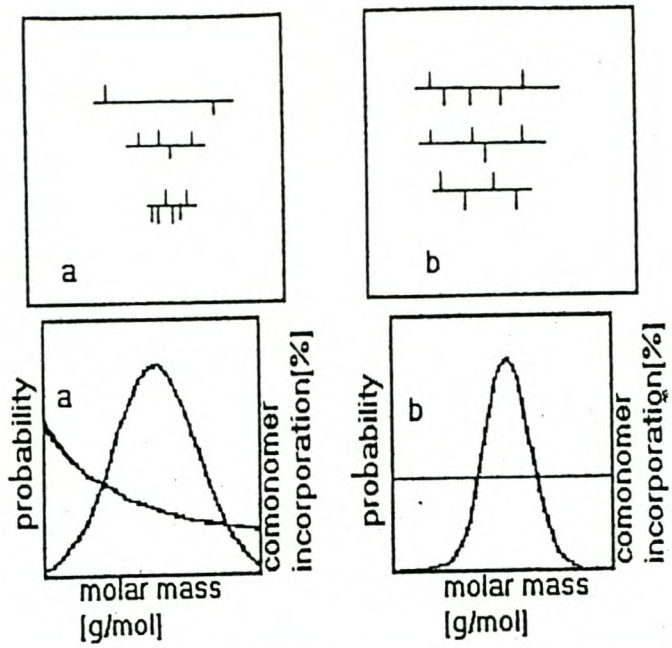

FIGURE 4-4: Molar Mass Distribution and Comonomer Incorporation of Multi-Site Ziegler–Natta Catalysts (a), Compared to Single–Site Metallocene Based Catalysts (b)[42]

(a) Copolymers consist of a complex mixture of homo- and copolymers with comonomers frequently incorporated in the low molar mass fractions, broad molar mass distrubution (M_w/M_n = 5–40).

(b) Uniform comonomer incorporation, narrower molar mass distribution ($M_w/M_n \approx 2$).

4.2.2 Advantages and Disadvantages of Metallocene/Alumoxane Catalysts

The major **advantages** of these homogeneous metallocene/ alumoxane (MAO) catalysts are:

(a) They exhibit high catalytic activities.

(b) Small quantites of catalyst are required.

(c) They have the ability to polymerize a wide variety of monomers.

(d) They produce polymers with narrow molecular mass distributions approaching the theoretical value of 2.0 as predicted by the Schultz–Flory mechanism.

(e) They are able to polymerize α-olefins with almost any desired stereospecificity.

Disadvantages of these catalyst systems are:

(f) Decay–type kinetics are evident with ethene/higher α-olefin mixtures.

(g) High Al/Zr ratios are required for obtaining high catalytic activity and a relatively stable kinetic profile.

(h) The high cost of methylalumoxane (MAO).

(i) The short shelf lifetime of methylalumoxane.

(j) The inability of catalysts to be used in slurry or gas phase processes.

4.2.3 The Reaction Mecahnism for the Preparation of Copolymers Produced by Metallocene Catalysts

4.2.3.1 Catalyst Activation

Spectroscopic evidence[43, 44] is consistent with the assumption that Lewis acidic centers present in MAO are able to accept CH_3^- (or Cl^-) anions from the alkylated metallocene, thus generating a metallocene alkyl cation, the active polymerization species[45, 46], and poorly coordinating counterion (Figure 4-5)[47].

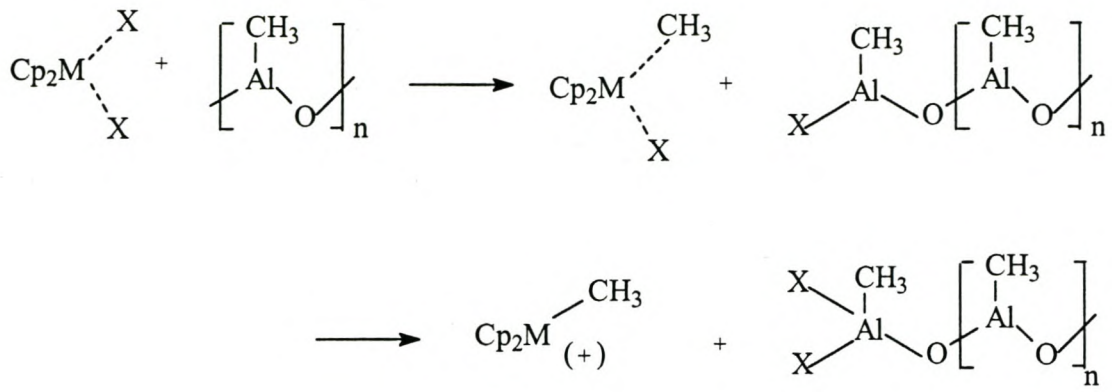

FIGURE 4-5: Formation of a Metallocene Alkyl Cation (the Active Species) by the Reaction between Metallocene and Methylalumoxane

4.2.3.2 Propagation

The polymerization reaction starts when ethene or an α-olefin molecule is inserted into the Zr–Me bond[44, 48, 49].

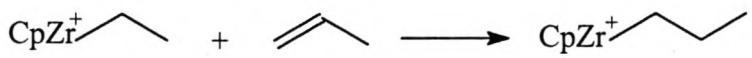

Eq. 4.1

During copolymerization, two or more different α-olefin molecules are competitively inserted into the transition metal–carbon bonds of the active centers. When two α-olefins, CH_2=CH-R' and CH_2=CH-R'', copolymerized, four chain–growth reactions (Eq. 4.2 to Eq. 4.5) should be considered:

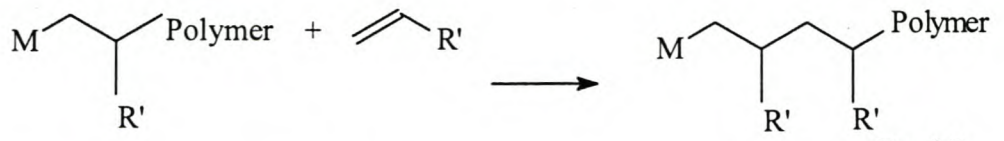

Eq. 4.2

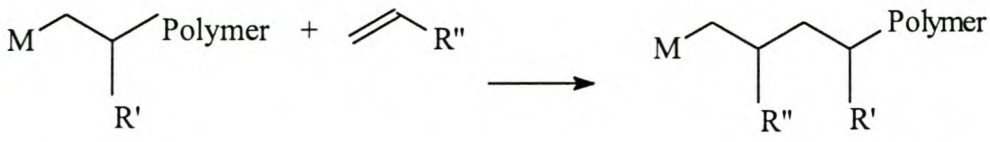

Eq. 4.3

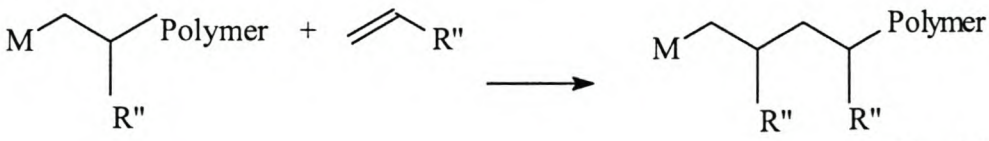

Eq. 4.4

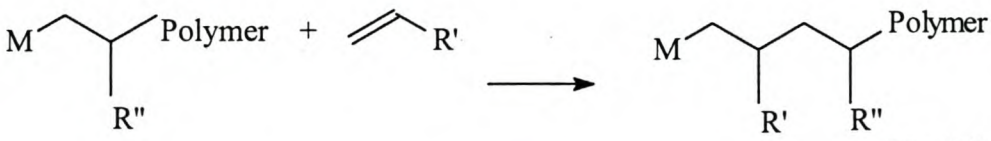

Eq. 4.5

Equations 4.2 and 4.4 represent homopolymerization growth processes (rate constants k_{11} and k_{22}), and the other two equations (4.3 and 4.5) represent copolymerization processes (rate constants k_{12} and k_{21}). The values of the four rate constants for Eq. 4.2–Eq. 4.5 are different, which means that the rate of the insertion reaction of a particular α-olefin into the Me-C bond depends not only on the structure of the α-olefin itself, but also on the structure of the last monomer unit attached to the transition metal atom before a given olefin insertion reaction. In copolymerization reactions, the four rate constants are traditionally grouped into two ratios named reactivity ratios:

$$r_1 = k_{11}/k_{12} \text{ and } r_2 = k_{22}/k_{21}.$$

In copolymerization reactions of ethene with propene and with other α-olefins or propene with other α-olefins, ethene and propene is always much more reactive than the α-olefin, independant of the last monomer unit in the

growing chain. Hence the r_1 value is always higher than 1 and the r_2 value is always lower than 1.

The insertion of an α-olefins in the metal-carbon bond may take place in two different ways[47]:

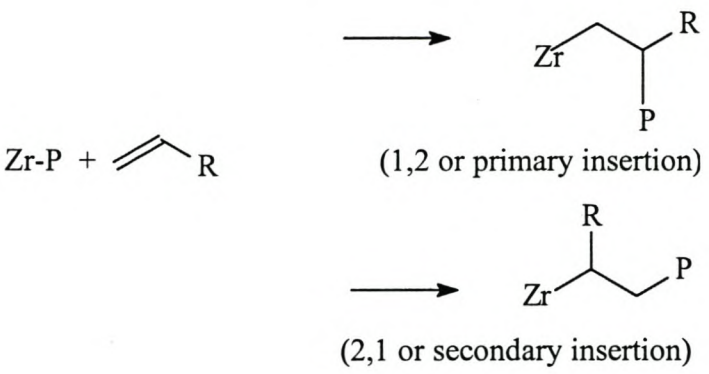

Eq. 4.6

It was proved, by chain–end group analysis, that the 1,2 insertion mode was evident in the isospecific polymerization of olefins with metallocene–based catalysts[29, 50]. Isospecific polypropene, obtained with chiral C_2–symmetric group 4 metallocenes (for example $Et(Ind)_2ZrCl_2$), includes a small number (about 1 %) of isolated regioirregular structural units resulting from the 2,1 and 3,1 insertion of the monomer, as follows:

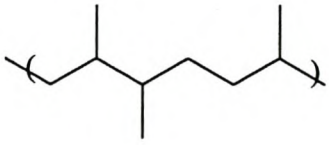

(2,1 insertion)

Eq. 4.7

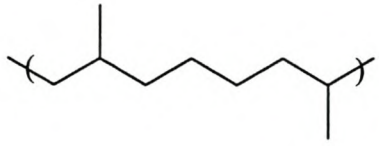

(3,1 insertion)

Eq. 4.8

This was revealed by the presence of $(CH_2)_2$ and $(CH_2)_4$ groups respectively[32, 51, 52].

The content of the two regioirregularities and their relative proportion depend on the σ-ligands, polymerization temperature, and monomer concentration[53].

4.2.3.3 Termination

The polymer chains are usually terminated in two reactions, a β-hydride elimination reaction (Eq. 4.9) and a chain transfer reaction to ethene or an α-olefin molecule (Eq. 4.10)[49, 53].

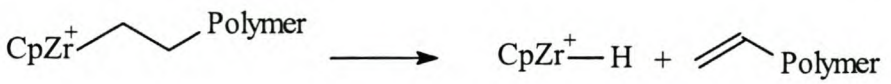

Eq. 4.9

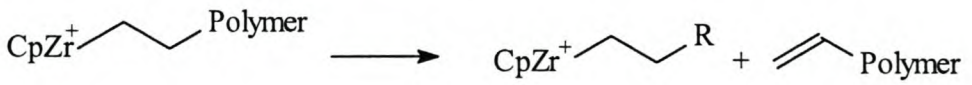

Eq. 4.10

4.2.4 Factors Influencing Copolymerization Behavior

The structures and properties of copolymers produced with metallocene catalysts can be changed by varying the following factors: (1) type of catalyst used, (2) [Al]/[Zr] ratios, (3) polymerization temperatures, (4) monomer feed ratios and (5) using different cocatalysts. Aspects of these variables are discussed in this Section.

4.2.4.1 Catalyst Used

Copolymerizations of ethene/α-olefins or propene/α-olefins with compositions covering the entire range of feasible copolymer ratios, were investigated as a function of metallocenes with different ligands, bridging groups and transition metal centers[37, 49, 54-71]. The non–bridged catalysts are traditionally used in the polymerization of ethene, whereas the bridged ones are used in the polymerization of propene and higher α-olefins.

4.2.4.2 Steric Control

In stereo- and regioselective metallocene–catalyzed propene polymerization, steric control depends primarily on the metallocene structure, especially metallocene symmetry. Metallocenes used in olefin polymerization have been classified on the basis of their symmetry (see Figure 4-6 and Table 4.2).

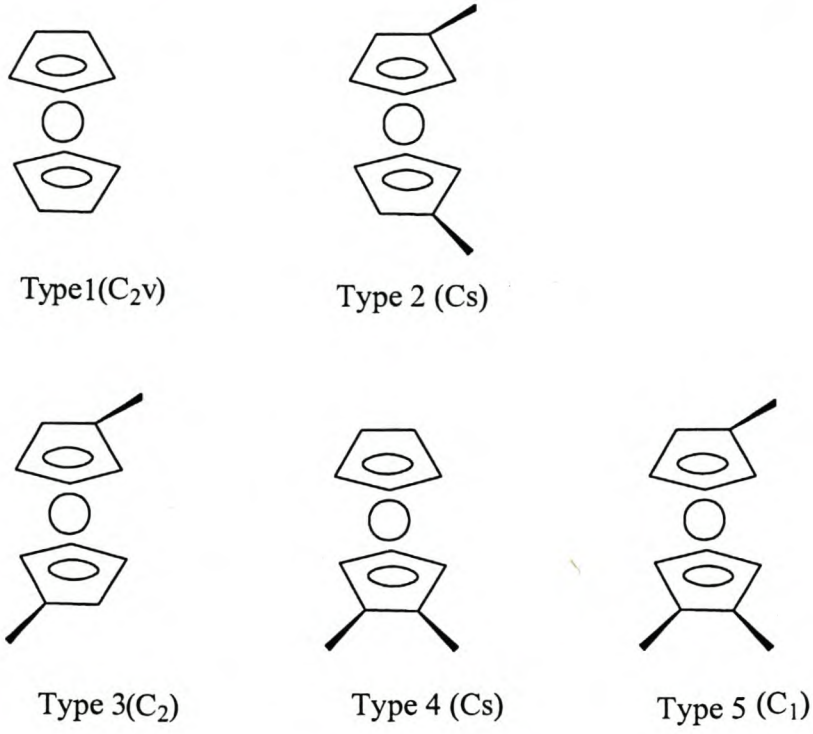

FIGURE 4-6: Steric Control as a Function of Metallocene Symmetry (Ewen's Symmetry Rules[72])

In Type 1, the two η^5-ligands can be bridged or not; whereas in the other classes they are bridged. In Types 1 and 2, the two active sites occupied by the η^5–ligands are bisected by a horizontal mirror plane and consequently are achirotopic; they are related by a two–fold rotation axis in Type 3 and are homotopic (equal). In Type 4, the two sites are related by a vertical mirror plane and are enantiotopic (mirror image to each other). No symmetry elements are present in Type 5, the two sites are diastereotopic (different). Table 4.2 shows the relationship between metallocene symmetry and polymer structure.

TABLE 4.2: Relationship between Metallocene Symmetry and Polymer Structure[73]

Idealised symmetry	Metallocene type	Examples	Polymer microstructure
C_{2v}	1	$Cp_2MCl_2Cp^*MCl_2$[a]	Atactic
C_s	2	meso-EBIMCl_2[b]	Atactic
C_2	3	rac-EBIMCl_2[c]	Isotactic
C_s	4	$Me_2C(Cp)(Flu)MCl_2$[d]	Syndiotactic
C_1	5	$Me_2C(MeCp)(Flu)MCl_2$[e]	Hemiisotactic

[a]Cp = cyclopetadienyl
Cp* = pentamethylcyclopentadienyl
[b]meso-EBI = meso- ethylene *bis* indenyl
[c]rac-EBI = racemic-ethylene *bis* indenyl
[d]Flu = fluorenyl
[e]MeCp = 3-methylcyclopentadienyl

4.2.4.3 Molecular Mass

The molecular mass of ethene/propene copolymers is dependant on the metallocene structure of the catalyst used in the polymerization (See Figure 4-6). Brintzinger[52] and Spaleck[74-76] discovered, almost simultaneously, that benzannelation, and especially the 2–methyl substitution of silylene-bridged *bis*-indenyl zirconocenes, clearly increases molecular weight. Molecular weight is thought to be limited by the occurrence of secondary or 2,1 insertion of α-olefins, which produces steric crowding at the active metal centre. This results in easier β-hydrogen abstraction and termination of polymerization. Substitution in the 2 and 4 positions of indenyl ligands have the two-fold role of lowering the number of 2,1 insertions as well as lowering the activation energy for olefin insertion. The latter was indicated, inter alia,

by Brintzinger[52], who showed that benzannelation of dimethylsilylbis(2-methyl indene)zirconium dichloride catalysts promoted the random incorporation of 1-octene. The result was in accord with recent force field modeling studies done by Schneider and Prosenc[77], where benzannelation accounted for substantially lower differences of activation energy of 1-octene insertion subsequent to ethene insertion or ethene subsequent to 1-octene, respectively. Although 2–methyl substitution did not effect randomness, it improved copolymer molar mass at the expense of catalytic activity.

4.2.4.4 Co-Monomer Incorporation

Copolymers obtained with metallocene catalysts contain higher amounts of higher α-olefins than those obtained with heterogeneous catalysts under similar conditions. In heterogeneous catalysts several active centers are present at the catalyst surface, and they show different selectivities towards the bulkier comonomer. Subsequently, the copolymers obtained are non-homogeneous and can be separated into fractions having different compositions. Conversely, the copolymers produced by metallocene–based catalysts consist of chains with uniform monomer composition and narrower molecular mass distribution, typical of single–centre catalysts[33–35, 37-41].

4.2.4.5 [Al]/[Zr] Ratios

In 1990 Resconi *et al* [78] proposed that the actual cocatalyst in the metallocene-MAO system is $AlMe_3$ (TMA) itself, with MAO acting as a soluble carrier–activator of the ion–pair formed upon reaction of the metallocene with TMA[2]. In these catalyst systems the following reaction is believed to take place[79]:

$$CpMX_2 + (\text{-AlMeO-})_n \rightarrow [CpMCH_3]^+[X_2(\text{-AlMeO-})_n]^-$$

Recent findings suggest that MAO serves both as an alkylating agent and as a template for poorly coordinating anions[80-83]. Other studies of metallocenes used for stereoregular α-olefin polymerization showed that polymerization activities, stereoregularities, and polymer molecular masses were strongly

dependant on the types of cocatalyst and their concentrations, suggesting strong, structure-sensitive ion–pairing effects[84-86].

The response of zirconocenes to changes in the [Al]/[Zr] ratio and MAO structure can be interpreted in terms of a mechanistic model involving ion pairs (see Figure 4-7)[40, 87, 88].

$$CpMX_2 + nMAO \rightarrow [Cp_2M\text{-}CH_3]^+ \bullet X \bullet [X\text{-}MAO]^- \bullet [MAO]_{n-1}$$

Contact ion pair

$$[Cp_2M\text{-}CH_3]^+ \bullet X \bullet [X\text{-}MAO]^- \bullet [MAO]_{n-1} \rightarrow [Cp_2M\text{-}CH_3]^+ \parallel [X_2\text{-}MAO]^- \bullet [MAO]_{n-1}$$

Solvent separated ion pair

FIGURE 4-7: Ion–Pair Model[79]

It is postulated that as the MAO ratio increases, the MAO aggregates become larger and the cationic species becomes further separated from the anions. This less sterically hindered species is largely responsible for the enhanced activity. The extent of ion pairing is dependant on the structure of the zirconocene composition.

The monomer moves through the channels to the active site where it joins the growing polymer chain.

With BuCpZr (*bis*(n-butylcyclopentadienyl)zirconium dichloride) catalyst at lower MAO/Zr ratios, some contact ion pairs are formed. As the MAO/Zr ratio increases, these eventually become solvent–separated ion pairs. These 'free' cations are responsible for the enhanced activity and improved comonomer response. The 'free' cations should facilitate β-hydride elimination by creating a four–centered, coplanar transition state for chain transfer[79].

The acceleration of the polymerization rate with metallocene catalysts in the presence of α-olefins may also be related to perturbations of the ion pair at the active site. α-Olefins can function not only as reactants but also as

ligands at the active site and, in such a role, serve to reduce the extent of interaction of the cationic zirconium center and the alumoxane counterion. The chemical nature of the counterion can have a profound effect on polymerization activity and stereoregularity, with 'inert', non–coordinating couteranions providing a route to higher activity[33, 86, 87].

The catalytic productivity of the zirconocene–alumoxane catalyst system depends on the [Al]/[Zr] ratios. It is well known that a high excess of MAO is needed to achieve optimum polymerization activity with metallocene catalysts. It is likely that the excess of MAO converts all the metallocene molecules into active centers, but it is also proposed that it reconverts the inactive intermediates which form, into the active species by an alkyl exchange reaction[89]. Both these effects give rise to an increase in the population of active species, which accounts for the increased activity.

In 1997 Forlini *et al* [90] showed that there is a high increase in activity for [Al]/[Zr] ratios between 1 000 and 3 000, but it becomes slower at higher MAO concentrations. A clear increase in molecular masses is also observed in the homo- and copolymerization as the [Al]/[Zr] ratio increases. This indicates that there is an increase in the rate of propagation, which is higher than that of chain termination, due to the higher activity and/or stability of the catalytic complexes in the presence of MAO[90].

It was found that an increase in the [Al]/[Zr] ratio did not have any influence on the homo- and copolymerization microstructure. Therefore, the excess MAO, that leads to an increase in the number of active species and makes the catalyst more active, and more stable, does not favour the insertion of certain comonomers above another. (Reactivity ratios remain constant.)

4.2.4.6 Polymerization Temperature

The temperature dependence of the copolymerization parameter of, for example, ethene/propene copolymers was investigated by Chien and Xu using *rac*-Et[Ind]$_2$ZrCl$_2$[37]. The copolymerization parameter of the bulkier α-olefin increased with increasing temperature. Mülenbrock and Fink[91]

reported temperature-dependant copolymerization parameters for ethene/1-hexene copolymerization, opposite to those of Chien and Xu[37]. Shum *et al* [55] found that an increase in temperature or a decrease in ethene concentration markedly influenced the copolymer's molecular mass, while for 1-octene incorporation in ethene/1-octene copolymers it remained constant. They concluded that the solution enthalpy of the different monomers has a potential influence on copolymerization parameters. In the copolymerization of ethene with 1-hexene or 1-octene, incorporation of 1-octene or 1-hexene increased with decreasing temperature, despite using different metallocenes and transition–metal to aluminium ratios for copolymerization.

4.2.4.7 Different Monomer Feed Ratios

Koivumäki *et al* [92] found that with the $Me_2C(Cp)(Flu)ZrCl_2$/MAO catalyst, above the [comonomer]/[ethene] ratio of one the polymerization rate of ethene: (1) increases markedly with 1-hexene, (2) increases slightly with 1-dodecene, and (3) decreases with 1-octadecene. The larger the comonomer the more difficult it is for the ethene monomer unit to insert itself and the ethene propagation reaction becomes slower. With the catalyst system *rac*-$Et[IndH_4]_2ZrCl_2$/MAO, the polymerization rate increased steadily, to a maximum at a [1-octadecene]/[ethene] ratio of two. Above this the rate decreased sharply.

Lehtinen *et al* [93] found that there were no great differences in the incorporation of hexene and hexadecene in the ethene/hexene and ethene/hexadecane copolymers. The molar contents in these copolymers remained low, even with very high comonomer ratios in the polymerization process. This was due to the low activity of the $Et(Ind)_2ZrCl_2$ catalyst used.

4.2.4.8 Different Cocatalysts

MAO is a relatively expensive chemical and Kaminsky–Sinn catalysts require a high concentration of it to achieve high activity. A major improvement towards simpler and cheaper metallocene–based systems will be to use other cocatalysts instead of MAO. Boron compounds, such as $B(C_6F_5)_3$, NR_3H^+ $B(C_6F_5)_4^-$ and $Ph_3C^+B(C_6F_5)_4^-$, in combination with metallocene dimethyls, can

be used as cocatalysts[94- 98]. Typically, cationic metallocene complexes can be formed by reactions of perfluorinated triphenylborane or trityltetrakis(pentafluorophenyl) borate:

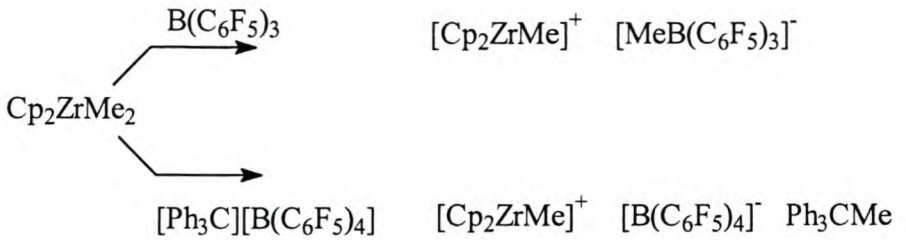

Whereas the ratio of MAO to metallocene needs to be around 5 000 : 1 for active catalyst systems, the required ratio of borate to metallocene is 1 : 1. As these systems are not able to scavenge impurities, a large part of the activated catalyst has to be sacrificed for that purpose. Better results have been achieved by adding small amounts of aluminium alkyls (AlR_3) to the borate catalyst system. AlR_3 scavenges impurities and alkylates the metallocene so that the simpler metallocene dichloride can be used[99, 100].

4.2.5 Conclusions

On the basis of the information available in the literature, as discussed in Section 4.2, some conclusions can be drawn, as they relate to **this** study.

(1) Bridged metallocene catalysts are more active in the copolymerization of propene than the non–bridged complexes.

(2) Copolymers obtained with metallocene catalysts contain higher amounts of α-olefins than those obtained with heterogeneous catalysts.

(3) The type of metallocene catalyst used will have an influence on the polymer microstructure, molecular mass and comonomer incorporation.

(4) A temperature study might be useful as the solution enthalpy of the different monomers at different temperature has an influence on the copolymerization parameters and therefore the incorporation of the comonomer. Molecular mass is also dependant on the polymerization

temperature, with an increasing reaction temperature leading to a decrease in molecular mass.

(5) The monomer feed ratio could have an influence on the incorporation of the comonomer, but it depends on the catalyst system and the different monomers used.

4.3 POLYMERIZATION REACTIONS OF 3-PHENYL-1-PROPENE WITH HIGHER α-OLEFINS

4.3.1 Introduction

In order to compare the relative effect of the adamantyl group and a phenyl group on the physical and thermal properties of the polymers such as T_g, an analogous series of copolymers were planned. This series comprised the copolymerization of 3-phenyl-1-propene with higher α-olefins using the C_2 symmetric *ansa* metallocene catalyst, *rac*-[(ethylene*bis*(1-indenyl)]zirconium dichloride ($Et(Ind)_2ZrCl_2$) with MAO as cocatalyst. Possible chain transfer reactions which occur during the copolymerization of 3-phenyl-1-propene with ethene using the metallocene catalyst, *rac*-[(ethylene*bis*(1-indenyl)]zirconium dichloride and MAO as cocatalyst, needs to be discussed. This information about the chain transfer reactions can lead to a better understanding of the copolymerization mechanism of 3-phenyl-1-propene as well as 3-(1-adamantyl)-1-propene and higher α-olefins.

4.3.2 Chain Transfer Reactions during the Copolymerization of Ethene with 3-phenyl-1-propene

Two chain transfer processes, β-hydride elimination and chain transfer to aluminium, are known as major chain transfer reactions in homogeneous Ziegler–Natta polymerization reactions[101]. It is reported that β-hydride elimination is the dominant chain transfer process during ethene polymerization with homogeneous metallocene catalysts[102, 103]. There are only a few reports that chain transfer to aluminium is a predominant chain transfer process with homogeneous metallocene catalysts[104].

Buyn *et al* reported that the chain transfer process occurred selectively depending upon catalysts in the metallocene–catalyzed 3-phenyl-1-propene polymerization[105]. A schematic representation of chain transfer reactions during the copolymerization of ethene and 3-phenyl-1-propene is shown in Scheme 4-1.

Buyn *et al* reported that chain transfer mainly occurred not through β-hydride elimination in the copolymerization of ethene with 3-phenyl-1-propene, but through chain transfer to aluminium[106]. ^{1}H NMR spectrum of the ethene-3-phenyl-1-propene did not show any peaks corresponding to vinyl or vinylidene end groups. This finding was corroborated in later studies[105].

Chain transfer to aluminium in the ethene-3-phenyl-1-propene copolymerization may be induced by the 3-phenyl-1-propene unit incorporated at the propagating chain end (see Scheme 4-1). The chain transfer reaction (H to Al) limits molecular weight of the copolymers. This could cause similar effects in the 3-(1-adamantyl)-1-propene polymer structures, where the presence of the even more bulky adamantyl group will hinder incorporation of the next monomer even more, while transfer to aluminum will occur more easily.

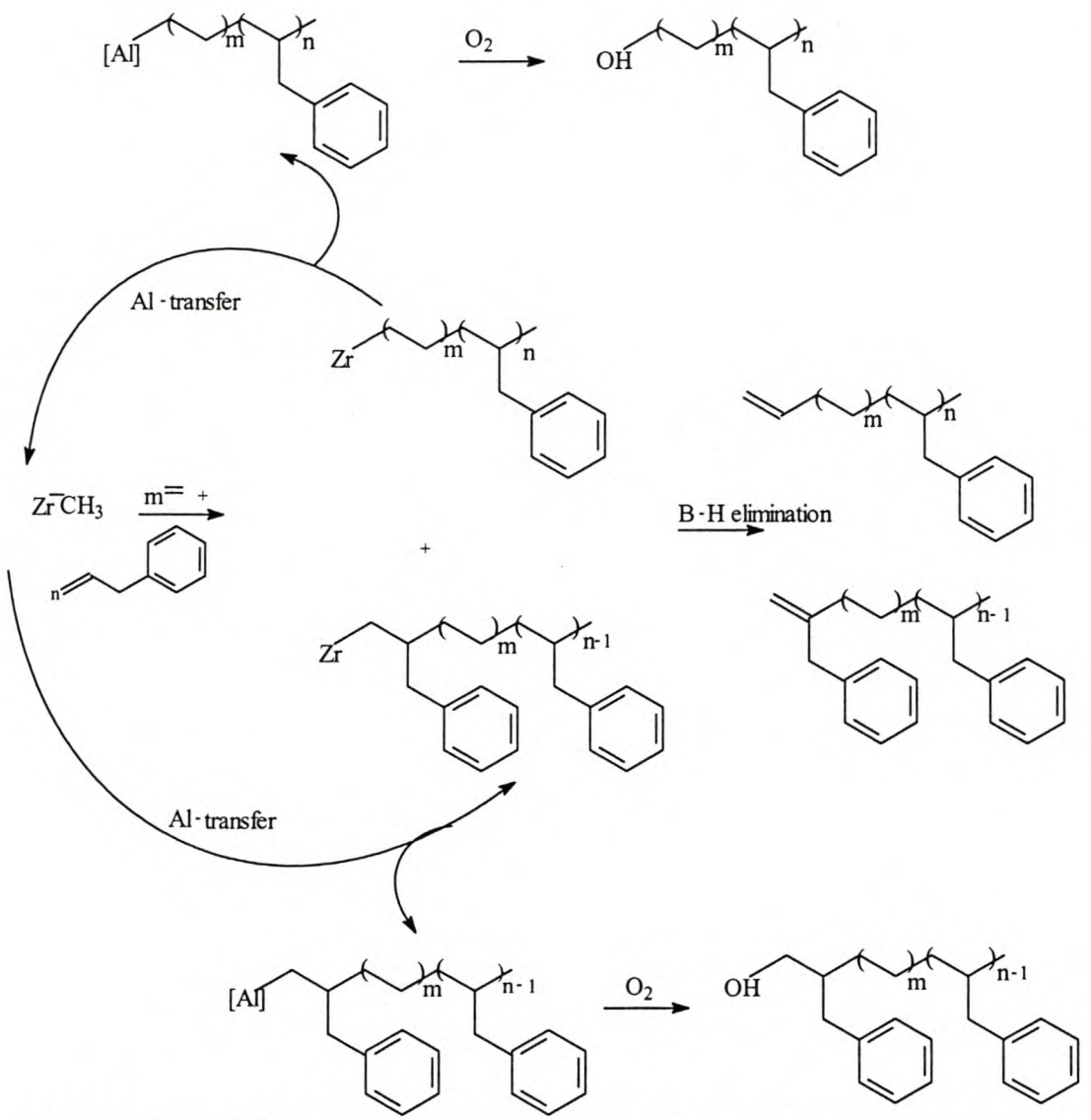

SCHEME 4–1: Schematic Representation of Chain Transfer Reaction in the Ethene-3-phenyl-1-propene Copolymerization

The catalysts of choice for the polymerization reactions of 3-(1-adamantyl)-1-propene as well as 3-phenyl-1-propene with α-olefins are the stereorigid, C_2-symmetric *ansa* metallocene ethylene *bis*(indenyl)zirconiumdichloride, $Et(Ind)_2ZrCl_2$, the unbridged *bis*(indenyl)zirconiumdichloride, Ind_2ZrCl_2 and a titanium based, silicon bridged constrained geometry catalyst, dimethylsilyl(*t*-butylamido)(tetramethylcyclpentadienyl)titaniumdimethyl.

Toluene was selected for use as solvent and an excess of MAO as cocatalyst. The effect of different amounts of 3-(1-adamantyl)-1-propene as well as 3-phenyl-1-propene in the copolymers on the physical and thermal properties, will be investigated.

4.4 GENERAL EXPERIMENTAL CONSIDERATIONS

In this Section, a general discussion concerning the materials, solvents, monomers, catalysts and cocatalysts used in the polymerization reactions of 3-(1-adamantyl)-1-propene as well as 3-phenyl-1-propene is done. The discussion includes the special handling and drying methods where necessary.

4.4.1 Materials

The most important factor in the preparation of reagents for the polymerization reactions was to ensure that all reagents had been adequately dried because of the moisture and air sensitivity of the catalyst systems used. All experiments with air- and moisture sensitive compounds were conducted in a nitrogen atmosphere, either by using standard Schlenk techniques or working in a dry box. Glassware as well as the reactors used were dried overnight at 120 °C before use, assembled hot and cooled in a nitrogen atmosphere.

4.4.1.1 Solvents

Toluene

Toluene was obtained from Saarchem.

Toluene (500 mL) was dried over sodium pieces and boiled under reflux, with a small amount of benzophenone, until the toluene had a dark blue color. Benzophenone was used as indicator to indicate when the toluene was dry. Toluene was then distilled onto 4 Å molecular sieve.

Methanol

Methanol was obtained from Saarchem and used without further purification.

4.4.1.2 Monomers

Ethene

Ethene (Copolymerization grade, 99 % minimum) was obtained from Fedgas and was used without further purification.

Propene

Propene was obtained from Messer Fedgas and was purified by passing through three columns containing BASF catalysts R3–11G and R3–12 and molecular sieve (3 Å) obtained from Polifin.

4-Methyl-1-Pentene

4-Methyl-1-pentene was obtained from Aldrich and used without further purification.

1-Pentene, 1-Hexene and 1-Octene

1-Pentene, 1-Hexene and 1-Octene was obtained from SASOL α-olefins. 1-Pentene (500 mL) was boiled under reflux[107] for 30 minutes over 0.5 g of lithium aluminium hydride ($LiAlH_4$) and distilled onto 4 Å molecular sieve.

3-(1-Adamantyl)-1-Propene

3-(1-Adamantyl)-1-propene was synthesized as described in Section 3.7. 3-(1-Adamantyl)-1-propene was dried over calcium hydride (CaH_2) and filtered through a GPC filter before it was used.

3-phenyl-1-propene

3-phenyl-1-propene was obtained from Aldrich. The monomer (250 mL) was dried over 2 g of calcium chloride ($CaCl_2$) and was used without further distillation.

4.4.1.3 Catalysts

Both catalysts were weighed out into Schlenk tubes in a dry box under a nitrogen atmosphere because of the air and moisture sensitivity of these catalysts. The catalysts were dissolved in toluene under a nitrogen atmosphere.

rac-[Ethylene _bis_(1-indenyl)] Zirconium Dichloride

rac-[Ethylene _bis_(1-indenyl)]zirconium dichloride was obtained from Aldrich and used without further purification.

Typically, ethylene bis(indenyl)zirconium dichloride, (5 mg; 1.2 x 10^{-5} mole) was weighed out in a dry box into a Schlenk tube and dissolved in 10 mL of toluene under nitrogen. For each polymerization reaction, 1 mL of the catalyst solution was used.

bis(1-Indenyl) Zirconium Dichloride

bis(1-Indenyl) zirconium dichloride was obtained from Aldrich and used as received.

Typically, _bis_(indenyl)zirconium dichloride, (5 mg; 1.3 x 10^{-5} mole) was weighed out in a dry box into a Schlenk tube and dissolved in 10 mL of toluene under nitrogen. For each polymerization reaction, 1 mL of the catalyst solution was used.

4.4.1.4 Cocatalyst

In all the polymerization reactions carried out with the two different catalytic systems, methyl alumoxane (MAO), obtained in a 10 % solution in toluene from Aldrich, was used as cocatalyst without further purification. MAO was chosen as cocatalyst because it can also act as a scavenger in the polymerization reactions.

The ratio of MAO to transition metal for both catalytic systems mentioned was maintained at 5 000 : 1.

4.4.2 Equipment used in the Polymerization Reactions

In this Section, a general discussion concerning the equipment used in the polymerization reactions of 3-(1-adamantyl)-1-propene as well as 3-phenyl-1-propene is done. The discussion includes the special handling and drying methods where necessary.

4.4.2.1 Plas Labs Dry Box[108]

Because of the air and moisture sensitive nature of the catalysts used in the polymerization reactions, the catalysts were weighed out in a nitrogen Plas Labs dry box, as was mentioned previously.

A nitrogen cylinder was connected to the dry box and nitrogen was dried by passage through an activated 4 Å molecular sieve column and a silica gel column before entering the dry box. A vacuum pump was connected to the loading compartment of the dry box.

A humidity meter was used to gain a rough measure of the moisture content during the preparation of the dry box. Surgical gloves were worn for working inside the dry box to prevent the evaporation of any skin moisture into the dry box.

4.4.2.2 Reactor

A 350 mL teflon–lined stainless–steel Parr autoclave was used in the copolymerization reactions of 3-(1-adamantyl)-1-propene with ethene and propene. The reactor was equipped with a fitted silicon ring, a pressure gauge and two inlets to work under nitrogen.

4.4.2.3 Schlenk Tubes

50 mL Schlenk tubes, equipped with a side arm and a stopcock to be able to work under a nitrogen atmosphere, were used for all the polymerization reactions as well as the copolymerization reactions of 3-(1-adamantyl)-1-propene with the higher α-olefins.

4.4.2.4 Syringes

50 mL, 20 mL, 10 mL, 5 mL and 2 mL Hamilton glass syringes as well as 1 mL disposable syringes were used for transfer of monomer, solvent, catalyst and MAO into the reactor or Schlenk tubes.

4.4.3 Analytical Methods and Instrumentation

The polymers formed were characterized by the following methods using the equipment described below.

4.4.3.1 Dfferential Scanning Caolrimetry (DSC) and Thermogravimetric Analyses (TGA)

See Section 3.4.4.1.

4.4.3.2 Infrared (IR) Spectroscopy

See Section 3.4.4.2.

4.4.3.3 Nuclear Magnetic Resonance Spectroscopy (NMR)

^{1}H and ^{13}C NMR spectra were recorded on a Varian VXR 300 Spectrometer at ambient temperature (20 °C) using 7 mm rotors and spinning rates of about 5 500 Hz. $CDCl_3$ was used as solvent throughout.

High temperature ^{1}H and ^{13}C NMR spectra were recorded on a Varian VXR 300 Spectrometer at 100 °C using 7 mm rotors and spinning rates of about 5 500Hz. A solvent mixture of 1:10 C_6D_6:1,2,4-trichlorobenzene was used for the high temperature NMR analyses.

The solid state ^{13}C Cross Polarization Magic Angle Spinning (CP MAS) spectra of the polymers were recorded at 75 MHz on a Varian VXR 300 spectrometer at ambient temperature (20 °C) using 7 mm rotors and spinning rates of about 5 500 Hz.

^{13}C NMR spectroscopy can be used to investigate the microstructure of 3-(1-adamantyl)-copolymers as well as 3-phenyl-1-propene copolymers with

respect to comonomer sequence disruption. It can also be used to determine ethyl, propyl and butyl branches concentrations independantly of the saturated end-groups. ^{13}C NMR spectroscopy therefore has a distinct advantage over corresponding infrared measurements because the latter technique can only detect methyl groups, irrespective of whether the methyl groups belongs to a butyl branch or chain end.

^{13}C NMR spectra were recorded by using the technique of full decoupling. The carbon–hydrogen interactions were decoupled by multiple irradiation. Such a spectrum then consists only of a number of singlets corresponding to carbon atoms in different chemical environments. The chemical shifts, as well as the multiplicity, could be determined by using the APT–pulse sequence, without a great loss in sensitivity. In order to distinguish between different carbon atoms, the ^{13}C signals were converted to negative and positive signals. The conditions are chosen in such a manner that CH_3- and CH-carbon atoms are characterized by negative amplitudes, while CH_2- and C-carbon atoms are characterized by positive amplitudes.

4.4.3.4 Dynamic Mechanical Analysis (DMA)

DMA analyses were performed using a Perkin Elmer Dynamic Mechanical Analyzer (7e). Samples were melt–casted at 120 °C for 15 minutes in a 9 mm (outside diameter) cup. The samples were allowed to reach room temperature before it was used. A 5 mm probe was used to do the analyses. The samples were cooled to –145 °C and held for three minutes before heating to 50 °C at a rate of 5 °C/min.

4.5 SYNTHESIS OF POLYMERS

4.5.1 General

4.5.1.1 Laboratory Safety

Almost without exception, polymerization reactions carry some element of danger. During the polymerization reactions under discussion, safety precautions beyond those routinely observed in any chemical laboratory are

required. Furthermore, the air and moisture sensitive nature of the catalysts used for these polymerizations required additional care to be exercised in its handling to avoid contact with air and moisture. The catalysts were therefore only handled in a nitrogen atmosphere.

The cocatalyst, MAO, used in these polymerization reactions is highly pyrophoric and special care had to be taken when handling it. MAO is also toxic and the primary health hazards which are associated with inhalation are nausea and that of skin contact is skin irritation.

4.5.1.2 Preparation of the Nitrogen Dry Box[108]

Because of the air and moisture sensitive nature of the catalysts used in the polymerization reactions, the catalysts were weighed out in a nitrogen dry box, as was mentioned previously.

The floor of the dry box was covered with a lining of plastic for protection against catalyst spills. The equipment used for weighing out the required amount of the catalysts, such as the balance, Schlenk tubes and spatula, were placed inside the dry box prior to closing the door. The window and other possible sources of air leaks were also sealed with silicon sealant.

Dry nitrogen gas was passed through the box, the nitrogen flow at an outlet being continuously monitored to ensure constant positive pressure. Thereafter the dry box was evacuated by switching on the vacuum pump for about 30 seconds (not longer, as the cabinet could not tolerate a very high negative pressure). Sucessive (three) evacuation and nitrogen flush cycles were carried out.

Close monitoring of the pressure was required during any operations carried out inside the dry box, otherwise the high positive pressure would have made it impossible to work. With the nitrogen from the cylinder flowing through the dry box, a very dry 'atmosphere' was constantly ensured while operations in the dry box were carried out. With the above-mentioned system in place, and dry nitrogen gas flushing the system, the humidity inside the dry box was low enough for the catalyst systems to be handled freely inside the dry box.

4.5.2 Polymerization Reactions with 3-(1-Adamantyl)-1-Propene

The homopolymerization reaction of 3-(1-adamantyl)-1-propene was carried out with the C_2 symmetric *ansa* metallocene catalyst, *rac*-[ethylenebis(1-indenyl)]zirconium dichloride. Copolymerization reactions of 3-(1-adamantyl)-1-propene with ethene, propene, 4-methyl-1-pentene, 1-pentene, 1-hexene and 1-octene were carried out with both the C_2 symmetric *ansa* metallocene catalyst, *rac*-[ethylenebis(1-indenyl)]zirconium dichloride and dimethylsilyl(*t*-butylamido)(tetramethylcyclpentadienyl) titaniumdimethyl.

The procedure followed for the polymerization reactions with 3-(1-adamantyl)-1-propene was a combination of those described in literature for similar reactions[109, 110]. The procedure is described below.

All required glassware, as well as the reactor were kept overnight in an oven at 120 °C to remove any residual moisture that could deactivate the metallocene catalyst system. The glassware was then cooled under a nitrogen atmosphere to prevent condensation of moisture that might cause possible contamination during the removal of the glassware from the oven. Whether the polymerization reactions were carried out either in the reactor or in Schlenk tubes, the reactor or the Schlenk tubes were charged under nitrogen. The precise amount of the prepared catalyst needed for the reaction, was weighed on a balance inside the Plas Labs nitrogen dry box.

4.5.2.1 Homopolymerization Reaction of 1-(3-Adamantyl)-1-Propene

The homopolymerization reaction of 3-(1-adamantyl)-1-propene was conducted in a 50 mL Schlenk tube under a nitrogen atmosphere. 3-(1-Adamantyl)-1-propene (1 g; 6 x 10^{-3} mole) was dissolved in 5 mL of toluene in a Schlenk tube equipped with a magnetic follower, side-arm and stopcock.

MAO (3.5 mL of a 10 % solution in toluene) was added. The catalyst *rac*-ethylenebis(indenyl)zirconium dichloride, (1.2 x 10^{-6} mole in 1 mL of toluene) was added. The Al : Zr ratio was 5 000 : 1. The Schlenk tube was

closed, heated to 80 °C and kept at that temperature for 18 hours. The Schlenk tube was then cooled and vented, and the polymer precipitated in acidic methanol (10 % HCl). The mixture was stirred for 24 hours, filtered, the product well washed with methanol and dried under reduced pressure.

4.5.2.2 Copolymerization Reactions of 1-(3-Adamantyl)-1-Propene with Ethene and Propene

Copolymerization reactions of 3-(1-adamantyl)-1-propene with ethene and propene were conducted in a 350 mL Parr autoclave under a nitrogen atmosphere. Typically, 3-(1-adamantyl)-1-propene (0.65 g; 4 x 10^{-3} mole) was dissolved in 10 mL of dry toluene and added to the reactor. The catalyst *rac*-ethylenebis(indenyl)zirconium dichloride or Cp_2ZrCl_2, (3.8 x 10^{-5} mole in 1 mL of toluene) and MAO (4 mL of a 10 % solution in toluene) were also added. The Al : Zr ratio for all the copolymerizations was maintained at 5 000 : 1. The reactor was sealed and pressurized to a pressure of 300 Psi with the gaseous monomer (ethene or propene). The reactor was heated to 80 °C and kept at that temperature for 18 hours. The reactor was then cooled and vented, and the polymer precipitated in acidic methanol (10 % HCl). The mixture was stirred for 24 hours, filtered, the product well washed with methanol and dried under reduced pressure.

4.5.2.3 Copolymerization Reactions of 3-(1-Adamantyl)-1-Propene with Higher α-Olefins

A series of copolymerizations of 3-(1-adamantyl)-1-propene with 4-methyl-1-pentene, 1-pentene, 1–hexene and 1–octene were carried out. The catalyst used in these copolymerizations was *rac*-[ethylenebis(1-indenyl)]zirconium dichloride. MAO was used as cocatalyst. The ratio of Al : catalyst was maintained at 5 000 : 1 for all the copolymerizations.

Typically, 4-methyl-1-pentene (1 g; 1 x 10^{-2} mole) and 3-(1-adamantyl)-1-propene (0.8 g; 5 x 10^{-3} mole) were dissolved in 5 mL of toluene in a Schlenk tube equipped with a magnetic follower, side-arm and stopcock. The

reaction mixture was repeatedly frozen in liquid nitrogen, evacuated and thawed. After the last freeze-thaw cycle, the reaction mixture was covered with a nitrogen atmosphere. The *rac* (ethylenebis(indenyl)zirconium dichloride (7×10^{-4} mole in 0.5 mL of toluene) was added by syringe, followed by 2.5 mL of a 10 % solution of MAO in toluene. The reaction flask was then placed in an oil bath at 40 °C and the reaction mixture stirred for three hours. The polymer was precipitated in acidic methanol and worked up as described in Section 4.5.2.2.

A series of copolymerizations of 4-methyl-1-pentene and different concentrations of 3-(1-adamantyl)-1-propene were done. The concentration of 3-(1-adamantyl)-1-propene used in the reaction mixture in these copolymerizations varied from 10 mole % to 30 mole %. NMR analysis as well as DMA analysis was done to investigate the physical and thermal properties of these copolymers. A comparison between the properties of the different copolymers with different concentrations of 3-(1-adamantyl)-1-propene incorporated, was done.

In the copolymerization reactions where 1-pentene, 1-hexene and 1-octene were copolymerized with 3-(1-adamantyl)-1-propene, it was not necessary to freeze–thaw the α-olefins, because the monomers were dried and purified as described in Section 4.4.1.2. These copolymerization reactions were carried out at 80 °C for 18 hours.

4.5.3 Polymerization Reactions with 3-Phenyl-1-Propene

The homopolymerization reaction of 3-phenyl-1-propene as well as the copolymerization reactions of 3-phenyl-1-propene with higher α-olefins were carried out with the bridged metallocene catalyst, *rac*-ethylenebis(indenyl)zirconium dichloride.

The procedure followed for the polymerization reactions with 3-phenyl-1-propene was described in literature for similar reactions[110]. The procedure is described below.

All experimental procedures involving the polymerization reactions, were conducted in a nitrogen atmosphere.

All glassware required were kept overnight in an oven at 120 °C to remove any residual water that could poison the metallocene catalyst system. The glassware were then cooled under a nitrogen atmosphere to remove any air or moisture that might cause possible contamination during the removal of the glassware from the oven. The required amount needed for the polymerization reactions, was weighed out using a balance inside the Plas Labs nitrogen dry box.

4.5.3.1 Homopolymerization Reaction of 3-Phenyl-1-Propene

The homopolymerization reaction of 3-phenyl-1-propene was conducted in a 50 mL Schlenk tube under a nitrogen atmosphere. 3-Phenyl-1-propene (1 g; 8.5×10^{-3} mole) was dissolved in 5 mL of toluene in a Schlenk tube equipped with a magnetic follower, side-arm and stopcock.

MAO (3.5 mL of a 10 % solution in toluene) was added. The bridged catalyst $Et(Ind)_2ZrCl_2$, (1.2×10^{-5} mole in 1 mL of toluene) was added. The Al : Zr ratio was 5 000 : 1. The Schlenk tube was closed, heated to 80 °C and kept at that temperature for 18 hours. The Schlenk tube was then cooled and vented, and the polymer precipitated in acidic methanol (10 % HCl). The mixture was stirred for 24 hours, filtered, the product well washed with methanol and dried under reduced pressure.

4.5.3.2 Copolymerization Reactions of 3-Phenyl-1-Propene with Higher α-Olefins

A series of copolymerizations of 3-phenyl-1-propene with 4-methyl-1-pentene, 1-pentene, 1–hexene and 1–octene were carried out. The catalyst used in all these copolymerizations was $Et(Ind)_2ZrCl_2$. MAO was used as cocatalyst. The ratio of Al : Zr was maintained at 5 000 : 1 for all the copolymerizations.

Typically, 4-methyl-1-pentene (1.33 g; 1.69×10^{-2} mole) and 3-phenyl-1-propene (1 g; 8.5×10^{-3} mole) were dissolved in 5 mL of toluene in a

Schlenk tube equipped with a magnetic follower, side-arm and stopcock. The reaction mixture was repeatedly frozen in liquid nitrogen, evacuated and thawed. After the last freeze-thaw cycle, the reaction mixture was covered with a nitrogen atmosphere. The ethylene *bis*(indenyl)zirconium dichloride (1.2×10^{-6} mole in 1 mL of toluene) was added by syringe, followed by 3.5 mL of a 10 % solution of MAO in toluene. The reaction flask was then placed in an oil bath at 40 °C and the reaction mixture stirred for 18 hours. The polymer was precipitated in acidic methanol and worked up as described in Section 4.5.2.1. Yield: 0.86 g (51 %).

All the other copolymerization reactions were carried out at 80 °C for 18 hours.

4.6 RESULTS AND DISCUSSION

4.6.1 Polymerization Reactions

The homopolymerization of 3-(1-adamantyl)-1-propene proceeded to a good yield compared with that reported in the Ziegler–Natta catalyzed polymerization (Yield: 12.5 %[109]). The powdery polymer product of poly[(3-(1-adamantyl)-1-propene] proved to be insoluble in all common organic solvents, even in chlorinated aromatic solvents at elevated temperatures.

3-(1-Adamantyl)-1-propene was successfully copolymerized with ethene, propene, 1-pentene, 4-methyl-1-pentene, 1-hexene and 1-octene with *rac*-ethylenebis(indenyl)zirconium dichloride.

The reaction mixtures used in the polymerization reactions done with the *rac*-ethylenebis(indenyl)zirconium dichloride, and their yields, are given in Table 4.3. Reaction temperatures for the polymerization of 3-(1-adamantyl)-1-propene with ethene, propene, 4-methyl-1-pentene, 1-pentene, 1-hexene and 1-octene varied from 40 °C to 80 °C. The Al/Zr ratio was maintained at 5 000 : 1 for all the reactions.

In all the copolymerization reactions of 3-(1-adamantyl)-1-propene with higher α-olefins, the yields of copolymer were lower than the corresponding olefin hompolymerization reaction. Nevertheless, reasonable yields were obtained in all cases. Most copolymers were insoluble in common organic solvents.

TABLE 4.3: Polymerization Reaction Mixtures and Yields for the Polymerization of 3-(1-adamantyl)-1-propene [3-7] with Ethene, Propene and Higher α-Olefins

Polymer	**[3-7]** (mole%)	α-olefin (mole%)	Temp (°C)	Yield(%)
Poly(1-octene)	0	100	60	55
Poly(1-octene-co-**[3-7]**)	37	63	60	50
Poly(1-hexene)	0	100	60	65
Poly(1-hexene-co-**[3-7]**)	33	67	60	60
Poly(4-methyl-1-pentene)	0	100	45	88
Poly(4-methyl-1-pentene-co-**[3-7]**)	28	72	45	53
Poly(4-methyl-1-pentene-co-**[3-7]**)	12	88	45	63
Poly(1-pentene)	0	100	35	83
Poly(1-pentene-co-**[3-7]**)	8.5	91.5	35	60
Poly(propene-co-**[3-7]**)			60	72
Poly(ethene-co-**[3-7]**)			60	72
Poly(**[3-7]**)	100	0	60	55

4.6.2 Thermal Analyses by Differential Scanning Calorimetry (DSC)

The 3-(1-adamantyl)-1-propene homopolymer was analyzed by DSC to determine the melting point. The sample was heated from ambient temperature to 300 °C, at a heating rate of 5 °C/min, in a nitrogen atmosphere with a flow rate of 58.2 mL/min. An average sample mass of 10 mg polymer was used.

The polymer showed no melting prior to degradation, but did show a glass transition temperature at 235 °C.

In addition to the homopolymer of 3-(1-adamantyl)-1-propene, homopolymers of ethene, propene, 4-methyl-1-pentene, 1-pentene, 1-hexene and 1-octene were also synthesized and analyzed, then compared with the copolymers of 3-(1-adamantyl)-1-propene and the α-olefins. In general, the homopolymers were isolated in good yields, although some difficulty in quantitatively isolating the viscous homopolymers of 1-octene and 1-hexene has resulted in the yield values reported in Table 4.3 being lower than the actual yields. Melting and glass transition temperatures for the homopolymers were reasonably close to the literature values for the Ziegler–Natta catalyzed poly(α-olefins), with the exception of poly(4-methyl-1-pentene), for which the T_m was noticeably lower for the metallocene catalyzed polymers (210 °C vs 245 °C).

The 1-ethene copolymers were found to be insoluble in all common organic solvents. While they exhibited DSC melting points, they showed no visual melting before the onset of degradation. These polymers also showed a glass transition temperature of 10 to 15 °C, albeit a small transition. No other transitions were observed at lower temperatures. The copolymer of ethene with 3-(1-adamantyl)-1-propene still showed a crystalline melting point (DSC) but did not become fluid prior to the onset of degradation.

The 1-propene copolymers were found to be insoluble in all common organic solvents. While they exhibited DSC melting points, they showed no visual melting before the onset of degradation. These polymers also showed a

glass transition temperature of about –10 °C. No other transitions were observed at lower temperatures.

The copolymerization of 3-(1-adamantyl)-1-propene with 1-octene yielded an amorphous material with a T_g of –19 °C, which is 54 °C higher than the corresponding α-olefin homopolymer (Figure 4-8). Similarly, the T_g of the copolymers of 3-(1-adamantyl)-1-propene with 1-hexene and 3-(1-adamantyl)-1-propene with 1-pentene resulted in amorphous materials with T_g values higher than those of the homopolymer. In the case of poly[3-(1-adamantyl)-1-propene-co-1-pentene], the melting point present in the 1-pentene homopolymer disappears in the copolymer, making it clear that the presence of the bulky adamantylmethyl substituent severely disrupts the crystallinity as well as influencing the T_g. In the case of this poly[3-(1-adamantyl)-1-propene-co-1-pentene] copolymer, the T_g only differs by 10 °C for the homopolymer, but as only 8.5 mole % of 3-(1-adamantyl)-1-propene was used in this reaction, its incorporation into the copolymer is probably very limited.

In the case of the copolymerization of 3-(1-adamantyl)-1-propene with 4-methyl-1-pentene, where the poly(α-olefin) has a glass transition temperature of 45 °C, the following was found. In the copolymer formed when the concentration of 3-(1-adamantyl)-1-propene in the reaction mixture was low (12 mole %), the T_g was not affected to a large degree, although the crystallinity was apparently disrupted. Evidence for this was a lower melting point and a decreased heat of fusion. When the concentration of 3-(1-adamantyl)-1-propene in the reaction mixture was increased to 28 mole %, the resultant copolymer showed no crystallinity whatsoever, and a T_g of 69 °C. After heating and fusion, these copolymers appeared translucent. Table 4.4 shows the glass transition and melting temperatures of the homo- and copolymers of 3-(1-adamantyl)-1-propene and higher α-olefins.

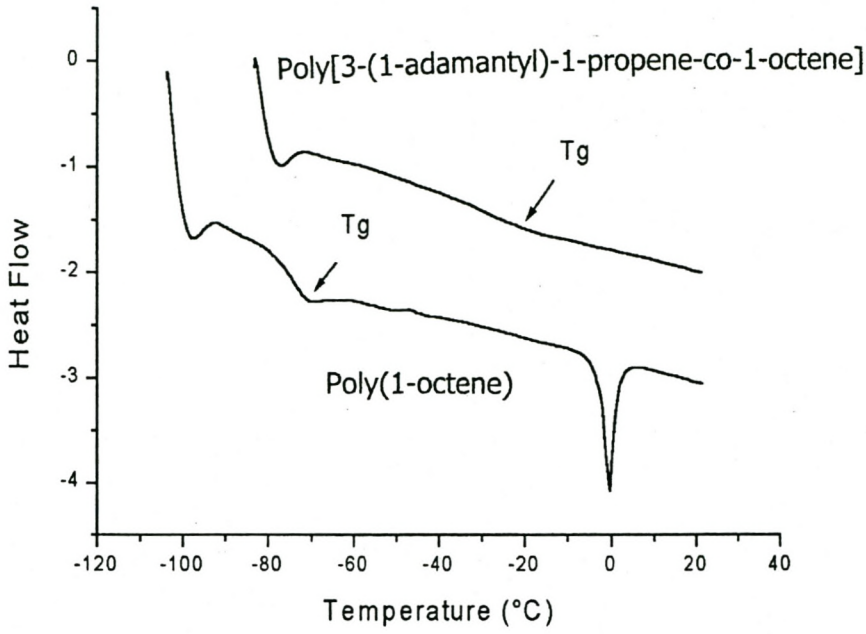

FIGURE 4-8: DSC Scan of poly(1-octene) and poly[(3-(1-adamantyl)-1-propene-co-1-octene]

TABLE 4.4: Glass Transition and Melting Temperatures of Homo- and Copolymers of 3-(1-adamantyl)-1-propene [3-7] and Higher α-Olefins

Polymer	Tg (°C)	Tm (°C)
Poly(1-octene)	-73	-0.5
Poly(1-octene-co-**[3-7]**)	-19	ND
Poly(1-hexene)	-53	ND
Poly(1-hexene-co-**[3-7]**)	-13	ND
Poly(1-pentene)	-38	75
Poly(1-pentene-co-**[3-7]**)	-25	ND
Poly(4-methyl-1-pentene)	45	210
Poly(4-methyl1-pentene-co-**[3-7]**)A	69	ND
Poly(4-methyl-1-pentene-co-**[3-7]**B)	47	168
Poly(ethene)	5	138
Poly(ethene-co-**[3-7]**)	12	124
Poly(propene)	-10	130
Poly(propene-co-**[3-7]**)	ND	128
Poly(**[3-7]**)	235	ND

4.6.2.1 DSC Analyses: Conclusions

(1) The glass transition temperatures as well as the melting points for the α-olefin homopolymers were reasonably close to the literature values for the Ziegler-Natta catalyzed poly(α-olefins) with the exception of poly(4-methyl-1-pentene), for which the T_m was noticeably lower for the metallocene–catalyzed polymers (210 °C vs. 245 °C).

(2) The homopolymer of 3-(1-adamantyl)-1-propene showed no melting prior to degradation, but did show a T_g at 235 °C.

(3) The T_g's of most of the 3-(1-adamantyl)-1-propene-α-olefin copolymers were higher than those of the corresponding homopolymers.

(4) From the T_g results it is clear that the incorporation of the bulky adamantyl pendant group severely disrupts the crystalline structure as well as influencing the T_g's of the polymers.

4.6.3 Compositional Analyses

Infrared spectroscopy (IR) and nuclear magnetic resonance spectroscopy (NMR) were used to determine the physical structure of the polymers synthesized as described in Section 4.5.2. ^{13}C NMR spectroscopy was used to investigate the microstructure of 3-(1-adamantyl)-1-propene homo- and copolymers. It was used to determine the concentrations of ethyl, propyl and butyl branches concentrations independant of the saturated end–groups. ^{13}C NMR spectroscopy therefore has a distinct advantage over corresponding infrared measurements because the latter technique can only detect methyl groups, irrespective of whether the methyl groups belong to a butyl branch or chain end.

4.6.3.1 Photo-Acoustic Infrared Spectroscopy (PAS-IR)

A Perkin Elmer FTIR instrument in conjunction with a photo–acoustic detector system, was used. This method obviates sample preparation and gives spectra that compare well with those obtained with other IR techniques. The spectral characteristics expected for the 3-(1-adamantyl)-1-propene homopolymer can be predicted.

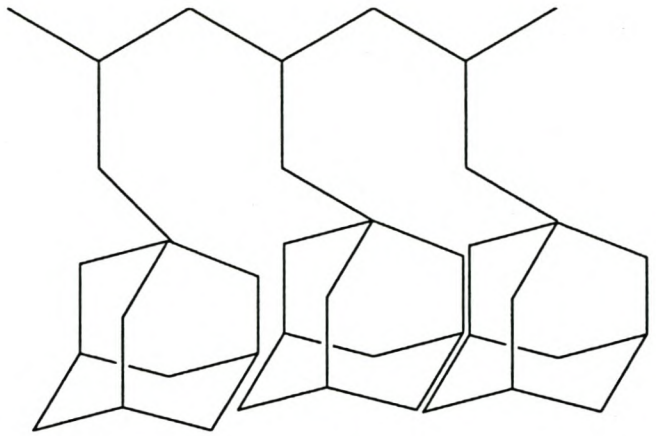

For the CH_2– and CH- groups in the polymer backbone the following are expected:

- C–H stretch vibrations, both symmetrical at 2 900 cm^{-1} and asymmetrical at 2 844 cm^{-1}
- $-CH_2-$ scissor vibrations at 1 450 cm^{-1}

For the adamantyl group:

- C-H stretch vibrations, both symmetrical at 2 900 cm^{-1} and assymetrical at 2 844 cm^{-1}
- $-CH_2$ wag vibrations, assymetrical at 1 260 cm^{-1} due to HCC angle bending
- C-H vibrations at 1 100 cm^{-1} due to deformation

The FTIR analysis of the homopolymer of 3-(1-adamantyl)-1-propene shown in Figure 4-9 confirmed the expected structure.

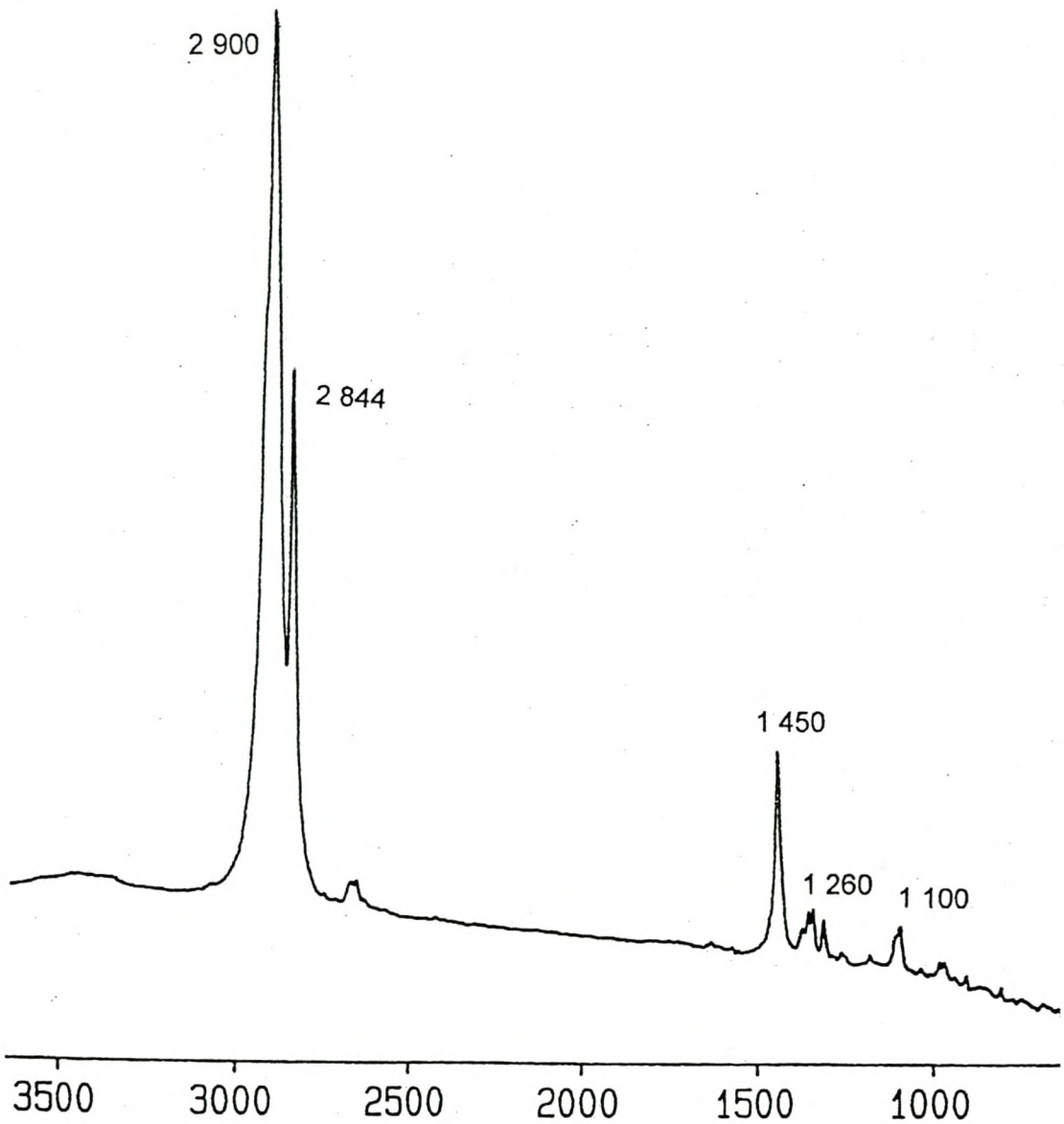

FIGURE 4-9: IR Spectrum of poly[(3-(1-adamantyl)-1-propene]

4.6.3.2 Nuclear Magnetic Resonance Spectroscopy (NMR)

^{13}C NMR spectroscopy can be used to investigate the microstructure of 3-(1-adamantyl)-copolymers with respect to comonomer sequence distribution. It can also be used to determine ethyl, propyl and butyl branch concentrations independantly of the saturated end–groups. ^{13}C NMR

spectroscopy therefore has a distinct advantage over corresponding infrared measurements because the latter technique can only detect methyl groups, irrespective of whether the methyl groups belongs to a butyl branch or chain end.

(i) Homopolymerization Reaction

The solid state NMR spectrum of poly[3-(1-adamantyl)-1-propene] is shown in Figure 4–10 and the chemical shift values are given in Table 4.5.

TABLE 4.5: Comparison of Expected and Observed ^{13}C NMR Chemical Shifts (δ) of poly[(3-(1-adamantyl)-1-propene]

Carbon	Expected	Observed
a	27.90*	29.99
b	36.90*	38 - 34
c	43.60*	44.84
d	27.0**	N/D
e	49.0**	52 - 49
f	25.0**	25.63
g	41.0**	N/D

*: Based on monomer spectra; **: Based on spectra of poly(4-methyl-1-pentene) and related polymers.

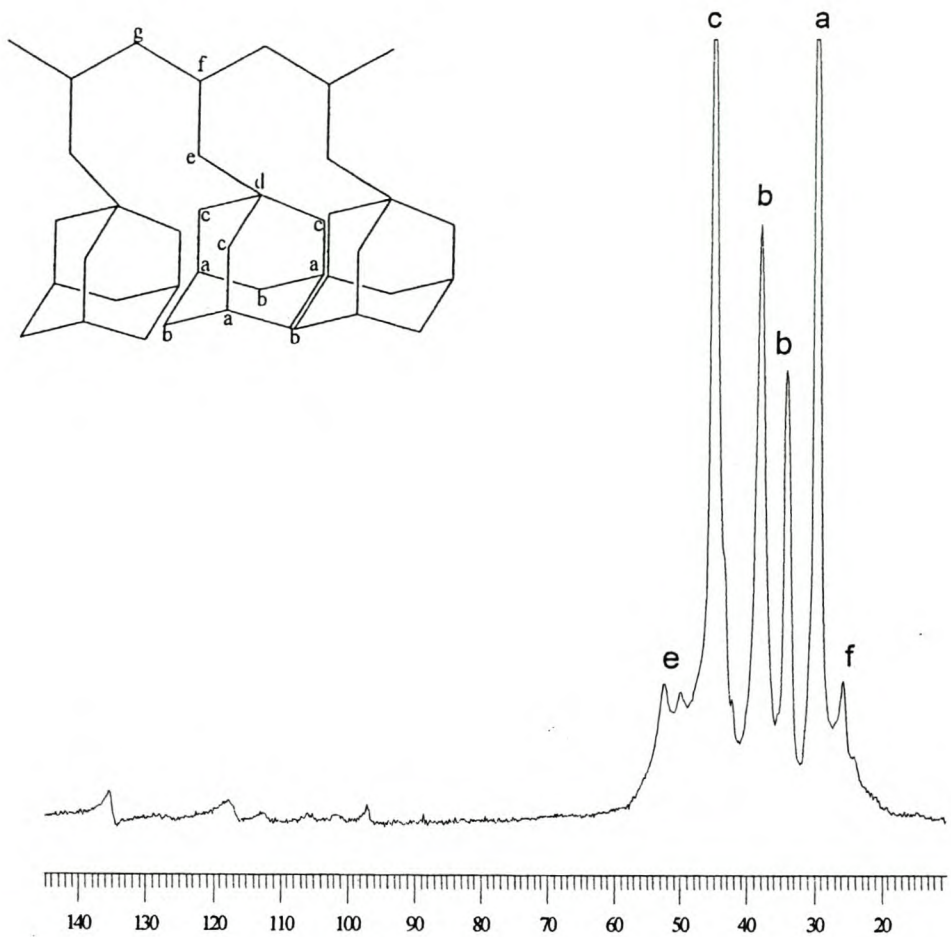

FIGURE 4-10: Solid State ^{13}C NMR Spectrum of poly[(3-(1-adamantyl)-1-propene]

From Table 4.5 one can see a very good comparison of the chemical shifts expected from similar hydrocarbon polymers (with $-CH_2$ groups in the α-position relative to the carbon chain and branching in the β-position) and the chemical shifts observed from the ^{13}C NMR spectrum. The spectrum is consistent with the structure shown above. In the case of carbons **d** and **g**, it is very difficult to observe the peaks from the ^{13}C NMR spectrum, as the areas in which these peaks are expected are hidden under larger peak areas, although a shoulder on the peak at 44.84 ppm could be the main-chain carbon peak at ca 41 ppm. Similarly it is possible that carbon **d** lies underneath the broad shoulder of the peak at 29.99 ppm. The signals at 29.99 ppm and 44.84 ppm represent the two adamantane signals of carbons **a** and **c**. The signal for carbons **b** (34 -38 ppm) appears to be split, probably

due to steric effects. Similarly the signal for carbon **e** seems to be split in two discernable signals. The reason for this is not clear.

The presence of the two small peaks at 118 ppm and 136 ppm could be because of residual monomers present or unsaturation at the chain end.

(ii) Copolymerization Reactions

(a) Copolymers with Ethene

The solid state ^{13}C NMR spectrum (Figure 4-11) clearly indicates the incorporation of 3-(1-adamantyl)-1-propene in the copolymer, with the peak assignments shown in Table 4.6. The reason for the infusibility of these materials is unclear. A possibility is the occurrence of crosslinking, but a possible mechanism for the crosslinking is not immediately obvious.

TABLE 4.6: Comparison of Expected and Observed ^{13}C NMR Chemical Shifts (δ) of poly[(3-(1-adamantyl)-1-propene-co-ethene]

Carbon	Expected	Observed
a	27.90*	29.88
b	36.90*	38.03
c	43.60*	43.32
d	27.0**	N/D
e	49.0**	N/D
f	25.0**	N/D
g	41.0**	32.94

*: Based on monomer spectra; **: Based on spectra of poly(ethylene) and related polymers.

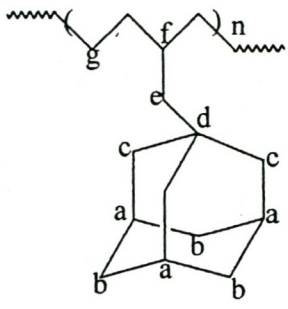

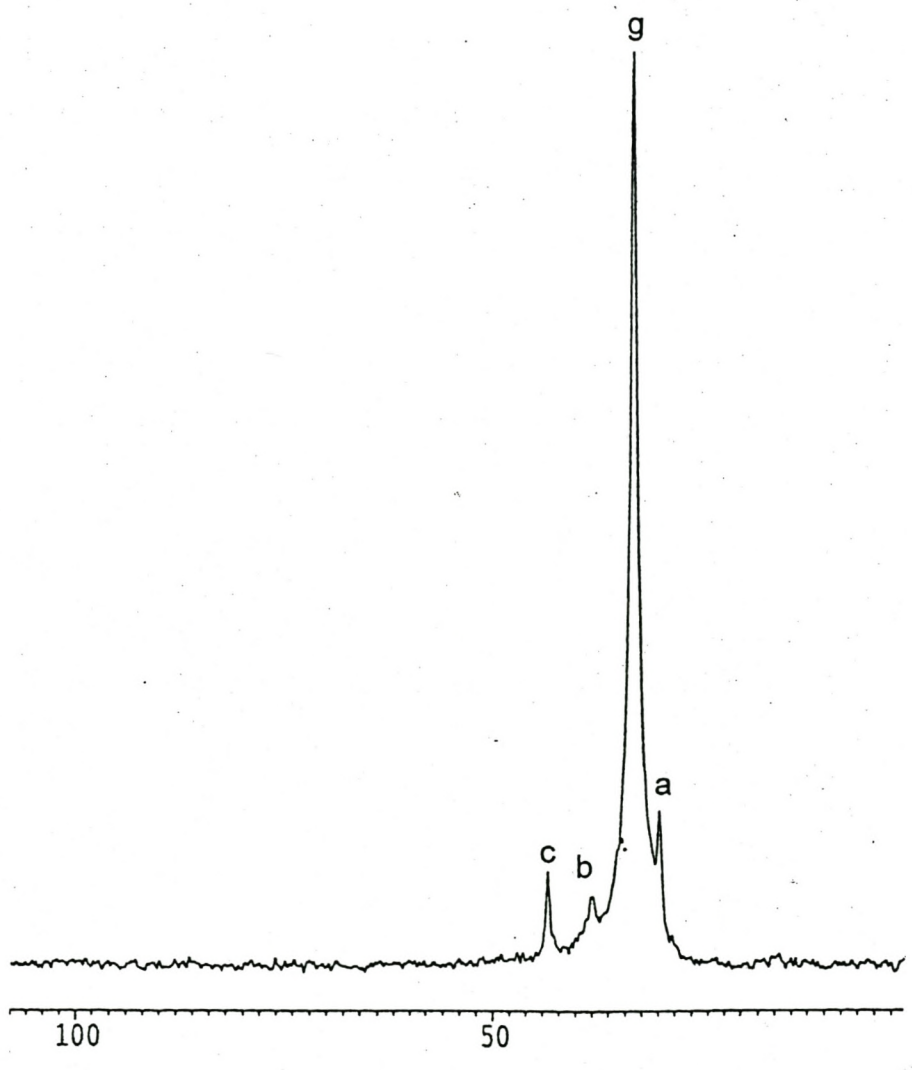

FIGURE 4-11: Solid State ^{13}C NMR Spectrum of poly[3-(1-adamantyl)-1-propene-co-ethene]

From Table 4.6 one can see a very good comparison of the chemical shifts expected from poly(ethylene) polymers (with $-CH_2$ groups in the α-position relative to the carbon chain and branching in the β-position) and the chemical shifts observed from the ^{13}C NMR spectrum. We expect the polymer to be predominantly poly(ethylene) with a small amount of 3-(1-adamantyl)-1-propene incorporated. The spectrum is consistent with the structure shown above. The signals at 29.88 ppm, 38.03 ppm and 43.32 ppm represent the three adamantane signals of carbons **a**, **b** and **c**. In this case, the signal at 32.94 ppm, which represents the poly(ethylene) backbone signal **g**, has a very high intensity relative to the other signals. Therefore, as one can see from the spectrum, the intensity of the signals that represent the adamantane carbons are very small relative to the intensity of the ethene peak. In the case of carbons **d**, **e** and **f**, it is very difficult to observe the peaks from the ^{13}C NMR spectrum, as the areas in which these peaks are expected are hidden under larger peak areas. Another factor that could attribute to the fact that carbon **d** can't be seen from the spectrum is the steric hinderance from the adamantane ring as well as the poly(ethylene) backbone. Therefore, only four signals are present in the ^{13}C NMR spectrum. From the ^{13}C NMR spectrum of poly[3-(1-adamantyl)-1-propene-co-ethene] it is clear that only a small amount of 3-(1-adamantyl)-1-propene was incorporated into the poly(ethylene) backbone.

(b) Copolymers with Propene

The solid state ^{13}C NMR spectrum (Figure 4-12) clearly indicates the incorporation of 3-(adamantyl)-1-propene in the copolymer, with the peak assignments shown in Table 4.7. The reason for the infusibility of these materials is unclear. A possibility is the occurrence of crosslinking, but a possible mechanism is not immediately obvious.

TABLE 4.7: Comparison of Expected and Observed ^{13}C NMR Chemical Shifts (δ) of poly[(3-(1-adamantyl)-1-propene-co-propene]

Carbon	Expected	Observed
a	27.90*	29.10
b	36.90*	38-34
c	43.60*	46.16
d	27.0**	N/D
e	41.0**	N/D
f	31.0**	33.43
g	41.0**	40.15
h	20.0**	17.57
i	28.0**	22.34

*: Based on monomer spectra; **: Based on spectra of poly(propylene).

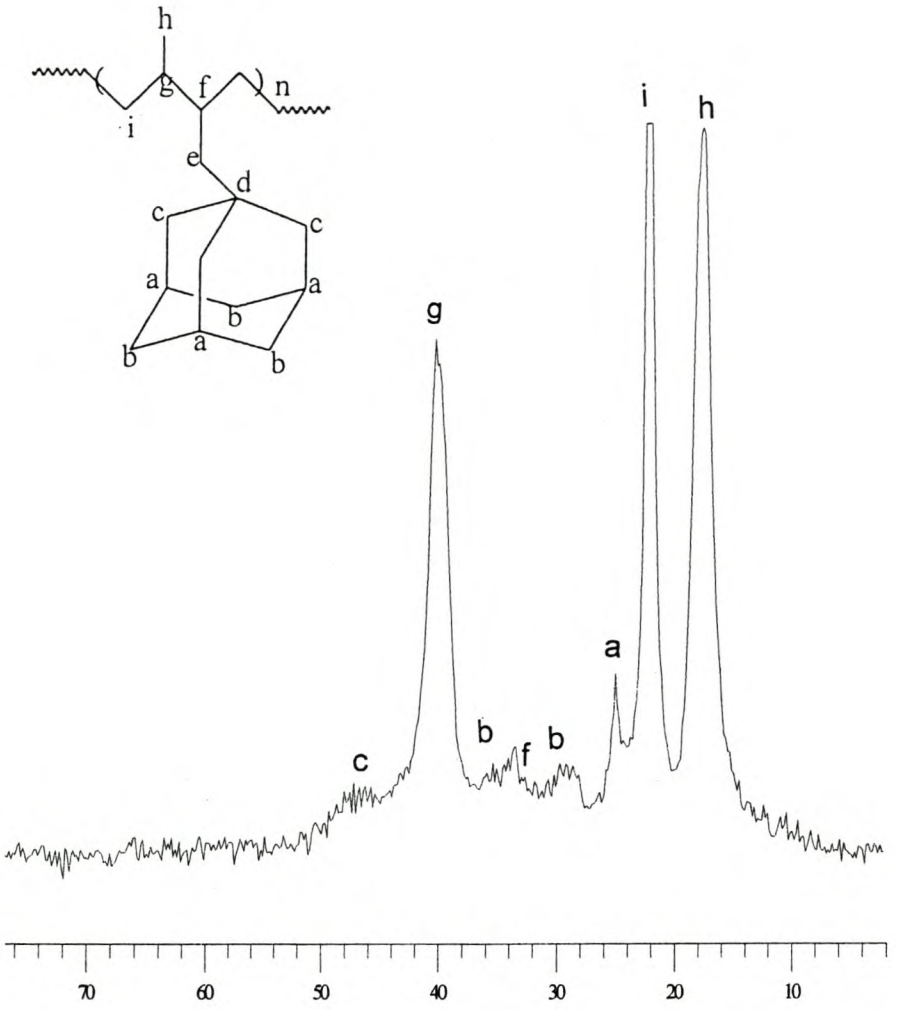

FIGURE 4-12: Solid State ^{13}C NMR Spectrum of poly[(3-adamantyl)-1-propene-co-propene]

Form Table 4.7 one can see a very good comparison of the chemical shifts expected from poly(propylene) polymers (with $-CH_2$ groups in the α-position relative to the carbon chain and branching in the β-position) and the chemical shifts observed from the ^{13}C NMR spectrum. We expect the polymer to be predominantly poly(propylene) with a small amount of 3-(1-adamantyl)-1-propene incorporated. The spectrum is consistent with the structure shown above. In the case of carbons **d** and **e**, it is very difficult to observe the peaks from the ^{13}C NMR spectrum, as the areas in which these peaks are expected are hidden under larger peak areas. Similarly it is possible that carbon **d** lies underneath the broad peak at 29.10 ppm. Another factor that could attribute to the fact that carbon **d** can't be seen from the spectrum is the

steric hinderance from the adamantane ring as well as the poly(propylene) backbone. The signals at 29.10 ppm and 46.16 ppm represent the two adamantane signals of carbons **a** and **c**. The signal for carbons **b** (34-38 ppm) may be hidden underneath the broad shoulder of the peak appearing at 40.15 ppm In this case, the signal at 22.34 ppm, which represents carbon **i**, is one of the poly(propylene) backbone signals and has a very high intensity. The signals representing carbons **f** and **g**, appear at chemical shifts of 33.43 ppm and 40.15 ppm respectively. The signal at 17.57 ppm, represents carbon **h**. There is no logical explanation for the appearance of the peak at 24.86 ppm.

(c) Copolymers with Higher α-Olefins

A typical solid–state ^{13}C NMR spectrum of the copolymer of 3-(1-adamantyl)-1-propene and 4-methyl-1-pentene is shown in Figure 4-13. Figure 4-14 is the ^{13}C NMR spectrum of poly(4-methyl-1-pentene). The spectrum of poly(4-methyl-1-pentene) was used to identify the peaks in the spectrum of poly[3-(1-adamantyl)-1-propene-co-4-methyl-1-pentene]. Peak assignments for the spectrum of poly[3-(1-adamantyl)-1-propene-co-4-methyl-1-pentene] are given in Table 4.8. Peak assignments for the copolymers of 3-(1-adamantyl)-1-propene with 1-pentene, 1-hexene and 1-octene are given in Tables 4.9 to 4.12.

TABLE 4.8: Comparison of Expected and Calculated ^{13}C NMR Chemical Shifts (δ) of poly[(3-(1-adamantyl)-1-propene-co-4-methyl-1-pentene]

Carbon	Expected	Observed
a	27.90*	29.10
b	36.90*	38.17
c	43.60*	43.68
d	27.0**	N/D
e	49.0**	N/D
f	23.0**	23.12
g	26.0**	25.78
h	32.0**	33.97
i	40.0**	42.35
j	44.0**	46.40

*: Based on monomer spectra; **: Based on spectra of poly(4-methyl-1-pentene) (See Figure 4-14) and related polymers.

From Table 4.8 one can see a very good comparison of the chemical shifts expected from poly(4-methyl-1-pentene) polymers (with $-CH_2$ groups in the α-position relative to the carbon chain and branching in the β-position) and the chemical shifts observed from the ^{13}C NMR spectrum. We expect the polymers to be predominantly poly(4-methyl-1-pentene) with a small amount of 3-(1-adamantyl)-1-propene incorporated. The NMR spectra of poly(4-methyl-1-pentene) (bottom spectrum, B) and poly[3-(1-adamantyl)-1-propene-co-4-methyl-1-pentene] (A) are shown in Figure 4-13. The arrows denote the peaks due to the adamantane ring carbons. The bridgehead methine carbons are clearly visible, while the methylene carbons (**c**) appear as a shoulder on the peak at 43 ppm. The other carbons due to the adamantyl-containing units are not visible, as they are most likely hidden under the poly(4-methyl-1-pentene) peaks. Noticeable is that the peak at 33 ppm which is visible in the spectrum of poly(4-methyl-1-pentene) is shifted slightly downfield in the copolymer spectrum, and is greatly reduced. This is due to the disruption of the microstructure of the 4-methyl-1-pentene sequences. It is interesting to note that the solid state spectrum (B) of

poly(4-methyl-1-pentene) is significantly different from the high-temperature liquid-phase ^{13}C NMR spectrum of the same polymer (Figure 4-14). From Figure 4-13 we can conclude that 3-(1-adamantyl propene) was successfully copolymerized with 4-methyl-1-pentene.

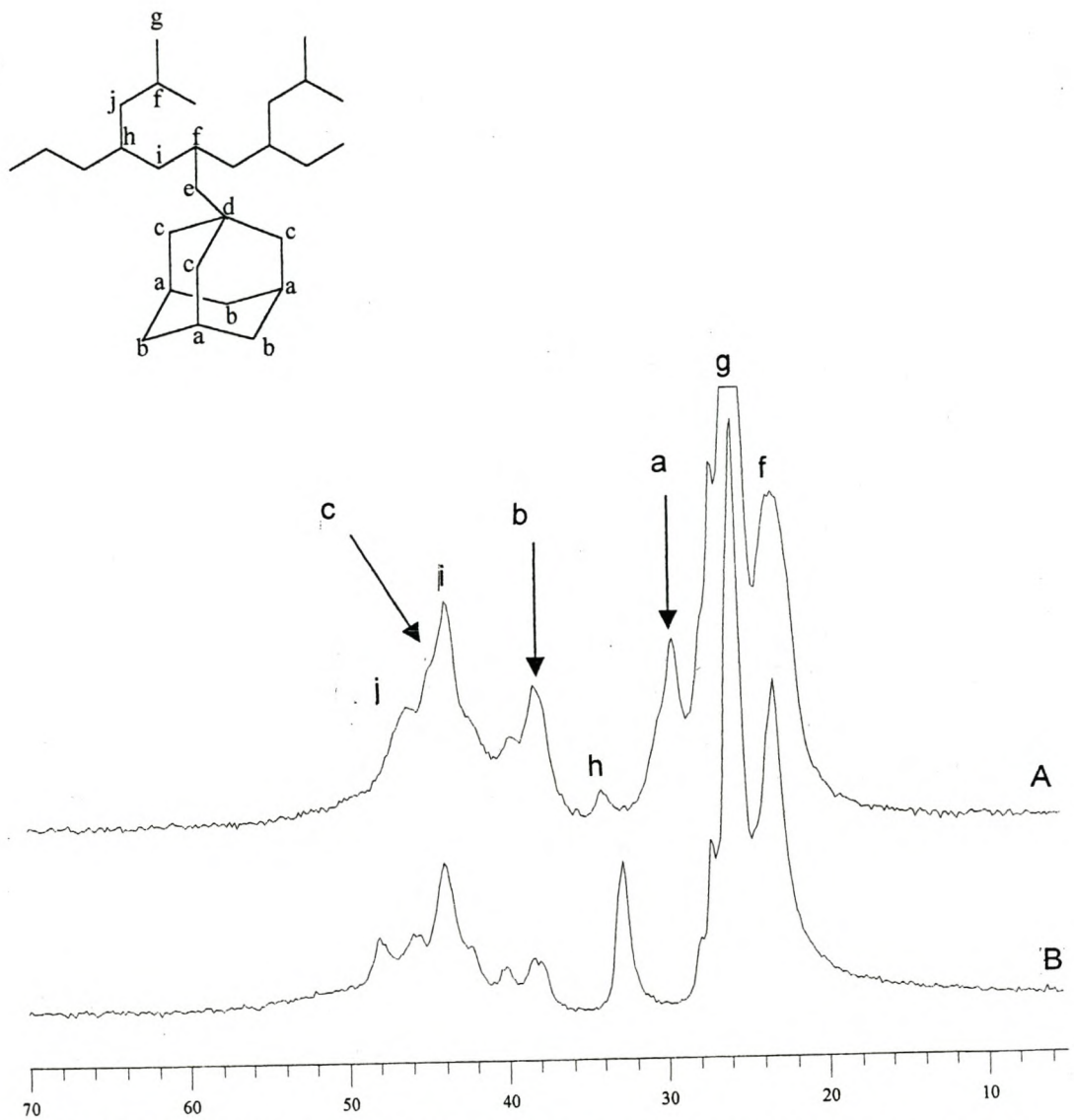

Figure 4-13. The solid state 13C NMR spectra of poly(4-methyl-1-pentene) and poly[(3-(1-adamantyl)-1-propene-co-4-methyl-1-pentene]

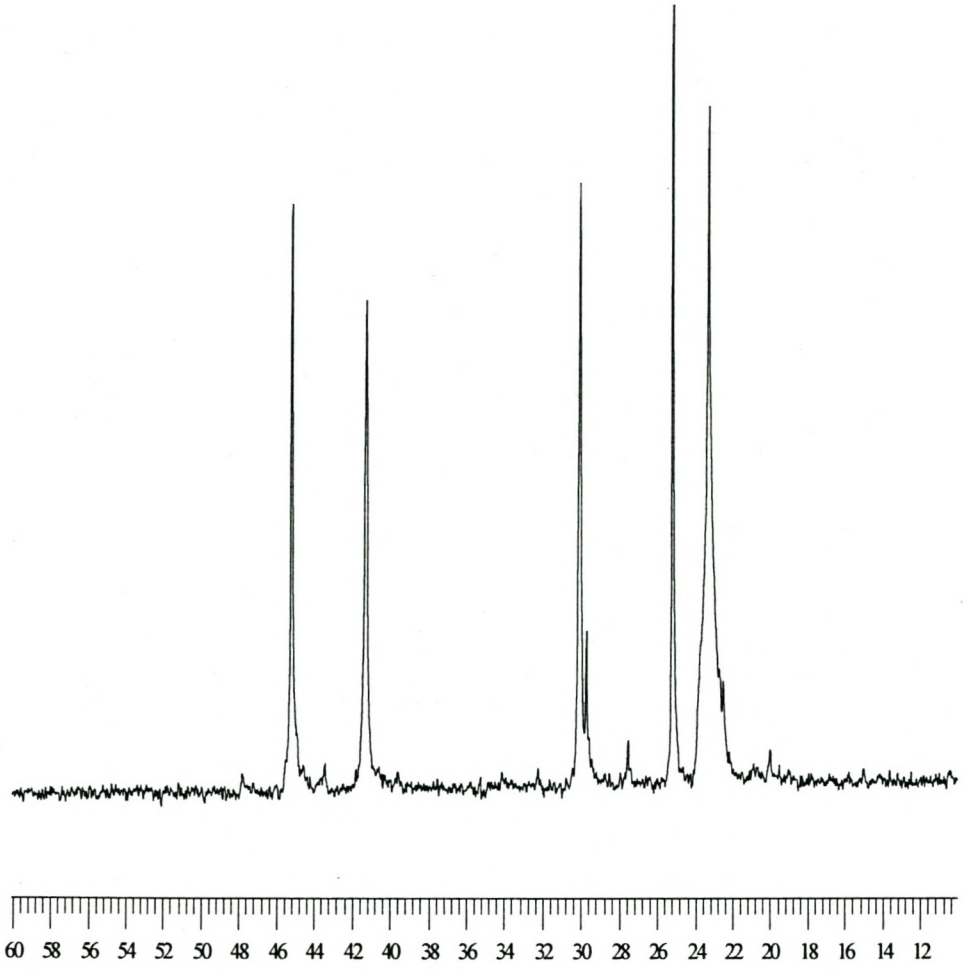

FIGURE 4-14: ^{13}C NMR Spectrum of poly(4-methyl-1-pentene)

A schematic representation of poly[3-(1-adamantyl)-1-propene-co-1-pentene] is presented below:

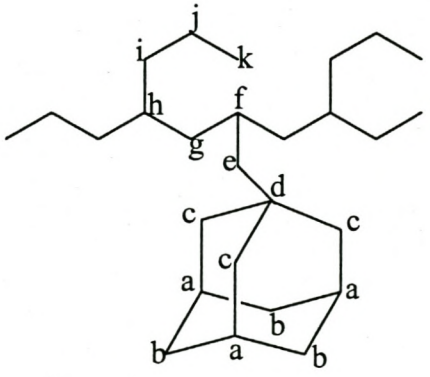

We expect the polymers to be predominantly poly(α-olefins) with a small amount of 3-(1-adamantyl)-1-propene incorporated. The expected ^{13}C NMR shift values for the poly(α-olefins) are given in Table 4.9.

TABLE 4.9: ^{13}C NMR Chemical Shifts (ppm) in $CDCl_3$ and Assignment of the Signals to the Respective C Atom for Poly(α-Olefins)[110]

	C1	C2	C3	C4	C5	C6	C8
Poly(1-pentene)	40.47	32.48	37.52	19.65	14.69		
Poly(1-hexene)	40.43	32.55	34.76	28.85	23.34	14.24	
Poly(1-octene)	40.43	32.58	35.14	26.60	30.07	32.16	14.18

In the above Table, the carbons are numbered as follows: The main-chain methylene carbons are denoted as C1. The main-chain methine carbons as C2, and the side-chain carbons numbered sequentially with the highest number representing the methyl group (e.g C5 for poly(1-pentene) and C8 for poly(1-octene)), and the lowest number the methylene carbon adjacent to C2.

TABLE 4.10: Comparison of Expected and Observed ^{13}C NMR Chemical Shifts (δ) of poly[(3-(1-adamantyl)-1-propene-co-1-pentene]

Carbon	Expected	Observed
a	27.90*	28.10
b	36.90*	38.10
c	43.60*	43.88
d	27.0**	N/D
e	37.52**	35.80
f	25.0**	25.40
g	40.47**	41.40
h	32.48**	32.90
i	37.52**	36.40
j	19.65**	20.80
k	14.69**	18.20

*: Based on monomer spectra; **: Based on spectra of poly(1-pentene).

Form Table 4.10 one can see a very good comparison of the chemical shifts expected from poly(1-pentene) polymers (with $-CH_2$ groups in the α-position relative to the carbon chain and branching in the β-position) and the chemical shifts observed from the ^{13}C NMR spectrum. We expect the polymers to be predominantly poly(α-olefins) with a small amount of 3-(1-adamantyl)-1-propene incorporated. The spectrum is consistent with the structure shown above. In the case of carbon **d**, it is very difficult to observe the peak from the ^{13}C NMR spectrum. Another factor that could attribute to the fact that carbon **d** can't be seen from the spectrum is the steric hinderance from the adamantane ring as well as the poly(1-pentene) backbone. In this case, the signal at 41.40 ppm, represents carbon **g** and is one of the poly(1-pentene) backbone carbons. The signals representing the α-carbons relative to carbon **g**, carbons **f** and **h**, appear at chemical shifts of 25.40 ppm and 32.90 ppm. The signal representing carbon **i** appears at 36.40 ppm. The signal at 35.80 ppm, represents the other β-carbon relative to carbon **g**, carbon **e**. The signal at 18.20 ppm represents carbon **k**. The signals at 28.10 ppm, 38.10 ppm and 43.88 ppm represent the three adamantane carbon signals of carbons **a**, **b** and **c.** The signal at 20.80 ppm represents carbon **j**.

A schematic representation of poly[3-(1-adamantyl)-1-propene-co-1-hexene] is presented below:

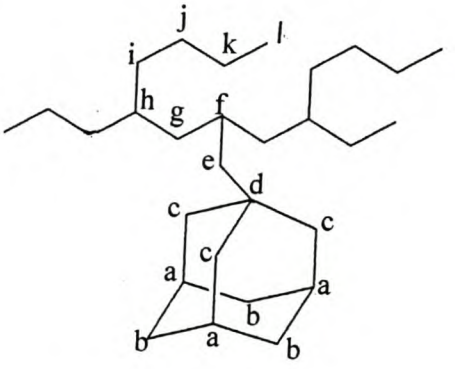

TABLE 4.11: Comparison of Expected and Observed ^{13}C NMR Chemical Shifts (δ) of poly[(3-(1-adamantyl)-1-propene-co-1-hexene]

Carbon	Expected	Observed
a	27.90*	28.10
b	36.90*	36.60
c	43.60*	43.60
d	27.0**	N/D
e	49.0*	49.60
f	25.0**	25.30
g	40.43**	41.35
h	32.55**	32.60
i	34.76**	33.50
j	28.85**	27.10
k	23.34**	23.80
l	14.24**	18.10

*: Based on monomer spectra; **: Based on spectra of poly(1-hexene).

Form Table 4.11 one can see a very good comparison of the chemical shifts expected from poly(1-hexene) polymers (with $-CH_2$ groups in the α-position relative to the carbon chain and branching in the β-position) and the chemical shifts observed from the ^{13}C NMR spectrum. We expect the polymers to be predominantly poly(α-olefins) with a small amount of 3-(1-adamantyl)-1-propene incorporated. The spectrum is consistent with the structure shown above. In the case of carbon **d**, it is very difficult to observe the peak from the ^{13}C NMR spectrum. Another factor that could attribute to the fact that carbon **d** can't be seen from the spectrum is the steric hinderance from the adamantane ring as well as the poly(1-hexene) backbone. In this case, the signal at 41.35 ppm, represents carbon **g** and is one of the poly(1-hexene) backbone carbons. The signals representing the α-carbons relative to carbon **g**, carbons **f** and **h**, appear at chemical shifts of 25.30 ppm and 32.60 ppm. The signal representing carbon **i** appears at 33.50 ppm. The signal at 49.60 ppm, represents the other β-carbon relative to carbon **g**, carbon **e**. The signal at 23.80 ppm represents carbon **k**. The signals at 28.10 ppm,

36.60 ppm and 43.60 ppm represent the three adamantane carbon signals of carbons **a**, **b** and **c**. The signals at 27.10 ppm and 18.10 ppm represent carbons **j** and **l** respectively.

A schematic representation of poly[3-(1-adamantyl)-1-propene-co-1-octene] is presented below:

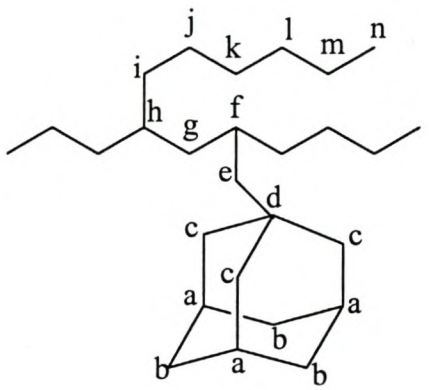

TABLE 4.12: Comparison of Expected and Observed ^{13}C NMR Chemical Shifts (δ) of poly[(3-(1-adamantyl)-1-propene-co-1-octene]

Carbon	Expected	Observed
a	27.90*	27.80
b	36.90*	35.50
c	43.60*	46.50
d	27.0**	N/D
e	49.0**	49.36
f	25.0**	24.50
g	40.43**	38.40
h	32.58**	32.60
i	35.14**	35.50
j	26.60**	26.70
k	30.07**	30.25
l	32.16**	31.40
m	22.85**	23.60
n	14.18**	17.30

*: Based on monomer spectra; **: Based on spectra of poly(1-octene).

Form Table 4.12 one can see a very good comparison of the chemical shifts expected from poly(1-octene) polymers (with $-CH_2$ groups in the α-position relative to the carbon chain and branching in the β-position) and the chemical shifts observed from the ^{13}C NMR spectrum. We expect the polymer to be predominantly poly(1-octene) with a small amount of 3-(1-adamantyl)-1-propene incorporated. The spectrum is consistent with the structure shown above. In the case of carbon **d**, it is very difficult to observe the peak from the ^{13}C NMR spectrum. Another factor that could attribute to the fact that carbon **d** can't be seen from the spectrum is the steric hinderance from the adamantane ring as well as the poly(1-octene) backbone. In this case, the signal at 38.40 ppm, represents carbon **g** and is one of the poly(1-octene) backbone carbons. The signals representing the α-carbons relative to carbon **g**, carbons **f** and **h**, appear at chemical shifts of 24.50 ppm and 32.60 ppm. The signal representing carbon **i** apperas at 35.50 ppm. The signal at 49.36 ppm, represents the other β-carbon relative to carbon **g**, carbon **e**. The signal at 30.25 ppm represents carbon **k**. The signals at 27.80 ppm, 35.50 ppm and 46.50 ppm represent the three adamantane carbon signals of carbons **a**, **b** and **c.** The signal at 26.70 ppm represents carbon **j**. The signal at 31.40 ppm represents carbon **l**. The signals at 23.60 ppm and 17.30 ppm represent carbons **m** and **n** .

From the data compiled in Tables 4.7 to 4.12, it was possible to propose structures for both the homopolymer, poly[3-(1-adamantyl)-1-propene] and the copolymers of 3-(1-adamantyl)-1-propene with α-olefins.

The solid state NMR spectra of both the homopolymer as well as the copolymers showed the expected amount of signals and confirmed the proposed structure. Because of the similarity of the solid state ^{13}C NMR spectra of the copolymers of 3-(1-adamantyl)-1-propene and higher α-olefins, only the spectrum of poly[3-(1-adamantyl)-1-propene-co-4-methyl-1-pentene] is shown.

4.6.4 Conclusions

(1) The homopolymer of 3-(1-adamantyl)-1-propene was successfully prepared using a metallocene catalyst, *rac*-[ethylene*bis*(1-indenyl)]zirconium dichloride with MAO as cocatalyst.

(2) In addition, the copolymerization of 3-(1-adamantyl)-1-propene with ethene, propene and a series of higher α-olefins have been demonstrated.

(3) The glass transition temperatures as well as the melting points for the α-olefin homopolymers were reasonably close to the literature values for the Ziegler-Natta catalyzed poly(α-olefins) with the exception of poly(4-methyl-1-pentene), for which the T_m was noticeably lower for the metallocene-catalyzed polymers (210 °C vs. 245 °C). The homopolymer of 3-(1-adamantyl)-1-propene showed no melting prior to degradation, but did show a T_g at 235 °C. The T_g's of most of the 3-(1-adamantyl)-1-propene-α-olefin copolymers were higher than those of the corresponding homopolymers. From the T_g results it is clear that the incorporation of the bulky adamantyl pendant group severely disrupts the crystalline structure as well as influencing the T_g's of the polymers.

(4) High temperature liquid ^{13}C NMR spectroscopy proved to be an effective method in determining the homo- and copolymer structures.

(5) High temperature liquid ^{13}C NMR spectroscopy also clearly showed the incorporation of 3-(1-adamantyl)-1-propene during the copolymerization reactions.

4.7 RESULTS AND DISCUSSION: 3-PHENYL-1-PROPENE POLYMERS

4.7.1 Polymerization Reactions

The reaction mixtures used in the polymerization reactions of 3-phenyl-1-propene done with $Et(Ind)_2ZrCl_2$, and their yields, are given in Table 4.13. Reaction temperatures for the polymerization of 3-phenyl-1-propene with higher α-olefins varied from 35 °C to 80 °C. The Al/Zr ratio was maintained at 5 000 : 1 for all the reactions.

The homopolymerization of 3-phenyl-1-propene proceeded to a good yield. The powdery polymer product of poly(3-phenyl-1-propene) proved to be insoluble in all common organic solvents, but dissolved in 1,2,4-trichlorobenzene at 100 °C. The high temperature liquid ^{13}C NMR spectrum of the polymer confirmed the expected structure.

In addition to the homopolymer of 3-phenyl-1-propene, homopolymers of the higher α-olefins were also synthesized and analyzed, then compared with the analyses of the copolymers of 3-phenyl-1-propene and the α-olefins. In general, the homopolymers were isolated in good yields, although some difficulty in quantitatively isolating the viscous homopolymers of 1-hexene and 1-octene have resulted in the yield values reported in Table 4.13 being lower than the actual yields.

3-Phenyl-1-propene was successfully copolymerized with 4-methyl-1-pentene, 1-pentene, 1-hexene and 1-octene with $Et(Ind)_2ZrCl_2$ used as catalyst .

In all the copolymerization reactions of 3-phenyl-1-propene with higher α-olefins, the yields of copolymer were lower than the corresponding olefin hompolymerization reaction. Nevertheless, reasonable yields were obtained in all cases. Most copolymers were insoluble in common organic solvents, but dissolved in 1,2,4-trichlorobenzene at 100 °C. The high temperature liquid ^{13}C-NMR spectra of the homopolymer as well as the copolymers discussed in Section 4.5.3. confirmed the expected structures.

TABLE 4.13: Polymerization Reaction Mixtures and Yields for the Polymerization of 3-Phenyl-1-Propene with Higher α-Olefins

Polymer	**3-phen-1-propene** (mole%)	α-olefin (mole%)	Temp (°C)	Yield(%)
Poly(1-octene)	0	100	60	55
Poly(1-octene-co-**3-phen-1-propene**)	36	64	60	60
Poly(1-hexene)	0	100	60	65
Poly(1-hexene-co-**3-phen-1-propene**)	23	77	60	60
Poly(4-methyl-1-pentene)	0	100	45	88
Poly(4-methyl-1-pentene-co-**3-phen-1-propene**)	23	77	45	51
Poly(1-pentene)	0	100	35	83
Poly[(1-pentene-co-**3-phen-1-propene**)	27	73	35	50
Poly(**3-phen-1-propene**)	100	0	60	50

4.7.2 Thermal Transition Analysis by Dynamic Mechanical Analysis (DMA)

The 3-phenyl-1-propene homopolymer was analyzed by DMA to determine the melting point. The sample was kept at –50 °C for three minutes before it was heated from –50 °C to 150 °C, at a heating rate of 5 °C/min.

The polymer showed a glass transition temperature at –9 °C.

In addition to the homopolymer of 3-phenyl-1-propene, homopolymers of 4-methyl-1-pentene, 1-pentene, 1-hexene and 1-octene were also synthesized and analyzed, then compared with the analyses of the copolymers of 3-(1-adamantyl)-1-propene and the α-olefins as well as the copolymers of 3-phenyl-1-propene.

The copolymerization of 3-phenyl-1-propene with 1-octene yielded an amorphous material with a T_g of –65 °C, which is 8 °C higher than the corresponding α-olefin homopolymer. Similarly, the T_g of the copolymers of 3-phenyl-1-propene with 1-octene and 3-phenyl-1-propene with 1-hexene resulted in amorphous materials with T_g values slightly higher than those of the corresponding homopolymer. In the case of poly(3-phenyl-1-propene-co-1-pentene) as well as the poly(3-phenyl-1-propene-co-4-methyl-1-pentene), the T_g of the copolymers are lower than that of the corresponding homopolymer. This could be because of little incorporation of 3-phenyl-1-propene into the copolymer.

TABLE 4.14: Glass Transition Temperatures of Homo- and Copolymers of 3-Phenyl-1-Propene and Higher α-Olefins

Polymer	Tg (°C)
Poly(1-octene)	-73
Poly(1-octene-co-**3-phen-1-propene**)	-65
Poly(1-hexene)	-53
Poly[1-hexene-co-**3-phen-1-propene**)	-45
Poly(1-pentene)	-38
Poly(1-pentene-co-**3-phen-1-propene**)	-45
Poly(4-methyl-1-pentene)	45
Poly(4-methyl1-pentene-co-**3-phen-1-propene**)	2
Poly(**3-phen-1-propene**)	-9

4.7.2.1 Comparison between Tg's of 3-(1-Adamantyl)-1-Propene-α-Olefin Copolymers and 3-Phenyl-1-Propene-α-Olefin Copolymers

In Table 4.15 the T_g's of the 3-(1-adamantyl)-1-propene-α-olefin copolymers as well as the 3-phenyl-1-propene-α-olefin copolymers and the T_g's of the corresponding homopolymers, are shown.

TABLE 4.15: T_g's of 3-(1-Adamantyl)-1-Propene-α-Olefin Copolymers as well as 3-Phenyl-1-Propene-α-Olefin Copolymers and the Corresponding Homopolymers

Polymer	T_g
Poly(3-**phen**-1-propene)	-9
Poly[3-**(1-ada)**-1-propene]	235
Poly(1-octene)	-73
Poly(3-**phen**-1-propene-co-1-octene)	-65
Poly[3-**(1-ada)**-1-propene-co-1-octene]	-19
Poly(1-hexene)	-53
Poly(3-**phen**-1-propene-co-1-hexene)	-45
Poly[3-**(1-ada)**-1-propene-co-1-hexene]	-13
Poly(1-pentene)	-38
Poly(3-**phen**-1-propene-co-1-pentene)	-45
Poly[3-**(1-ada)**-1-propene-co-1-pentene]	-25
Poly(4-methyl-1-pentene)	45
Poly[3-**phen**-1-propene-co-4-methyl-1-pentene)	1
Poly[3-**(1-ada)**-1-propene-co-4-methyl-1-pentene]	69

When the T_g's of the two different series of copolymers with α-olefins are compared, it is clear that the T_g's of the copolymers of 3-(1-adamantyl)-1-propene and α-olefins are all higher compared to those of the 3-phenyl-1-propene and α-olefins. It is a well known fact that the adamantyl group has a much bigger influence on the T_g and disruption of the structure of the copolymers than the phenyl group. A further point to prove this is shown in

the comparison of the T_g values of the various copolymers with the corresponding homopolymers. It is clear that the difference in T_g's of the copolymers of 3-(1-adamantyl)-1-propene and α-olefins and the homopolymers of the corresponding α-olefins is much greater than that of the T_g's of the copolymers of 3-phenyl-1-propene and α-olefins and the corresponding homopolymers. Therefore, the incorporation of 3-(1-adamantyl)-1-propene into α-olefins has a greater influence on the properties of the polymers as discussed in Section 4.5.2 than the incorporation of 3-phenyl-1-propene into α-olefins. The presence of the planar phenyl group doesn't disrupt the structure as much as the adamantylmethyl substituents which severely disrupt the crystallinity as well as influencing the T_g. It has to be pointed out that the assumption was made that reasonably similar amounts of 3-phenyl-1-propene and 3-(1-adamantyl)-1-propene were incorporated in the copolymers. There was, due to the insolubility of the adamantyl-containing polymers, no way of calculating the copolymer composition.

4.7.2.2 DMA Analyses: Conclusions

(1) The homopolymer of 3-phenyl-1-propene showed a T_g at –9 °C.

(2) The T_g's of poly(3-phenyl-1-propene-co-1-octene) and poly(3-phenyl-1-propene-co-1-hexene) were slightly higher than those of the corresponding homopolymers.

(3) The T_g's of poly(3-phenyl-1-propene-co-1-pentene) and poly(3-phenyl-1-propene-co-4-methyl-1-pentene) were lower than those of the corresponding homopolymers.

(4) From the T_g results it is clear that the incorporation of the bulky phenyl pendant group doesn't have such a big influence on the T_g's or the structures of the polymers.

4.7.3 Compostional Analysis

4.7.3.1 Nuclear Magnetic Resonance Spectroscopy (NMR)

^{13}C NMR spectroscopy can be used to investigate the microstructure of the 3-phenyl-1-propene homopolymer as well as the 3-(1-phenyl)-copolymers with respect to comonomer sequence disruption. In the high temperature liquid ^{13}C NMR spectra of the homopolymer of 3-phenyl-1-propene as well as the copolymers of 3-phenyl-1-propene and α-olefins, the peaks between 127 ppm and 128 ppm, are triplets of the solvent system (mixture of C_6D_6 and 1,2,4-trichlorobenzene). Two representative spectra of the poly(3-phenyl-1-propene) copolymers are shown in the next Section.

(i) Homopolymerization Reaction

The chemical shift values for the high temperature liquid ^{13}C NMR spectrum of poly(3-phenyl-1-propene) are given in Table 4.16. A schematic representation of poly(3-phenyl-1-propene) is presented below:

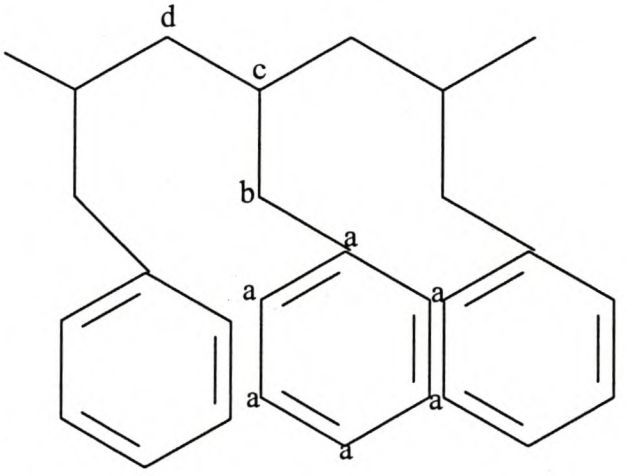

TABLE 4.16: Comparison of Expected and Observed ^{13}C NMR Chemical Shifts (δ) of poly(3-phenyl-1-propene)

Carbon	Expected	Observed
a	128.50*	128.40
b	30.30**	31.20
c	32.70**	33.40
d	41.60**	40.90

*: Based on monomer spectra; **: Based on spectra of related polymers.

From Table 4.16 one can see a very good comparison of the chemical shifts expected from similar hydrocarbon polymers (with $-CH_2$ groups in the α-position relative to the carbon chain and branching in the β-position) and the chemical shifts observed from the ^{13}C NMR spectrum. The spectrum is consistent with the structure shown above. In this case, the signal at 40.90 ppm, represents carbon **d**, which is the CH_2 backbone of the polymer. The signal representing an α-carbon relative to carbon **d**, carbon **c**, appears at 33.40 ppm. The signal at 31.20 ppm, represents a β-carbon relative to carbon **d**, carbon **b**. The signal at 128.40 ppm represents the carbons of the phenyl ring, carbons **a**.

(ii) Copolymers with Higher α-Olefins

The spectra of the copolymers with 1-pentene and 1-octene are shown, in Figures 4-15 and 4-16, as typical examples. Peak assignments for all the higher α-olefin copolymers are given in Tables 4.17 to 4.20. A schematic representation of poly(3-phenyl-1-propene-co-4-methyl-1-pentene) is presented below:

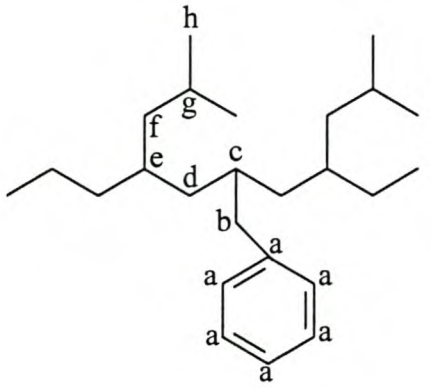

TABLE 4.17: Comparison of Expected and Observed ^{13}C NMR Chemical Shifts (δ) of poly(3-phenyl-1-propene-co-4-methyl-1-pentene)

Carbon	Expected	Observed
a	128.50*	127.90
b	28.10**	28.90
c	35.50**	33.10
d	39.70**	34.90
e	30.02**	32.25
f	44.40**	40.90
g	26.30**	23.20
h	22.60**	13.90

*: Based on monomer spectra; **: Based on spectra of related polymers.

Form Table 4.17 one can see a very good comparison of the chemical shifts expected from poly(4-methyl-1-pentene) polymers (with $-CH_2$ groups in the α-position relative to the carbon chain and branching in the β-position) and the chemical shifts observed from the ^{13}C NMR spectrum. The spectrum is consistent with the structure shown above. In this case, the signal at 40.90 ppm, represents carbon **f**, which is the CH_2 backbone of the polymer. The signal at 34.90 ppm represents carbon **d**. The signal representing an α-carbon relative to carbon **d**, carbon **c**, appears at 33.10 ppm. The signal at 32.25 ppm represents the other α-carbon relative to carbon **d**, carbon **e.** The signal at 28.90 ppm, represents a β-carbon relative to carbon **d**, carbon **b**. The signals appearing at 23.20 ppm and 13.90 ppm represents carbons **g**

and **h** respectively. The signal at 127.90 ppm represents the carbons of the phenyl ring, carbons **a**.

TABLE 4.18: Comparison of Expected and Observed ^{13}C NMR Chemical Shifts (δ) of poly(3-phenyl-1-propene-co-1-pentene)

Carbon	Expected	Observed
a	128.5*	130.5
b	28.10**	N/D
c	35.50**	N/D
d	39.40**	41.0
e	32.70**	33.10
f	37.50**	37.80
g	20.90**	19.60
h	14.30**	14.40

*: Based on monomer spectra; **: Based on spectra of related polymers.

Form Table 4.18 one can see a very good comparison of the chemical shifts expected from poly(1-pentene) polymers (with $-CH_2$ groups in the α-position relative to the carbon chain and branching in the β-position) and the chemical shifts observed from the ^{13}C NMR spectrum. The spectrum is consistent with the structure shown below. In this case, the signal at 41.0 ppm, represents carbon **d**, a backbone carbon of poly(1-pentene). The signal representing an α-carbon relative to carbon **d**, carbon **e**, appears of 33.10 ppm. The signals representing carbons **b** and **c** are not detected. This could be because of the steric hinderance of the phenyl ring as well as the poly(1-pentene) backbone. Another factor could be because of the high concentration of the poly(1-pentene) backbone to the low concentration of 3-phenyl-1-propene incorporated into the copolymer The signals representing carbons **g** and **h** appear at 19.60 ppm and 14.40 ppm respectvely. The signal representing carbon **f** appears at 37.80 ppm. The signal at 130.5 ppm represents the carbons of the phenyl ring, carbons **a**. The spectrum is consistent with the structure shown below.

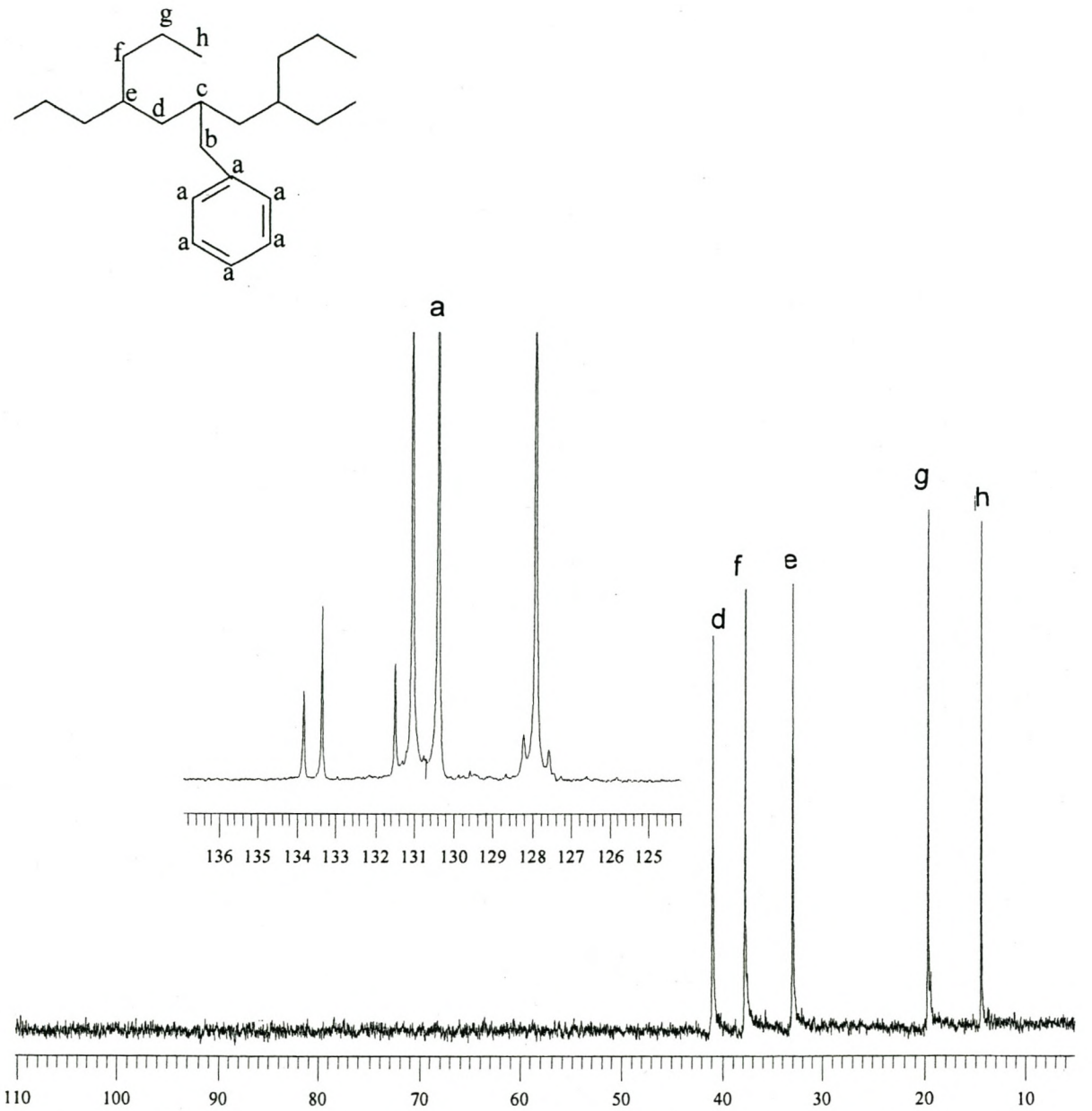

FIGURE 4-15: High Temperature ^{13}C NMR Spectrum of poly(3-phenyl-1-propene-co-1-pentene). The aromatic region is shown as a separate expanded region.

A schematic representation of poly(3-phenyl-1-propene-co-1-hexene) is presented below:

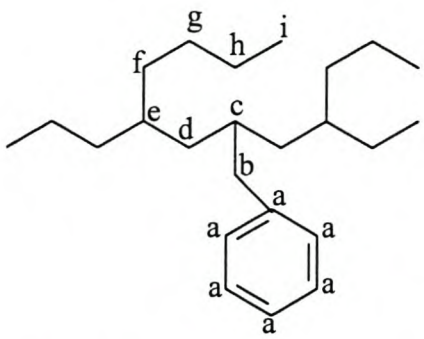

TABLE 4.19: Comparison of Expected and Observed ^{13}C NMR Chemical Shifts (δ)of poly(3-phenyl-1-propene-co-1-hexene)

Carbon	Expected	Observed
a	128.50*	130.5
b	28.10**	N/D
c	35.50**	N/D
d	39.40**	40.90
e	33.0**	33.10
f	35.0**	34.90
g	30.30**	28.80
h	23.40**	23.20
i	14.0**	13.80

*: Based on monomer spectra; **: Based on spectra of related polymers.

Form Table 4.19 one can see a very good comparison of the chemical shifts expected from poly(1-hexene) polymers (with $-CH_2$ groups in the α-position relative to the carbon chain and branching in the β-position) and the chemical shifts observed from the ^{13}C NMR spectrum. The spectrum is consistent with the structure shown below.In this case, the signal at 40.90 ppm, represents carbon **d**, a backbone carbon of poly(1-hexene). The signal representing an α-carbon relative to carbon **d**, carbon **e**, appears of 33.10 ppm. The signals representing carbons **b** and **c** are not detected. This could be because of the

steric hinderance of the phenyl ring as well as the poly(1-hexene) backbone. Another factor could be because of the high concentration of the poly(1-hexene) backbone to the low concentration of 3-phenyl-1-propene incorporated into the copolymer The signals representing carbons **g** and **h** appear at 28.80 ppm and 23.20 ppm respectvely The signals representing carbons **f** and **i** appear at 34.90 ppm and13.80 ppm. The signal at 130.5 ppm represents the carbons of the phenyl ring, carbons **a**.

TABLE 4.20: Comparison of Expected and Observed ^{13}C NMR Chemical Shifts (δ) of poly(3-phenyl-1-propene-co-1-octene)

Carbon	Expected	Observed
a	128.50*	130.5
b	28.10**	N/D
c	35.50**	N/D
d	39.40**	41.10
e	33.0**	33.30
f	35.30**	35.50
g	28.10**	26.80
h	30.30**	30.20
i	32.50**	32.20
j	23.10**	22.80
k	14.0**	14.0

*: Based on monomer spectra; **: Based on spectra of related polymers.

Form Table 4.20 one can see a very good comparison of the chemical shifts expected from poly(1-octene) polymers (with $-CH_2$ groups in the α-position relative to the carbon chain and branching in the β-position) and the chemical shifts observed from the ^{13}C NMR spectrum. The spectrum is consistent with the structure shown below. In this case, the signal at 41.10 ppm, represents carbon **d**, a backbone carbon of poly(1-octene). The signal representing an α-carbon relative to carbon **d**, carbon **e**, appears of 33.30 ppm. The signals representing carbons **b** and **c** are not detected. This could be because of the

steric hinderance of the phenyl ring as well as the poly(1-octene) backbone. Another factor could be because of the high concentration of the poly(1-octene) backbone to the low concentration of 3-phenyl-1-propene incorporated into the copolymer. The signals representing carbons **g** and **h** appear at 26.80 ppm and 30.20 ppm respectvely. The signals representing carbons **f** and **i** appear at 35.50 ppm and 32.20 ppm. The signals representing carbons **j** and **k** appear at 22.80 ppm and 14.0 ppm respectively. The signal at 130.5 ppm represents the carbons of the phenyl ring, carbons **a**.

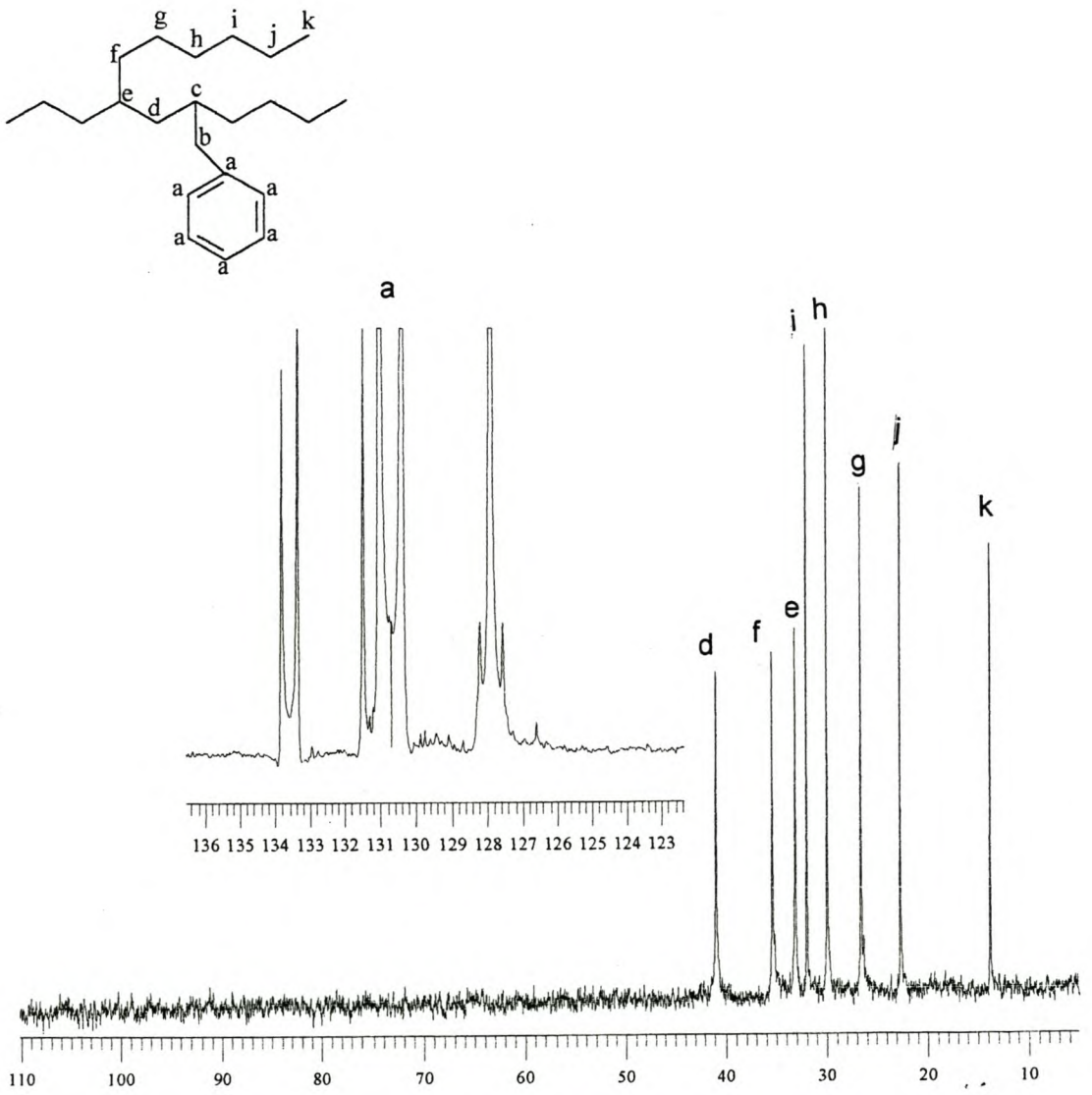

FIGURE 4-16: High Temperature ^{13}C NMR Spectrum of poly(3-phenyl-1-propene-co-1-octene). The aromatic region is shown as a separate expanded region.

4.7.3.2 NMR: Conclusions

From the data compiled in Tables 4.16 to 4.20, it was possible to propose structures for both the homopolymer, poly(3-phenyl-1-propene) and the copolymers of 3-phenyl-1-propene with α-olefins.

The high temperature liquid ^{13}C NMR spectra of both the homopolymer as well as the copolymers showed the expected amount of signals and confirmed the proposed structure.

4.7.4 Conclusions

(1) The homopolymer of 3-phenyl-1-propene was successfully prepared using a metallocene catalyst, *rac*-ethylenebis(indenyl)zirconium dichloride with MAO as cocatalyst.

(2) In addition, the copolymerization of 3-phenyl-1-propene with a series of higher α-olefins have been demonstrated.

(3) The presence of the bulky phenyl pendant group resulted in a slight increase in T_g in the case of poly(3-phenyl-1-propene-co-1-octene) and poly(3-phenyl-1-propene-co-1-hexene) compared to the corresponding α-olefin homopolymers. In the case of poly(3-phenyl-1-propene-co-1-pentene) and poly(3-phenyl-1-propene-co-4-methyl-1-pentene) the T_g is lower compared to those of the corresponding α-olefin homopolymers. It is clear that the bulky phenyl pendant group has little effect on the T_g's of the 3-phenyl-1-propene-α-olefin copolymers as well as the structure of these copolymers.

(4) High temperature liquid ^{13}C NMR spectroscopy proved to be an effective method in determining the homo- and copolymer structures.

(5) High temperature liquid ^{13}C NMR spectroscopy also clearly showed the incorporation of 3-phenyl-1-propene during the copolymerization reactions.

(6) From a comparison done between the T_g's of the 3-(1-adamantyl)-1-propene-α-olefin copolymers and the T_g's of the 3-phenyl-1-propene-α-olefin copolymers it was clear that the bulky adamantyl pendant group has a much bigger influence on the T_g's as well as the crystalline structure of the copolymers than the phenyl group.

4.8 REFERENCES

1. Breslow D.S., Newburg N.R., *J. Am. Chem. Soc.*, 1957, **79**, 5 072.

2. Natta G., Pino P., Mazzanti G., Giannini U., *J. Am. Chem. Soc.*, 1957, **79**, 2 957.

3. Geldenhuys M., M.Sc Thesis, University of Stellenbosch, 1999.

4. Wild F.R.W.P., Zsolani L., Huttner G., Brintzinger H.H., *J. Organomet. Chem.*, 1982, **232**, 233.

5. Kaminsky W., Miri M., Sinn H., Woldt R., *Macromol. Chem. Rapid Commun.*, 1983, **4**, 417.

6. Sinn H., Kaminsky, W., *Adv. Organomet. Chem.*, 1980, **18**, 99.

7. Kaminsky W., Kulper K., Brintzinger H.H., Wald F.R., *Angew. Chem. Int. Ed. Engl.*, 1985, **24**, 507.

8. Kaminsky W. in *History of Polyolefins.* Seymour R.B., Cheng T., Eds. Plenum Press, New York, 1987, 361.

9. Mashima K., Nakayama Y., Nakamura A., *Adv. Polym. Sci.*, 1997, **133**, 1.

10. Matkovsy P.E., Belov G.P., Kissin Y.V., Chrikov N.M., *Vysokomol. Soed.*, 1970, **A12**, 2 286.

11. Berlov G.P., Belova V.N., Raspopov L.N., Kissin Y.V., Birkenshtein K.A., Chirkov N.M., *Polym. J.*, 1972, **3**, 681.

12. Ewen J.A., Jones R.L., Razavi A., Ferrara J.P., *J. Am. Chem. Soc.*,1988, **110**, 6 255.

13. Wilkinson G., Birmingham I.M, *J. Am. Chem. Soc.*, 1954, **76**, 4 281.

14. Reichert K.M., Meyer K.R., *Macromol. Chem.*, 1973, **169**, 163.

15. Long W.P., Berslow D.S., *Justus Liebigs Ann. Chem.*, 1975, 463.

16. Andersen A., Cordes H.G., Herwig J., Kaminsky K., Merck A., Mottweiler R., Pein J., Sinn H., Vollmer H.J., *Angew. Chem. Int. Ed. Engl.*, 1976, **15**, 630.

17. Wild F.R.W.P., Wasincionek M., Huttner G., Brintzinger H.H., *J. Organomet. Chem.*, 1985, **288**, 63.

18. Kaminsky W., Miri M., *J. Polym. Sci., Chem. Ed.*, 1985, **23**, 2 151.

19. Kaminsky W., Drögenmüller H., *Macromol. Chem., Rapid Commun.*, 1990, **11**, 89.

20. Heiland K., Kaminsky W., *Macromol. Chem.*, 1992, **193**, 601.

21. Tait P.J.T., Berry I.G., *Comprehensive Polymer Science*, Vol. 4 (Eds: Eastmond G.C., Ledwith A., Russo S., Sigwalt), Pergamon Press, Oxford, 1989, **4**, 575.

22. *Encyclopedia of Polymer Science and Engineering* (Eds.: Mark H.F., Bikales N.B., Overnerger C.G., Menges G., Kroschwitz J.I.) John Wiley & Sons. New York, 1988, **13**, 500.

23. Guidetti G.P., Busi P., Giulianelli I., Zanneti R., *Eur. Polym. J.*, 1983, **19**, 757.

24. Busico V., Corradini P., De Rosa C., Di Benedetto E., *Eur. Polym. J.*, 1985, **21**, 239.

25. Avella M., Martuscelli E., Volpe G.D., Segre A., Rossi E., Simonazzi T., *Makromol. Chem.*, 1986, **187**, 1 927.

26. Davis D.S., *Proc. Annu. Tech. Conf. Reinf. Plast. Compos. Inst. Soc. Plast. Ind.*, 1992, **50**, 628.

27. Zimmerman J., *Macromol. Sci.*, 1993, **B32**, 141.

28. Zambelli A., Ammendola P., Grassi A., Longo P., Pronto A., *Macromolecules*, 1986, **19**, 2 703.

29. Zambelli A., Longo P., Ammendola P., Grassi A., *Gazz. Chim. Ital.*, 1986, **116**, 731.

30. Zambelli A., Ammendola P., *Gazz. Chim. Ital.*, 1986, **116**, 329.

31. Grassi A., Zambelli A., Resconi L., Albizatti E., Mazzocchi R., *Macromolecules*, 1988, **21**, 617.

32. Chien J.C.W., He D., *J. Polym. Sci. Part A*, 1991, **29**, 1 585.

33. Chien J.C.W., He D., *J. Polym. Sci. Part A*, 1991, **29**, 1 595.

34. Chien J.C.W., He D., *J. Polym. Sci. Part A*, 1991, **29**, 1 603.

35. Chien J.C.W., He D., *J. Polym. Sci. Part A*, 1991, **29**, 1 609.

36. Chien J.C.W., Nozaki T., *J. Polym. Sci. Part A: Polym. Chem.*, 1993, **31**, 227.

37. Chien J.C.W., Xu B., *Makromol. Chem. Rapid Commun.*, 1993, **14**, 109.

38. Uozumi T., Soga K., *Makromol. Chem.*, 1992, **193**, 823.

39. Tsutsui T., Kashiwa N., *Polym. Commun.*, 1988, **29**, 180.

40. Tsutsui T., Mizuno A., Kashiwa N., *Polymer*, 1989, **30**, 428.

41. Suhm J., Schneider M.J., Mülhaupt R., *J. Molecular Catalysis A: Chem.*, 1998, **128**, 215.

42. Heiland K., Kaminsky W., *Makromol. Chem.*, 1992, **193**, 601.

43. Siedle A.R., Lamanna W.M., Newmark R.A.A., *Makromol. Chem. Macromol. Symp.*, 1993, 66, 215.

44. Shista C., Hatorn R.M., Marks T.J., *J. Am. Chem. Soc.*, 1992, **114**, 1 112.

45. Jordan R.F., Bajgur C.S., Willet R., Scott B., *J. Am. Chem. Soc.*, 1986, **108**, 7 410.

46. Jordan R.F., *Adv. Organomet. Chem.*, 1991, **32**, 325.

47. Edward P. Moore, Jr., *Polypropylene Handbook*, Hanser Publishers, Munic, Vienna, New York, 1996.

48. Tritto I., Li S.X., Sacchi M.C., Lacatelli P., Zannoni G., *Macromolecules*, 1995, **28**, 5 358.

49. Rossi A., Zhang J., Odian G., *Macromolecules*, 1996, **29**, 2 331.

50. Ewen J.A., *J. Am. Chem. Soc.*, 1984, **106**, 6 355.

51. Soga K., Shiono T., Takemura S., Kaminsky W., *Macromol. Chem. Rapid Commun.*, 1987, **8**, 305.

52. Stehling U., Diebold J., Kirsten R., Röll W., Brintzinger H.H., Jüngling S., Mülhaupt R., Langhauser F., *Organometallics*, 1994, **13**, 964.

53. Resconi L., Fait A., Piemontesi F., Colonnesi M., Rychlicki H., Ziegler R., *Macromolecules*, 1995, **28**, 6 667.

54. Quijada R., Dupont J., Lacerda Miranda M.S., Scipioni R.S., Galland G.B., *Macromol. Chem. Phys.*, 1995, **196**, 3 991.

55. Suhm J., Schneider M.J., Mülhaupt R., *J. Polym. Sci.: Part A: Polym. Chem.*, 1997, **35**, 735.

56. Uozumi S., Soga K., *Macromol. Chem.*, 1992, **193**, 823.

57. Zambelli A., Grassi A., *Macromol. Chem., Rapid Commun.*, 1991, **12**, 523.

58. Tsai W-M, Chien J.C.W., *J. Polym. Sci., Part A*, 1994, **32**, 149.

59. Soga K., *Macromol. Chem.*, 1989, **190**, 37.

60. Soga K., *Macromol. Chem.*, 1988, **189**, 2 839.

61. Usami T., Gotoh Y., Takayama S., *Macromolecules*, 1986, **19**, 2 722.

62. Jüngling S., Mülhaupt R., Fischer D., Langhauser F., *Angew. Makromol. Chem.*, 1995, **229**, 93.

63. Koivumäki J., *Polym. Bull.*, 1996, **36**, 7.

64. Arnold M., Henscke O., Knorr J., *Macromol. Chem. Phys.*, 1996, **197**, 563.

65. Soga K., Quzumi S., Nakamura S., Toneri T., Teranishi T., Sano T., Arai T., *Macromol. Chem.*, 1996, **197**, 4 237.

66. Benadente R., Josi J.M., Perena M., Bello A., Perez E., Locatelli P., Fan Z.O., Zucchi D., *Polym. Bull.*, 1996, **36**, 249.

67. Galland G.B., Mauler R.S., De Menezes S.C., Quida R., *Polym. Bull.*, 1995, **34**, 599.

68. Bailey A.L., Tchir L.T., Kale W.J., *J. Appl. Polym. Sci.*, 1994, **51**, 547.

69. Koivumäki J., Lathi M., Seppällä J.V., *Angew. Makromol. Chem.*, 1994, **221**, 117.

70. Koivumäki J., Seppällä J.V., *Macromolecules*, 1994, **27**, 2 008.

71. Kaminsky W., *Angew. Makromol. Chem.*, 1986, **146**, 149.

72. Resconi L., Cavallo L., Fait A., Piemontesi F., *Chem. Rev.*, 2000, **100**, 1263.

73. Zucchini U., Dall Occo T., Resconi L., *Indian J. Tech.*, 1993, **31**, 247.

74. Spaleck W., Antberg M., Rohrmann M., Winter A., Bachmann B., Behm J., Hermann W.A., *Angew. Chem.*, 1992, **104**, 1 373.

75. Spaleck W., Kuber F., Winter A., Rohrmann M., Bachmann B., Antberg M., Dolle V., Paulus E.F., *Organometallics*, 1994, **13**, 954.

76. Spaleck W., Antberg M., Dolle V., Klein R., Rohrmann J., Winter A., *New J. Chem.*, 1990, **14**, 499.

77. Schneider M.J., Suhm J., Mülhaupt R., Prosenc M-H, Brintzinger H.H., *Macromolecules*, 1997, **30**, 3 164.

78. Resconi L., Bossi S., Abis L., *Macromolecules*, 1990, **23**, 20, 4 489.

79. Karol F.J., Kao S., Wasserman E.P., Brady R.C., *New J. Chem.*, 1997, **21**, 797.

80. Tritto I., Sanxi L., Sacchi M.C., Locatelli P., Zanneni G., *Macromolecules*, 1995, **28**, 5 358.

81. Tritto I., Sanxi L., Sacchi M.C., Aznnoni G., *Macromolecules*, 1993, **26**, 7111.

82. Pieter P.J.J., Van Beeck J.A.M., Van Tol M.F.H., *Macromol. Rapid Commun.*, 1995, **16**, 463.

83. Harlan C.J., Bott S.G., Barrow A.R., *J. Am. Chem. Soc.*, 1995, **117**, 6 465.

84. Giardello M.A., Eisen M.S., Stern C.L., Marks T.J., *J. Am. Chem. Soc.*, 1993, **115**, 3 326.

85. Giaardello M.A., Eisen M.S., Stern C.L., Marks T.J., *J. Am. Chem. Soc.*, 1995, **117**, 12 114.

86. Chien J.C.W., Song W., Rausch M.D., *J. Polym. Sci., Part A: Polym. Chem.*, 1994, 32, 2 387.

87. Eisch J.J., Pombrik S.I., Zheng G.X., *Organometallics*, 1993, **12**, 3 856.

88. Eisch J.J., Pombrik S.I., in *Catalyst Design for Tailor–made Polyolefins*, Soga K., Teranno M., Eds., Kodansha, Tokyo, p. 221 and references therein.

89. Kaminsky W., *Macromol. Symp.*, 1995, **97**, 79.

90. Forlini F., Fan Z.Q., Tritto I., Locatelli P., Sacchi M.C., *Makromol. Chem. Phys.*, 1997, **198**, 2 397.

91. Muhlenbrock P., Fink G., Naturforsch Z., B-A, *J. Chem. Sci.*, 1995, **50b**, 423.

92. Koivumäki J., Fink G., Seppällä J.V., *Macromolecules*, 1994, **27**.

93. Lehtinen C., Starck P., Löfgren B., *J. Polym. Sci., Part A: Polym. Chem.*, 1997, **35**, 307.

94. Yang X., Stern C.L., Marks T.J., *J. Am. Chem. Soc.*, 1991, **113**, 3 623.

95. Yang X., Stern C.L., Marks T.J., *J. Am. Chem. Soc.*, 1994, **116**, 10 015.

96. Boschmann M., Lancaster S.J., *Organometallics*, 1993, **12**, 633.

97. Chien W.C.J., Tsai W., Rausch M.D., *J. Am. Chem. Soc.*, 1991, **113**, 8570.

98. Herfert N., Fink G., *Makromol. Chem. Rapid Commun.*, 1993, **14**, 91.

99. Idemitsu, *Eur. Patent Appl.*, 1992, 513 380.

100. Tsai W., Rausch M.D., Chien J.C.W., *Appl. Organomet. Chem.*, 1993, **7**, 71.

101. Chien J.C.W., Wang B.P., *J. Polym. Sci., Polym. Chem. Ed.*, 1990, **28**, 15.

102. Okano Y., Masuda T., Higashimura T., *J. Polym. Sci., Polym. Chem. Ed.*, 1985, 23, 2 527.

103. Resconi L., Piemontesi F., Franciscono G., Abis L., Fiorani t., *J. Am. Chem. Soc.*, 1992, **114**, 1 025.

104. Morgstad A.L., Waymouth R.M., *Macromolecules*, 1992, **25**, 2 282.

105. Buyn D.J., Shin D.K., Kim S.Y., *Polym. Bull.*, 1999, **42**, 301.

106. Buyn D-J, Shin D-K, Kim S.Y., *Macromol. Rapid Commun.*, 1999, **20**, 419.

107. Grant M., M.Sc Thesis, University of Stellenbosch, 1993.

108. Barkhuysen L., M.Sc Thesis, University of Stellenbosch, 1997.

109. Capaldi E., Borchert A.E., US Patent, 1969, 3 457 318.

110. Brüll R., Pasch H., Raubenheimer H.G., Sanderson R.D., Wahner U.M., *J. Polym. Sci.: Part A: Polym. Chem.*, 2000, **38**, 2 333.

CHAPTER 5

THE PREPARATION OF 1-(1-ADAMANTYL)-4-VINYLBENZENE

5.1 INTRODUCTION

In this Chapter, different methods for the preparation of 1-(1-adamantyl)-4-vinylbenzene are discussed. 1-(1-Adamantyl)-4-vinylbenzene was later used in a series of polymerizations with α-olefins and styrene, using different catalytic systems. (See Chapter six.) The effect of the incorporation of the adamantane-substituted monomer on the physical and thermal properties of the polymers synthesized was investigated and are discussed in Chapter six.

The incorporation of bulky pendant groups like the adamantyl group has been shown to significantly affect the glass transition temperatures (T_g) of polymers (Chapter four, see Section 4.6.2). Adamantyl groups can be incorporated in polymers as part of the main chain[1-3] and as side groups[4-9]. The use of α-olefins having adamantyl-benzene substituents has not been reported in the literature.

5.2 THEORETICAL BACKGROUND

5.2.1 Preparation Methods

The preparation of 1-(1-adamantyl)-4-vinylbenzene (*para*-adamantyl styrene) has been reported by Bräse *et al* [10], although this method in our hands proved to be unsuccessful because of numerous side reactions.`

Scheme 5–1 is a summary of the three approaches which were followed to synthesize 1-(1-adamantyl)-4-vinylbenzene.

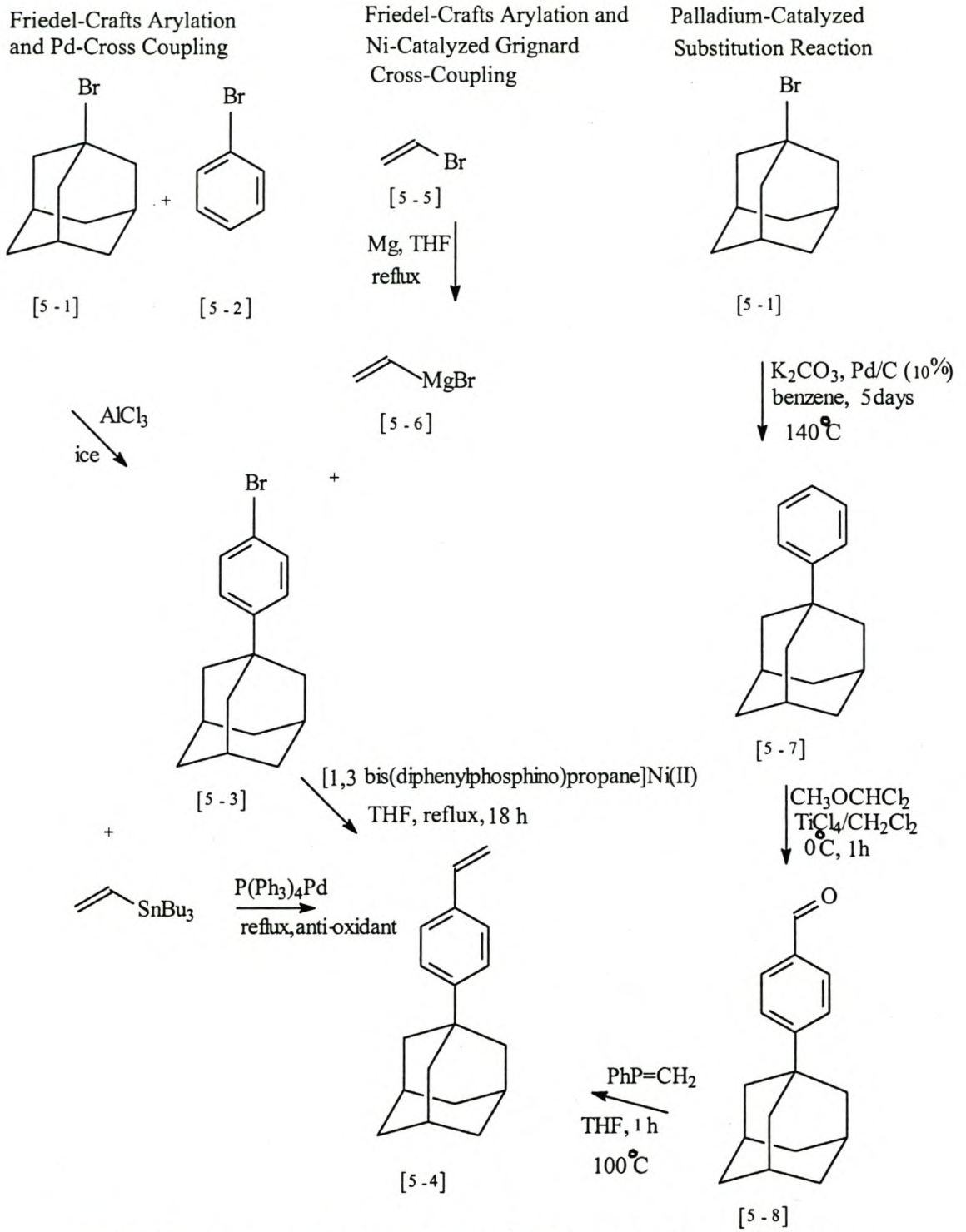

SCHEME 5–1: Summary of the Three Approaches Followed to Synthesize 1-(1-Adamantyl)-4-Vinylbenzene

Palladium–catalyzed coupling reactions of alkyl halides with unsaturated compounds are practically unknown, whereas the corresponding aryl and alkenyl halide couplings, in the so-called Heck–reaction, are well documented[11, 12]. The palladium–catalyzed vinylation of organic halides

provides a very convenient method for forming carbon–carbon bonds at unsubstituted vinylic positions[12]. This reaction usually does not require anhydrous or anaerobic conditions although it is advisable to limit an excess of oxygen when arylphosphines are used as a component of the catalyst. The transformation of anaerobic conditions to aerobic conditions first used by Heck *et al* [11] is valuable because the palladium-catalyzed vinylation of organic halides cannot be carried out in a single step by any other known method, except in certain Meerwein reactions[12]. The general reaction for the palladium–catalyzed vinylation of organic halides is

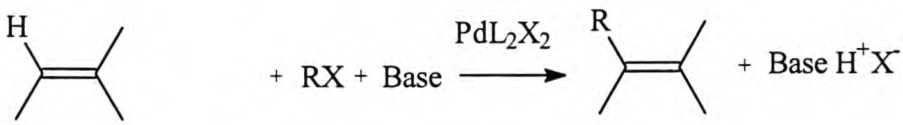

R = Aryl, hetrocyclic, benzyl or vinylic

X = Bromide, iodide or (rarely) chloride

L = A ligand

The organic halide used is limited to aryl, hetrocyclic benzyl or vinyl types, and bromides and iodides are the most frequently used. Halides with an easily eliminated β–hydrogen atom (i.e. alkyl derivatives) cannot be used since they form only olefins by elimination under the normal reaction conditions. The base needed may be a secondary or tertiary amine, sodium or potassium acetate, carbonate or bicarbonate.

The catalyst commonly used is palladium acetate, although palladium chloride or preformed triarylphosphine palladium complexes, as well as palladium on charcoal, have also been used[12]. A reactant, product or solvent may serve as the ligand, L, in reactions involving organic iodides, but generally a triarylphosphine or a secondary amine is required when organic bromides are used. The reaction takes place between 50 °C and 160 °C, and proceeds homogeneously. Although solvents are often unnecessary, these that have been used are acetonitrile, dimethylformamide, hexamethylphosphoramide, N-methylpyrrolidinone and methanol. The procedure is applicable to a wide range of reactants and yields are generally good to excellent.

Several variations of the reaction are known in which the organic halide is replaced by other reagents such as organometallics, diazonium salts or aromatic hydrocarbons.

5.2.2 Mechanism for Palladium–Catalyzed Coupling Reactions

Stoichiometric reactions with organopalladium compounds indicate that they are involved in vinylic substitution[13, 14]. If a palladium(II) complex or salt is the catalyst introduced, then it must be reduced under the reaction conditions, presumably by oxidizing some of the olefin present[15]. The palladium(0) complex or finely divided metal so formed then reacts with the organic halide to form the organopalladium-halide intermediate. This species is generally solvated or coordinated with a pair of two-electron donating ligands. The organopalladium complex adds to the double bond of the olefin. The resulting adduct is believed to undergo elimination of a hydridopalladium halide if an sp^3-bonded hydrogen, beta to the palladium group, is present. The reaction is catalyzed by palladium in the presence of a base because the hydridopalladium halide dissociates reversibly and the base shifts the equilibrium to the palladium(0) species. This latter compound reacts with the organic halide and the cycle begins again.

Catalyst formation:

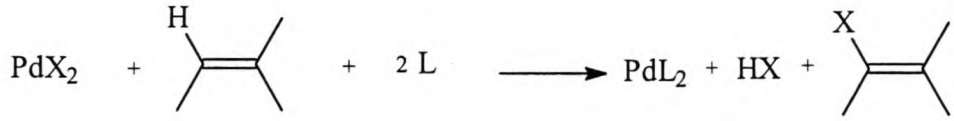

Catalytic cycle:

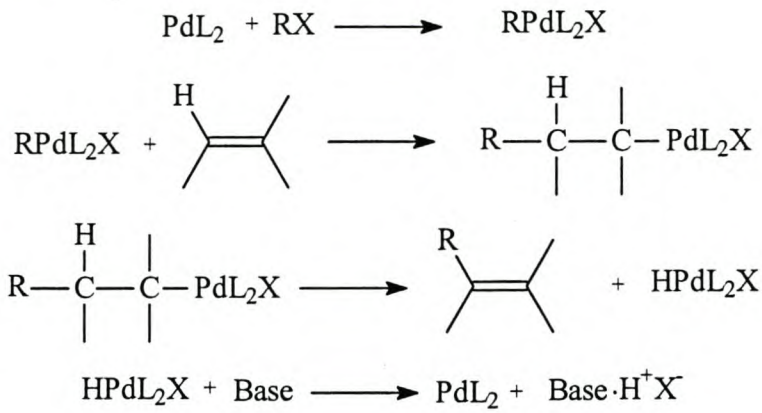

SCHEME 5–2: Mechanism for Palladium–Catalyzed Coupling Reactions

The direction of addition of the organopalladium species to unsymmetrically substituted double bonds appears to be largely sterically controlled. The organic group behaves as the larger part of the palladium complex, and it attaches to the less substituted carbon atom of the double bond[14]. If an electron-withdrawing group is attached to one carbon of the double bond, however, addition of the organic group generally takes place exclusively or, at least, predominantly on the other carbon atom. The presence of an electron-donating substituent often causes mixtures of products to be formed, with the sterically favored isomer predominating[16].

A series of vinylic bromides have been reacted with 1-hexene and with piperidine or morpholine as the base[17]. Vinyl bromide and 2-bromo-propene add exclusively terminally, but β-substituted vinylic bromides give mixtures.

A complication in the reaction may appear if there is more than one sp^3-bonded hydrogen atom beta to the palladium group in the olefin adduct[12]. A mixture of geometric isomers may result or the double bond may be moved from its original position.

Substitution with vinylic halides as substrates may produce another complication. In these cases π-allylic complexes are often formed by palladium hydride elimination and readdition in the reverse direction[18]. If the π-allylic complex undergoes palladium hydride elimination, double bond migration from the initial position may result. In many reactions the π-allylic complexes are sufficiently stable that they either do not decompose or do so only slowly under the usual reaction conditions with a tertiary amine as the base.

When π-allylic complexes are formed, the stereochemistry about the double bond of the vinylic halide is lost because there is a facile equilibration of the *syn* and *anti* forms of the π-allylic complexes. The preferred isomers are those having the largest allylic substituents furthest away from the metal.

5.2.3 Scope and Limitations in Palladium Coupling Reactions

In this Section, the limitations in the selection of the organic halide as well as the reactivity of the olefin in palladium coupling reactions are discussed. A comparison between the Heck-reaction and other related reactions is also discussed.

5.2.3.1 The Organic Halide

The major limitation related to selection of the organic halide is that sp^3-bonded hydrogen atoms beta to the halide group cannot be present[12]. The palladium alkyls formed from these halides undergo palladium hydride elimination more rapidly than addition to olefins, and only elimination products are produced. Aryl, many hetrocyclic, benzyl and vinylic halides react normally, however. Other halides without beta sp^3-bonded hydrogens exist but, for various reasons, they do not react normally. Methyl halides, haloacetate esters, phenacyl bromide and neopentyl bromide do not yield the expected products.

A second limitation concerns the halogen atom to be used. Iodides and bromides undergo comparable reactions in most instances, with the iodides

usually being a little more reactive. For example, both bromo- and iodobenzene react with *cis*-1-phenyl-1-propene at 100 °C in the presence of a palladium acetate–triphenylphosphine catalyst. The reaction product mixtures were essentially the same, but the iodide reacted a little more than twice as rapidly as the bromide[14]. Chlorides generally do not undergo reactions.

A very wide range of substituents may be present in the organic halides[19]. The only substituent known to stop the reaction in an aromatic compound is an *ortho*-carboxyl group, although the *ortho*–methyl ester reacts normally. Low yields of products are obtained when aromatic bromides containing strongly electron–donating substituents are used. The reason for the low yields is that the phosphine in the catalyst is usually quaternized in a palladium-catalyzed reaction and/or the halide is reduced to a hydrocarbon.

Quite sterically hindered organic halides may be employed, but the reaction rates are usually low. For example, the reaction of 2,5-diisopropylbromobenzene and methyl acrylate occurs in 79 % yield at 125 °C in 20 hours. Some limitations occur with heterocyclic halides as well.

A potential problem with the reactions of benzyl chloride or bromide is quaternization of both the amine base and the phosphine, if one is used[12]. Best results are obtained with hindered amines (diisopropylethylamine) and phosphines. Vinylic halides that are activated for base–catalyzed elimination, such as methyl 2-bromoacrylate, also do not undergo the vinylic substitution reaction, presumably because elimination is favored over substitution.

5.2.3.2 The Olefin

The primary factor in determining the reactivity of the olefin is the size and number of the substituents on the double–bond carbon atoms[12]. Rates of reaction and yields of products generally decrease with increasing size and number of substituents around the double bond. Ethene is the most reactive olefin[20]. Most monosubstituted ethenes also react well. Even disubstituted

ethenes often react in reasonable yields, but at lower rates. Poor yields are often obtained with trisubstituted ethenes.

Dimerization of the halides is frequently observed as a side reaction when the olefinic compounds are unreactive. Mixtures of products are sometimes produced from unsymmetrically substituted ethene derivatives. The presence of electron-withdrawing substituents on a double bond carbon atom generally directs the incoming organic group selectively to the other double bond carbon atom. However, electron-donating substituents generally cause addition to both carbon atoms. The amount of addition to each carbon atom in these reactions is strongly influenced by steric effects in both the halide and olefin. The organic group of the organopalladium complex preferentially attacks the less substituted carbon atom of the double bond.

Double bond isomers are often formed when the possibility exists for elimination of different β–hydrogen atoms. If *cis* or *trans* products are possible, the thermodynamically more stable olefin is favored[12]. Some isomerization may occur even in reactions when there is only a eliminatable β–hydrogen because of reverse hydride readdition and elimination of a hydrogen atom from a different carbon atom. This type of isomerization is suppressed by inclusion of a phosphine[18].

Some specific olefins that do not react well in the vinylic substitution are vinyl acetate, acrolein and 3-buten-2-one. Vinyl acetate tends to produce mixtures of products, largely with loss of the acetate group. Allylic halides also fail in the reaction as either olefins or halides.

5.2.4 Palladium–Catalyzed Coupling Reactions of 1-Bromoadamantane with Styrenes and Arene

The palladium–catalyzed reaction of 1-bromoadamantane with styrene and donor-substituted styrenes gives the corresponding Heck–type coupling products in moderate yields (15–41 %), while the palladium-catalyzed reaction of 1-bromoadamantane with various arenes under palladium

catalysis gave the corresponding adamantyl-substituted arenes in good to excellent yields (35-98 %)[10].

Thus, the reaction of 1-bromoadamantane with styrene[21], yields 1-styryladamantane in the *E*-configuration, while the treatment of bromoadamantane with benzene gives 4-phenyladamantane in good yield. To explore the scope of the latter reaction, halobenzenes were also investigated. As expected, fluorobenzene reacted rather slowly (two days, reflux), but gave the corresponding product in good yield (56 %), while chloro- and bromobenzene reacted smoothly. The required amount of catalyst depended on the electron density of the arene used. Bromobenzene gave the corresponding coupling product 1-bromo-4-adamantyl-benzene in 85 % yield, but some 1-bromo-3-(4'-bromophenyl)adamantane was also formed.

1-Phenyladamantane was shown to be converted to 4-adamantylstyrene in high overall yield by formylation and a subsequent Wittig olefination reaction of the (4'-formylphenyl)adamantane thus formed. Thus, the use of Pd/C as a catalyst can be extended to the arylation of bridgehead bromides like 1-bromoadamantane[22].

5.2.5 Cross-Coupling Reaction of Grignard Reagents with Organic Halides

In this Section the cross-coupling reaction of Grignard reagents with organic halides with phosphine palladium and phosphine nickel complexes as catalysts, is discussed.

5.2.5.1 Phosphine–Palladium Complexes

Phosphine–palladium complexes are known to catalyze the cross–coupling of aromatic and alkenyl halides with organometallics, such as Grignard reagents, organo–zinc, -aluminum and –zirconium compounds[23]. Of the palladium complexes, tetrakis(triphenylphosphine)palladium(0) has been the most extensively studied, and proved to be an effective catalyst. The organometallics successfully used for the palladium-catalyzed reaction have, unfortunately, been limited to aryl, alkenyl, alkynyl and benzyl derivatives.

The reaction with alkyl derivatives containing β-hydrogens has not been successful (with a few exceptions), probably because an alkylpalladium species generated in the catalytic cycle is prone to undergo β-hydride elimination, giving an alkene and palladium hydride.

Table 5.1 shows the cross-coupling reaction of *sec*-butylmagnesium chloride with halides catalyzed by palladium catalyst complexes.

Table 5.1: Cross-Coupling of *sec*-Butylmagnesium Chloride (1) with Halides (2) Catalyzed by Palladium Catalyst Complexes [a]

Catalyst	Halide(2) (RBr)	Reaction Temp	Conditions Time (h)	Yield (%)[b] *sec*-BuR(3)	Yield (%)[b] *sec*-BuR(4)	%
$Pd(dppf)Cl_2$	PhBr(2a)	r.t.	1	95 (80)[c]	0	(0)[d]
$Pd(dppf)Cl_2$[e]		r.t.	24	0	92	(2)[d]
$Pd(PPh_3)_4$		r.t.	24	4	6	(31)[d]
$Pd(PPh_3)_2Cl_2$		r.t.	24	5	6	(9)[d]
$Pd(dppe)Cl_2$		r.t.	48	0	0	(96)[d]
$Pd(dppe)Cl_2$		reflux	8	4	1	(30)[d]
$Pd(dppp)Cl_2$		r.t.	24	43	19	(23)[d]
$Pd(dppb)Cl_2$		r.t.	8	51	25	(1)[d]
$Pd(dppf)Cl_2$	PhCH=CHBr (2b)[f]	0° C	2	97 (78)[c]	0	(0)[g]
$Pd(dppf)Cl_2$		r.t.	24	93	0	(0)[g]
$Pd(dppf)Cl_2$		r.t.	20	0	90	
$Pd(PPh_3)_4$		0° C	3	33	36	(4)[g]
$Pd(dppe)Cl_2$		0° C	5	3	3	(38)[g]
$Pd(dppp)Cl_2$		0° C	5.5	76	5	(6)[g]
$Pd(dppb)Cl_2$		0° C	3.5	53	25	(8)[g]
$Pd(dppf)Cl_2$	CH_2=CMeBr (2c)	0° C	8	80	0	

[a] 1/2 = 1.5; catalyst/2 = 10^{-2}, unless otherwise noted. [b] Determined by glpc using an internal standard. [c] Isolated yield. [d] Recovered bromobenzene (%). [e] *n*-Butylmagnesium cholride was used instead of *sec*-butylmagnesium chloride. [f] Coupling products, *sec*-butyl- and *n*-butylstyrene have *E* configuration (> 99 %). [g] Yield (%) of styrene. [h] Catalyst/2b = 10^{-4}. r.t. = room temperature. dppe = diphenyl phosphino ethane dppp = diphenyl phosphino propane, dppb = diphenyl phosphino butane, dppf = diphenyl phosphino ferrocene.

From Table 5.1 it is clear that $Pd(dppf)Cl_2$ is the only catalyst giving exclusively *sec*–butylated derivatives. Other palladium complexes induced, as side reactions, isomerization of the butyl group and reduction of organic halides to some extent.

The efficiency of the triphenylphosphine–palladium complexes in the coupling of alkyl Grignard reagents can be attributed to the dissociation of triphenylphosphine from palladium, which promotes the β-elimination by forming unsaturated species[23]. Since bidentate phosphines are known to stabilize an alkyl–metal moiety against β-hydride elimination, by inhibiting loss of one coordinated phosphine, the palladium catalysts complexed with a bidentate phosphine are expected to be more efficient than the triphenylphosphine-palladium catalyst. It is rather surprising that the dppf ligand can completely suppress the side reactions while other bidentate phosphine ligands (dppe, dppp and dppb) cannot. Although the precise role of the ferrocene moiety in dppf in the coupling reaction remains to be clarified, it is likely that the delicate steric and electronic changes in phosphine ligands bring about marked differences in catalytic activity and selectivity.

5.2.5.2 Phosphine–Nickel Complexes

The cross–coupling of organic groups by the reaction of Grignard reagents with organic halides can be done with a variety of transition metal halides[24]. These reactions are, however, seldom used in practice due to the formation of substantial amounts of homocoupling products and a variety of disproportionation products.

Kiso *et al* [25] reported a preparative method of synthesizing unsaturated compounds; it involved the selective cross–coupling of a Grignard reagent with a vinyl or aryl halide, catalyzed by a phosphine–nickel complex. A possible mechanism for this synthesis is shown in Scheme 5–3.

First, two organic groups on a nickel complex are released by reaction of an organic halide to undergo coupling, where the complex itself is converted to the corresponding (halo)(organic)nickel complex. Second, such a

halogen-nickel bond reacts with a Grignard reagent to form the corresponding organonickel bond, is a well–known fact. These facts suggest that dihalodiphosphinenickel has catalytic ability for the coupling of a Grignard reagent with an organic halide.

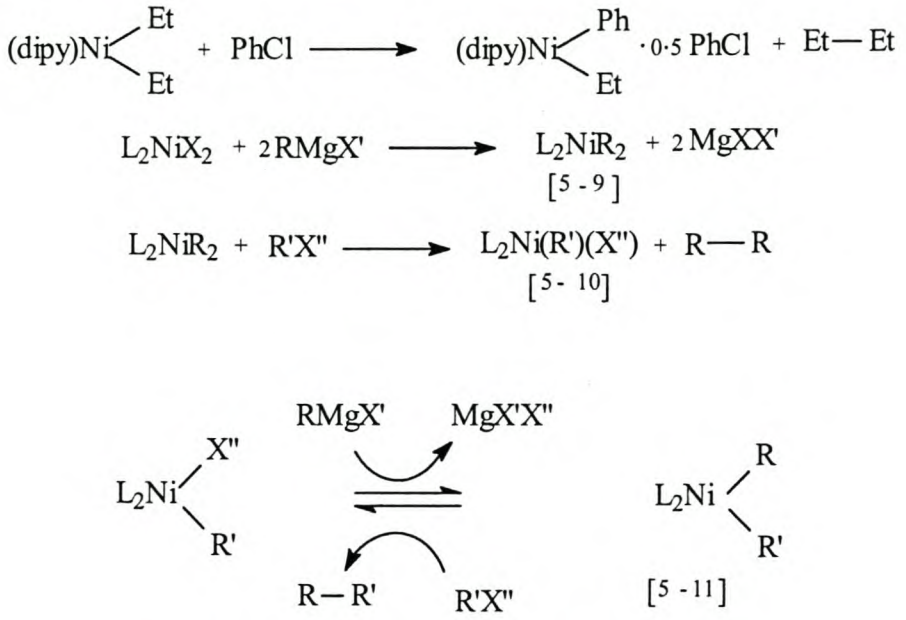

dipy = Ligand of Nickel – phosphine complex

SCHEME 5–3: Cross–Coupling Mechanism of Grignard Reagent with Organic Halides, Catalyzed by a Phosphine–Nickel Complex

Thus, a dihalodiphosphine nickel reacts with a Grignard reagent to form the intermediate diorganonickel complex **[5–9]** which is subsequently converted to the (halo)–(organo)nickel complex **[5–10]** by an organic halide. The subsequent reaction of **[5–10]** with the Grignard reagent leads to the formation of a new diorgano complex **[5–11]**, from which the cross-coupling product is released by the attack of the organic halide. The original complex **[5–10]** is thereby regenerated to complete the catalytic cycle.

This coupling reaction can be achieved by the addition of a Grignard reagent to an organic halide in the presence of a catalytic amount of a dihalodiphosphinenickel, and the yields of product are generally very high.

There are some significant features of this method of selective carbon-carbon bond formation.

- A variety of Grignard reagents in ether as solvent are applicable and high yields are obtained even from alkylmagnesium reagents containing β-hydrogen atoms. Therefore, the alkyl derivatives of aromatic compounds, which are not readily obtained by conventional preparation methods can be prepared in one step.

- Only C_{sp}^2 halides, such as vinylic and aromatic halides, can be used. The high reactivity of chlorides, especially, is most remarkable.

- As a ligand, a bidentate diphosphine exhibits remarkable catalytic activity.

- The use of diethyl ether as a solvent is definitely superior to tetrahydrofuran, in contrast with Tamura's catalysts[26].

5.3 SYNTHESIS AND CHARACTERIZATION OF 1-(1-ADAMANTYL-4-VINYLBENZENE – GENERAL EXPERIMENTAL CONSIDERATIONS

5.3.1 Materials and Methods

All operations involving air- and moisture sensitive compounds were conducted in a nitrogen atmosphere, either by using standard Schlenk techniques or working in a Plas Labs dry box. Solvents were thoroughly dried before use, using standard procedures. Glassware was dried overnight at 120 °C before use, assembled hot and cooled in a nitrogen atmosphere.

5.3.1.1 Reagents

All the chemicals used were obtained from Aldrich except THF, DMSO dichloromethane, pentane, methanol, petroleum ether (bp = 40–60 °C) and diethyl ether, which were obtained from Saarchem.

5.3.1.2 Solvents

Solvents were thoroughly dried, under nitrogen before use, except for pentane, methanol, petroleum ether and diethyl ether which were used as received.

Toluene

Toluene (500 mL) was dried over sodium pieces and boiled under reflux, with a small amount of benzophenone, until the toluene had a dark blue color. Benzophenone was used as indicator to indicate when the toluene is dry. Toluene was then distilled onto 4 Å molecular sieve.

Tetrahydrofuran (THF)

THF (200 mL) was dried over sodium pieces and boiled under reflux, with a small amount of benzophenone, until the THF had a dark blue color. Benzophenone was used as indicator to indicate when the THF is dry. THF was then distilled onto 4 Å molecular sieve and used immediately.

Dimethyl Sulfoxide (DMSO)

DMSO (500 mL) was boiled under reflux for one hour before distilling it by means of a high vacuum distillation onto 4 Å molecular sieve.

Dichloromethane

Dichloromethane (500 mL) was dried over P_2O_5 for 24 hours before it was boiled under reflux for one hour. Dichloromethane was then distilled onto 4 Å molecular sieve.

5.3.2 Equipment

Apparatus for the preparation of 1-bromo-(4-adamantyl)-benzene [5-3], 1-(1-adamantyl)-4-vinylbenzene [5–4], vinyl magnesiumbromide [5–6], 1-phenyl adamantane [5–7] and 1-formyl-(4-adamantyl)-benzene [5–8]

Apparatus for the preparation of **[5–3]** comprised a 50 mL round bottom flask and a condenser.

Apparatus for the preparation of **[5–4]** comprised a 50 mL conical flask, a 50 mL round bottom flask, condenser, nitrogen inlet, rubber septum, disposable syringe and a separating funnel.

Apparatus for the preparation of **[5–6]** comprised a 50 mL two-neck round bottom flask, condenser, nitrogen inlet, dropping funnel and glass wool.

Apparatus for the preparation of **[5–7]** comprised a 400 mL Parr stainless steel autoclave equipped with a nitrogen inlet.

Apparatus for the preparation of **[5–8]** comprised a 50 mL two–neck round bottom flask, condenser, nitrogen inlet, disposable syringe and a separating funnel.

5.3.3 Laboratory Safety

The necessary safety precautions for an exothermic reaction had to be taken into account during the synthesis of **[5–3]**. A water bath was used as a trap for the HCl gas that formed as by product during the formation of **[5–3]**. Care had to be taken in the synthesis of **[5–4]** to exclude all moisture due to the hygroscopic nature of the catalyst. Therefore, the whole procedure involving the preparation of **[5–4]** was conducted under nitrogen. The standard safety procedures for the preparation of a Grignard reagent were taken into account during the synthesis of **[5–6]**. High reactivity of the magnesium with water could easily cause an explosion. Care had to be taken to exclude all moisture when drying the THF, because of its hygroscopic nature.

5.3.4 Analytical Methods and Instrumentation

For DSC, NMR and IR, see Section 4.4.3.

5.3.4.1 Gas Chromatography (GC)

A Hewlett Packard 5 890 Series 2 gas chromatograph was used to follow the progress of the monomer synthesis as well as to determine the purity of the monomer.

5.4 *FIRST APPROACH: PALLADIUM-CATALYZED CROSS-COUPLING REACTION VIA THE INTERMDIATE 1-BROMO-(4-ADAMANTYL)-BENZENE*

After an extensive study of the relevant literature a two–step synthesis, comprising a combination of classical Heck-cross coupling conditions[11–16, 27] and a Friedel–Crafts arylation[21] was used to develop a method by which the target monomer, 1-(1-adamantyl)-4-vinylbenzene was prepared. The latter was synthesized via the intermediate, 1-bromo-(4-adamantyl)-benzene. The first step involved a Friedel–Crafts arylation reaction to form the intermediate, 1-bromo-(4-adamantyl)-benzene. The second step involved the Heck–type palladium-catalyzed coupling reaction to form the required monomer, 1-(1-adamantyl)-4-vinylbenzene.

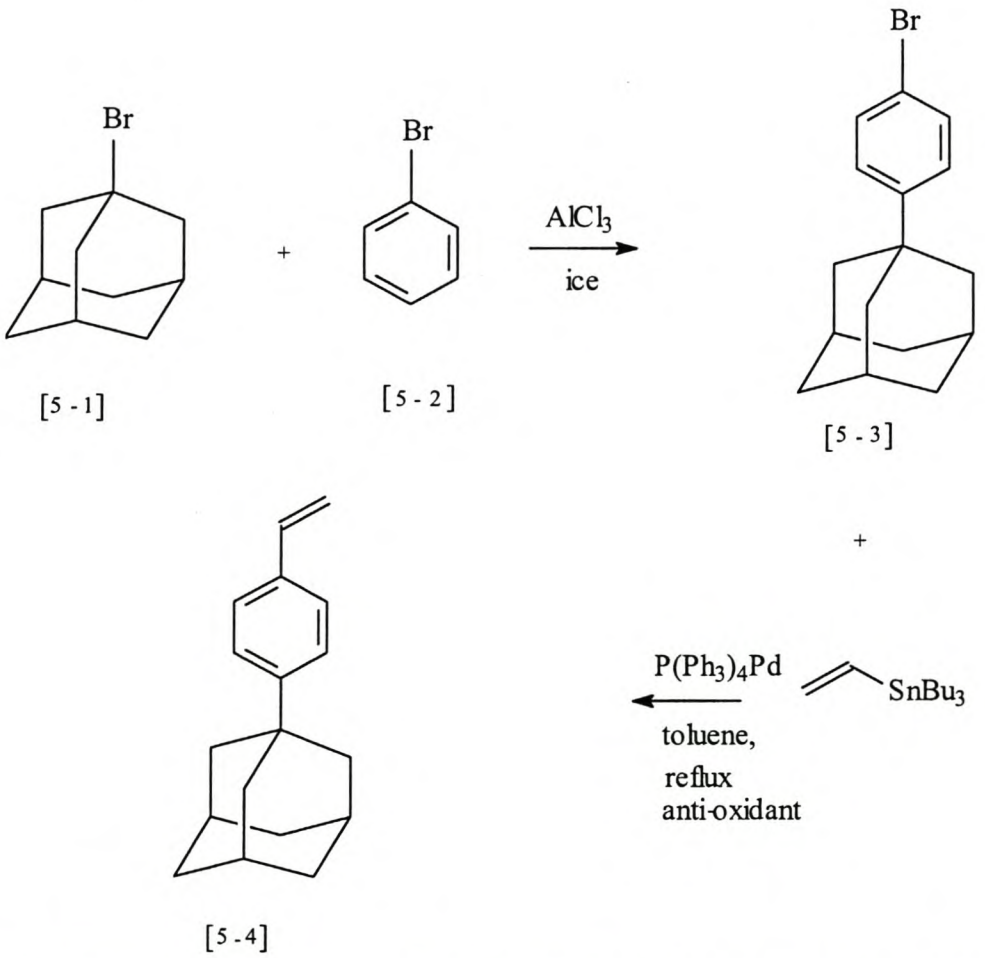

SCHEME 5-4: Proposed Synthesis of [5–4] via the Intermediate, [5–3], Using a Combination of Friedel–Crafts Arylation and Palladium Cross-Coupling Reactions

5.4.1 Preparation of 1-Bromo-(4-Adamantyl)-Benzene [5–3]

[5–1] (4 g; 1.8 x 10^{-2} mole) was dissolved in **[5 –2]** (4 mL; 3.8 x 10^{-2} mole) at 0 °C. A small amount of $AlCl_3$ was added and an exothermic reaction started immediately. The HCl–gas that evolved was trapped in a water bath. The reaction was kept at 0 °C for seven hours and monitored by gas chromatogtaphy. The reaction was quenched by pouring the mixture into an ice–water bath. The water was decanted and the reaction mixture poured slowly into methanol to precipitate. The methanol mixture was placed in the fridge for 24 hours to ensure maximum precipitation. The methanol was then decanted, the white microcrystals air-dried, and 4.6 g (88 %) of 1-bromo-(4-adamantyl)benzene isolated. The product was purified by sublimation under reduced pressure at 60 °C. T_m = 86 °C.

5.4.1.1 Results and Discussion

The ^{13}C NMR spectrum of **[5–3]** is shown in Figure 5-1 and the chemical shift values are given in Table 5.2.

TABLE 5.2: ^{13}C NMR Chemical Shifts (δ) of [5–3] in $CDCl_3$

Carbon	Chemical shift (ppm)
a	29.08
b	36.90
c	43.28
d	35.20
e	150.67
f	131.31
g	127.03
h	119.30

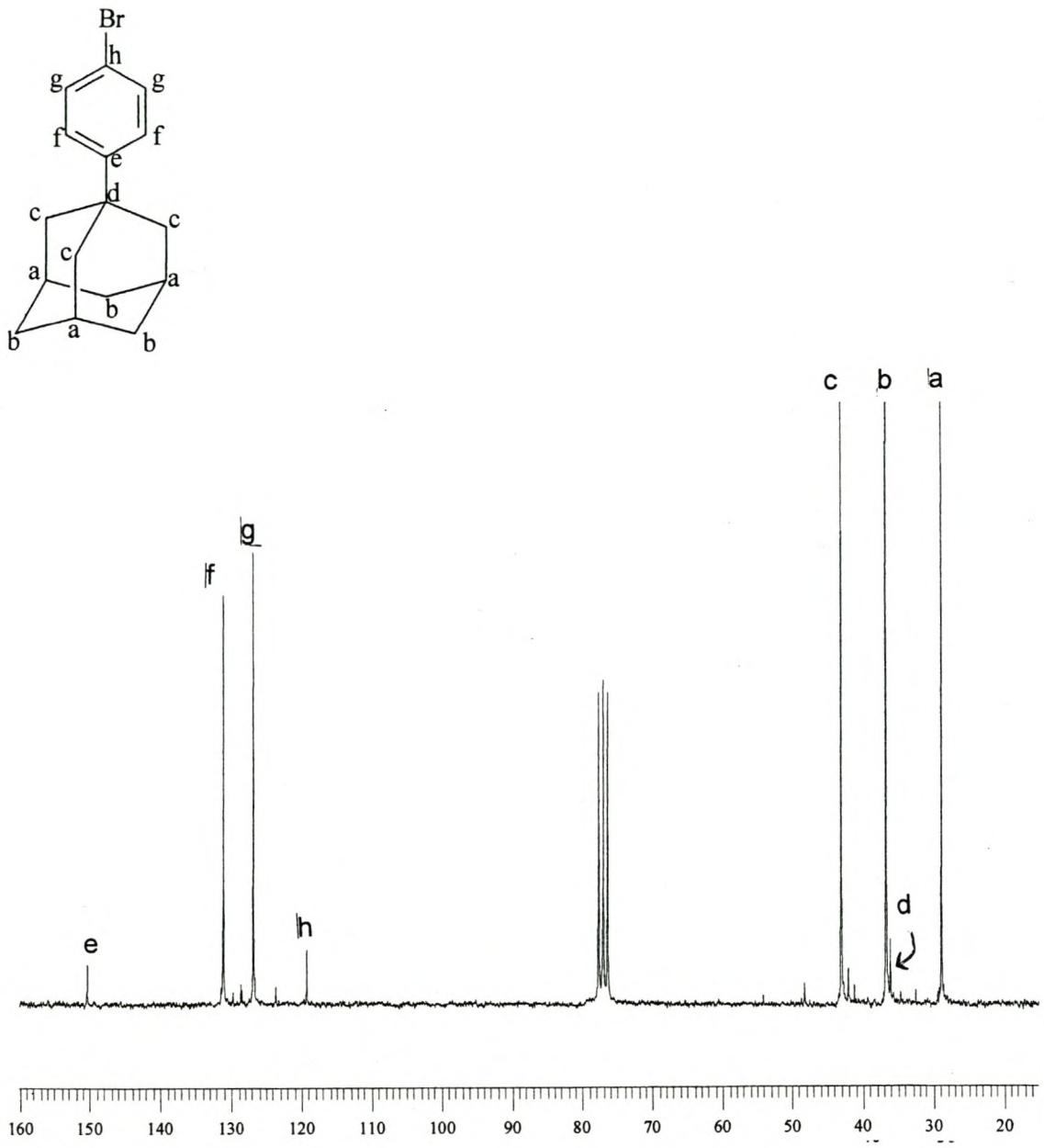

FIGURE 5-1: ^{13}C NMR Spectrum of [5–3] in $CDCl_3$

The ^{13}C NMR spectrum of **[5–3]** showed the four adamantane signals as well as the four phenyl ring signals, as expected. The signals at 119.30 ppm and 150.67 ppm, represent carbons **e** and **h** respectively. The signal at 35.20 ppm, represents the quaternary carbon **d**, and therefore the intensity is very low. The spectrum is consistent with the structure of the intermediate, 1-bromo-(4-adamantyl)-benzene, shown above.

NMR analysis of **[5-3]** revealed that this method, in which a Friedel–Crafts arylation reaction is used to synthesize the intermediate, 1-bromo-(4-adamantyl)-benzene, was suitable. Results also showed that high vacuum sublimation was an excellent method by which to purify **[5–3]** (>96 % purity as determined by GC). There are, however, a couple of disadvantages associated with using this method. The purification of the intermediate is a very time consuming process, because only small quantities of **[5–3]** can be purified at a time. It was therefore decided to attempt other methods to synthesize a substantial amount of **[5-3]**. Synthetic methods for which it was not necessary to synthesize an intermediate were also considered.

5.4.2 Preparation of 1-(1-Adamantyl)-4-Vinylbenzene [5–4]

In a conical flask equipped with a reflux condenser and nitrogen inlet, **[5–3]** (0.42 g; 2 x 10^{-3} mole) was dissolved in 10 mL dry toluene. Tributylvinyl tin (0.6 mL; 2 x 10^{-3} mole) was added dropwise to the reaction mixture. The reaction mixture was degassed three times using the freeze–thaw method.

$Pd(PPh_3)_4$ (0.053 g; 4.5 x 10^{-5} mole) was weighed in a dry box, under nitrogen, and dissolved in 3 mL dry toluene. The catalyst mixture was added dropwise to the reaction mixture after the last freeze–thaw cycle. 2,6-Di-tert-butyl-p-cresol (0.05 g; 1 x 10^{-5} mole), which acted as an anti–oxidant, was added to the reaction mixture. The reaction mixture was stirred at 140 °C for 24 hours, after which time it had a yellow–brown color.

The reaction mixture was allowed to cool to room temperature. A saturated aqueous solution of KF (3 g in 5 mL water) in 20 mL hexane was added to the reaction mixture and the mixture stirred for 24 hours. The reaction mixture was filtered and the filtrate washed with 4 x 10 mL diethyl ether. The combined ether extracts were washed with water once, aqueous (10 %) HCl twice, water once and saturated $NaHCO_3$ once, then dried over $MgSO_4$ for one hour. The diethyl ether was removed under reduced pressure. 0.3 g Crude **[5–4]** (65 %) was isolated and purified by chromatography on silica gel (column 2 x 20 cm, hexane/Et_2O, 5:1) to give 0.2 g (43 %) of **[5–4]** as a pale yellowish oil.

5.4.2.1 Results and Discussion

The ^{13}C NMR spectrum of **[5–4]** is shown in Figure 5–2.

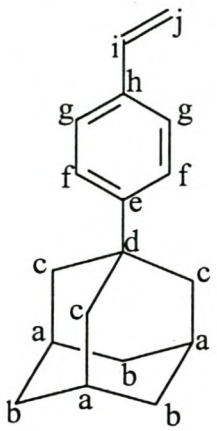

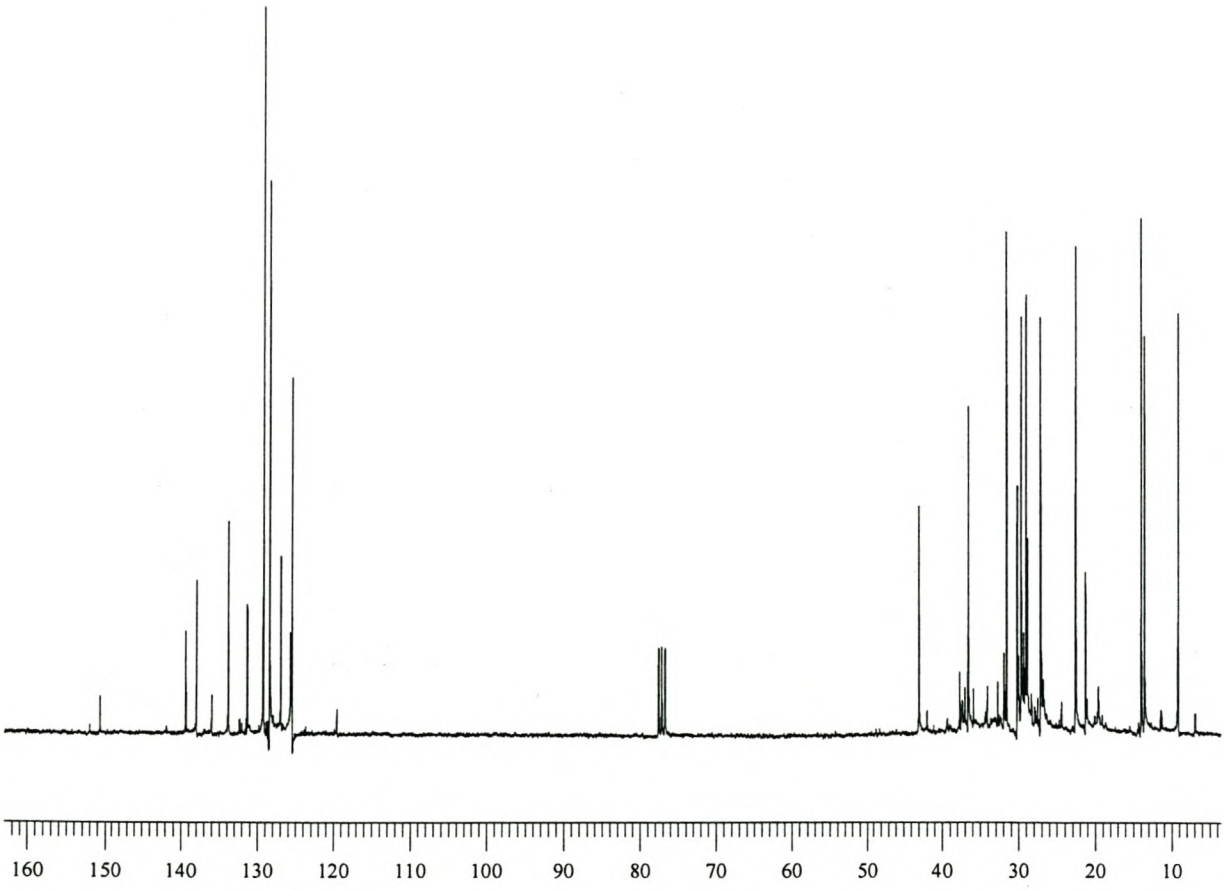

FIGURE 5-2: ^{13}C NMR Spectrum of [5–4] in $CDCl_3$

The ^{13}C NMR spectrum of **[5–4]** showed more than the expected eight signals, indicating that the product was not pure. Signals at 138.50 ppm, 132.99 ppm, 12.62 ppm and 8.26 ppm suggested that tributylvinyl tin was still present after purification by chromatography.

NMR analysis of **[5-4]** revealed that this method, where a Heck–type palladium coupling reaction is used to synthesize **[5–4]**, proved to be unsuitable. The use of chromatography proved to fail to purify **[5-4]**. Another possible method by which to remove the tin component could be high vacuum distillation. However, because of the low yield of **[5–4]** achieved by using this method, it was decided to rather consider other methods to synthesize a substantial amount of pure **[5-4]**.

5.5 SECOND APPROACH: NICKEL-CATALYZED GRIGNARD CROSS-COUPLING REACTION

After an extensive study of the relevant literature a three–step synthesis comprising a combination of a nickel–catalyzed Grignard cross coupling reaction[24-26, 28] and a Friedel–Crafts arylation[21], were used to develop another method by which to prepare the target monomer, 1-(1-adamantyl)-4-vinylbenzene. The first step involved the preparation of the Grignard reagent, vinyl magnesium bromide. The second step involved a Friedel-Crafts arylation reaction, to form 1-bromo-(4-adamantyl)-benzene, as discussed in Section 5.4.1. The third step involved a nickel-catalyzed Grignard cross-coupling reaction to form the required monomer, 1-(1-adamantyl)-4-vinylbenzene **[5-4]**. See Scheme 5-5.

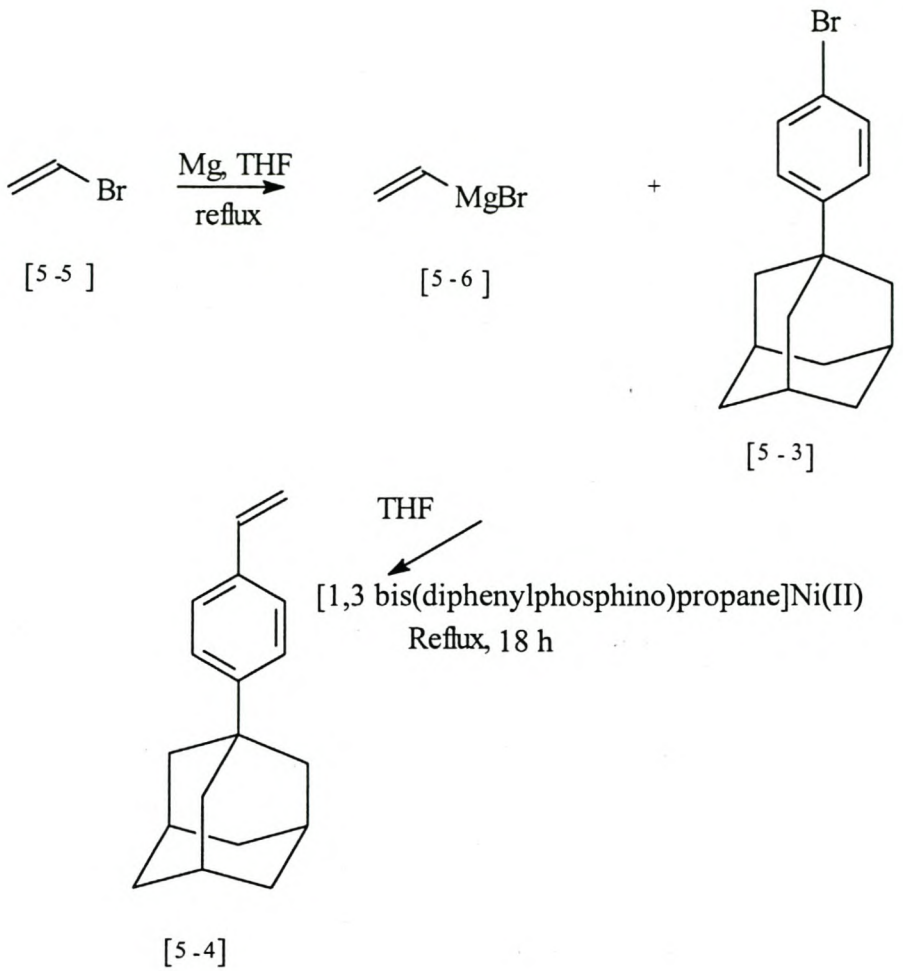

SCHEME 5-5: **Proposed Synthesis of [5–4] Using a Combination of Friedel-Crafts Arylation and Nickel–Catalyzed Grignard Cross–Coupling Reactions**

5.5.1 Preparation of 1-Bromo-(4-Adamantyl)-Benzene

See Section 5.4.1.

5.5.1.1 Preparation of Vinyl Magnesium Bromide [5-6]

The entire preparation of **[5–6]** was conducted under nitrogen because of the hygroscopic nature of the THF.

A solution of vinyl magnesium bromide (Grignard reagent) was prepared from magnesium turnings (0.06 g; 0.003 mole) and vinyl bromide **[5-5]** (2.9 mL; 3×10^{-3} mole) in 10 mL of dry THF. The magnesium turnings were weighed out into the round bottom flask, together with 10 mL of dry THF, and boiled

under reflux. **[5-5]** was then added dropwise, over a period of 30 minutes, and the mixture boiled under reflux for a further hour. The Grignard reagent was filtered through glass wool to remove the excess magnesium turnings.

5.5.1.2 Preparation of 1-(1-Adamantyl)-4-Vinylbenzene [5–4]

In a two–neck round bottom flask equipped with a reflux condenser and nitrogen inlet, **[5–3]** (0.36 g; 1 x 10^{-3} mole) was dissolved in 10 mL dry THF.

[1,3 *bis*(Diphenylphosphino)propane]Ni(II) (0.36 g; 1 x 10^{-3} mole) was weighed in the dry box under nitrogen and added to the reaction mixture. The Grignard reagent **[5–6]** was added dropwise to the reaction mixture, through a disposable syringe, over a period of 30 minutes. The reaction mixture was refluxed for 18 hours, after which it had an orange–brown color.

The reaction mixture was allowed to cool to room temperature and hydrolyzed with aqueous (30 %) HCl. The reaction mixture became dark yellow. The organic layer was separated and the water layer extracted with 4 x 10 mL of diethyl ether. The reaction mixture was filtered and the filtrate washed with 4 x 10 mL diethyl ether. The combined ether extracts were washed with water once, saturated $NaHCO_3$ once and water once, then dried over $CaCl_2$ for two hours. After two hours, the mixture was filtered, and the solvent removed under reduced pressure on a rotary evaporator to yield a yellowish solid, 1-(1-adamantyl)-4-vinylbenzene **[5-4]**, 0.4 g, 56 %. Tm = 89–93 °C.

5.5.2 Results and Discussion

The ^{13}C NMR spectrum of **[5–4]** is shown in Figure 5–3.

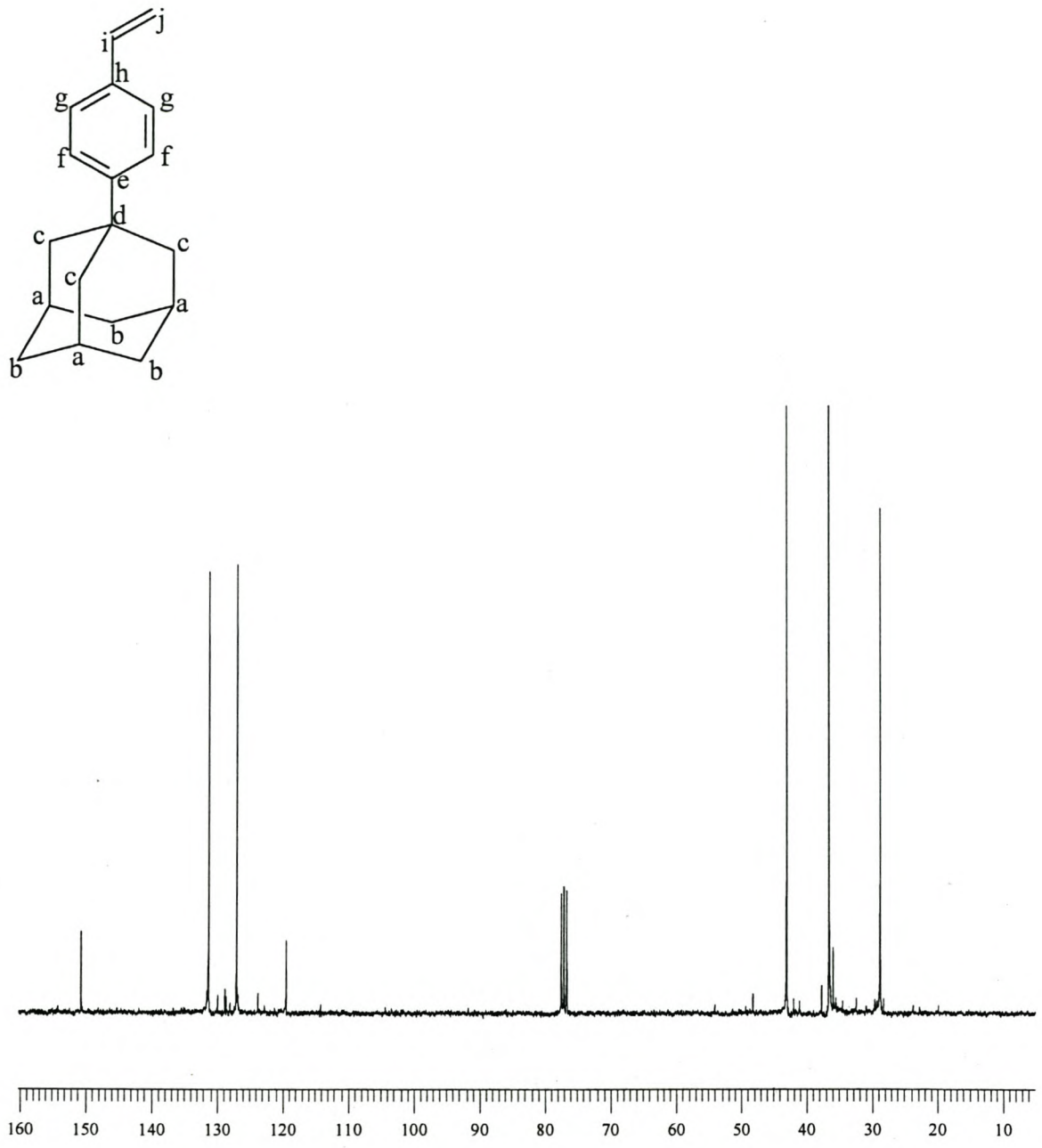

Figure 5–3: ^{13}C NMR Spectrum of [5–4] in $CDCl_3$

The ^{13}C NMR spectrum of **[5–4]** showed that the nickel-catalyzed Grignard cross-coupling reaction wasn't that successful. Considering the results from the ^{13}C NMR spectrum, it was clear that only a limited amount of coupling took place and only a small amount of the product was **[5–4]**. The major component in the ^{13}C NMR spectrum is **[5–3]**. The melting point of the product (89–93 °C) was in the same region as the melting point of **[5–3]** (86 °C).

Considering the low yield of required product **[5–4]** and the time factor involved in a three-step synthesis, it was therefore decided to attempt still other methods to synthesize a substantial amount of pure **[5-4]**.

5.6 THIRD APPROACH: PALLADIUM-CATALYZED SUBSTITUTION REACTION ON 1-BROMOADAMANTANE [5-1]

The synthesis of 1-(1-adamantyl)-4-vinylbenzene **[5–4]** has been reported by Bräse *et al* [10]. The proposed three–step synthesis can be described as a palladium–catalyzed substitution on **[5–1]**. The first step of the synthesis is a Friedel–Crafts arylation, the second step is a formylation reaction and the third step is a subsequent Wittig olefination, to form **[5–4]**. This proposed method of Bräse *et al* [10] was unsuccessful in our hands, because only small amounts of impure 1-(1-adamantyl)-4-vinylbenzene was synthesized. Therefore, using the relevant information in Bräse's method[10], the following three–step synthesis was proposed for the synthesis of pure and sufficient amounts of **[5–4]**.

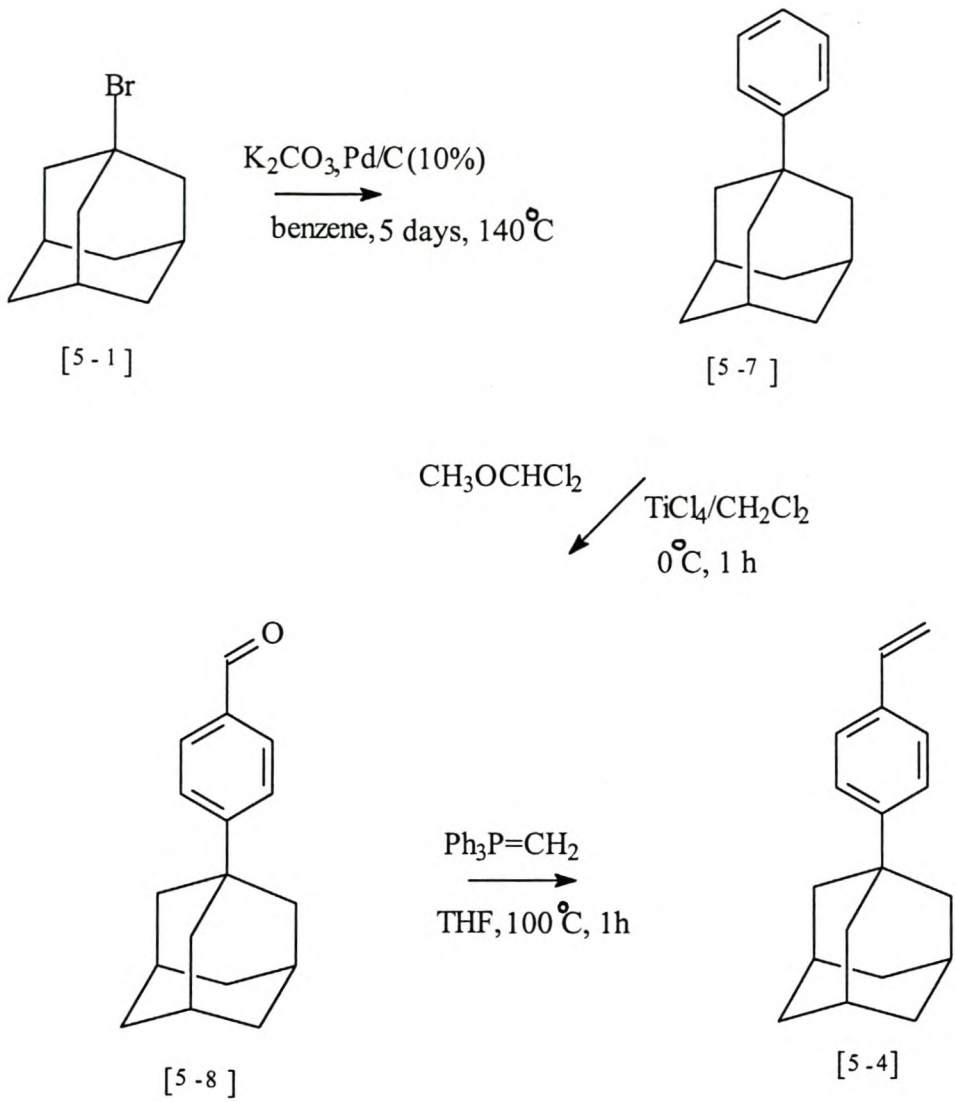

SCHEME 5-6: Proposed Synthesis of [5–4] Using a Palladium–Catalyzed Substitution Reaction on [5–1]

5.6.1 Preparation of 1-Phenyl Adamantane [5–7]

A mixture of **[5–1]** (4.4 g; 1 x 10^{-2} mole), K_2CO_3 (3.4 g; 1.2 x 10^{-2} mole), and Pd/C (10 %) (1 g; 5 x 10^{-4} mole) was stirred under nitrogen in a 400 mL stainless steel Parr autoclave for 60 hours at 140 °C. The reaction was monitored by gas chromatogtaphy until the peak for **[5–1]** had disappeared. The mixture was allowed to cool to room temperature then filtered. Evaporation of the solvent and recrystallization from methanol gave the corresponding wet product **[5–7]**. The product was then dried under vacuum for 24 hours to yield 2 g **[5–7]** (94 %) of fluffy white crystals. Tm = 85–86 °C.

5.6.1.1 Characterization of 1-Phenyl Adamantane by NMR Spectroscopy

The ^{13}C NMR spectrum of **[5–7]** is shown in Figure 5–4 and the chemical shift values are given in Table 5.3.

TABLE 5.3: ^{13}C NMR Chemical Shifts (δ) of [5–7] in $CDCl_3$

Carbon	Chemical shift (ppm)
a	29.08
b	37.0
c	43.30
d	36.30
e	150.80
f	128.50
g	125.90
h	125.20

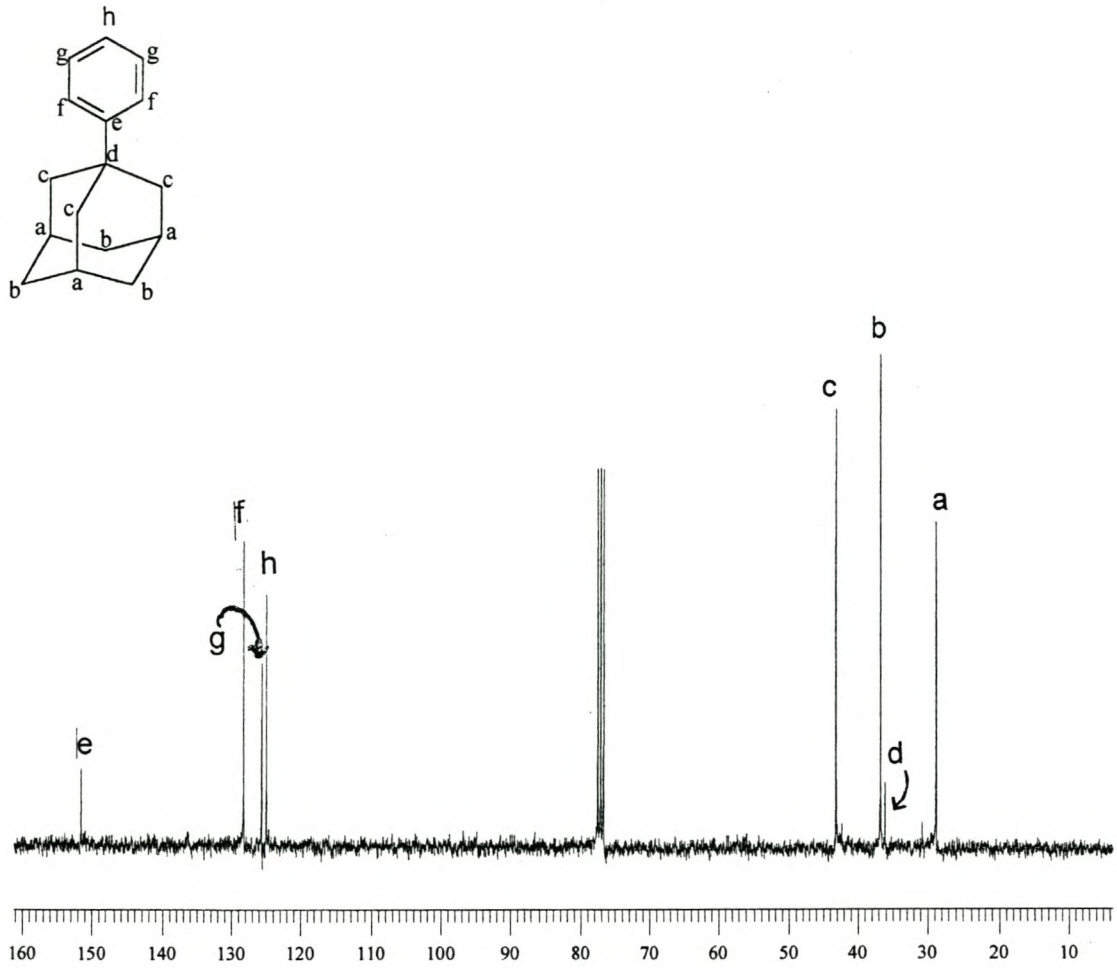

FIGURE 5-4: ^{13}C NMR Spectrum of [5–7] in $CDCl_3$

The ^{13}C NMR spectrum of **[5–7]** showed eight signals. The spectrum is consistent with the proposed structure shown above.

5.6.1.2 Results and Discussion

NMR analysis of **[5-7]** revealed that this method, where a Friedel–Crafts arylation reaction is used to synthesize **[5–7]**, was satisfactory. The reaction proceeded to a very high yield. From the NMR analysis it was clear that recrystallization from methanol was an efficient method for the purification of **[5-7]**, a purity of 96 % was achieved and no further purification was necessary.

5.6.2 Preparation of 1-Formyl-(4-Adamantyl)-Benzene [5–8]

$TiCl_4$ (2.3 mL; 1.7 x 10^{-2} mole) was rapidly added to a solution of **[5–7]** (3.5 g; 1.7 x 10^{-2} mole) in 25 mL of anhydrous dichloromethane at 0 °C, in a two-neck round bottom flask. Dichloromethyl methyl ether (1.5 mL; 1.7 x 10^{-2} mole) was then added rapidly while stirring. The reaction started immediately, with evolution of HCl-gas. After the mixture was stirred for one hour at 0 °C it was poured onto crushed ice and dichloromethane (100 mL) was added. The reaction mixture turned from cherry–red to bright yellow. The organic phase was separated and washed with water (50 mL) once, saturated $NaHCO_3$ (50 mL) twice and brine (50 mL) twice. After drying the product over $MgSO_4$ for four hours, the solvent was evaporated under reduced pressure to give 3 g (75 %) of crude **[5–8]** as a yellowish solid. **[5–8]** was purified by chromatography on silica gel [column 2 x 20 cm, petroleum ether (bp 40-60 °C)/Et_2O, 5:1] to yield 2.5 g (63 %) of pure **[5-8]**. Tm = 67 °C.

5.6.2.1 Characterization of 1-Formyl-(4-Adamantyl)-Benzene by NMR Spectroscopy

The ^{13}C NMR spectrum of **[5–8]** is shown in Figure 5–5 and the chemical shift values are given in Table 5.4.

TABLE 5.4: ^{13}C NMR Chemical Shifts (δ) of [5–8] in $CDCl_3$

Carbon	Chemical shift (ppm)
a	27.90
b	35.70
c	42.0
d	32.10
e	133.60
f	129.10
g	125.0
h	158.0
i	191.60

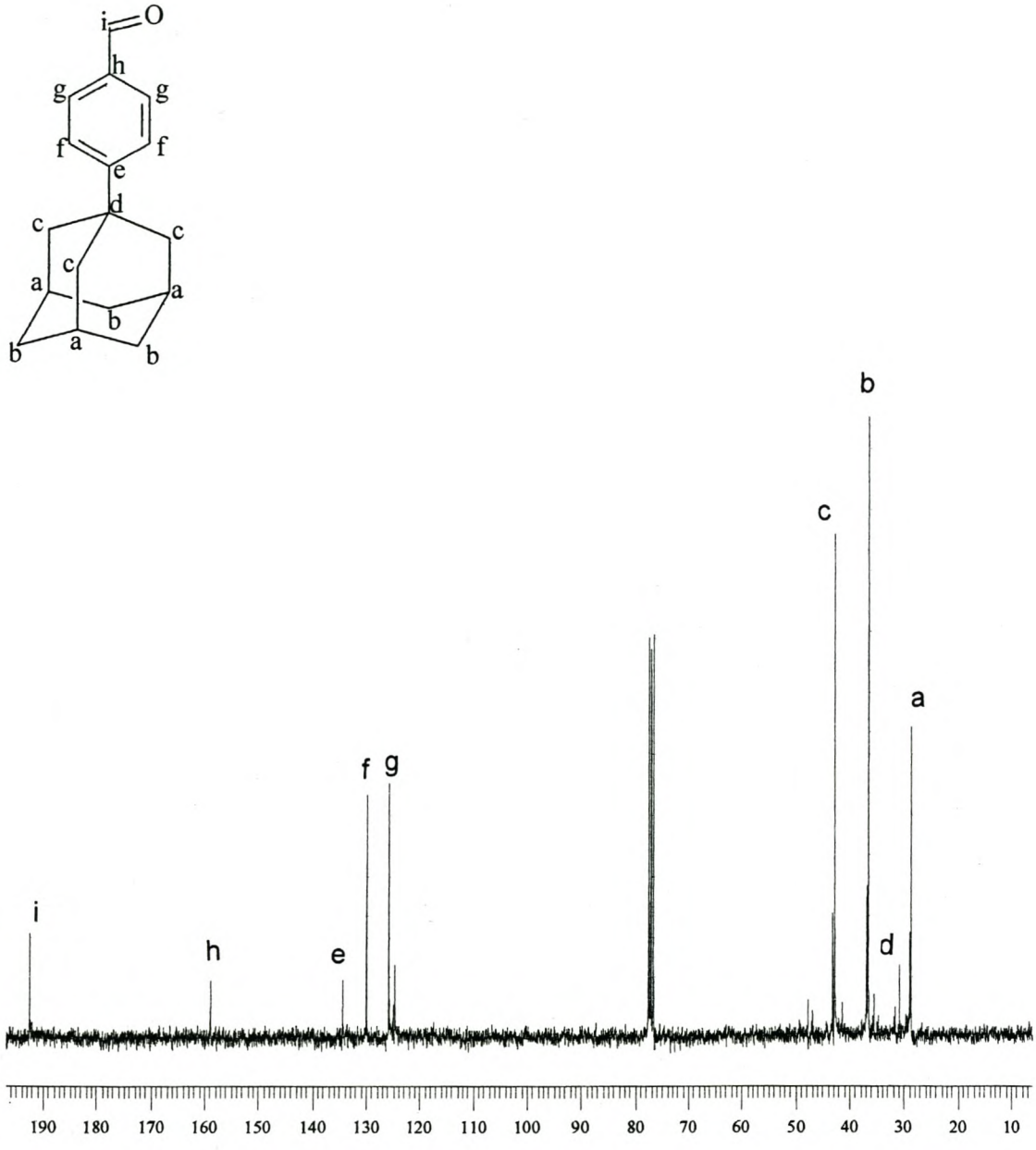

FIGURE 5-5: ^{13}C NMR Spectrum of [5–8] in $CDCl_3$

The ^{13}C NMR spectrum of **[5–8]** showed nine signals. The spectrum is consistent with the proposed structure shown above.

5.6.2.2 Results and Discussion

NMR analysis of **[5-8]** revealed that this method, where a formylation reaction is used to synthesize the **[5–8]**, proved to be very efficient. The reaction

proceeded to a good yield. From the NMR analysis it was clear that chromatography was an efficient method for the purification of **[5–8]**.

5.6.3 Preparation of 1-(1-Adamantyl)-4-Vinylbenzene [5–4]

Anhydrous DMSO (3.7 mL; 5.6 x 10^{-2} mole) was added to a suspension of NaH (0.24 g; 1 x 10^{-2} mole) in 50 mL of anhydrous THF in a two–neck round bottom flask. The reaction mixture was heated at 100 °C for 40 minutes. After cooling to 0 °C, a solution of methyl triphenylphosphonium bromide (3.6 g; 1 x 10^{-2} mole) in DMSO (5 mL) was added dropwise over a period of ten minutes. This mixture was stirred at 20 °C for ten minutes before **[5–8]** (2.2 g; 9 x 10^{-3} mole) was added. The final reaction mixture was stirred at 100 °C for one hour, then allowed to cool to room temperature and poured into water (50 mL). The aqueous phase was extracted with pentane (4 x 20 mL) and the combined organic phase dried over $MgSO_4$ for four hours. The reaction mixture was filtered and the solvent evaporated under reduced pressure to give 1.6 g (75 %) of crude **[5–4]** as a yellowish solid. **[5-4]** was purified by chromatography on silica gel [column 2 x 20 cm, petroleum ether (bp 40–60 °C)/Et_2O, 5:1] to give 1.4 g (65 %) of pure **[5-4]**. T_m = 75–77 °C.

5.6.3.1 Characterization of 1-(1-Adamantyl)-4-Vinylbenzene by NMR Spectroscopy

The ^{13}C NMR spectrum of **[5–4]** is shown in Figure 5–6 and the chemical shift values are given in Table 5.5.

TABLE 5.5: ^{13}C NMR Chemical Shifts (δ) of [5–4] in $CDCl_3$

Carbon	Chemical shift (ppm)
a	28.10
b	35.90
c	42.30
d	34.70
e	123.90
f	125.40
g	124.40
h	136.10
i	150.60
j	112.30

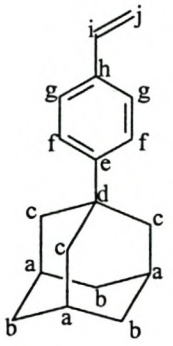

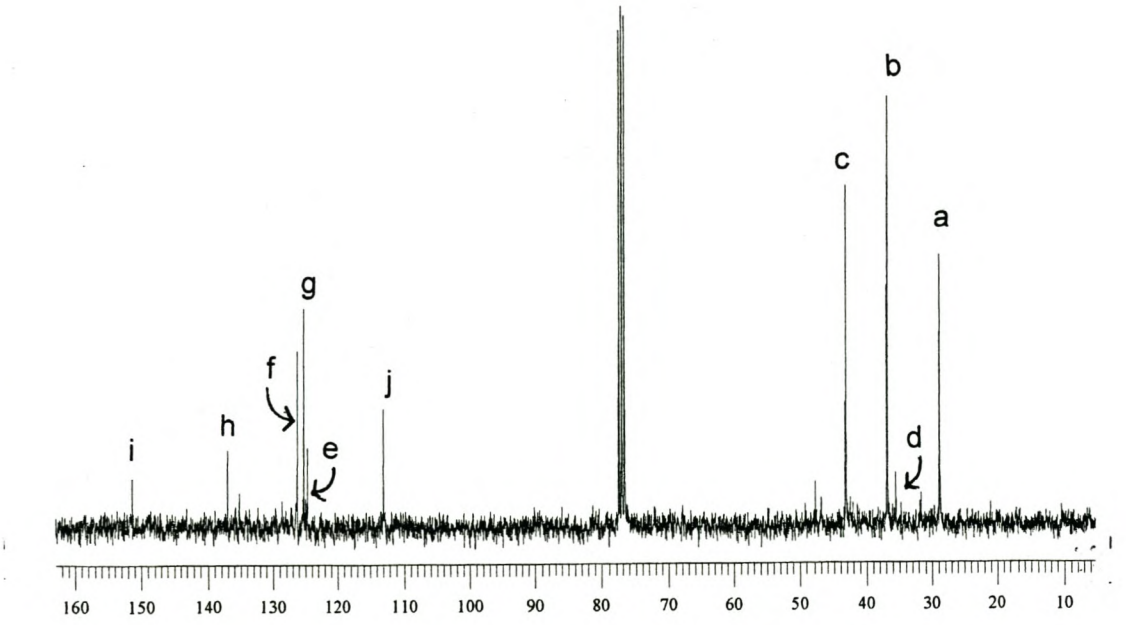

FIGURE 5-6: ^{13}C NMR Spectrum of [5–4] in $CDCl_3$

The ^{13}C NMR spectrum of **[5–4]** showed ten signals as expected. The spectrum is consistent with the proposed structure shown above.

5.6.3.2 Results and Discussion

NMR analysis of **[5-4]** revealed that this method, where a Wittig olefination reaction is used to synthesize **[5–4]**, proved to be very efficient. The reaction proceeded to a good yield. From the NMR analysis it was clear that chromatography was an efficient method for purification of **[5–4]**.

Analysis by FTIR spectroscopy was done to confirm the proposed structure of **[5–4]**. The spectral characteristics expected for **[5–4]** can be predicted.

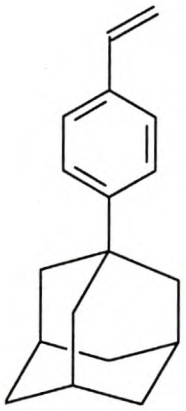

[5 – 4]

For the vinyl group the following are expected:

- Conjugated C=C stretch vibrations at 1 628 cm^{-1}
- $CHR_1=CH_2$ deformation vibrations at 3 083 cm^{-1}

For the phenyl group:

- =C-H stretch vibrations at 3 083 cm^{-1}
- C=C in–plane stretch vibrations at 1 628 cm^{-1}
- C-H in-plane bend vibrations at 1 012 cm^{-1} and 1 259 cm^{-1}, due to deformation
- C-H out–of–plane bend vibrations at 838 cm^{-1}, due to deformation

For the adamantyl group:

- C-H stretch vibrations, both symmetrical at 2 920 cm^{-1} and asymetrical at 2 848 cm^{-1}
- $-CH_2$ wag vibrations, asymmetrical at 1 344 cm^{-1} due to HCC angle bending
- C-H vibrations at 1 102 cm^{-1} due to deformation
- -C-C-C angle bending vibrations at 987 cm^{-1}

The FTIR analysis of **[5–4]** shown in Figure 5-7 confirmed the expected structure.

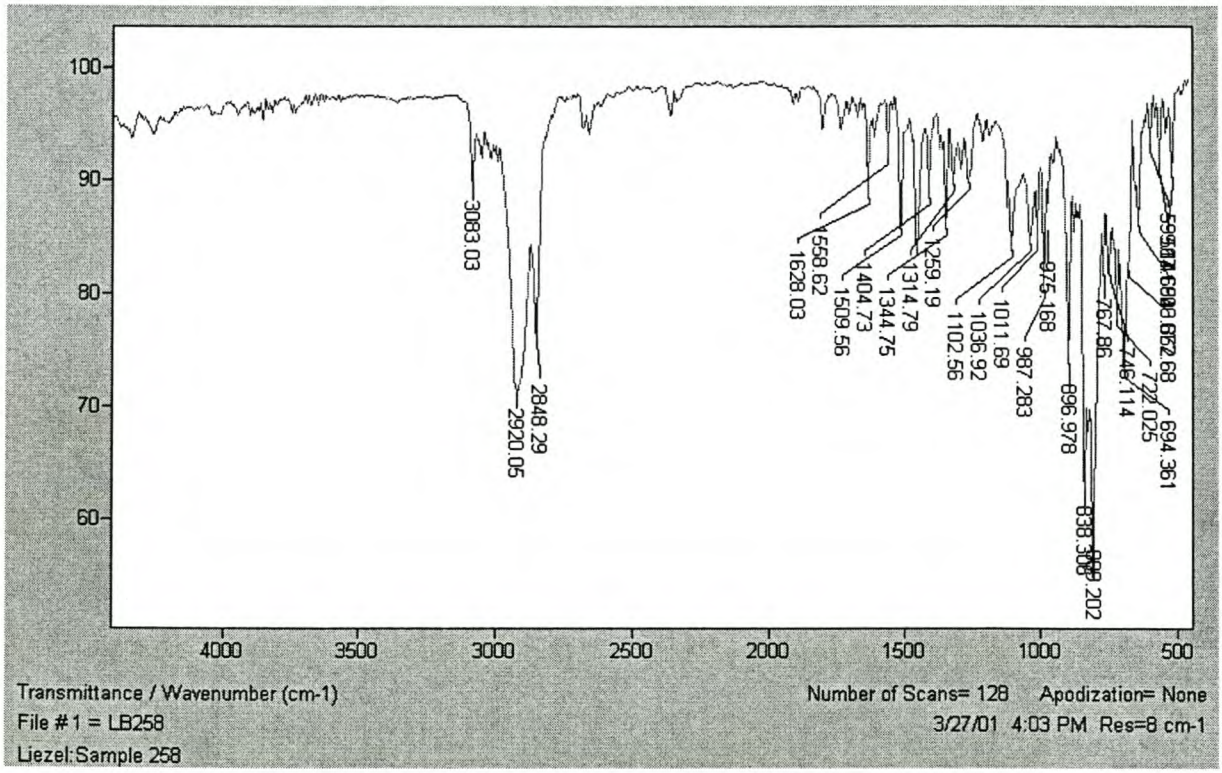

FIGURE 5-7: FTIR Spectrum of [5–4]

NMR analysis and the IR spectrum of **[5–4]** revealed that this proposed three-step synthesis, which can be described as a palladium–catalyzed substitution on **[5–1]**, was successful for the synthesis of high purity **[5-4]** which was suitable for use as monomer in polymerization reactions. This method was much more suitable than the other two proposed methods

discussed in Sections 5.4 and 5.5. Although this palladium–catalyzed substitution reaction comprised a three-step synthesis, the methods used to purify the product/s of the individual steps were very easy and not time consuming.

From the NMR analysis it was clear that chromatography was an excellent method for purification of **[5–4]**.

5.7 CONCLUSIONS

In conclusion, three different approaches were applied to synthesize **[5–4]** that was pure enough to be polymerized or incorporated into polymers. All three approaches comprised a three-step synthesis.

The first approach, a Heck–type palladium coupling proved to be unsuitable for the synthesis of **[5-4]**. The use of chromatography proved to fail to purify **[5-4]**. Another possible method which was considered to purify **[5-4]** was high vacuum distillation. However, because of the low yield of **[5–4]** achieved by using this method, it was decided to rather consider other methods to synthesize a substantial amount of pure **[5-4]**.

The second approach, a nickel-catalyzed Grignard cross-coupling reaction wasn't that successful either. Considering the results from the ^{13}C NMR spectrum, it was clear that only a limited amount of coupling took place and only a small amount of the product was **[5–4]**. The major component in the ^{13}C NMR spectrum proved to be **[5–3]**.

The third approach, a palladium–catalyzed substitution reaction, proved to be the most successful. From the NMR analysis it was clear that chromatography was an excellent method of purification of **[5–4]**.

5.8 REFERENCES

1. Chern Y.T., Wang J.J., *Macromolecules*, 1995, **28**, 5 554.
2. Chern Y.T., Chung W.H., *J. Polym.Sci.: Part A: Polym. Chem.*, 1996, **34**, 117.
3. Pixton M.R., Paul D.R., *Polymer*, 1995, **36**, 3 165.
4. Wang J.J., Chern Y.T., Chung M.A., *J. Polym. Sci., Polym. Chem. Ed.*, 1996, **34**, 3 345.
5. Chern Y.T., *Polym. Bull.*, 1996, **36**, 59.
6. Mathias L.J., Reichert V:R., Muir A.V.G., *Chem. Mat.*, 1993, **5**, 4.
7. Matsumoto A., Tanaka S., Otso T., *Macromolecules*, 1991, **24**, 4 017.
8. Avci D., Kusefoglu S.H., Thompson R.D., Mathias L.J., *Macromolecules*, 1994, **27**, 2 937.
9. Tsuda T., Mathias L.J., *Macromolecules*, 1993, **26**, 4 743.
10. Bräse S., Waegell B., de Meijere A., *Organic Synthesis*, 1998, **2**, 148.
11. Heck R.F., Trost B.M., Fleming I., *Comprehensive Organic Synthesis*, Eds., Pergamon: Oxford, 1991, **4**, 833.
12. Heck R.F., *Organic Reactions*, 1982, **27**, 345.
13. Heck R.F., *J. Am. Chem. Soc.*, 1968, **90**, 5 518.
14. Dieck H.A., Heck R.F., *J. Am. Chem. Soc.*, 1974, **96**, 1 133.
15. Heck R.F., Nolley J.P., Jr., *J. Org. Chem.*, 1972, **37**, 2 320.
16. Heck R.F., *Acct. Chem. Res.*, 1979, **12**, 146.
17. Patel B.A., Heck R.F., *J. Org. Chem.*, 1978, **43**, 3 898.
18. Dieck H.A., Heck R.F., *J. Org. Chem.*, 1975, **40**, 1 083.

19. Ziegler C.B., Jr., Heck R.F., *J. Org. Chem.*, 1978, **43**, 2 941.

20. Plevyak J.E., Heck R.F., *J. Org. Chem.*, 1978, **43**, 2 454.

21. Spencer A., *J. Organomet. Chem.*, 1984, **270**, 115.

22. Stetter H., Weber J., Wulff C., *Chem. Ber.*, 1964, **97**, 3 488.

23. Hayashi T., Konishi M., Kumada M., *Tett. Lett.*, 1979, **21**, 1 871.

24. Tamura M., Kochi J., *J. Am. Chem. Soc.*, 1971, **93**, 1 483.

25. Kiso Y., Yamamoto K., Tamao K., Makoto K., *J. Am. Chem. Soc.*, 1972, **94**, 4 374.

26. Tamura M., Kochi J., *Synthesis*, 1971, 303.

27. Heck R.F., *Pure and Appl. Chem.*, 1978, **50**, 691.

28. Farady L., Bencze L., Makó L., *J. Organometal. Chem.*, 1969, **17**, 107.

CHAPTER 6

POLYMERIZATION REACTIONS OF 1-(1-ADAMANTYL)-4-VINYLBENZENE

6.1 INTRODUCTION

In this Chapter, the homopolymerization reaction of 1-(1-adamantyl)-4-vinylbenzene as well as the polymerization reactions with ethene, styrene and higher α-olefins are discussed. Two different metallocene catalyst systems were used, namely a half-sandwich catalyst pentamethylcyclopentadienyl zirconium trichloride and a bridged C_s symmetric catalyst, iso-propylidene(cyclopentadienyl)(9-fluorenyl) zirconium dichloride. Stannic chloride ($SnCl_4$) was used in a cationic homopolymerization as well as copolymerization reactions with the 1-(1-adamantyl)-4-vinylbenzene and styrene monomers. In both the metallocene catalyst systems used, methylaluminoxane (MAO) was used as cocatalyst. An historical and theoretical background to metallocene-catalyzed polymerization reactions with ethene, propene and higher α-olefins has been presented in Section 4.2. Only a brief background to mainly the metallocene-catalyzed styrene polymerizations will therefore be discussed here.

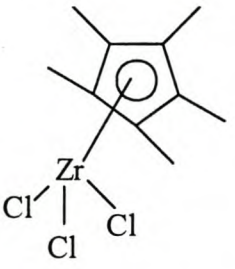

Figure 6–1: Pentamethyl Cyclopentadienyl Zirconium Trichloride

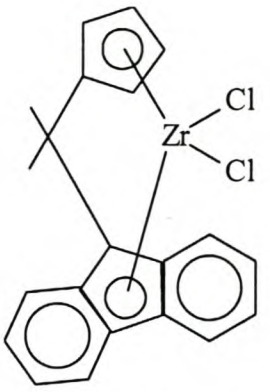

Figure 6–2: Iso-Propylidene(cyclopentadienyl)(9-fluorenyl)Zirconium Dichloride

6.2 METALLOCENE CATALYZED POLYMERIZATION REACTIONS WITH ETHENE, STYRENE AND HIGHER α-OLEFINS

6.2.1 Introduction

Since the discovery of the Ziegler–Natta catalyst systems, extensive studies concerning the stereospecific polymerization of olefins have been carried out[1]. In most cases, isotactic polymers are obtained, and syndiotactic polymers are rare. In principle, polystyrene can occur with isotactic, atactic or syndiotactic configurations, but the latter was unknown until the late 1980s[2, 3]. Ishihara *et al* [4] reported the first example of a syndiotactic polystyrene, with a very high syndiotacticity and high degree of crystallinity. The long-known isotactic polystyrene, which shows a slow crystallization rate, is useless for most industrial applications. The syndiotactic material shows a fast crystallization rate and a higher melting point of 275 °C compared to 240 °C, the melting point for the isotactic polymer. The glass transition temperature of the common atactic polymer[5] is 100 °C. These new properties, which are similar to those of some expensive engineering plastics[5] are the reason for the interest in syndiotactic polystyrene (sPS).

A variety of alkoxy, cyclopentadienyl and pentamethylcyclopentadienyl complexes of titanium, zirconium and hafnium have been investigated by Ishihara[1], Zambelli[6], Chien[7], Grassi[8] and Soga[9] for the syndiospecific

polymerization of styrene. Table 6.1 shows a variety of typical catalysts for the syndiospecific polymerization of styrene.

TABLE 6.1: Typical Catalysts for the Syndiospecific Polymerization of Styrene

Catalyst	T (°C)	10^{-4}[M] (mol/L)	[S] (mol/L)	Al:M	A	10^{-3} M_w	Ref
$TiCl_4$	50	4.07	1.63	800	8.5		1
$Ti(OEt)_4$	50	4.07	1.63	800	19.8		1
$TiBz_4$	50	6.25	3.26	100	18.3	153	6
$CpTiCl_3$	50	4.07	1.63	600	207		1
$Cp*TiCl_3$	50	4.07	1.63	600	157		1
$IndTiCl_3$	30	1.00	4.3	1000	260		1
(1-PhInd)$TiCl_3$	50	0.5	0.88	4000	3400	424	10
(2-methylbenz[*e*]indenyl)$TiCl_3$	50	0.5	0.88	4000	8000	424	10
$CpTiCl_2$	50	4.07	1.63	600	92		1
Cp_2TiCl_2	50	4.07	1.63	600	2.1		1
$Ti(acac)_2$	50	6.25	3.26	100	6.4	327	6
(η^6-C_6H_5Me)$Ti(Cl_2AlCl_2)$	50	27	2.6	700	1.8	1190	9
$CpTiCl_3/(Bu_3Sn)_2$	25	1.8	1.74	1244	11.9		11
$Cp*TiBz_3/B(C_6F_5)_3$	50	27.5	2.72		409		12
$ZrBz_4$	50	6.25	3.26	100	3.4	9	6
$Zr(OPr)_4$	50	0.09			1.8 x 10^{-5}	14	13

T = polymerization temperature, [M] = concentration of the catalyst, [S] = styrene concentration, Al:M = molar ratio (cocatalyst MAO), A (activity) = (kg of sPS)/(mol of M h), M_w = molecular weight. Et = ethyl, Bz = benzyl, Cp = cyclopentadienyl, Cp* = pentamethylcyclopentadienyl, Ind = indenyl, acac = acetylacetonato, Bu = butyl, Pr = propyl, Ph = phenyl.

Table 6.2 shows a summary of the polymerization conditions for the synthesis of syndiotactic polystyrene with different titanium and zirconium/MAO catalytic complexes.

TABLE 6.2: Synthesis of Syndiotactic Polystyrene with Different Titanium and Zirconium/MAO Complexes

Catalyst	T (°C)	A	Mp (°C)	M_w	M_w/M_n
$CpTiCl_3$	50	1100	258	140 000	1.9
$CpTiF_3$	50	3000	250	100 000	2.0
Cp^*TiCl_3	30	3.5	277	186 000	2.3
Cp^*TiCl_3	50	15	275	169 000	3.6
Cp^*TiF_3	30	300	277	700 000	1.8
Cp^*TiF_3	50	690	275	660 000	2.0
Cp^*ZrCl_3	50	0.08	249	16 000	1.6
Cp^*ZrF_3	50	0.9	248	38 000	2.5
$(MeCp)_2TiF_2$	50	1.8	264	121 000	2.4
$(MeSiCp)_2TiF_2$	10	0.2	275	290 000	1.7

T = polymerization temperature, A = activity, Mp = melting point , M_w = molecular weight, M_w/M_n = molecular weight distribution

If the cyclopentadienyl ligand in the metallocene (Table 6.2) is changed to a pentamethylcyclopentadienyl ligand (Cp∗), which is a stronger electron donor and exerts a greater steric hinderance, the polymerization activity is lower[5]. On the other hand, hydrogen transfer reactions tend to occur less often, so that the molecular weight of the obtained polystyrene increases. If the chlorine atoms are substituted by fluorine atoms, the activity rises drastically.

The catalyst Cp^*TiF_3 is highly active, producing syndiotactic polystyrene with a very high melting point of 277 °C and a high molecular weight (660 000 $g.mol^{-1}$ at 50 °C). The catalyst shows thermal stability up to polymerization temperatures of 70 °C, while the chlorinated analogue has a strongly reduced activity and its use results in a lower molecular weight polymer[5].

The activity of fluorinated complexes decreases drastically when zirconium or hafnium compounds are used instead of titanium (Table 6.2). In comparison

to the chlorinated compounds, the fluorinated systems are again much more active, but on a lower level. The same decrease in activity is found for substituted *bis*(cyclopentadienyl)titanium difluorides. Their activity is lower than that of the half sandwich complexes by a factor of 1 000–5 000. The two Cp rings hinder the polymerization and make a higher Al:Ti ratio necessary[5].

6.3 GENERAL EXPERIMENTAL CONSIDERATIONS

6.3.1 Materials

See Section 4.4.1.

6.3.1.1 Solvents

See Sections 4.4.1.1 and 5.3.1.2.

6.3.1.2 Monomers

The purification and drying of ethene, 1-pentene, 1-hexene and 1-octene is described in Section 4.4.1.2.

Styrene

Before use, the styrene monomer was purified from any inhibitors and/or impurities by distillation[14]. The monomer was first washed with a 0.3 M potassium hydroxide (KOH) solution to remove the hydroquinone inhibitor. To do this, 400 mL of styrene monomer and 100 mL of the KOH solution in a 500 mL separation funnel was carefully shaken to ensure that most of the inhibitor is washed out into the aqueous KOH phase. This was done three times with venting in–between to prevent pressure build–up in the funnel. The separation funnel was then left to stand for a few minutes for the phases to separate after which the bottom KOH layer was carefully removed. The monomer was then transferred to a one liter round bottom flask and boiling stones added. Distillation was done under vacuum and with a low heat applied to the flask. Care had to be taken that the temperature of the vapor did not exceed 55 °C as spontaneous polymerization could then occur.

The first 40 mL fraction collected was discarded to ensure that the distilled monomer was free from any impurities and also water. The second fraction collected was therefore considered pure and was stored at –8 °C to retard polymerization. $CaCl_2$ was also added to ensure a completely water–free product. The distilled styrene monomer used in all further reactions was never more than five days old.

1-(1-Adamantyl)-4-Vinylbenzene

1-(1-adamantyl)-4-vinylbenzene was synthesized as described in Section 5.6.3 and used without further purification.

6.3.2 Catalysts

Both the metallocene catalysts were weighed out into Schlenk tubes in a Plas Labs dry box because of the air and moisture sensitivity of these catalysts. The catalysts were dissolved in toluene under a nitrogen atmosphere.

In the case of the cationic polymerizations, a stannic chloride ($SnCl_4$) solution was prepared in anhydrous dichloromethane and used without further precautions involving moisture and air sensitivity.

6.3.2.1 Pentamethylcyclopentadienyl Zirconium Trichloride

The half-sandwich metallocene catalyst pentamethylcyclopentadienyl zirconium trichloride was obtained from Aldrich. It was used in the homopolymerization reactions of 1-(1-adamantyl)-4-vinylbenzene as well as the copolymerization reactions with ethene, 1-pentene, 1-hexene and 1-octene.

Typically, pentamethylcyclopentadienyl zirconium trichloride, (0.5 mg; 1.5×10^{-6} mole) was weighed out in a Plas Labs dry box into a Schlenk tube and dissolved in 4.4 mL of a 10 % solution of MAO in toluene under nitrogen.

6.3.2.2 Iso-Propylidene(cyclopentadienyl)(9-fluorenyl) Zirconium Dichloride

Iso-propylidene(cyclopentadienyl)(9-fluorenyl) zirconium dichloride was obtained from Aldrich. Typically, iso-propylindene(cyclopentadienyl)(9-fluorenyl) zirconium dichloride (0.5 mg; 1.7 x 10^{-5} mole) was weighed out in a Plas Labs dry box into a Schlenk tube and dissolved in 10 mL of toluene under nitrogen. For each polymerization reaction, 2.5 mL of the catalyst solution was used.

6.3.2.3 Stannic Chloride ($SnCl_4$)

Stannic chloride was obtained from Aldrich. Typically, stannic chloride, (0.9 mL; 7 x 10^{-5} mole) was injected to a Schlenk tube and diluted with 40 mL of anhydrous dichloromethane. For each polymerization reaction, 4 mL of the catalyst solution was used. The stannic chloride solution was kept at 0 °C.

6.3.3 Cocatalyst

See Section 4.4.1.4.

6.4 EQUIPMENT USED IN THE POLYMERIZATION REACTIONS

Descriptions of the Dry Box, the reactors and Schlenk tubes, as well as syringes can be found in Sections 4.4.2.1-4.4.2.4.

6.5 ANALYTICAL METHODS AND INSTRUMENTATION

The polymers formed were characterized by Infrared Spctroscopy, Nuclear Magnetic Resonance (NMR) Spectroscopy, Differential Scanning Calormetry (DSC) and Dynamic Mechanical Analysis (DMA). These techniques were discussed in Sections 4.4.3.1-4.4.3.4.

6.5.1 Gel Permeation Chromatography

GPC analysis was used to determine the molecular weight as well as molecular weight distribution of the polymers. The GPC system consisted of

a Waters 510 pump, Waters 486 tuneable absorbance detector at 260 nm, Waters 410 differential refractometer and a TSP (Thermo Separations Products) Spectra Series AS 100 autosampler. Five columns and a pre-column filter were used. The column oven was set at 30 °C. PSS WinGPC Scientific V 4.02 was used for data analysis. Tetrahydrofuran (THF) was used as a solvent and the flow rate was 1.06 mL/min. The volume of the samples injected was 180 μL.

Sample preparation was done as follows. Typically, one mg of polymer was dissolved in one mL of THF and filtered by means of a GPC filter before being injected into the GPC.

6.6 SYNTHESIS OF POLYMERS

6.6.1 General

Notices on laboratory safety and the preparation of the Dry Box can be found in Sections 4.5.1.1. and 4.5.1.2.

6.6.2 Polymerization Reactions of 1-(1-Adamantyl)-4-Vinylbenzene

The homopolymerization reaction of 1-(1-adamantyl)-4-vinylbenzene was carried out with the half–sandwich metallocene catalyst, pentamethylcyclopentadienyl zirconium trichloride, as well as by means of cationic polymerization using stannic chloride ($SnCl_4$) as catalyst. Copolymerization reactions of 1-(1-adamantyl)-4-vinylbenzene with ethene, 1-pentene, 1-hexene and 1-octene were carried out with both the bridged C_s symmetric metallocene catalyst, iso-propylidene(cyclopentadienyl)(9-fluorenyl) zirconium dichloride, and the half-sandwich metallocene catalyst, pentamethylcyclopentadienyl zirconium trichloride. Copolymerization reactions of 1-(1-adamantyl)-4-vinylbenzene with styrene were carried out with the half–sandwich metallocene catalyst, pentamethylcyclopentadienyl zirconium trichloride as well as by means of cationic polymerization using stannic chloride ($SnCl_4$) as catalyst.

The procedure followed for the polymerization reactions with 1-(1-adamantyl)-4-vinylbenzene was a combination of those described in literature for similar reactions[15-17]. The procedure is described below in Sections 6.6.2.1-6.6.2.4.

The reactor and all glassware were kept overnight in an oven at 120 °C to remove any residual water that could poison the metallocene catalyst system. The glassware was then cooled under a nitrogen atmosphere to prevent condensation of moisture that might cause possible contamination during the removal of the glassware from the oven. Whether the polymerization reactions were carried out either in the reactor or in Schlenk tubes, both were charged under nitrogen. The precise amount of the prepared catalyst needed for the reaction was weighed on a balance inside the Plas Labs nitrogen dry box.

6.6.2.1 Homopolymerization Reaction of 1-(1-Adamantyl)-4-Vinylbenzene

(i) Half–Sandwich Metallocene Catalyst

The homopolymerization reaction of 1-(1-adamantyl)-4-vinylbenzene was conducted in a 50 mL Schlenk tube, equipped with a magnetic follower under a nitrogen atmosphere. 1-(1-adamantyl)-4-vinylbenzene (0.5 g; 2 x 10^{-3} mole) was dissolved in 5 mL of toluene in a Schlenk tube equipped with a magnetic follower, side-arm and stopcock.

The half–sandwich catalyst, pentamethylcyclopentadienyl zirconium trichloride, (5 x 10^{-4} g; 1.5 x 10^{-6} mol) was dissolved in MAO (4.4 mL of a 10 % solution in toluene) and added. The Al : Zr ratio was 5 000 : 1. The Schlenk tube was closed, heated to 50 °C and kept at that temperature for 18 hours. The Schlenk tube was then cooled and vented, and the polymer precipitated in acidic methanol (10 % HCl). The mixture was stirred for 24 hours, filtered, the product well washed with methanol and dried under reduced pressure.

(ii) Cationic Polymerization using Stannic Chloride ($SnCl_4$)

The cationic homopolymerization reaction of 1-(1-adamantyl)-4-vinylbenzene was conducted in a 50 mL Schlenk tube equipped with a magnetic follower. Anhydrous dichloromethane (40 mL) was added to the Schlenk tube and cooled to 0 °C. The cold stannic chloride solution (4 mL) was added to the dichloromethane in the Schlenk tube. 1-(1-adamantyl)-4-vinylbenzene (0.3 g; 1×10^{-3} mole) was added to the catalyst mixture. The mixture was stirred for one hour at 0 °C then poured into a flask containing 100 mL of methanol. The polymer was filtered, washed with methanol and dried under reduced pressure.

6.6.2.2 Copolymerization Reaction of 1-(1-Adamantyl)-4-Vinylbenzene with Ethene

The copolymerization reaction of 1-vinyl-(4-adamantyl)-1-benzene with ethene was conducted in a 350 mL Parr autoclave under a nitrogen atmosphere. Typically, 1-(1-adamantyl)-4-vinylbenzene (0.3 g; 1×10^{-3} mole) was dissolved in 10 mL of dry toluene and added to the reactor. The half-sandwich catalyst, pentamethylcyclopentadienyl zirconium trichloride (5×10^{-4}g; 1.5×10^{-6} mole) was dissolved in MAO (4.4 mL of a 10 % solution in toluene) and after ageing for 30 minutes, was added to the toluene in the reactor. The Al : Zr ratio for all the copolymerization reactions was 5 000 : 1. The reactor was sealed and pressurized to a pressure of 300 Psi with the gaseous monomer (ethene). The reactor was heated to 80 °C and kept at that temperature for 18 hours. The reactor was then cooled and vented, and the polymer precipitated in acidic methanol (10 % HCl). The mixture was stirred for 24 hours, filtered, the product well washed with methanol and dried under reduced pressure.

6.6.2.3 Copolymerization Reactions of 1-(1-Adamantyl)-4-Vinylbenzene with Higher α-Olefins

A series of copolymerizations of 1-(1-adamantyl)-4-vinylbenzene with 1-pentene, 1–hexene, 1–octene and styrene were carried out. The catalysts used in all these copolymerizations were pentamethylcyclopentadienyl

zirconium trichloride and iso-propylindene(cyclopentadienyl)(9-fluorenyl) zirconium dichloride. MAO was used as cocatalyst. The ratio of Al : Zr was 5 000 : 1 for all the copolymerizations.

Typically, 1-pentene (6.4 g; 9 x 10^{-2} mole) and 1-(1-adamantyl)-4-vinylbenzene (0.3 g; 1 x 10^{-3} mole) were dissolved in 5 mL of toluene in a Schlenk tube equipped with a magnetic follower, side-arm and stopcock. The iso-propylindene(cyclopentadienyl)(9-fluorenyl)zirconium dichloride (0.001 g; 2.9 x 10^{-6} mole) was added by syringe, followed by 8.4 mL of a 10 % solution of MAO in toluene. In the case of the half–sandwich catalyst, pentamethylcyclopentadienyl zirconium trichloride (5 x 10^{-4} g; 1.5 x 10^{-6} mole) was dissolved in MAO (4.4 mL of a 10 % solution in toluene) and after ageing for 30 minutes, was added to the monomer in solution. The reaction flask was then placed in an oil bath at 40 °C and the reaction mixture stirred for 18 hours. The polymer was precipitated in acidic methanol, stirred for 24 hours, filtered, the product well washed with methanol and dried under reduced pressure.

6.6.2.4 Cationic Copolymerization Reaction of 1-(1-Adamantyl)-4-Vinylbenzene with Styrene

The cationic copolymerization reaction of 1-(1-adamantyl)-4-vinylbenzene and styrene was conducted in a 50 mL Schlenk tube equipped with a magnetic follower.

Anhydrous dichloromethane (40 mL) was added to the Schlenk tube and cooled to 0 °C. Styrene (4.55 g; 5 x 10^{-2} mole) was added to the Schlenk tube containing 40 mL of dichloromethane. The cold stannic chloride solution (4 mL) was added to the dichloromethane in the Schlenk tube. 1-(1-Adamantyl)-4-vinylbenzene (0.3 g; 1 x 10^{-3} mole) was added to the catalyst mixture. The mixture was stirred for one hour at 0 °C then poured into a flask containing 100 mL of methanol. The polymer was filtered and washed with methanol and dried under reduced pressure.

6.7 RESULTS AND DISCUSSION

6.7.1 Polymerization Reactions

The homopolymerization of 1-(1-adamantyl)-4-vinylbenzene proceeded to a good yield. The powdery polymer product of poly[(1-(1-adamantyl)-4-vinylbenzene] obtained by using the half–sandwich catalyst, pentamethylcyclopentadienyl zirconium trichloride, was insoluble in all common organic solvents, even in chlorinated aromatic solvents at elevated temperatures. The powdery polymer product of poly[(1-(1-adamantyl)-4-vinylbenzene] obtained by cationic polymerization was soluble in some organic solvents.

1-(1-Adamantyl)-4-vinylbenzene was successfully copolymerized with ethene by using the half–sandwich metallocene catalyst, pentamethylcyclopentadienyl zirconium trichloride. The powdery polymer product of poly[(1-(1-adamantyl)-4-vinylbenzene-co-ethene] was insoluble in all common organic solvents.

In the copolymerization reactions of 1-(1-adamantyl)-4-vinylbenzene with 1-pentene, 1-hexene and 1-octene using the half–sandwich metallocene catalyst, pentamethylcyclopentadienyl zirconium trichloride, only poly[(1-(1-adamantyl)-4-vinylbenzene] was formed. In the case where styrene was used as comonomer the powdery product, poly[(1-(1-adamantyl)-4-vinylbenzene-co-styrene], was formed. This could be because of the ease with which the styrene–derived monomer is polymerized with the half-sandwich catalyst. In the copolymerization reactions of 1-(1-adamantyl)-4-vinylbenzene with 1-pentene, 1-hexene, 1-octene and styrene using the bridged metallocene catalyst, iso-propylindene(cyclopentadienyl)(9-fluorenyl) zirconium dichloride, no polymers were formed. This could be because of the steric hindrance of the bridged catalyst and the steric nature of the 1-(1-adamantyl)-4-vinylbenzene monomer.

1-(1-Adamantyl)-4-vinylbenzene was also successfully copolymerized with styrene cationically, using stannic chloride ($SnCl_4$) as catalyst. The powdery

polymer product of poly[(1-(1-adamantyl)-4-vinylbenzene-co-styrene] proved to be soluble in most common organic solvents.

6.7.2 GPC Analyses

The 1-(1-adamantyl)-4-vinylbenzene homopolymer and 1-(1-adamantyl)-4-vinylbenzene-co-styrene copolymer, synthesized cationically, were analyzed by GPC to determine the molecular weight and molecular weight distribution. 100 µL of a 1 mg/mL sample was injected. The column oven was at a constant temperature of 30 °C and the run time was 60 minutes. GPC results are shown in Table 6.3.

TABLE 6.3: GPC Results of poly[(1-(1-adamantyl)-4-vinylbenzene] and poly[(1-(1-adamantyl)-4-vinylbenzene-co-styrene]

Polymer	Molecular Weight (Mw)	Polydispersity
Poly[(1-(1-adamantyl)-4-vinylbenzene]	1 823	1.5
Poly[(1-(1-adamantyl)-4-vinylbenzene-co-styrene]	21 229	2.4

The GPC analysis of the homopolymer of 1-(1-adamantyl)-4-vinylbenzene showed that it was an oligomer that consisted of about 8 repeating units. It had a Mw of 1 823 $g.mol^{-1}$.

GPC analysis of the copolymer of 1-vinyl(4-adamantyl)-benzene-co-styrene showed that it was polymeric, and has a Mw of 21 229 $g.mol^{-1}$.

The polydispersity of both the homopolymer and the copolymer was quite narrow for a cationic polymerization.

6.7.3 Thermal Analysis by DSC

The 1-(1-adamantyl)-4-vinylbenzene homopolymers synthesized with the metallocene catalysts, as well as cationically, were analyzed by DSC to determine the melting points. A sample was heated from ambient

temperature to 300 °C, at a heating rate of 5 °C/min, in a nitrogen atmosphere with a flow rate of 58.2 mL/min. An average sample mass of eight mg polymer was used.

The polymers showed no melting prior to degradation.

Poly[(1-(1-adamantyl)-4-vinylbenzene-co-ethene] synthesized with the half-sandwich metallocene catalyst was insoluble in all common organic solvents. This copolymer showed a melting point at 142 °C. No other transitions were observed at lower temperatures. Although analysis by DSC showed a crystalline melting point, the sample did not become fluid prior to the onset of degradation.

Poly[(1-(1-adamantyl)-4-vinylbenzene-co-styrene] synthesized with the half-sandwich metallocene catalyst was insoluble in all common organic solvents. No melting point was observed prior to degradation.

Poly[(1-(1-adamantyl)-4-vinylbenzene-co-styrene] synthesized cationically, using stannic chloride ($SnCl_4$) as catalyst, was soluble in most common organic solvents. No melting point was observed prior to degradation, indicating no tacticity in the formed polymer.

Because of the higher sensitivity to hard-to detect transitions of the DMA, T_g analyses were to be done using this technique.

6.7.4 Dynamic Mechanical Analysis (DMA)

The 1-(1-adamantyl)-4-vinylbenzene homopolymer synthesized cationically, using stannic chloride ($SnCl_4$) as catalyst, was analyzed by DMA to determine its melting point. The sample was kept at –50 °C for three minutes before it was heated from –50 °C to 150 °C, at a heating rate of 5 °C/min.

The polymer showed a glass transition temperature at –9 °C. This very low value is due to the oligomeric nature of the material.

In the case of poly[(1-(1-adamantyl)-4-vinylbenzene-co-styrene], the sample was kept at 10 °C for one minute before it was heated from 10 °C to 200 °C, at a heating rate of 5 °C/min.

The polymer showed a glass transition temperature at 100.9 °C, which is very close to that of polystyrene homopolymer.

6.7.5 COMPOSITIONAL ANALYSIS

Infrared spectroscopy (IR) and nuclear magnetic resonance spectroscopy (NMR) were used to determine the physical structure of the polymers synthesized (Sections 6.6.2.1-6.6.2.4). ^{13}C NMR spectroscopy was used to investigate the microstructure of 1-(1-adamantyl)-4-vinylbenzene homo- and copolymers.

6.7.5.1 Photo–Acoustic Infrared Spectroscopy (PAS-IR)

A Perkin Elmer FTIR instrument in conjunction with a photo–acoustic detector system, was used. This method obviates sample preparation and gives spectra that compare well with those obtained with other IR techniques.

The spectral characteristics expected for poly[(1-(1-adamantyl)-4-vinylbenzene] can be predicted.

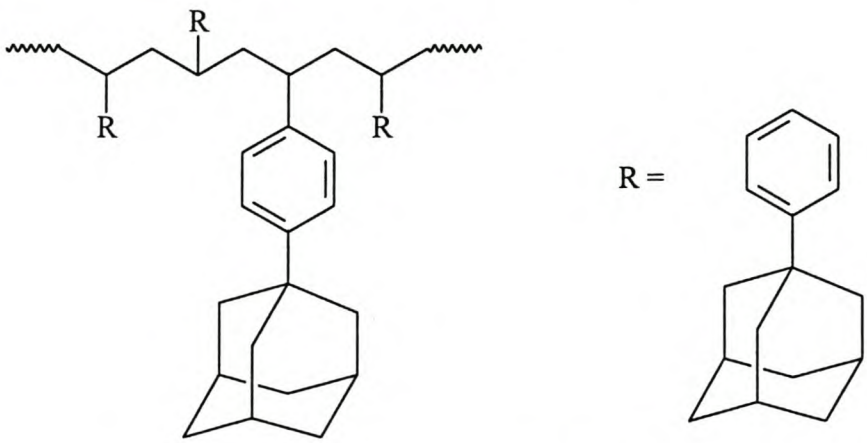

For the $-CH_2-$ groups and –CH-groups in the backbone the following are expected:

- $-CH_2$ scissor deformation vibrations at 1 511 cm^{-1}-1 453 cm^{-1}

- C-H stretch vibrations, both symmetrical at 2 904 cm^{-1} and asymmetrical at 2 847 cm^{-1}

For the phenyl group:

- =C-H stretch vibrations at 3 085 cm^{-1}
- C-H out–of-plane bend vibrations at 806 cm^{-1} due to deformation

For the adamantyl group:

- C-H stretch vibrations, both symmetrical at 2 904 cm^{-1} and assymetrical at 2 847 cm^{-1}

The FTIR analysis of poly[(1-(1-adamantyl)-4-vinylbenzene] shown in Figure 6-3 confirmed the expected structure.

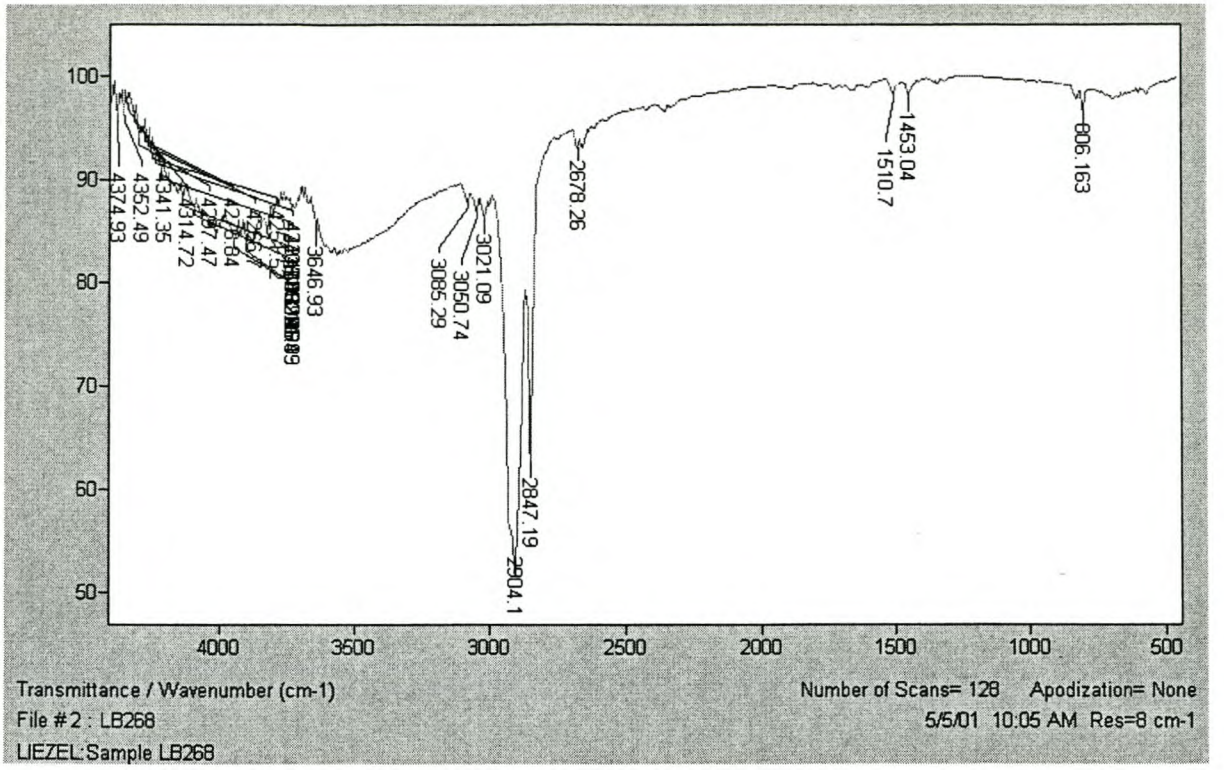

FIGURE 6-3: IR Spectrum of poly[(1-(1-adamantyl)-4-vinylbenzene]

Likewise, the spectral characteristics expected for poly[(1-(1-adamantyl)-4-vinylbenzene-co-styrene] can be predicted.

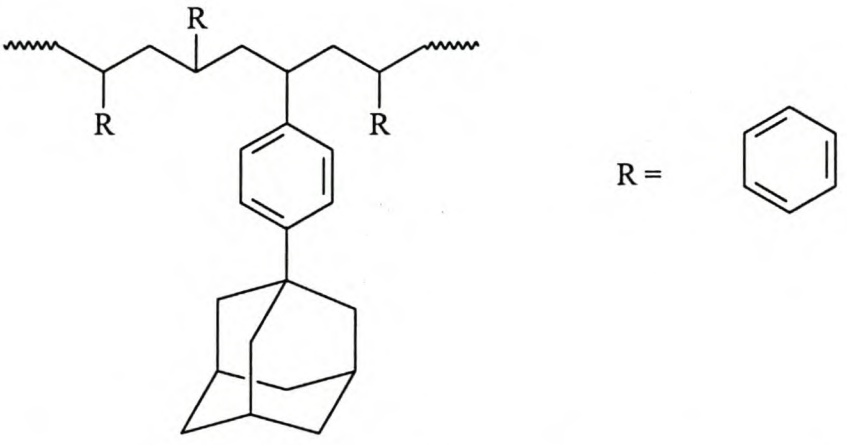

For the -CH_2- groups and –CH-groups in the backbone the following are expected:

- -CH_2 scissor deformation vibrations at 1 493cm^{-1}-1 453 cm^{-1}

- C-H stretch vibrations, both symmetrical at 2 924 cm^{-1} and asymmetrical at 2 848 cm^{-1}
- $-CH_2-CH_2-$skeletal vibrations at 757 cm^{-1}

For the phenyl group:

- =C-H stretch vibrations at 3 081 cm^{-1}
- C=C in–plane stretch vibrations at 1 601 cm^{-1}
- C-H in-plane bend vibrations at 1 027 cm^{-1}, due to deformantion

For the adamantyl group:

- C-H stretch vibrations, both symmetrical at 2 924 cm^{-1} and assymetrical at 2 848 cm^{-1}
- $-CH_2$ wag vibrations, assymetrical at 1 453 cm^{-1}-1 493 cm^{-1} due to HCC angle bending
- C-H vibrations at 1 027 cm^{-1}, due to deformantion

The FTIR analysis of poly[(1-(1-adamantyl)-4-vinylbenzene-co-styrene] shown in Figure 6-4 confirmed the expected structure.

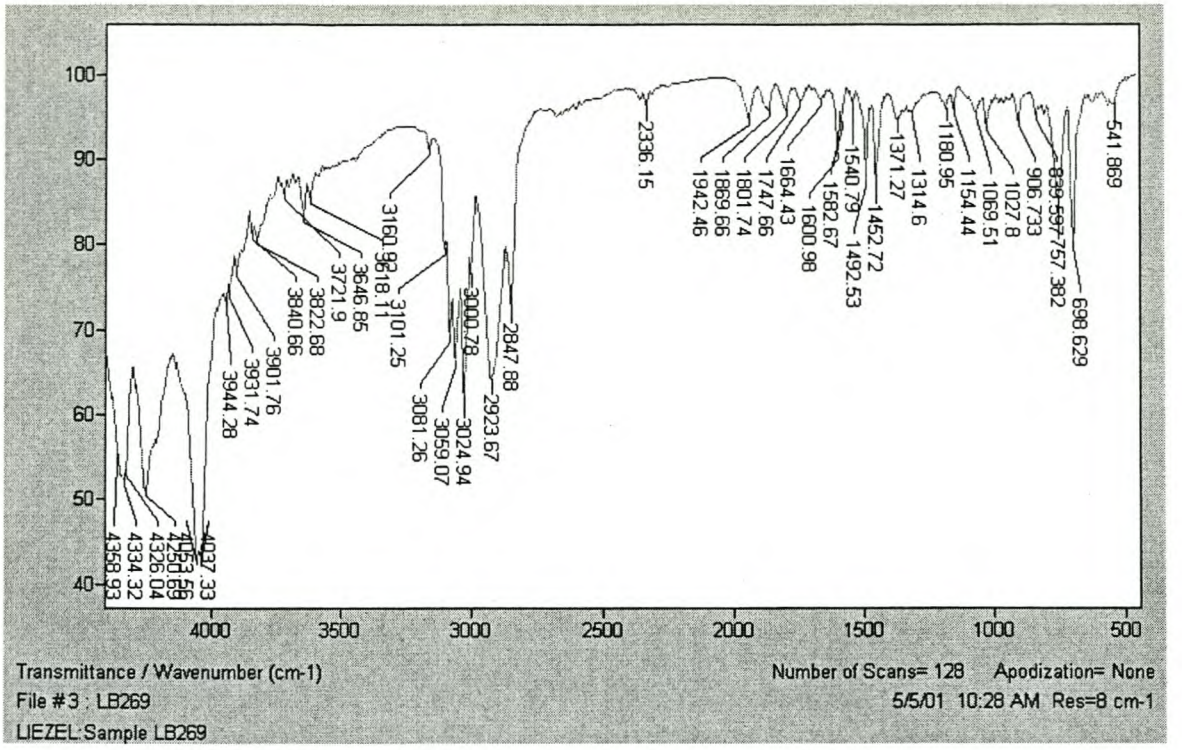

FIGURE 6-4: IR Spectrum of poly[(1-(1-adamantyl)-4-vinylbenzene-co-styrene]

From the data compiled from the IR–analyses of the homopolymer poly[(1-(1-adamantyl)-4-vinylbenzene] and the copolymer of 1-(1-adamantyl)-4-vinylbenzene with styrene, it was possible to propose structures for the above-mentioned polymers.

The IR spectra of the homopolymer as well as the copolymer confirmed the proposed structure.

6.7.5.2 Nuclear Magnetic Resonance Spectroscopy (NMR)

(i) Homopolymerization Reaction

The ^{13}C NMR spectrum of poly[1-(1-adamantyl)-4-vinylbenzene] is shown in Figure 6–5 and chemical shift values are given in Table 6.4.

TABLE 6.4: Comparison of Expected and Observed ^{13}C NMR Chemical Shifts (δ) of poly[(1-(1-adamantyl)-4-vinylbenzene]

Carbon	Expected	Observed
a	28.10*	29.10
b	35.90*	37.0
c	42.30*	43.40
d	27.0**	N/D
e, h	135.0**	127.90
f, g	128.2**	124.90
i	37.70**	N/D
j	24.40**	N/D

*: Based on monomer spectra; **: Based on spectra of poly(styrene) and related polymers.

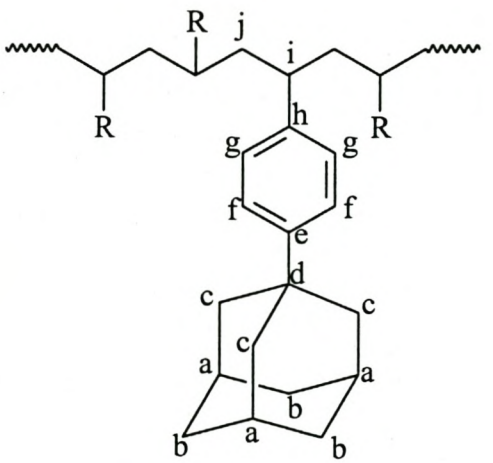

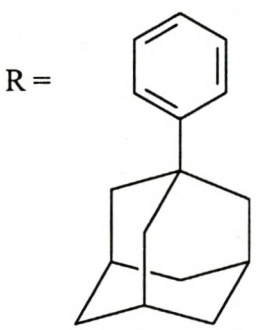

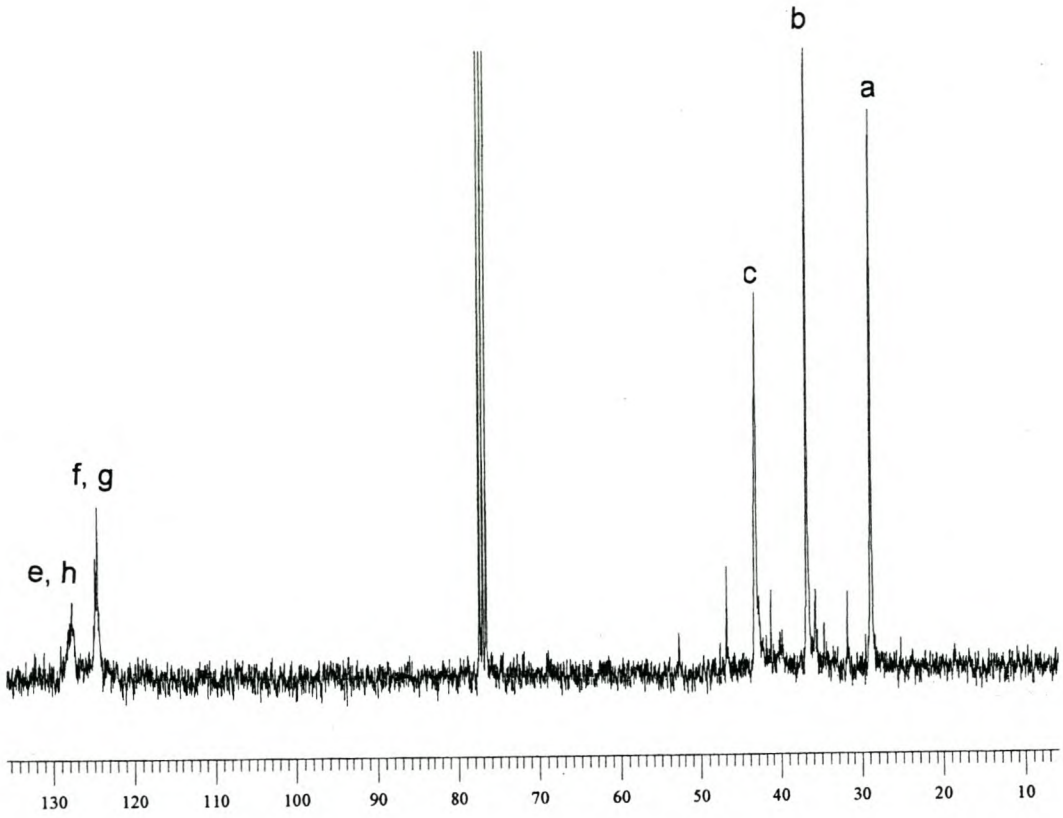

FIGURE 6-5: ^{13}C NMR Spectrum of poly[(1-(1-adamantyl)-4-vinylbenzene] in $CDCl_3$

From Table 6.4 one can see a very good comparison of the chemical shifts expected for similar hydrocarbon polymers (with $-CH_2$ groups in the α-position relative to the carbon chain and branching in the β-position) and the chemical shifts observed from the ^{13}C NMR spectrum. The spectrum is consistent with the structure shown above. In the case of carbon **d** it is very difficult to observe the peak from the ^{13}C NMR spectrum, as the area in which this peak is expected is hidden under the larger peak area at ca 29 ppm. The signals at 29.10 ppm, 37.0 ppm and 43.40 ppm represent the three adamantane signals of carbons **a**, **b** and **c**. The signals at 124.90 ppm and represents the four phenyl ring signals of carbons **f**, **g**, **e** and **h**. There is no logical explanation for the appearance of the signal at ca 47 ppm.

(ii) Copolymerization Reactions

(a) Copolymer with Ethene

The high temperature ^{13}C NMR spectrum (Figure 6-6) clearly indicates the incorporation of 1-(1-adamantyl)-4-vinylbenzene in the copolymer. The peak assignments are shown in Table 6.5.

TABLE 6.5: Comparison of Expected and Observed ^{13}C NMR Chemical Shifts (δ) of poly[(1-(1-adamantyl)-4-vinylbenzene-co-ethene]

Carbon	Expected	Observed
a	28.10*	29.12
b	35.90*	36.90
c	42.30*	43.40
d	27.0**	N/D
e, h	125.50**	N/D
f, g	128.40**	124.50
i	32.0**	N/D
j	30.90**	29.50
k	27.80**	31.20

*: Based on monomer spectra; **: Based on spectra of poly(ethylene) and related polymers.

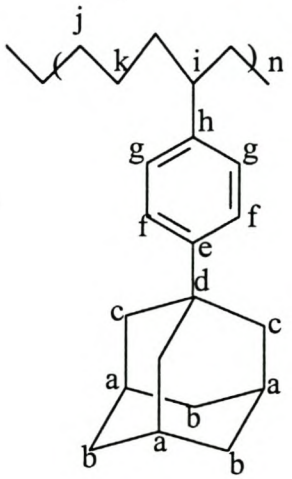

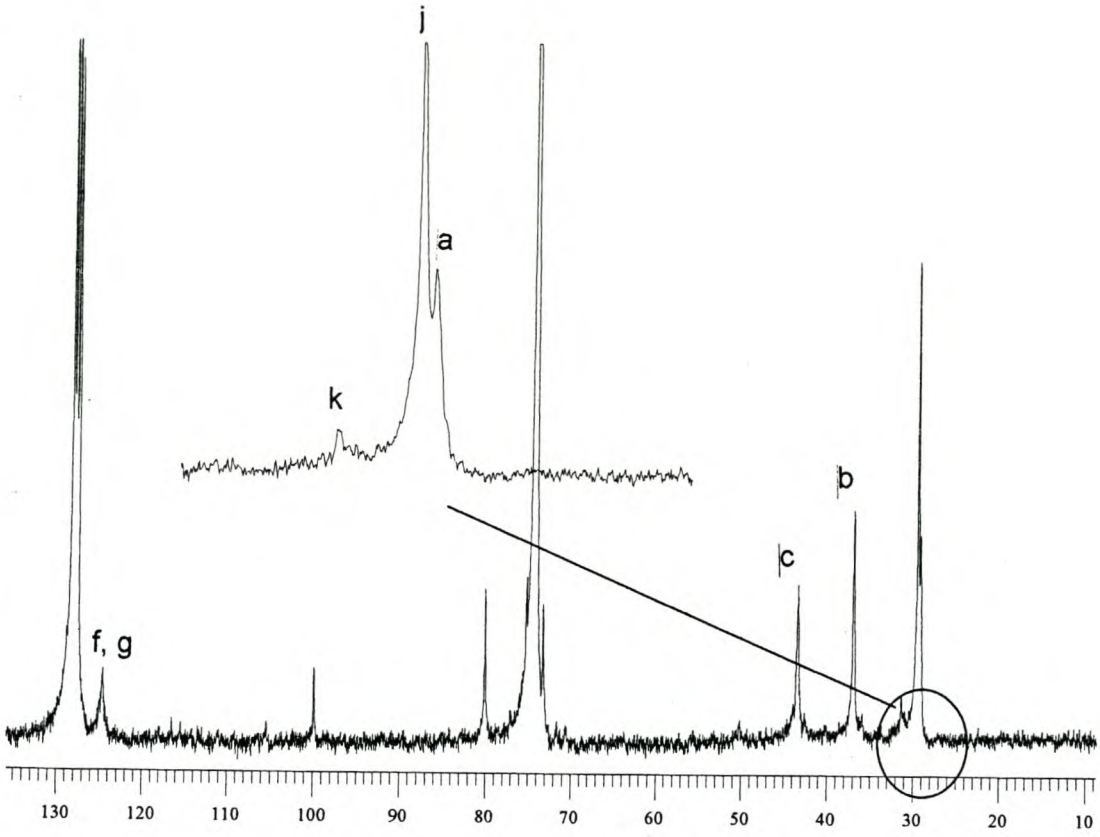

FIGURE 6-6: High Temperature ^{13}C NMR Spectrum of poly[1-(1-adamantyl)-4-vinylbenzene-co-ethene]

From Table 6.5 one can see a very good comparison of the chemical shifts expected from poly(ethylene) polymers (with $-CH_2$ groups in the α-position relative to the carbon chain branching in the β-position) and the chemical shifts observed from the ^{13}C NMR spectrum. We expect the polymers to be predominantly poly(α-olefins) with a small amount of 1-(1-adamantyl)-4-vinylbenzene incorporated. The spectrum is consistent with the structure shown above. The signals at 29.12 ppm, 36.90 ppm and 43.40 ppm represent the three adamantane signals of carbons **a**, **b** and **c**. In the case of carbon **d** it is very difficult to observe the peak from the ^{13}C NMR spectrum, as the area in which this peak is expected is hidden under the larger peak area at ca 29 ppm. The signal at 124.50 ppm represents the phenyl ring carbons, carbons **f** and **g**. In this case, the signal representing carbons **e** an **h** may be hidden under the larger peak area at ca 127 ppm representing the deuterated benzene carbons. The signal representing carbon **i** may be hidden under the larger peak area at ca 29 ppm. The signal at 29.50 ppm

represents the poly(ethylene) pentads, carbon **j**. The signal representing carbon **k** at 31.20 ppm is due to branching in the poly(ethylene) backbone The signals at ca 100 ppm, 80 ppm and 74 ppm represent tetrachloroethylene which was used in combination with deuterated benzene (signal at ca 127 ppm) as high temperature solvent.

From the ^{13}C NMR spectrum of poly[(1-(1-adamantyl)-4-vinylbenzene-co-ethene] it is clear that only a small amount of comonomer was incorporated into the polyethylene backbone.

(b) Copolymer with Styrene

The ^{13}C NMR spectrum (Figure 6-7) clearly indicates the incorporation of 1-(1-adamantyl)-4-vinylbenzene in the copolymer, with the peak assignments shown in Table 6.6.

TABLE 6.6: Comparison of Expected and Observed ^{13}C NMR Chemical Shifts (δ) of poly[(1-(1-adamantyl)-4-vinylbenzene-co-styrene]

Carbon	Expected	Observed
a	28.10*	29.20
b	35.90*	36.90
c	42.30*	43.40
d	27.0**	N/D
e, h	125.50**	125.80
f, g	128.40**	124.60
i	27.0**	N/D
j	44.70**	50.20

*: Based on monomer spectra; **: Based on spectra of poly(styrene) and related polymers.

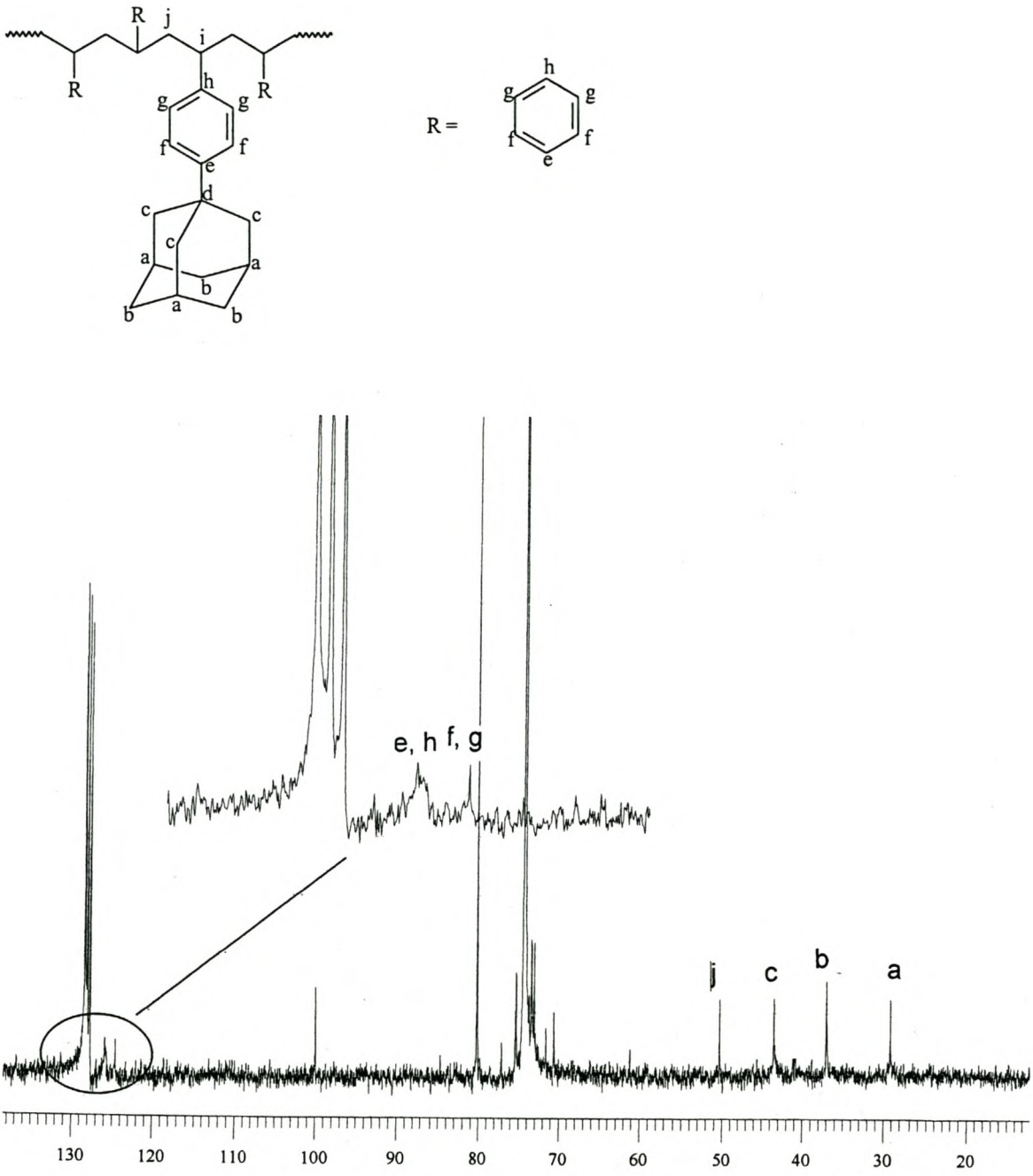

FIGURE 6-7: ^{13}C NMR Spectrum of poly[1-(1-adamantyl)-4-vinylbenzene-co-styrene]

From Table 6.6 one can see a very good comparison of the chemical shifts expected from poly(styrene) polymers (with $-CH_2$ groups in the α-position relative to the carbon chain branching in the β-position) and the chemical shifts observed from the ^{13}C NMR spectrum. We expect the polymer to be

predominantly poly(styrene) with a small amount of 1-(1-adamantyl)-4-vinylbenzene incorporated. The spectrum is consistent with the structure shown above. The signals at 29.20 ppm, 36.90 ppm and 43.40 ppm represent the three adamantane signals of carbons **a**, **b** and **c**. In the case of carbon **d** it is very difficult to observe the peak from the ^{13}C NMR spectrum, as the area in which this peak is expected is hidden under the larger peak area at ca 29 ppm. The signals at 124.60 ppm and 125.80 ppm represent the phenyl ring carbons, carbons **f**, **g**, **e** and **h**. The signal representing carbon **i**, predicted at ca 27 ppm, may be buried underneath the signal of carbon **a**, which represents one of the adamantane ring carbons, at 29.20 ppm. The signal at 50.20 ppm may represent carbon **j**, the CH_2 backbone of poly(styrene). The signals at ca 100 ppm, 80 ppm and 74 ppm represent tetrachloroethylene which was used in combination with deuterated benzene (signal at ca 128 ppm) as high temperature solvent.

From the ^{13}C NMR spectrum of poly[(1-(1-adamantyl)-4-vinylbenzene-co-styrene] it is clear that a large amount of styrene was incorporated into the copolymer.

From the data compiled in Tables 6.4 to 6.6, it was possible to propose structures for the homopolymer, poly[(1-(1-adamantyl)-4-vinylbenzene] and the copolymers of 1-(1-adamantyl)-4-vinylbenzene with ethene and styrene.

The ^{13}C NMR spectra of the homopolymer as well as the copolymers showed the expected amount of signals and confirmed the proposed structure.

6.8 CONCLUSIONS

(1) The homopolymer of 1-(1-adamantyl)-4-vinylbenzene was successfully prepared using a half–sandwich metallocene catalyst, pentamethylcyclopentadienyl zirconium trichloride with MAO as cocatalyst, as well as cationically, using stannic chloride ($SnCl_4$) as catalyst.

(2) The copolymerization of 1-(1-adamantyl)-4-vinylbenzene with ethene using a half–sandwich metallocene catalyst, pentamethylcyclopentadienyl zirconium trichloride, was demonstrated.

(3) The copolymerization of 1-(1-adamantyl)-4-vinylbenzene with styrene using a half–sandwich metallocene catalyst, pentamethylcyclopentadienyl zirconium trichloride, as well as cationic polymerization using stannic chloride as catalyst, have been demonstrated.

(4) In the case of the copolymerization of 1-(1-adamantyl)-4-vinylbenzene with pentene, hexene and octene using a half–sandwich metallocene catalyst, pentamethylcyclopentadienyl zirconium trichloride, only poly[(1-(1-adamantyl)-4-vinylbenzene] was formed. In the case where styrene was used as comonomer, a powdery product, poly[(1-(1-adamantyl)-4-vinylbenzene-co-styrene], was formed. This may be because of the ease with which the styrene-derived monomer is polymerized with the half–sandwich catalyst. In the copolymerization reactions of 1-(1-adamantyl)-4-vinylbenzene with 1-pentene, 1-hexene, 1-octene and styrene using the bridged metallocene catalyst, iso-propylindene(cyclopentadienyl)(9-fluorenyl) zirconium dichloride, no polymers were formed. This may be because of the steric hindrance of the bridged catalyst and the steric nature of the 1-(1-adamantyl)-4-vinylbenzene monomer.

(5) ^{13}C NMR spectroscopy proved to be an effective method in determining the homo- and copolymer structures.

(6) GPC analysis of the 1-(1-adamantyl)-4-vinylbenzene homopolymer showed that it is an oligomer (Mw = 1 823 $g.mol^{-1}$) consisting of about eight repeating units. The polydispersity is quite low for a cationic homopolymerization.

(7) GPC analysis of the 1-(1-adamantyl)-4-vinylbenzene copolymer with styrene showed that it was polymeric, with a Mw of 21 229 $g.mol^{-1}$. The polydispersity is again quite low for a cationic copolymerization.

(8) DMA analyses of the 1-(1-adamantyl)-4-vinylbenzene homopolymer showed a Tg at –9 °C. The very low value is indicative of the oligomeric nature of the material.

(9) DMA analysis of the 1-(1-adamantyl)-4-vinylbenzene copolymer with styrene showed a Tg at 100.9 °C, which is very close to that of the polystyrene homoplymer.

(10) IR spectroscopy was another method that was successfully used to determine the structure of the homopolymer.

(11) ^{13}C NMR spectroscopy also clearly showed the incorporation of 1-(1-adamantyl)-4-vinylbenzene during the copolymerization reactions.

6.9 REFERENCES

1. Ishihara M., Kuramoto M., Uoi M., *Macromolecules*, 1988, **21**, 3 356.

2. Natta G., Pino P., Corradini P., Danusso F., Mantica E., *J. Am. Chem. Soc.*, 1955, **77**, 1 700.

3. Natta G., Danusso F., Sianesi D., *Makromol. Chem.*, 1958, **28**, 253.

4. Ishihara N., Seimiya T., Kuramoto M., *Macromolecules*, 1986, **19**, 2 464.

5. Kaminsky W., Lenk S., Scholtz V., *Macromolecules*, 1997, **30**, 7 647.

6. Zambelli A., Oliva L., Pellecchia C., *Macromolecules,* 1989, **22**, 2 129.

7. Chien J.C.W., Ready T.E., Rausch M.D., *J. Organomet. Chem.*, 1996, **21**, 519.

8. Grassi A., Zambelli A., Longo P., Pellecchia C., *Macromolecules*, 1987, **20**, 2 035.

9. Soga K., Yu C.H., Shiono T., *Makromol. Chem., Rapid Commun.*, 1988, **9**, 351.

10. Foster P.F., Chien J.C.W., Rausch M.D., *Organometallics*, 1996, 15, 2 404.

11. Kissin Y.V. (Mobil Oil Corp.), US Patent 5 326 837, 1994, *Chem. Abstr.*, 1995, 12 232 333.

12. Pellecchia C., Longo P., Proto A., Zambelli A., *Makromol. Chem., Rapid Commun.*, 1992, **13**, 265.

13. Campell R.E., Jr., Schmidt G.F. (Dow Chemical Corp.), US Patent 4 774 301, 1988, *Chem. Abstr.*, 1988, 110, 24 453.

14. Van Zyl A.P.J., M.Sc Thesis, University of Stellenbosch, 1999.

15. Capaldi E., Borchert A.E., US Patent 3 457 318, 1969.

16. Brüll R., Pasch H., Raubenheimer H.G., Sanderson R.D., Wahner U.M., *J. Polym. Sci.: Part A, Polym. Chem.*, 2000, **38**, 2 333.

17. Sandler, Karo Bonesteel, Pearce, in *Polymer Synthesis and Characterization, A Laboratory Manual*, Acedemic Press, 1998, 22.

CHAPTER 7
CONCLUSIONS

7.1 GENERAL

The following overall conclusions can be drawn from the work carried out on the incorporation of bulky pendant groups into α-olefin polymers.

1. A thorough literature study on the subject matter, namely adamantane, its structure, formation and properties, as well as adamantane–containing polymers was undertaken.

   Several synthetic techniques described in the literature were then successfully used to synthesize the two monomers 3-(1-adamantyl)-1-propene and 1-(1-adamantyl)-4-vinylbenzene, for use in this study.

   A number of unique materials, both oligomeric and polymeric in nature, such as the 3-(1-adamantyl)-1-propene homopolymer and copolymers with ethene, propene and higher α-olefins as well as the 1-(1-adamantyl)-4-vinylbenzene homopolymer and copolymers with ethene and styrene were also synthesized.
2. These homopolymers and copolymers mentioned in (1) were characterized for glass transition and melting point determination, composition analyses and molecular weight determination.
3. The relationship between the composition and physical properties of the homo- and copolymers mentioned in (1) was investigated. Conclusions were drawn regarding the physical, mechanical and thermal properties of the materials made.

7.2 3-(1-ADAMANTYL)-1-PROPENE

In the study of the synthesis of 3-(1-adamantyl)-1-propene the following conclusions were drawn:

1. Of the three different approaches used to synthesize 3-(1-adamantyl)-1-propene that was pure enough to be polymerized or incorporated into polymers, it was the third approach, by which 3-(1-adamantyl)-1-propene was synthesized using a Friedel–Crafts type reaction, that proved to be most suitable. The use of high vacuum sublimation proved to be an excellent method by which to purify 3-(1-adamantyl)-1-propene. This method also proved to be not as expensive as the method used in the second approach, where a trimethylsilylated unsaturated compound was used as proton sponge to minimize side reactions.
2. From the results obtained by NMR analysis, it was clear that the first approach used to synthesize 3-(1-adamantyl)-1-propene, a Grignard type procedure, was not suitable. It resulted in a low yield and a mixture of products. None of the three purification methods used to purify the crude product was successful.
3. A new method for the preparation of 3-(1-adamantyl)-1-propene, the second approach, using the relevant literature published by Sasaki *et al*[1] and adding a proton sponge, was developed in our hands. Use of the hindered pyridine, 2,6-di-tert-butyl pyridine, employed to act as a proton sponge, proved to be very successful in preventing the creation of an acidic reaction medium conducive to the occurrence of side reactions.

   This method, by which 3-(1-adamantyl)-1-propene was synthesized using trimethylsilylated unsaturated compounds, was reasonably successful. High vacuum sublimation proved to be an excellent method by which to purify 3-(1-adamantyl)-1-propene for polymerizations. Purity of the 3-(1-adamantyl)-1-propene monomer was > 96%. The only disadvantage of this method is that the hindered pyridine is very expensive, which makes it quite expensive to produce large quantities of the required monomer 3-(1-adamantyl)-1-propene.

7.2.1 Polymerization Reactions with 3-(1-Adamantyl)-1-Propene and 3-Phenyl-1-Propene

1. The homopolymers of 3-(1-adamantyl)-1-propene and 3-phenyl-1-propene were successfully prepared using the metallocene catalyst, *rac*-ethylenebis(indenyl)zirconium dichloride, with MAO as cocatalyst.
2. In addition, the copolymerizations of 3-(1-adamantyl)-1-propene with ethene, propene and a series of higher α-olefins were successfully carried out. In the case of 3-phenyl-1-propene, copolymerizations were carried out successfully with a series of higher α-olefins.

7.2.2 Characterization and Properties of 3-(1-Adamantyl)-1-Propene and 3-Phenyl-1-Propene Polymers

1. The glass transition temperatures as well as the melting points of the α-olefin homopolymers were reasonably close to the literature values for the Ziegler-Natta-catalyzed poly(α-olefins) with the exception of poly(4-methyl-1-pentene), for which the T_m was noticeably lower for the metallocene-catalyzed polymers (210°C vs. 245°C). The homopolymer of 3-(1-adamantyl)-1-propene showed no melting prior to degradation, but did show a T_g at 235°C. The T_g's of most of the 3-(1-adamantyl)-1-propene-α-olefin copolymers were higher than those of the corresponding homopolymers. From the T_g results it was clear that the incorporation of the bulky adamantyl pendant group severely disrupted the crystalline structure and influenced the T_g's of the polymers.
2. The presence of the bulky phenyl pendant group resulted in a slight increase in T_g's of poly[3-phenyl-1-propene-co-1-octene] and poly[3-phenyl-1-propene-co-1-hexene], compared to the corresponding α-olefin homopolymers. The T_g's of poly[3-phenyl-1-propene-co-1-pentene] and poly[3-phenyl-1-propene-co-4-methyl-1-pentene] were lower than those of the corresponding α-olefin homopolymers. The bulky phenyl pendant group

had little effect on the T_g's of the 3-phenyl-1-propene-α-olefin copolymers and their structures.

3. From a comparison done between the T_g's of the 3-(1-adamantyl)-1-propene-α-olefin copolymers and the T_g's of the 3-phenyl-1-propene-α-olefin copolymers it was clear that the bulky adamantyl pendant group had a much bigger influence on the T_g's and the crystalline structures of the copolymers than the phenyl group did.
3. High-temperature liquid ^{13}C NMR spectroscopy as well as solid state NMR spectroscopy proved to be effective methods in determining the homo- and copolymer structures. Results clearly showed the incorporation of 3-(1-adamantyl)-1-propene and 3-phenyl-1-propene during the copolymerization reactions.
4. The solid state NMR spectra of both the homopolymer of 3-(1-adamantyl)-1-propene as well as the copolymers showed the expected number of signals and confirmed the proposed structures.
5. The 3-(1-adamantyl)-1-propene homopolymer as well as the copolymers were insoluble in most organic solvents, including trichlorobenzene at high temperatures.
6. IR spectroscopy was also successfully used to confirm the structure of the 3-(1-adamantyl)-1-propene homopolymer.
7. The 3-phenyl-1-propene homopolymer as well as the copolymers were insoluble in most organic solvents, with the exception of trichlorobenzene at high temperatures.

7.3 1-(1-Adamantyl)-4-Vinylbenzene

In the study of the synthesis of 1-(1-adamantyl)-4-vinylbenzene the following conclusions were drawn:

1. Three different approaches were used to synthesize 1-(1-adamantyl)-4-vinylbenzene that was pure enough to be polymerized or incorporated into polymers.

2. The first method used to prepare 1-(1-adamantyl)-4-vinylbenzene was successful. This method was a two–step synthesis; a combination of classical Heck cross-coupling conditions and a Friedel–Crafts arylation. The target monomer, 1-(1-adamantyl)-4-vinylbenzene, was synthesized via the intermediate 1-bromo-(4-adamantyl)-benzene. 1-(1-adamantyl)-4-vinylbenzene could not be purified by chormatography. Because of the low yield of 1-(1-adamantyl)-4-vinylbenzene achieved using this method, high vacuum distillation was not considered as a method of purification. Alternate methods to synthesize a substantial amount of pure 1-(1-adamantyl)-4-vinylbenzene were required.
3. The second method used to prepare 1-(1-adamantyl)-4-vinylbenzene was also unsuccessful. This method was three–step synthesis; a combination of a nickel-catalyzed Grignard cross coupling reaction and a Friedel-Crafts arylation. From the ^{13}C NMR spectrum it was clear that only a limited amount of coupling took place and that the major component of the crude product was 1-bromo-(4-adamantyl)-benzene. Considering the low yield of the desired 1-(1-adamantyl)-4-vinylbenzene and the time factor involved in this three-step synthesis, further methods by which to synthesize substantial amounts of pure 1-(1-adamantyl)-4-vinylbenzene were considered.
4. The third method used was a three–step synthesis which can be described as a palladium–catalyzed substitution on 1-bromoadamantane. The first step of the synthesis is a Friedel–Crafts arylation. The second step entailed a formylation reaction and a subsequent Wittig olefination, to form 1-(1-adamantyl)-4-vinylbenzene. This method proposed by Bräse *et al*[2] was unsuccessful in our hands. Therefore, using the relevant information in Bräse's method, the following three-step synthesis was developed in this study to synthesize pure and sufficient amounts of 1-(1-adamantyl)-4-vinylbenzene.

   This method, by which 1-(1-adamantyl)-4-vinylbenzene is synthesized using a palladium–catalyzed substitution on 1-bromo adamantane, proved to be

very successful. The use of chromatography proved to be an excellent method by which to purify the desired product. This method was ultimately successful and less time consuming than the other two approaches attempted to synthesize substantial amounts of pure 1-(1-adamantyl)-4-vinylbenzene.

7.3.1 Polymerization reactions with 1-(1-Adamantyl)-4-Vinylbenzene

1. The homopolymerization reaction of 1-(1-adamantyl)-4-vinylbenzene was carried out sucessfully with the half–sandwich metallocene catalyst, pentamethylcyclopentadienyl zirconium trichloride, as well as by means of cationic polymerization using stannic chloride ($SnCl_4$) as catalyst. The powdery polymer product of poly[(1-(1-adamantyl)-4-vinylbenzene] obtained by using the half–sandwich catalyst, was insoluble in all common organic solvents, even in chlorinated aromatic solvents at elevated temperatures. The powdery polymer product of poly[(1-(1-adamantyl)-4-vinylbenzene] obtained by cationic polymerization on the other hand, was soluble in all common organic solvents.
2. 1-(1-adamantyl)-4-vinylbenzene was successfully copolymerized with ethene by using the half–sandwich metallocene catalyst, pentamethylcyclopentadienyl zirconium trichloride. The powdery polymer product of poly[(1-(1-adamantyl)-4-vinylbenzene-co-ethene] was insoluble in all common organic solvents, even in chlorinated aromatic solvents at elevated temperatures.
3. Of the copolymerization reactions of 1-(1-adamantyl)-4-vinylbenzene with 1-pentene, 1-hexene and 1-octene, using the half–sandwich metallocene catalyst, pentamethylcyclopentadienyl zirconium trichloride, only poly[(1-(1-adamantyl)-4-vinylbenzene] was formed. When styrene was used as comonomer, the powdery product poly[(1-(1-adamantyl)-4-vinylbenzene-co-styrene] was formed.
4. In the copolymerization reactions of 1-(1-adamantyl)-4-vinylbenzene with 1-pentene, 1-hexene, 1-octene and styrene using the bridged metallocene

catalyst, iso-propylindene(cyclopentadienyl)(a-fluorenyl) zirconium dichloride, no polymers were formed.

5. 1-(1-adamantyl)-4-vinylbenzene was also successfully copolymerized with styrene, cationically, using stannic chloride ($SnCl_4$) as catalyst. The powdery polymer product of poly[(1-(1-adamantyl)-4-vinylbenzene-co-styrene] was soluble in most organic solvents.

7.3.2 Charaterization of 1-(1-Adamantyl)-4-Vinylbenzene Polymers

The 1-vinyl(4-adamantyl)-benzene polymers were characterized and showed the following:

1. From the data obtained from the ^{13}C NMR spectra, it was possible to obtain structures for the homopolymer, poly[(1-vinyl)-(4-adamantyl)-benzene], and the copolymers of 1-(1-adamantyl)-4-vinylbenzene with ethene and styrene.
2. GPC analysis of the 1-(1-adamantyl)-4-vinylbenzene homopolymer showed that it was an oligomer (Mw = 1823 $g.mol^{-1}$) consisting of about eight repeating units. The polydispersity was quite low for a cationic homopolymerization.
3. GPC analysis of the 1-(1-adamantyl)-4-vinylbenzene copolymer with styrene showed that it was polymeric, with a Mw of 21 229 $g.mol^{-1}$. The polydispersity was quite low for a cationic copolymerization.
4. DMA analysis of the 1-(1-adamantyl)-4-vinylbenzene copolymer with styrene showed a Tg at 100.9 °C.
5. IR spectroscopy was also successfully used to confirm the structure of the 1-(1-adamantyl)-4-vinylbenzene homopolymer.

7.4 REFERENCES

1. Sasaki T., Usuki A., Ohno T., *J. Org. Chem.*, 1980, **45**, 3 559.
2. Bräse S., Waegell B., de Meijere A., *Organic Synthesis*, 1998, **2**, 148.